

NORTHWEST GEOLOGY

The Journal of The Tobacco Root Geological Society

Volume 49, July 2020

45th Annual Field Conference

**Geology of the Bitterroot Region and
Other Papers**

July 23–27, 2020



Published by The Tobacco Root Geological Society, Inc.

P.O. Box 118

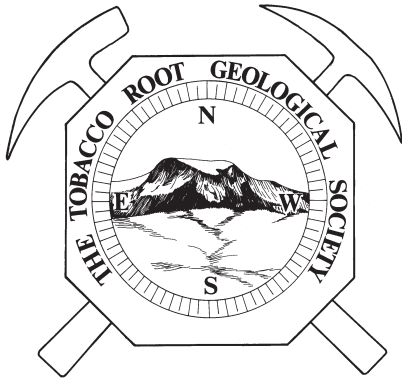
Butte, Montana 59703

<http://trgs.org>

Edited by: Jeff Lonn, Alan English, Katie McDonald, and Phyllis Hargrave



Cover photo: Tilted layers of mylonitic gneiss developed along the east-dipping Eocene Bitterroot detachment fault. Late Quaternary glaciers carved these spectacular exposures in Mill Creek Canyon near Hamilton. Jeff Lonn photo.



NORTHWEST GEOLOGY

The Journal of The Tobacco Root Geological Society

Volume 49, July 2020

45th Annual Field Conference

Geology of the Bitterroot Region and Other Papers

July 23–27, 2020

Published by The Tobacco Root Geological Society, Inc.

P.O. Box 118

Butte, Montana 59703

<http://trgs.org>

Edited by: Jeff Lonn, Alan English, Katie McDonald, and Phyllis Hargrave



The Tobacco Root Geological Society, Inc.

P.O. Box 118
Butte, Montana 59703

Officers, 2020:

President: Jesse Mosolf, Montana Bureau of Mines and Geology, Butte, MT
Vice-President: Alan English, Montana Bureau of Mines and Geology, Butte, MT
Treasurer: Katie McDonald, Montana Bureau of Mines and Geology, Butte, MT
Secretary: Sandy Underwood, Bozeman, MT
Corresponding Secretary: Lara Strickland, Columbus, MT
Webmasters: Petr Yakovlev, Montana Bureau of Mines and Geology, Butte, MT

Board of Directors, 2020:

Ted Antonioli, Geologist, Missoula, MT
Bruce E. Cox, Geologist (semi-retired), Missoula, MT
Larry Johnson, Consultant, Missoula, MT
Larry N. Smith, Dept. of Geological Engineering, Montana Tech, Butte, MT
Mike Stickney, Montana Bureau of Mines and Geology, Butte, MT
John Childs, Childs Geoscience Inc., Bozeman, MT
Emily Geraghty Ward, Geology Dept., Rocky Mountain College, Billings, MT

2020 Conference Organizers:

George Furniss, Jeff Lonn, Katie McDonald, Bruce Cox, Jesse Mosolf
Editors: Jeff Lonn, Alan English, Katie McDonald, and Phyllis Hargrave (MBMG)
Layout and Editing: Susan Barth (MBMG)

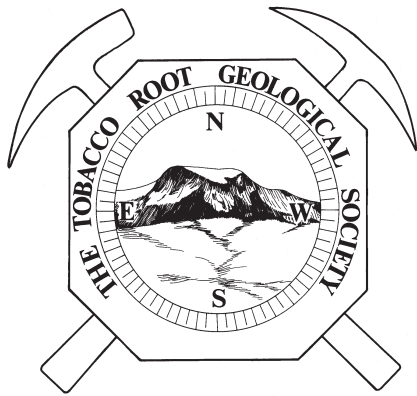
Printed by Insty-Prints, Butte, Montana

ISSN: 0096-7769

© 2020 The Tobacco Root Geological Society, Inc.

<http://trgs.org>





NORTHWEST GEOLOGY

The Journal of The Tobacco Root Geological Society

Volume 49, July 2020

Geology of the Bitterroot Region and Other Papers

TABLE OF CONTENTS

FIELD GUIDES

Skye W. Cooley	Sheeted clastic dikes in the megaflood region, WA-OR-ID-MT 1
Burmester, Lonn, and Lewis	Further speculation on Belt stratigraphy and structure around Salmon, Idaho: Alternative interpretations and tests..... 19
Lonn and Mosolf	Field guide to the geology of the Sleeping Child metamorphic complex, southern Sapphire Mountains, western Montana..... 35
Michael Stickney	Hanging wall rocks of the Bitterroot detachment fault exposed west of Victor, Montana..... 57
Gammons and Grondin	Field trip guide to Crystal Mountain fluorite mine..... 63
Michael Stickney	Late Quaternary fault scarps near Como Lake, Montana 71
Childs and Dean	New documentation of a major molybdenum–copper porphyry system in Lower Willow Creek, west of the Black Pine mine, Granite County, southwestern Montana..... 77
Jeff Lonn	Geology along the Late Quaternary Bitterroot fault scarps, and implications for seismicity in the Bitterroot Valley, western Montana..... 87
George Furniss	Roadside geologic traverse along the Bitterroot Front from Hamilton to Lake Como 97
J.W. Sears	Faults and floods of the Missoula Valley 103
Cox and Furniss	Roadside geologic traverse through the Sapphire Mountains, Montana: State Highway 38, west to east..... 119



TRGS 2020 SCHOLARSHIP AWARD WINNERS

- * Ethan Costello (Foster), Colorado State University
Mafic Rocks associated with ores of the Boulder Batholith, southwestern Montana
- * Stuart Parker (TRGS), Idaho State University
Response of exhumation to basin geometry in the Idaho/Montana fold-thrust Belt
- * Carlos Montejo (TRGS) Montana Tech
Quaternary geology of portions of the McGregor Peak, Marion, Murr Peak, and Hubbard Reservoir 7.5' quadrangles, Flathead County, Montana
- * Haley Thoresen (Skipp), University of Idaho
Basin record of the initiation of extension and core complex exhumation in western Montana and south east Idaho
- * Erin Young-Dahl (TRGS), University of Idaho
Using stable isotope paleoaltimetry of hydrated volcanic glass to reconstruct Eocene paleotopography across the northern United States Cordillera
- * Matthew Ellison (TRGS), Utah State University
The biggest snowball fight in Earth history: Sequence stratigraphy, facies analysis, and geochronology of the Cryogenian Pocatello Fm, SE Idaho, USA
- * Chance Ronemus (Harrison), Montana State University
Reconstructing the Proterozoic-recent thermal history of the Beartooth Mountains, Montana
- * Shannon Ahern (Kleinkopf), Stockton University
Geologic mapping of the Mount Powell Batholith, western Montana
- * Rudolph Engel (Kleinkopf), Stockton University
Petrophysical characterization of the Mount Powell Batholith, western Montana



TRGS CHARTER MEMBERS

Stanley W. Anderson
Clyde Cody
William S. Cordua
Lanny H. Fisk
Richard I. Gibson†
Thomas Hanley
Stephen W. Henderson
Thomas E. Hendrix
Mac R. Hooton
Inda Immega
Steven W. Koehler
Marian Millen Lankston†
Robert W. Lankston†
J. David Lazor
Joe J. Liteheiser, Jr.
Judson Mead*
Marvin R. Miller
Vicki M. Miller*
Allen H. Nelson
Alfred H. Pekarek
Patricia Price*
Donald L. Rasmussen
Raymond M. Rene

TRGS LIFETIME MEMBERS

John Childs
Rob Foster
Joan (Mrs. Jack) Harrison*
Karen Keefer
Layaka Mann
Chris Pool

† = co-founder

* = deceased



TRGS HAMMER AWARD RECIPIENTS

*Awarded for distinguished achievement
in the study of the geology of the
Northern Rocky Mountains*

1993: Ed Ruppel*
1994: Dick Berg
2003: Don Winston
2004: Dean Kleinkopf*
2009: Betty Skipp
2010: Jim Sears
2011: John Childs
2012: J. Michael O'Neill
2013: Paul Karl Link
2014: Reed Lewis
2015: Jeff Lonm
2016: Bruce Cox
2019: Susan Vuke

TRGS HONORARY MEMBERS

1980: Charles J. Vitaliano*
2008: Elizabeth Younggren*
(also honorary Board member)
2010: Dick Berg
2010: Bruce Cox
2010: Dean Kleinkopf*
2010: Dave Lageson
2011: Marie Marshall Garsjo
2011: Paul Link
2011: Rob Thomas
2012: Jeff Lonm
2012: Mitch Reynolds
2013: Reed Lewis
2015: Don Winston
2020: Ted Antonioli, Larry Smith,
Mike Stickney



PAPERS

SHEETED CLASTIC DIKES IN THE MEGAFLOOD REGION, WA-OR-ID-MT

Skye W. Cooley

Field Geologist, Ronan, Montana

ABSTRACT

Clastic dikes are sediment-filled fractures found worldwide in deformed sediments from the Precambrian to the Pleistocene. Most are soft sediment deformation features and the products of liquefaction caused by seismic shaking. The dikes described in this article are vertically sheeted and have other characteristics that contrast with typical liquefaction dikes. This study investigated unconsolidated sediments along the path of the Ice Age megafloods between Priest River, ID and The Dalles, OR and found clastic dikes in 262 of 488 exposures. Dike distribution, width, relative age, and association with syndepositional deformation indicate the dikes are nonseismic structures formed by rapid loading and hydrofracture during glacial outburst floods. They are flood injectites, not seismites. This study is the first to document large numbers of sheeted clastic dikes at a regional scale (>25,000 km²) in the Inland Pacific Northwest.

PREVIOUS WORK

Clastic dikes in megaflood deposits are noted in classic papers on the Channeled Scabland (Allison, 1941; Baker, 1973; Waitt, 1985; Smith, 1993; Atwater, 1986), but reports containing detailed descriptions of the dikes are few (Jenkins, 1925; Lupher, 1944; Black, 1979; Woodward-Clyde Associates, 1981), especially those containing field measurements (Alwin and Scott, 1970; Cooley and others, 1996; Neill and others, 1997; Ward and others, 2006). Several articles mention the dikes in passing and speculate on their origin, but contain little data (Flint, 1938; Newcomb, 1962; Bingham and Grolier, 1966; Jones and Deacon, 1966; Beaulieu, 1974; Carson and others, 1978; Shaw and others, 1999; Fecht and others, 1999; Pritchard and Cebula, 2016). Seventy years of reporting on Pleistocene deposits at the USDOE Hanford waste storage site (1,518 km²) provides no clarity on the dikes' origin. The Hanford literature collectively contains few field measurements and ample speculation, much of it contradictory (i.e., Bjornstad, 1982; Bjornstad and oth-

ers, 1990, 2001; Bjornstad and Teel, 1993; Bjornstad and Lanigan, 2007).

Four origins for the dikes have been proposed: earthquakes (Jenkins, 1925), ground ice (Black, 1979), desiccation (Lupher, 1944), and floodwater loading (Brown and Brown, 1962; Baker, 1973). A dubious fifth, "multigenetic" (Black, 1979; Fecht and others, 1999), suggests the dikes formed by a combination of these processes. Cooley (2015) provides a concise summary of the arguments for and against each.

THIS STUDY

I investigated unconsolidated sediments along the path of the Ice Age megafloods between Priest River, ID and The Dalles, OR (fig. 1). Clastic dikes with vertically sheeted fills were identified in 262 of 488 exposures (54%). Sites where soft sediment deformation was abundant were also recorded (starred locations on map). Dikes observed throughout the study area are identical with respect to sedimentology, age, structure, taper direction, and scale. All appear to have formed by the same mechanism.

TYPICAL CLASTIC DIKES

Clastic dikes are sediment-filled fractures found worldwide in deformed sediments from the Precambrian to the Pleistocene. Most clastic dikes are soft sediment deformation features and the products of liquefaction caused by seismic shaking. Strong shaking elevates pore fluid pressures in wet, unconsolidated sediment, causing it to mobilize and vent to the ground surface, forming sand blows (small wet-sediment volcanos). Therefore, most earthquake-generated clastic dikes have upward-tapering forms, contain massive sandy fills, and serve as feeder conduits to sand blows (e.g., Obermeier and others, 1993).

SHEETED INJECTITES IN THE ICE AGE FLOODWAY

The clastic dikes described here are different. They are sheeted, wedge-shaped structures that were filled

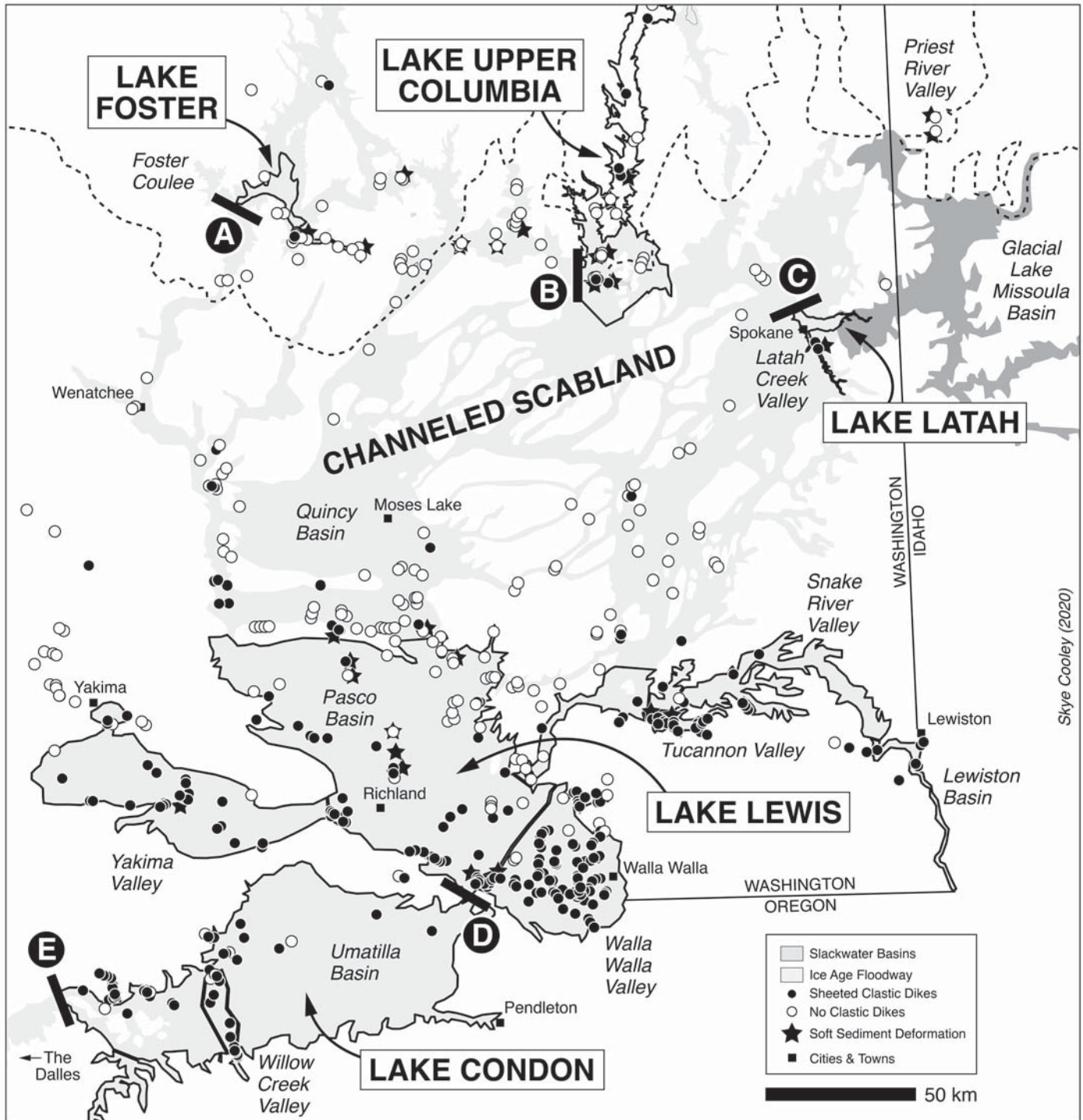


Figure 1. Study area map. Locations with sheeted clastic dikes are shown as black circles. White-filled circles denote locations where no dikes were observed. Stars denote locations with abundant soft sediment deformation. Star symbols are offset from outcrop circles for clarity. A dashed line approximates the Cordilleran Ice Sheet margin. Glacial Lake Columbia is shown at its 600 m elevation shoreline. Sediments observed at all locations ($n = 488$) consist primarily of unconsolidated Pleistocene-age flood and non-flood silts, sands, and gravels with mixed Neogene sediments and bedrock exposed at a few locations. Light gray areas show the extent of ephemeral slackwater lakes Lewis, Condon, Latah, Upper Columbia, and Foster that formed behind bedrock or ice constrictions (A,B,C,D,E). Dikes are common in southern part of the Channeled Scabland, where silty, sandy rhythmites were deposited. Dikes are sparse in gravel-dominated deposits in the Channeled Scabland and absent from Palouse Loess and lacustrine silts of the Glacial Lake Missoula basin.

from the top and taper downward (fig. 2). They formed by the forceful infilling of brittle tensional fractures propagated downward into sedimentary and bedrock substrates during the Pleistocene when glacial outburst floods inundated the Inland Pacific Northwest

(fig. 3). Injection style and timing are consistent with overloading and surface deformation by fast-moving, rapidly deepening floods and deep, slow-draining slackwater lakes >200 m deep in places.



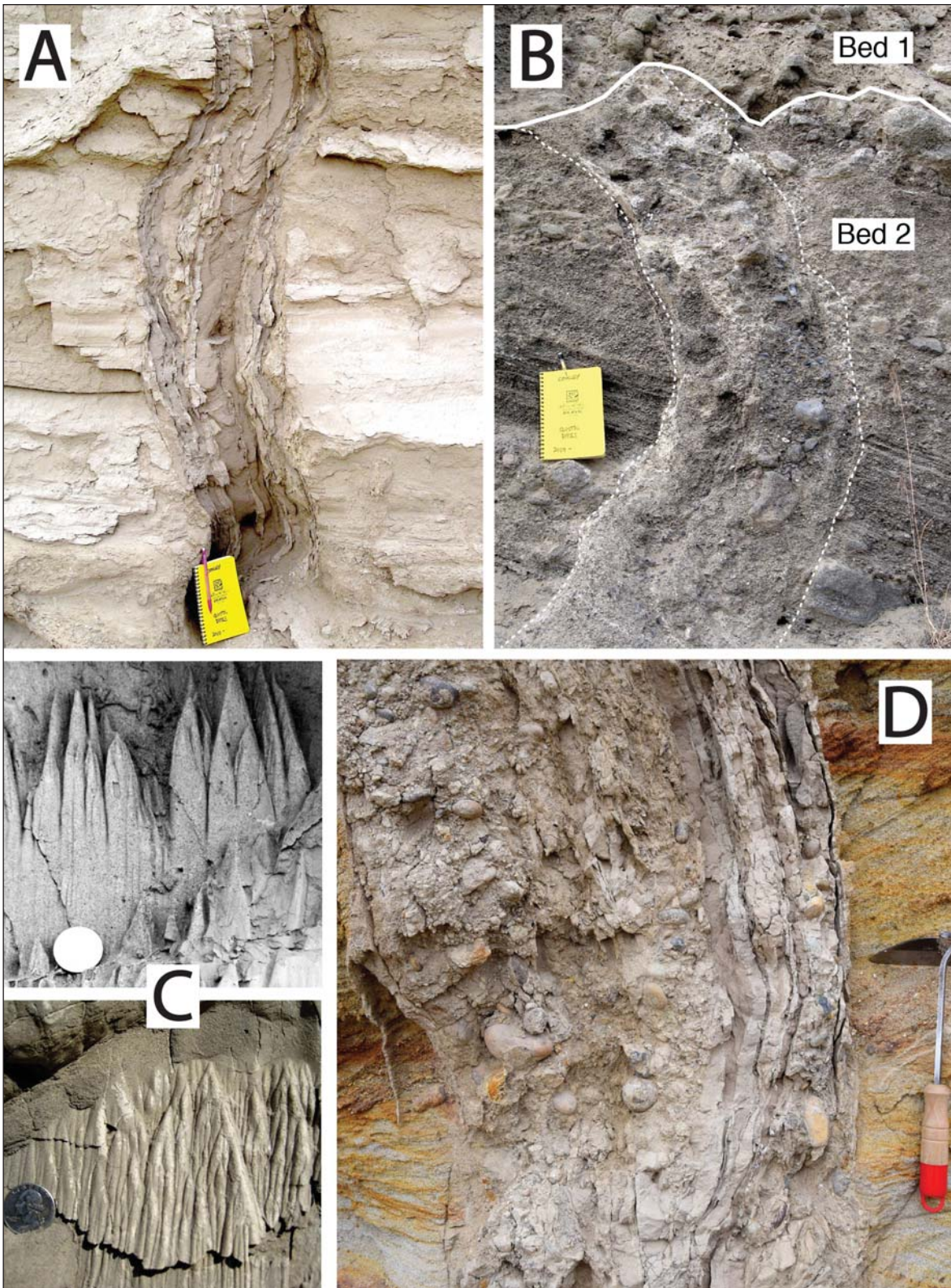


Figure 2. Examples of typical sheeted clastic dikes and flute casts. (A) A typical clastic dike in slackwater rhythmites (Touchet Beds) exhibits the characteristic vertical sheeting composed of darker fill bands (sheets) separated by light-colored silt skin partitions. This example contains ~12 sheets and is filled with silty, sandy sediment closely resembling the host material. Umatilla Basin at Cecil, OR (Slackwater Lake Condon). (B) A typical dike in gravelly deposits is truncated at its top by a second floodbed. Its fill is crudely sheeted and lacks silt skins. Dikes in coarse-grained deposits tend to have lower length-to-width ratio than dikes in fine-grained sediments. Umatilla Basin at Willow Creek, OR (Slackwater Lake Condon). (C) Examples of flute casts that ornament the faces of silt skins. Upward-pointing noses are clear directional indicators. Sediment entered the fractures from the top. Quarters for scale. Walla Walla Valley, WA (Slackwater Lake Lewis). (D) A sheeted dike, filled with a mix of silty, sandy flood sediment (Late Pleistocene) and quartzite-rich gravel from the Ellensburg Fm eroded from local exposures by floodwaters, intrudes micaceous, oxidized fluvial sandstones (Miocene) at Snipes Mountain. The dike contains ~10 sheets. Hoe is 28 cm long. Emerald Road at Granger, WA (Slackwater Lake Lewis).



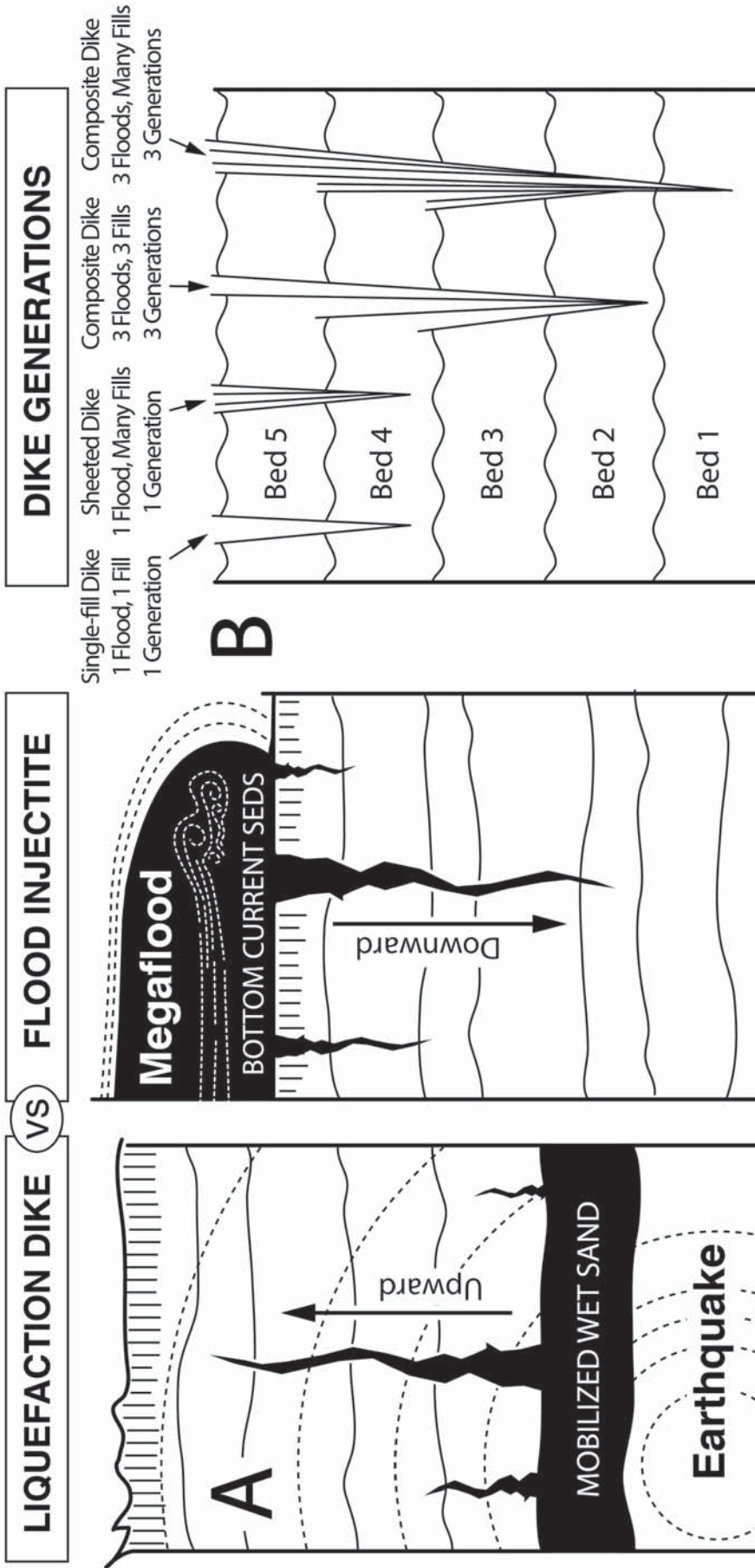


Figure 3. (A) A concept sketch illustrates the differences between clastic dikes formed by liquefaction (sand blows, fluid escape structures) and those formed by floodwater loading and hydrofracture (flood injectites). Liquefaction dikes propagate upward and are sourced in wet, sandy beds deposited sometime in the past and remobilized by strong shaking. Flood injectites are filled hydrofractures that propagate downward and are filled by sediment sourced in circulating bottom currents of glacial outburst floods (megafloods). (B) Generations concept for clastic dikes in aggrading flood sediments. Four examples represent the typical range of forms found in the study area (single-fill, multi-fill compound, and multi-fill composite).



Size

The dikes penetrate more than a dozen different geologic units, including Miocene basalt. The largest examples contain >100 vertical sheets (fill bands), are >2 m wide, and penetrate to depths >40 m. Typical features are <15 cm wide and contain fewer than a dozen sheets.

Sedimentary Fill

Sedimentology of the fill material reflects the local geology. Fills contain a mix of micaceous sandy sediment carried within floods (suspended-load) and coarser bed-load material eroded from localities along the floodway. For example, dikes at Snipes Mountain, WA (Yakima Valley) contain clasts from the Miocene–Pliocene Ellensburg Fm. Dikes at Foster Creek (upper Columbia Valley) contain Latah Fm gneiss shed from a granitic highland to the north. Dikes in the Walla Walla Valley contain Touchet Bed sediment (Jenkins, 1925; Cooley, 2015) and oxidized material deposited by “ancient” Scabland floods (Spencer and Jaffee, 2002; Bader and others, 2016).

Sheeting and Growth

The dikes are conspicuously sheeted “composite” structures (*sensu* Hyashi, 1966). Vertical sheeting records incremental widening by repeated crack-and-fill cycles (reinjection). Crosscutting relationships demonstrate that sheeting did not form during a single event or several events; rather, it developed over time in response to dozens of disturbances. New fractures opened alongside older ones and were filled by sediment delivered from the top; they grew by successive crack-and-fill cycles. Bladed cut-slopes that expose their plan view geometry (Silver and Pogue, 2002) reveal dikes coalesced and intertwined to form polygonal networks over time. Strong grain size contrasts between adjacent sheets are evidence of a variable and changing sediment source consistent with circulating bottom currents within floods. Sheet counts are highest in floodway basins that gathered many floods and lowest in coulees that received few. The largest dikes and those that contain the most sheets occur in slack-water areas near Wallula Gap, through which all floods flowed (Bretz, 1929; Baker and others, 2016).

Silt Skins

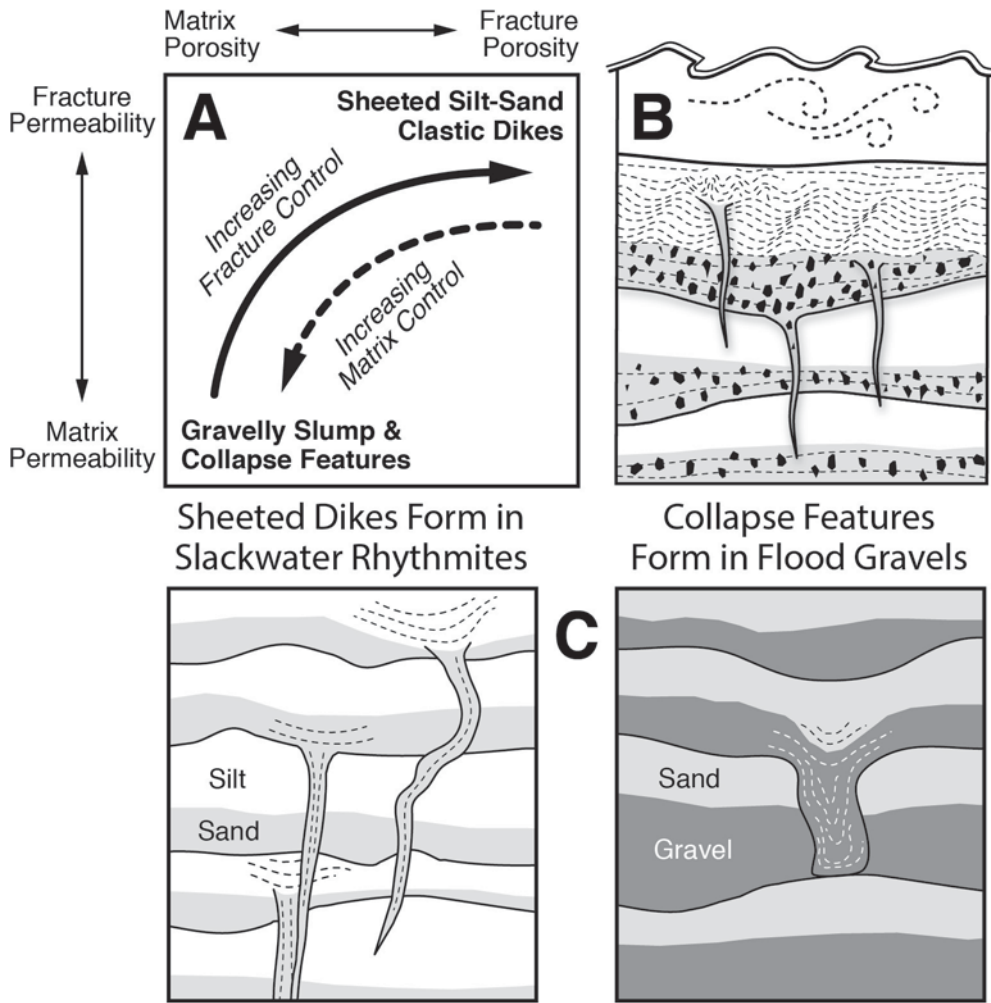
Thin silt partitions (silt skins) separate sheets of sediment inside dikes. Flute casts that ornament the faces of silt skins have upward-pointing noses, in-

dicating downward transport. Silt skins form when pore water migrates laterally out of wet sediment, through the fracture wall, and into the surrounding material. Fines are screened at the fracture walls and accumulate in continuous layers, sealing the fracture. The same filter-screening process forms slurry walls in concrete-filled trench foundations used in heavy construction. Silt skins in study area dikes are 1–10 mm thick. Skins between sheets indicate the younger fills dewatered into older, drier fills nearby. Skins that line the outer walls of dikes are fluted only on their interior faces. Exterior skin walls indicate the host sediment was well-drained, ice-free, and above the water table (vadose zone) at the time of the first injection and probably during all subsequent fillings. Dikes that penetrate impermeable bedrock lack exterior skin walls altogether.

Distribution

The dikes are widely distributed throughout the Ice Age floodway. Great distances separate outcrops containing nearly identical features. For example, more than 500 km separates the northernmost site in the study at Hunters, WA from the southernmost site known to contain dikes at Salem, OR (Ian Madin, photos and written commun.). Glenn (1965) reports dikes in silt-dominated strata exposed along the Willamette River. Sheeted dikes intruding late Pleistocene Willamette silt, which correlates to the Touchet Beds, were discovered in the basement of the Oregon Capitol Building during a recent remodel (Ray Wells, photos and written commun.). Dikes do not occur in the Palouse Loess above elevations of local maximum flood-stage indicators (trimlines), nor in unconsolidated sediments beyond the margins of the floodway. Dikes occur in close proximity to active Quaternary faults (i.e., Wallula fault zone) and at sites located far from them. They are most abundant, well-formed, and best-exposed in high-silt-content rhythmites (Touchet Beds) that form low benches in protected backwater valleys adjacent to high-energy flood coulees. Silty, sandy rhythmites contain dikes that are commonly long and slender with fills that contain delicate, pristinely preserved features (fine laminae, rip-ups, trace fossils, crisp truncations, etc.). Coarse-grained, high-energy flood channel gravels (“Pasco Gravels”) that contain little silt also contain few dikes. Dikes in flood gravels are typically crudely sheeted with low length-to-width ratios (fig. 4)





(6.8 ka). No dikes were found in Holocene deposits during this study and I am aware of no other studies from the region reporting sheeted dikes in Holocene alluvium. The dikes did not form prior to the Pleistocene or since.

Pleistocene-Holocene Liquefaction

Evidence of Pleistocene to Holocene liquefaction in the study area is sporadic and confined to tight corridors along Yakima Fold Belt structures. Foundation Sciences (1980) report liquefaction features in the Wallula fault zone at Finley Quarry, WA. The irregularly shaped features are small, trend with bedding, and their origin is disputed (Coppersmith and others, 2014; Sherrod and others, 2016). Liquefaction was not noted by Bennett and others (2016), who trenched the Burbank Fault near Yakima, WA or by Sherrod and others (2013), who opened trenches in the nearby Wenas Valley. A sparse set of thin, mud-filled dikes intrude certain fine-grained portions of the Ringold Fm in south-central Washington

Figure 4. Dike abundance and geometry differs in slackwater rhythmites vs. flood gravels. (A) Dike forms differ because fine and coarse materials respond differently to floodwater loads. Grain size governs whether pore fluid pressures will build or disperse, and whether fractures or collapses will form. (B) Dike injection appears to be primarily a slackwater phenomenon due to the necessary combination of silt deposition (low-velocity flow), overloading (deep water), and preservation (low erosion). (C) High-silt-content rhythmites (Touchet Beds) contain abundant clastic dikes with high length-to-width ratios. Dikes in gravelly flood deposits (bars) are typically stubby and crudely sheeted.

(Pasco and Othello Basins). The features are rarely thicker than a notebook, are entirely contained in Pliocene strata, are not described in detail elsewhere, and bear little resemblance to dikes of the Pleistocene set.

CLASTIC DIKES AS PALEOSEISMIC INDICATORS

Because clastic dikes are so commonly found in deformed sediments in earthquake-prone regions, data on dikes are often included in post-quake damage assessments and seismic hazard reports. Field measurements (width, length, distance from epicenter, etc.) are used to delineate the spatial extent of an earthquake's damage halo and to construct shake intensity maps. The value of such maps largely depends on the size

Age

Field relationships constrain the timing of dike injection to between ~1.5 Ma to ~14 ka, the period of ice sheet growth and Scabland flooding (Baker and others, 2016; Waitt and others, 2017). However, most injections occurred late, during the Missoula flood cycle (18–14 ka). The dikes penetrate all formations exposed to and inundated by Ice Age megafloods (fig. 5), including Late Wisconsin Missoula flood deposits, pre-Late Wisconsin scabland deposits (“ancient” flood gravels, silt diamicts, paleosols), Pliocene–Pleistocene alluvial fan gravels with thick CaCO₃ cements, Pliocene Ringold Fm basin-fill sediments, Miocene–Pliocene Ellensburg/Latah Fm sediments, and Miocene Columbia River Basalt. The dikes cut the Mount St. Helens Set S tephra (16 ka), but not the Mazama Ash



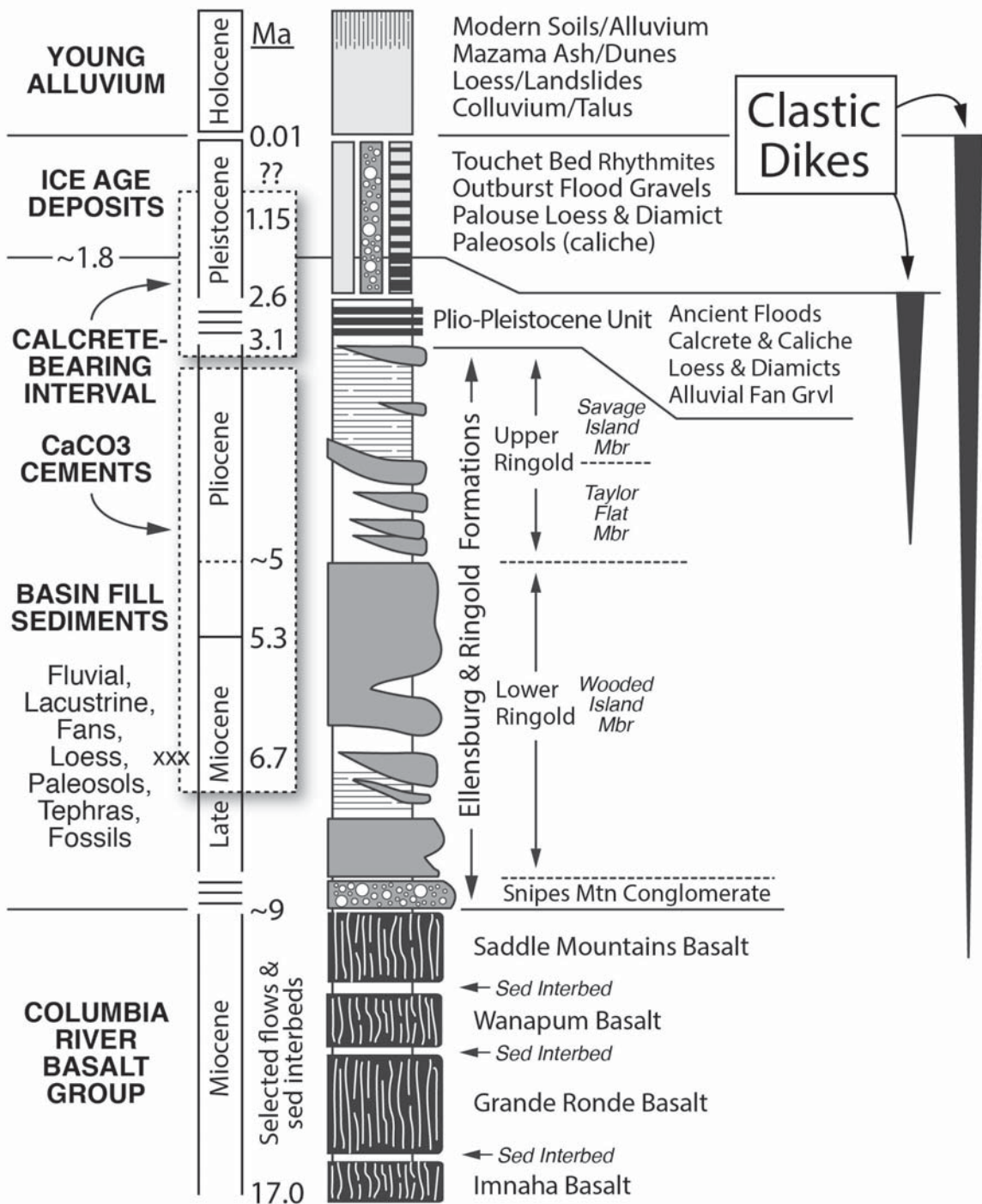


Figure 5. Sheeted clastic dikes in the Channeled Scabland are a Pleistocene phenomenon. Sheeted dikes originate in Pleistocene deposits, including both “ancient” flood deposits (>35 ka, pre-Late Wisconsin) and younger Missoula Flood deposits (<35 ka, Late Wisconsin). The vertically sheeted, wedge-shaped structures number in the tens of thousands (a conservative estimate), are visually distinctive, and occur only within the margins of the Ice Age floodway. They penetrate to many meters depth, including to basalt bedrock. Figure modified from Lindsey (1996).

of the dataset. A small number of measurements or measurements collected within a small area have low value because they lack statistical power and may underrepresent the wider effects of shaking. Standardized methods for mapping liquefaction features have been developed by USGS, state geological surveys, and consultants (Gohn and others, 1984; Atwater, 1994; Obermeier, 1996, 2009; Peterson and Madin, 1998; McCalpin, 2009; Holtzer and others, 2011).

Misinterpretation of features and relationships observed in the field can be a problem, especially for inexperienced staff or where exposures are poor. In the absence of quality exposures and observations, familiar explanations and faulty logic are too often employed, but can derail an investigation. The misguided notion that all dikes form by liquefaction, therefore all liquefaction features are earthquake-caused, has led some to conclude that all clastic dikes are seismites.



An international conference called to coordinate proper reporting with respect to the suite of features called seismites (Seilacher, 1969; Montenat and others, 2007; Van Loon, 2014) illustrates the need for caution (Feng, 2017). It seems “seimite” had been applied too liberally to features of nonseismic or ambiguous origin in journal articles, making it necessary for sites around the world touted as classic seimite localities to be reinspected. Participating geoscientists inside and outside the paleoseismology community reattributed many of the features to nonseismic processes, most commonly to rapid sedimentation and loading (Moretti and Van Loon, 2014; Shanmugam, 2016 and references therein). The following three quotes express the feelings of participants:

“Nonseismic events can create structures that are virtually indistinguishable from seismically-deformed sediments, or seismites. Therefore, paleoseismologists must correlate candidate seismites over regions and rule out nontectonic origins before concluding that an earthquake occurred.”

–L.B. Grant

“A great progress has been made in researches [SIC] of soft-sediment deformation structures (SSDs) and seismites in China. However, the research thought was not open-minded. About the origin of SSDs, it was almost with one viewpoint, i.e., almost all papers published in journals of China considered the beds with SSDs as seismites. It is not a good phenomenon.”

–Z-Z. Feng

“At present, there are no criteria to distinguish... soft-sediment deformation structures formed by earthquakes from SSDs formed by the other 20 triggering mechanisms...the current practice of interpreting all SSDs as “seismites” is a sign of intellectual indolence.”

–G. Shanmugam

MAXIMUM WIDTH METHOD INAPPROPRIATE FOR SHEETED CLASTIC DIKES

Liquefaction-extent maps prepared in the wake of damaging earthquakes are based on point data collected in the field, specifically the widths and locations of clastic dikes. The width of the widest dike is recorded at each site and the point data contoured or otherwise summarized cartographically. The “maximum width

method” is based on the recognition that seismic shaking is most intense near an epicenter and attenuates radially outward; therefore, large dikes will form in close proximity to it and smaller dikes away from it. Wider dikes indicate more lateral spreading and more intense shaking. Relationships between maximum dike width and shaking intensity are well established (Ambraseys, 1991; Galli, 2000).

The most well known example of liquefaction feature mapping is perhaps the New Madrid Seismic Zone located in the Mississippi River Valley (Fuller, 1912; Boyd and Schumm, 1995; Obermeier and others, 2005). Magnitude 7.2–8.2 quakes with Modified Mercalli Intensities >VIII struck the region in 1812, toppling structures, disrupting transportation networks, and changing local hydrology. Sand blows vented wet sediment to the surface over hundreds of square kilometers. Obermeier (1998a,b), using data from sand blows, successfully demonstrated liquefaction features can be used to determine the approximate location of a paleoepicenter.

But the USGS methodology for sand blows is inappropriate for downward-pinching, sheeted clastic dikes. The maximum width method assumes dikes are single-fill structures formed during single quakes (e.g., event structures). Measurements on composite (sheeted) dikes would not capture amount of spreading during the event that formed them, as sand blow measurements do, but the total amount of widening that took decades to millennia to develop. The data would describe two entirely different phenomena, reflect two different fracture modes, different geologic environments, and result in entirely different maps. The appropriate measurement, one that provides an apples-to-apples comparison, would be the width of the widest dike at a site (single-fill) vs. the width of the widest sheet in any dike at a site (sheeted).

SHAKING INTENSITY–LIQUEFACTION DISTANCE RELATIONSHIPS FAIL

Shallow, intraplate faults in the study area are believed capable of producing magnitude ~6.5 earthquakes and MMI VII–VIII shaking (Lidke and others, 2003). However, the dikes are found at distances far beyond the 100–125 km outer limit for soft sediment deformation established by Galli (2000; fig. 6). An epicenter placed at Finely, WA (Wallula fault zone) is located >225 km from the northernmost dikes at



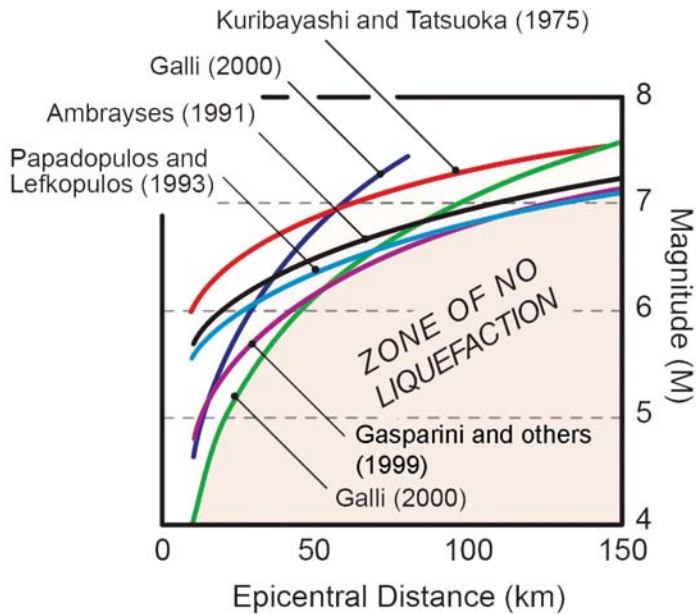


Figure 6. Magnitude–distance curves. Compiled curves from six studies by Galli (2000) show a similar relationship between earthquake magnitude and the distance away from an epicenter at which liquefaction features will form. Faults in the study area are believed capable of generating quakes as large as M6.5 (possibly up to M7.0), which corresponds with an epicentral distance limit of approximately 125 km. Many large dikes in the study area are found at distances greater than 125 km away from Yakima Fold Belt structures, the Hite fault, the Arlington–Shutler fault zone, and the Wallula fault zone.

Hunters, WA. An epicenter at Burbank Creek, WA (Umtanum–Gable Mountain fault) is >260 km from large dikes in Lewiston Basin, ID. An epicenter in the Blue Mountains (Hite fault zone) is >265 km from dikes near Granger, WA in western Yakima Valley. An epicenter placed near Arlington, OR (Arlington–Shutler fault zone) is >230 km from dikes in the central Willamette Valley. If the dikes were the products of seismic shaking, then a Yakima Fold Belt structure would be a likely candidate. However, the dikes are distributed over such a large area to attribute to a local structure (fig. 7). Seismicity at the Cascadia plate margin, located several hundred kilometers to the west, also seems far-fetched, as shaking would be greatly attenuated before reaching the Columbia Basin.

SILT SKIN SEALS FACILITATE HYDROFRACTURE

Sand-propped hydrofractures are commonly used in the petroleum industry to stimulate tight gas reservoirs, a process commonly known as fracking. Hydrofracturing is induced by shutting in the well bore and using pumps to jack up the fluid pressure inside until the formation yields and fractures propagate outward. Pressurized proppant (sand + water + chemicals)

immediately fills the fractures and holds them open, permitting hydrocarbons to flow back to the well.

The geometry of sand-propped hydrofractures closely resembles that of the natural clastic dikes found in the Channeled Scabland. Hydrofracturing was suspected by Pogue (1998), whose article summarized earlier studies that established the dikes as wedge-shaped, fracture-filling structures that penetrate to bedrock (Cooley and others, 1996; Niell and others, 1997).

Silt skins appear to have facilitated hydrofracturing of substrates during megafloods. Loading by floodwater raises fluid pressure in the formation that lasts for a period of seconds to minutes. Shallow natural weaknesses such as frost cracks, soil macropores, burrows, and joints provide nucleation planes for new fractures. During flooding, some of these become fractures that open by a few centimeters and sediment rapidly enters, dewateres, and forms a silt skin. The entering sediment is a slurry (natural proppant) sourced from the circulating flow at the base of the overriding flood. The skin-sealed crack now behaves as a pressure vessel. Continued loading of the sealed fracture raises pore fluid pressures (P_f) inside. The point at which fluid pressure exceeds the confining strength of the formation ($P_f \sim O_1$, $P_f > O_3$), breakout occurs, the fracture tip propagates, and a dike forms in the 01–02 plane (vertical). As the fluid pressure reaches equilibrium with the confining pressure ($P_f = O_3$), the tip halts, the crack completely fills, and pressure begins to build again. Each breakout causes a forward jump of the fracture tip and temporarily relieves fluid pressures in fractures. This load-crack-fill-seal cycle is responsible for the dikes' vertically sheeted fabric (fig. 8).

The direction of fracture propagation appears controlled, in part, by the orientation of older sheets and bedding (planes of weaknesses), in part by the vertically oriented water load, and in part by the orientation of the local fluid pressure gradient during overloading (inverted for downward-tapering dikes). In sand blow systems, by contrast, the pressure gradient decreases upward, toward the ground surface (free face), and the sediment that fills dikes is mobilized from *in situ* deposits at depth. While elevated pore pressure is also involved due to compaction of the source layer (pore space reduction), fluid escape proceeds in the opposite direction and forms dikes that pinch upward.



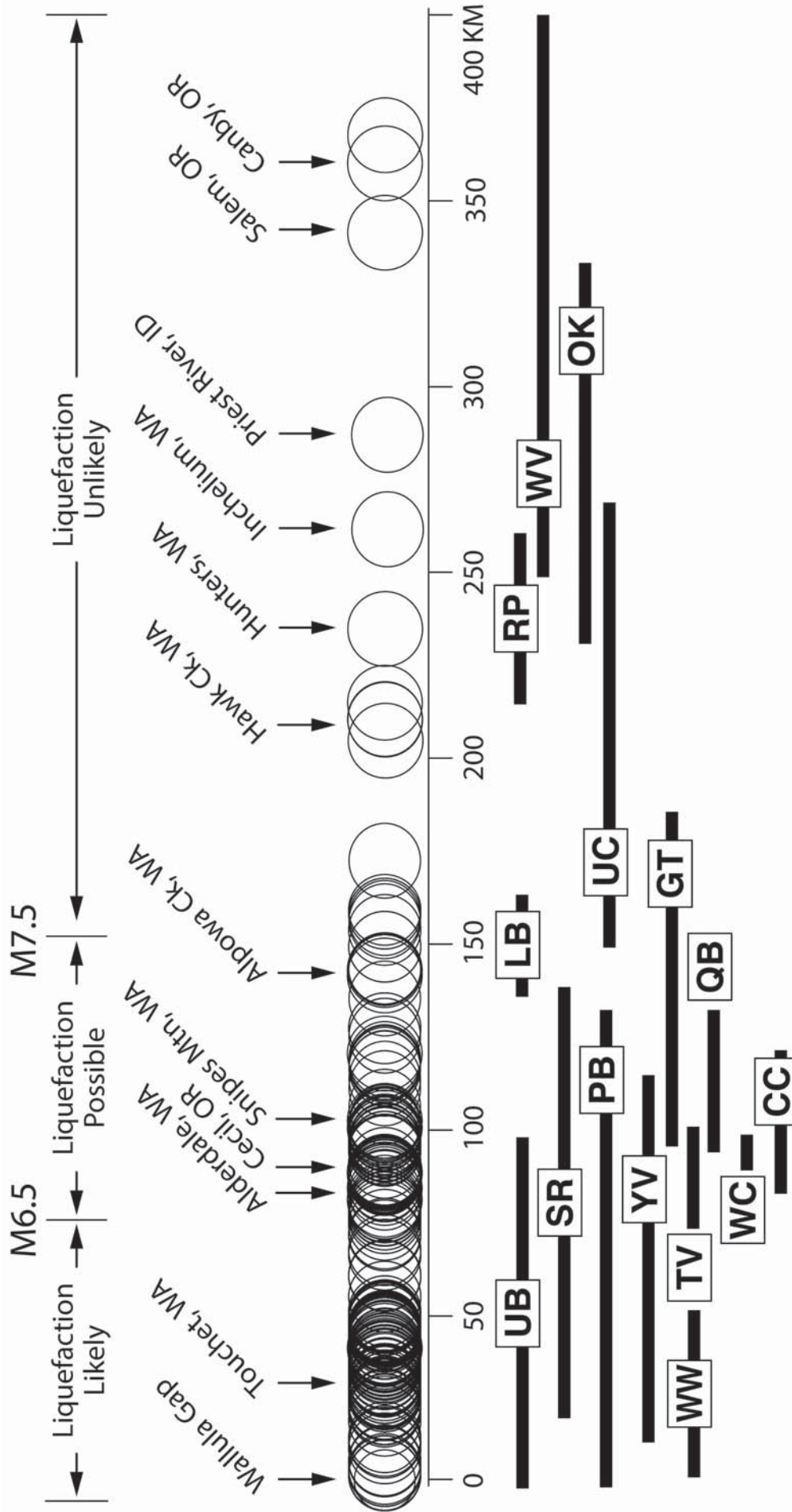


Figure 7. Distances between dike-bearing outcrops and the Wallula fault zone. Distances from outcrops containing clastic dikes (circles) were measured from an assumed epicenter located on the Wallula fault zone (Wallula Gap). Most dikes occur within 150 km of the assumed epicenter, but many occur at distances far beyond limits established by Galli (2000) for earthquake-caused liquefaction. Black bars show the span of various subbasins along the Ice Age floodway. Dikes are most abundant in valleys immediately upstream and downstream of Wallula Gap, specifically Walla Walla Valley, Pasco Basin, Umatilla Basin, and Willow Creek Valley. All megafloods flowed through these basins, formed deep, slow-draining slackwater lakes, and deposited thick sections of silty, sandy rhythmites. CC, Crab Creek Valley; GT, Gorge Tributary valleys downstream of Wallula Gap; LB, Lewiston Basin; OK, Okanogan Valley; PB, Pasco Basin; RP, Rathdrum Prairie; QB, Quincy Basin; SR, Snake River Valley; TV, Tucannon River Valley; UB, Umatilla Basin; UC, Upper Columbia River Valley; WC, Willow Creek Valley; WW, Walla Walla Valley; WV, Willamette Valley; YV, Yakima Valley.

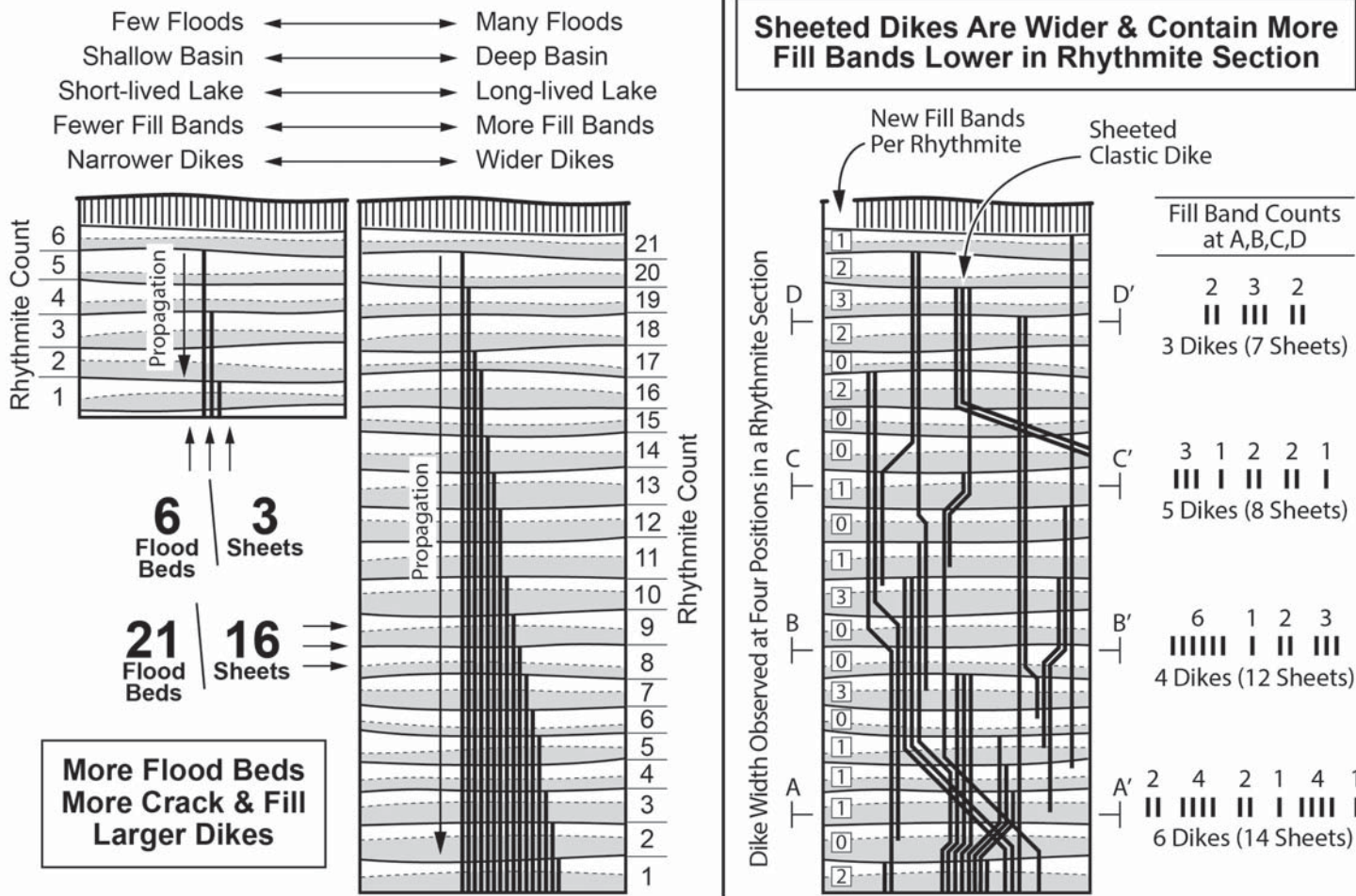


Figure 8. Flood counts and the development of vertical sheeting in the dikes. Stacks of rhythmites (Touchet Beds) deposited by Pleistocene megafloods accumulated to different thicknesses in different parts of the Channeled Scabland. Rhythmite counts vary depending on location. The most complete rhythmite sections occur in slackwater basins repeatedly filled by Lake Lewis, Lake Condon, and Lake Allison. Lake Lewis filled the Walla Walla Valley (Waitt, 1980, 1985), Lewiston Basin (Bretz, 1929; Webster and others, 1982), and Tucannon Valley (Smith, 1993). Lake Condon filled the Umatilla Valley (Benito and O'Connor, 2003), Willow Creek Valley (Cooley, 2015), and Sixmile Valley. Lake Allison filled the Willamette Valley (Glenn, 1965). Glacial Lake Columbia filled the Sanpoil Valley (Atwater, 1986), Upper Columbia Valley (Kiver and Stradling, 1982; Hanson and Clague, 2012), Latah Creek Valley (Rigby, 1982; Kiver and Stradling, 1982; Waitt, 1983; Meyer, 1999), and Foster Coulee (Russell, 1893). Rhythmites also occur in the Glacial Priest Lake basin (Walker, 1967; Breckenridge, 1989). The rhythmite count at a site approximates the flood count. All floods flowed through Wallula Gap and slackwater lakes that ponded there were the deepest anywhere in the region (>200 m). Consequently, the largest dikes occur in full rhythmite sections in the southern Pasco Basin, eastern Umatilla Basin, and western Walla Walla Valley. Fill band counts (sheet counts) record repeated flood-loading, substrate failure, and sediment injection. Sheet counts (injections) roughly scale with rhythmite counts (flood count), though a one-sheet-per-flood pattern is not robust. The count data suggest that fewer than 10 sheets form in any given dike during any given flood, depending on local conditions (flow regime, water depth, valley configuration, grain size, slackwater lake residence time, etc.). Because the dikes widened by the addition of new sediment via reinjection, their widest portions occur near the base of rhythmite stacks rather than their tops. Dikes can appear to taper upward because newer fills that tapped successively younger flood beds intruded alongside older fills, forming composite injection dikes.

Fast-moving currents in main flood channels deposited coarse-grained sediment. Suspended silt was swept downstream, making it unavailable to fill cracks. Slower-moving currents in off-channel and slackwater areas dropped their silty sediment loads, making it available to fill cracks. Dike injection appears to be primarily a slackwater phenomenon due to the necessary combination of silt deposition (low-velocity flow), overloading (deep water), and preservation (low erosion).

NONSEISMIC ANALOGS TO COLUMBIA BASIN DIKES

Per descendum clastic dikes that form by rapid overloading and hydrofracture are reported by others and appear analogous to features in this study. Sheeted, downward-pinching dikes intrude muddy deposits beneath tidewater glaciers (Von Brunn and Talbot, 1986; Jolly and Lonergan, 2002; Le Heron and Etienne, 2005; Phillips and others, 2013). Sheeted dikes with prominent silt(?) skins descend from the base of



lahar deposits on the side of an Aleutian volcano (Herriot and others, 2014). Dikes formed by hydrofracture propagate downward and laterally out of marine turbidites into their levees and distal fan-lobe complexes (Braccini and others, 2008; Cobain and others, 2016). Wedge-shaped sand dikes descend from the base of debris flow deposits at Black Dragon Canyon in the San Rafael Swell, UT (Cooley, unpublished field notes and photos). In all cases, overloading, rapid sedimentation, and hydrofracture produced clastic dikes with characteristics remarkably similar to those observed in the study area.

FIELD WORK MATTERS

The preceding examples teach a valuable lesson: when working in earthquake country, field projects should be appropriately scaled and employ methods matched to the geologic setting.

Project planning is the responsibility of the paleoseismologist. Paleoseismology is primarily a field-based discipline focused on determining the timing and effects of prehistoric earthquakes. Paleoseismic investigation results (fault slip rates, event dates, and shaking effects) are critical inputs to building codes, community planning documents, and land-use policies. Data collected in the field inform and often drive policymaking. Unlike technical trench wall logs and tables of recurrence probabilities, maps constructed from field data are easily understood by technical and non-technical audiences alike. They are uniquely influential and readily migrated into land-use policy documents, which tend to persist for decades.

Clastic dikes are ambiguous structures that do not necessarily require earthquakes to form. In fact, dikes are widely reported in a variety of geological settings where primarily nontectonic triggers operate (Shanmugam, 2016). Dikes are threshold features that, if interpreted one way, will brand a landscape as hazardous and unfit for human occupation and industrial development. Interpreted another way, the same dikes become Ice Age relicts of little importance to anyone other than academics and the odd (really odd) megaflood enthusiast. When anchored by evidence gathered at the outcrop, investigations into the origin of clastic dikes tilt toward a correct interpretation. Lab work, office-generated theories, and modeling serve geoscience and society best when they are rooted in and remain subordinate to field data.

Careful, comprehensive field work that involves a sufficient number of outcrops (samples) and a study area scaled to the geological phenomenon under investigation should be *de rigueur*. Slothful reporting on clastic dikes and other features highlighted by Shanmugam (2015), shoddy work, and methods successfully developed in one region, but uncritically applied to another (i.e., maximum width method on sheeted dikes) are unacceptable practices.

KEY CHARACTERISTICS ASSESSABLE IN THE FIELD

Three key physical characteristics of clastic dikes, (a) vertical sheeting, (b) taper direction, and (c) truncation, speak directly to dike origin and are readily assessable in the field.

- (a) **Vertical Sheeting**—Sheeting is the result of repeated fracturing and reinjection. If sheeting is present, the field geologist must ask why and endeavor to ascertain the cause. Dikes in the study area grew in staccato fashion by filling of newly opened fractures by new sheets of sediment. Sheeting in dikes found elsewhere likely records a similar pattern of reinjection along preexisting weaknesses. New sheets erode older ones; rip-ups derived from adjacent bands should be present. Small packages of parallel sheets, typically up to six or so in the case of study area dikes, commonly crosscut older packages and reveal variations in the way fractures propagate. If new sheets tap progressively younger source beds, small collapses should be present above fractures opening below. At some of my study sites, multiple collapses appear in successive rhythmites. Brief periods of active widening (floods) were separated by longer periods of inactivity (hiatus), a pattern that follows cyclic filling and spilling by proglacial lakes.
- (b) **Taper Direction**—Taper direction is strongly tied to dike origin and, whether upward or downward, must be assessed correctly, even when exposure is limited. Taper direction reveals how fractures propagate, the mode of fracture, and the orientation of the pressure gradient, and often reveals the source of dike fills. Upward-tapering dikes indicate a buried sediment source and correspond with upward fluid escape under



a normal pressure gradient. Fluid pressure in the mobilized bed exceeds the confining stress of the overburden. Downward-tapering dikes indicate downward injection within an inverted pressure gradient. Sediment from surficial materials fills descending dikes.

Downward-tapering (*per descendum*) dikes have few triggers. Where formed, the local stratigraphy will commonly contain low-pressure zones, such as openwork gravels or layers of coarse sand with abundant pore space. Such layers are resistant to compaction and cannot sustain pore pressures, thus may provide low-resistance pathways that mimic unconfined layers located near the ground surface. Coarse layers, commonly the basal portions of rhythmites, appear to control the direction of fracture tip propagation.

(c) **Truncations**—Understanding how dikes are truncated is a key to understanding how many dikes form. Truncation by bedding contacts or other surfaces is common in Touchet Bed rhythmite sections. Truncations are not just another characteristic in a checklist. Dikes with bedding-truncated tops connect the timing of deposition to the timing of injection. Tops truncated by multiple bedding contacts in a stack of rhythmites (or other strata) are powerful evidence for repeated deformation, reinjection, and feature growth over time.

CONCLUSIONS

This study documents sheeted dikes throughout a vast inland region located far from the plate margin and swept repeatedly by Ice Age megafloods. Sedimentology, age, structure, and scale of the dikes indicate they all share a common origin: repeated floodwater loading and hydrofracture. Hydrofracture was suspected by earlier workers (Baker, 1973; Pogue, 1998), but not tested. Based on the field data, I interpret the dikes as nontectonic structures. Fracture response of silty-sandy rhythmites and other substrates to repeated overloading by floodwaters best explains why, when, and where the dikes occur. Dike widths reflect local flood counts and sheeting reflects reinjection over time. Grain size contrasts between sheets is consistent with circulating bottom currents and changing sediment loads carried by numerous floods. Their

field-observable characteristics distinguish them from sand blows and related liquefaction structures formed elsewhere by strong recurrent earthquakes, strongly suggesting that clastic dikes in the megaflood region are flood injectites, not seismites.

REFERENCES

- Allison, I.S., 1941, Flint's fill hypothesis of origin of scabland: *Journal of Geology*, v. 49, p. 54–73.
- Alwin, J.A., and Scott, W.E., 1970, Clastic dikes of the Touchet Beds, southeastern Washington: *Northwest Science*, v. 44, p. 58.
- Ambraseys, N.N., 1991, Engineering seismology: *International Journal of Earthquake Structural Dynamics*, v. 17, p. 1–105.
- Atwater, B.F., 1986. Pleistocene glacial-lake deposits of the Sanpoil River Valley, northeastern Washington: *U.S. Geological Survey Bulletin* 1661, 39 p.
- Atwater, B.F., 1994, Geology of Holocene liquefaction features along the lower Columbia River at Marsh, Brush, Price, Hunting, and Wallace Island, Oregon and Washington: *U.S. Geological Survey Open-File Report* 94-209, 64 p.
- Bader, N.E., Spencer, P.K., Bailey, A.S., Gastineau, K.M., Tinkler, E.R., Pluhar, C.J., and Bjornstad, B.N., 2016, A loess record of pre-Late Wisconsin glacial outburst flooding, Pleistocene paleoenvironment, and Irvingtonian fauna from the Rulo site, southeastern Washington, USA: *Palaeogeography, Palaeoclimatology, Palaeoecology*, v. 462, p. 57–69.
- Baker, V.R., 1973, Paleohydrology and sedimentology of Lake Missoula flooding in Eastern Washington, *Geological Society of America Special Paper* 144, 79 p.
- Baker, V.R., Bjornstad, B.N., Gaylord, D.R., Smith, G.A., Meyer, S.E., Alho, P., Breckenridge, R.M., Sweeney, M.R., and Zreda, M., 2016, Pleistocene megaflood landscapes of the Channeled Scablands: *in* Lewis, R.S., and Schmidt, K.L., eds., *Exploring the geology of the Inland Northwest: Geological Society of America Field Guide* 41, 73 p.
- Beaulieu, J.D., 1974, Geologic hazards of Hood River, Wasco, and Sherman Counties, Oregon: *Oregon Department of Geology and Mineral Industries Bulletin*, v. 91, p. 18.



- Benito, G., and O'Connor, J.E., 2003, Number and size of last-glacial Missoula floods in the Columbia River valley between the Pasco Basin, Washington, and Portland, Oregon: Geological Society of America Bulletin, v. 115, p. 624–638.
- Bennett, S.E.K., Sherrod, B.L., Kelsey, H.M., Reedy, T.J., Lasher, J.P., Paces, J.B., and Mahan, S.A., 2016, History of recent surface-rupturing earthquakes on the Burbank fault, Yakima Folds, Central Washington: American Geophysical Union Fall Meeting, Abstract T41B-2908.
- Bingham, J.W., and Grolier, M.J., 1966, The Yakima Basalt and Ellensburg Formation of south-central Washington: U.S. Geological Survey Bulletin 1224-G, 15 p.
- Bjornstad, B.N., 1982, Catastrophic flood surging represented in the Touchet Beds of the Walla Walla Valley, Washington: American Quaternary Association 7th Biennial Conference Program and Abstracts, p. 72.
- Bjornstad, B.N., Fecht, K.R., and Tallman, A.M., 1990, Quaternary stratigraphy of the Pasco Basin area, south-central Washington: Rockwell International Report #RHO-BW-SA-563A, 24 p.
- Bjornstad, B.N., and Teel, S.S., 1993, Natural analog study of engineered protective barriers at the Hanford Site: Pacific Northwest Lab Report #PNL-8840 UC-510.
- Bjornstad, B.N., Fecht, K.R., and Pluhar, C.J., 2001, Long history of Pre-Wisconsin Ice Age cataclysmic floods: Evidence from southeastern Washington State: Journal of Geology, v. 109, p. 695–713.
- Bjornstad, B.N., and Lanigan, D.C., 2007, Geologic descriptions for the solid-waste low level burial grounds: Pacific Northwest National Lab Report #PNNL-16887.
- Black, R.F., 1979, Clastic dikes of the Pasco Basin, southeastern Washington: Rockwell Hanford Report #RHO-BWI-C-64, 65 p.
- Braccini, E., Boer, W., Hurst, A., Huuse, M., Vigorito, M., and Templeton, G., 2008, Sand injectites: Oilfield Review, v. 20, p. 34–49.
- Bretz, J.H., 1929, Valley deposits immediately east of the Channeled Scabland of Washington: Journal of Geology, v. 37, p. 393–427.
- Boyd, K.F., and Schumm, S.A., 1995, Geomorphic evidence of deformation in the northern part of the New Madrid seismic zone: U.S. Geological Survey Professional Paper 1538-R, p. 1–35.
- Brown, D.J., and Brown, R.E., 1962, Touchet clastic dikes in the Ringold Formation: Hanford Atomic Products Operation Report #HW-SA-2851, 11 p.
- Carson, R.J., McKhann, C.F., and Pizey, M.H., 1978, The Touchet Beds of the Walla Walla Valley, in Baker, V.R., and Nummedal, D., eds.: The Channeled Scabland: National Aeronautics and Space Administration, p. 173–177.
- Cobain, S.L., Hodgson, D.M., Peakall, J., and Shiers, M.N., 2016, An integrated model of clastic injectites and basin floor lobe complexes, implications for stratigraphic trap plays: Basin Research, v. 29, p. 816–835.
- Coppersmith, R., Hanson, K., Unruh, J., and Slack, C., 2014, Structural analysis and Quaternary investigations in support of the Hanford PSHA in Hanford Sitewide Probabilistic Seismic Hazard Analysis: Pacific Northwest National Laboratory Report #23361, 173 p.
- Cooley, S.W., 2015, The curious clastic dikes of the Columbia Basin, in Carson, R.J.: Many Waters, Natural history of the Walla Walla Valley and vicinity: Keokee Books, p. 90–91.
- Cooley, S.W., Unpublished photograph of clastic dikes descending from the base of a debris flow deposit in Black Dragon Canyon, San Rafael Swell, UT, https://commons.wikimedia.org/wiki/File:Dikes_in_black_dragon_canyon_UT.JPG [Accessed May 28, 2020].
- Cooley, S.W., Pidduck, B.K., and Pogue, K.R., 1996, Mechanism and timing of emplacement of clastic dikes in the Touchet Beds of the Walla Walla Valley, south-central Washington: Geological Society of America Abstracts with Programs, v. 28, p. 57.
- Fecht, K.R., Bjornstad, B.N., Horton, D.G., Last, G.V., Reidel, S.P., and Lindsey, K.A., 1999, Clastic injection dikes of the Pasco Basin and vicinity: Bechtell-Hanford Report #BHI-01103, 217 p.
- Feng, Z.Z., 2017, Preface of the Chinese version of “The seismite problem”: Journal of Palaeogeography, v. 6, p. 7–11.
- Flint, R.F., 1938, Origin of the Cheney–Palouse scabland tract: Geological Society of America Bulletin, v. 46, p. 169–194.



- Foundation Sciences, Inc., 1980, Geologic reconnaissance of parts of the Walla Walla and Pullman, Washington, and Pendleton, Oregon 1 x 2 degree AMS quadrangles: U.S. Army Corps of Engineers-Seattle District, Report #DACW67-80-C-0125, 144 p.
- Fuller, M.L., 1912, The New Madrid earthquake: U.S. Geological Survey Bulletin 494, 129 p.
- Galli, P., 2000, New empirical relationships between magnitude and distance for liquefaction: *Tectonophysics*, v. 324, p. 169–187.
- Glenn, J.L., 1965, Late Quaternary sedimentation and geologic history of the North Willamette Valley, OR: PhD Dissertation, Oregon State University, 248 p.
- Gohn, G.S., Weems, R.E., Obermeier, S.F., and Gelinias, R.L., 1984, Field studies of earthquake-induced, liquefaction-flowage features in the Charleston, South Carolina, area: U.S. Geological Survey Preliminary Report, 29 p.
- Hanson, M.A., Lian, O.B., and Clague, J.J., 2012, The sequence and timing of large late Pleistocene floods from glacial Lake Missoula: *Quaternary Science Reviews*, v. 31, p. 67–81.
- Herriott, T.M., Reger, C.J., Wartes, R.D., LePain, M.A., and Gillis, R.J., 2014, Geologic context, age constraints, and sedimentology of a Pleistocene volcanoclastic succession near Mount Spurr volcano, south-central Alaska: Alaska Division of Geological and Geophysical Surveys, Report of Investigation #RI-2014-2, 35 p.
- Holtzer, T.L., Noce, T.E., and Bennett, M.J., 2011, Strong ground motion inferred from liquefaction caused by the 1811–1812 New Madrid, Missouri, earthquakes: *Bulletin of the Seismological Society of America*, v. 105, p. 2589–2603.
- Hyashi, T., 1966, Clastic dikes in Japan: *Japanese Journal of Geology and Geography*, v. 37, p. 1–20.
- Jenkins, O.P., 1925, Clastic dikes of eastern Washington and their geologic significance *American Journal of Science*: v. 57, p. 234–246.
- Jolly, R.J., and Lonergan, L., 2002, Mechanisms and controls on the formation of sand intrusions: *Journal of the Geological Society*, v. 159, p. 605–617.
- Jones, F.O., and Deacon, R.J., 1966, Geology and tectonic history of the Hanford Area and its relation to the geology and tectonic history of the state of Washington and the active seismic zones of western Washington and western Montana: Douglas United Nuclear, Inc. Consultants Report #DUN-1410, 50 p.
- Kiver, E.P., Stradling, D.F., Roberts, S., and Fountain, D., 1982, Quaternary geology of the Spokane area: Tobacco Root Geological Society 1980 Field Conference Guidebook, p. 26–44.
- Le Heron, D.P., and Etienne, J.L., 2005, A complex subglacial clastic dyke swarm, Myrdalsjokull, southern Iceland: *Sedimentary Geology*, v. 181, p. 25–37.
- Lidke, D.J., Johnson, S.Y., McCrory, P.A., Personius, S.F., Nelson, A.R., Dart, R.L., Bradley, L., Haller, K., and Machette, M.N., 2003, Map and data for Quaternary faults and folds in Washington State: U.S. Geological Survey Open-file Report 03-428, 16 p.
- Lindsey, K.A., 1996, The Miocene to Pliocene Ringold Formation and associated deposits of the ancestral Columbia River system, south-central Washington and north-central Oregon: Washington Division of Geology and Earth Resources, Open-File Report 96-8, 176 p.
- Lupher, R.L., 1944, Clastic dikes of the Columbia Basin region, Washington and Idaho: *Bulletin of the Geological Society of America*, v. 55, p. 1431–1462.
- McCalpin, J.P., 2009, *Paleoseismology* (2nd ed.): Academic Press, 613 p.
- Meyer, S.A., 1999, Depositional history of pre-Late and Late Wisconsin outburst flood deposits in northern Washington and Idaho, Analysis of flood paths and provenance: Washington State University, MS Thesis, 91 p.
- Montenat, C., Barrier, P., d’Estevou, P.O., and Hibschi, C., 2007, Seismites: An attempt at critical analysis and classification: *Sedimentary Geology*, v. 196, p. 5–30.
- Moretti, M., and Van Loon, A.J., 2014, Restrictions to application of ‘diagnostic’ criteria for recognizing ancient seismites: *Journal of Palaeogeography*, v. 3, p. 162–173.



- Neill, A. R., Leckey, E.H., and Pogue, K.R., 1997, Pleistocene dikes in Tertiary rocks: Downward emplacement of Touchet Bed clastic dikes into co-seismic fissures, south-central Washington: Geological Society of America Abstracts with Programs, v. 29, p. 55.
- Newcomb, R.C., 1962, Hydraulic injection of clastic dikes in the Touchet Beds, Washington, Oregon, and Idaho: Geological Society of the Oregon Country Bulletin, v. 28, p. 70.
- Obermeier, S.F., 1996, Use of liquefaction-induced features for paleoseismic analysis: An overview of how seismic liquefaction features can be distinguished from other features and how regional distribution and properties of source sediment can be used to infer the location and strength of Holocene paleoearthquakes: Engineering Geology, v. 44, p. 1–76.
- Obermeier, S.F., 1998a, Liquefaction evidence for strong earthquakes of Holocene and latest Pleistocene ages in the states of Indiana and Illinois, USA: Engineering Geology, v. 50, p. 227–254.
- Obermeier, S.F., 1998b, Seismic liquefaction features: Examples from paleoseismic investigations in the continental United States: U.S. Geological Survey Open-file Report 98-488 (web version only), <https://pubs.usgs.gov/of/1998/of98-488>.
- Obermeier, S.F., 2009, Chapter 7: Using liquefaction-induced features for paleoseismic analysis, *in* McCalpin, J.P., ed., Paleoseismology: Academic Press, p. 497–564.
- Obermeier, S.F., Martin, J.R., Frankel, A.D., Youd, T.L., Munson, P.J., Munson, C.A., and Pond, E.C., 1993, Liquefaction evidence for one or more strong Holocene earthquakes in the Wabash Valley of southern Indiana and Illinois, with a preliminary estimate of magnitude: U.S. Geological Survey Professional Paper 1536, 27 p.
- Obermeier, S.F., Olson, S.M., and Green, R.A., 2005, Field occurrences of liquefaction-induced features: A primer for engineering geologic analysis of paleoseismic shaking: Engineering Geology, v. 76, p. 209–234.
- Peterson, C.D., and Madin, I.P., 1998, Coseismic paleoliquefaction evidence in the central Cascadia margin, USA: Oregon Geology, v. 59, p. 51–74.
- Phillips, E., Lipka, E., and van der Meer, J.J., 2013, Micromorphological evidence of liquefaction, injection and sediment deposition during basal sliding of glaciers: Quaternary Science Reviews, v. 81, p. 114–137.
- Pogue, K.R., 1998, Earthquake-generated(?) structures in Missoula flood slackwater sediments (Touchet Beds) of southeastern Washington: Geological Society of America Abstracts with Programs, v. 30, p. 398–399.
- Pritchard, C.J., and Cebula, L., 2016, Geologic and anthropogenic history of the Palouse Falls area: Floods, fractures, clastic dikes, and the receding falls, *in* Lewis, R.S., and Schmidt K.L., eds.: Geological Society of America Field Guide, v. 41, p. 75–92.
- Rigby, J.G., 1982, The sedimentary, mineralogy, and depositional environment of a sequence of Quaternary catastrophic flood-derived lacustrine turbidites near Spokane, WA: University of Idaho, MS Thesis, 132 p.
- Russell, I.C., 1893, A geological reconnaissance in central Washington: U.S. Geological Survey Bulletin 108, 108 p.
- Seilacher, A., 1969, Fault-graded beds interpreted as seismites: Sedimentology, v. 13, p. 155–159.
- Shanmugam, G., 2016, The seismite problem: Journal of Palaeogeography, v. 5, p. 318–362.
- Shaw, J., Munro-Stasiuk, M., Sawyer, B., Beaney, C., Lesemann, J., Musacchio, A., Rains, B., and Young, R.R., 1999, The Channeled Scabland: Back to Bretz?: Geology, v. 27, p. 605–608.
- Sherrod, B.L., Barnett, E.A., Knepprath, N., and Foit, F.F., Jr., 2013, Paleoseismology of a possible fault scarp in Wenas Valley, central Washington: U.S. Geological Survey Scientific Investigations Map 3239.
- Sherrod, B., Blakely, R.J., Lasher, J.P., Lamb, A.P., Mahan, S.A., Foit, F.F., and Barnett, E., 2016, Active faulting on the Wallula fault zone within the Olympic-Wallowa lineament, Washington State, USA: Geological Society of America Bulletin, v. 128, p. 1636–1659.
- Silver, M.H., and Pogue, K.R., 2002, Analysis of plan-view geometry of clastic dike networks in Missoula Flood slackwater sediments (Touchet Beds), southeastern Washington: Geological Society of America Abstracts with Programs, v. 34, p. 24.



- Smith, G., 1993, Missoula flood dynamics and magnitude inferred from sedimentology of slack-water deposits on the Columbia Plateau: Geological Society of America Bulletin, v. 105, p. 77–100.
- Spencer, P.K, and Jaffee, M., 2002, Pre-late Wisconsinan glacial outburst floods in southeastern Washington, the indirect record: Washington Geology, v. 30, p. 9–16.
- Van Loon, A.T., 2014, The Mesoproterozoic “seismites” at Laiyuan (Hebei Province, E China) reinterpreted: *Geologos*, v. 20, p. 139–146.
- Von Brunn, V., and Talbot, C.J., Formation and deformation of subglacial intrusive clastic sheets in the Dwyka Formation of northern Natal, South Africa: *Journal of Sedimentary Research*, v. 56, p. 35–44.
- Waitt, R.B., 1980, About forty last-glacial Lake Missoula jokulhlaups through southern Washington: *Journal of Geology*, v. 88, p. 653–679.
- Waitt, R.B., 1983, Tens of successive, colossal Missoula floods at north and east margins of Channeled Scabland: Friends of the Pleistocene Rocky Mountain Cell Guidebook for the 1983 Field Conference, 29 p.
- Waitt, R.B., 1985, Case for periodic, colossal jokulhlaups from Pleistocene glacial Lake Missoula: *Geological Society of America Bulletin*, v. 96, p. 1271–1286.
- Waitt, R.B., Breckenridge, R.M., Kiver, E.P, and Stradling, D.F., 2017, Chapter 17: Late Wisconsin Cordilleran Ice Sheet and colossal floods in northeast Washington and Northern Idaho, *in* Cheney, E.S., ed., *The Geology of Washington and Beyond, from Laurentia to Cascadia*: University of Washington Press, p. 233–256.
- Walker, E.H., 1967, Varved lake beds in northern Idaho and northeastern Washington: U.S. Geological Survey Professional Paper 575-B, p. 83.
- Ward, A., Conrad, M.E., Daily, W.D., Fink, J.B., Freedman, V.L., Gee, G.W., Hoverston, G.M., Keller, M.J., Majer, E.L., Murray, C.J., White, M.D., Yabusaki, S.B., and Zhang, Z.F., 2006, Vadose zone transport field study summary report, U.S. Department of Energy Report DE-AC05-76RL01830, 288 p.
- Woodward-Clyde Consultants, 1981, Task D3: Quaternary sediments study of the Pasco Basin and adjacent areas: Report to Washington State Public Power Supply System, 33 p.





FURTHER SPECULATION ON BELT STRATIGRAPHY AND STRUCTURE AROUND SALMON, IDAHO: ALTERNATIVE INTERPRETATIONS AND TESTS

Russell F. Burmester,¹ Jeffrey D. Lonn,² and Reed S. Lewis³

¹*Geology, Western Washington University*

²*Montana Bureau of Mines and Geology*

³*Idaho Geological Survey, University of Idaho*

ABSTRACT

Understanding the stratigraphy and structure of the Lemhi subbasin continues at a glacial pace despite global warming, but it progresses. Observations of the Apple Creek Formation in the Salmon River Mountains prompted us to favor the interpretation that the Freeman thrust carries fine-grained western facies Apple Creek strata over coarser grained, eastern facies Apple Creek Formation to the north and east. However, the nature of the North Fork fault and the identity of the rocks between it and the Diamond Creek fault remain uncertain. One possibility is that all rocks in between are also Apple Creek, but higher in the section than on the Freeman plate, requiring that the Diamond Creek fault is Gunsight Formation against Apple Creek despite similarity of lithologies and attitudes across the fault. An alternative is that all rocks between are Gunsight, with the North Fork fault being between them and the Apple Creek of the Freeman plate. Problems with this interpretation include young detrital zircon ages from those rocks near Lemhi Pass, and lack of evidence for large displacement between them and Lawson Creek Formation rocks across the Cow Creek fault. A third option, which combines the first two with a break across a gap in continuity of the rocks and faults, has mixed benefits and remaining problems. Some of the problems might be resolved with more isotopic ages from zircons and garnets in critical places.

INTRODUCTION

Our paper for the 2017 TRGS Leadore meeting (Burmester and others, 2017) proposed some changes to unit calls on the Salmon 30' x 60' map (Burmester and others, 2016a), but did not explore structural implications. Figure 1 shows the regional geology as proposed in 2017 with an insert from the 2016 publication. Figure 2 shows stratigraphic columns for the

three mountain ranges around Salmon. Points made in the 2017 paper were: (1) correlations on our early 7½' maps of the Beaverhead Mountains were based on stratigraphy of the type section of the Lemhi Group in the Lemhi Range southwest of Leadore; (2) our revised stratigraphy (Burmester and others, 2016b; Lonn, 2017) cast some of these early correlations in doubt; and (3) the Beaverhead Mountains contain a nearly complete section of Lemhi subbasin strata with negligible fault disruption, including the banded siltite member of the Apple Creek Formation, which we had earlier correlated with the Yellow Lake Formation of the Lemhi Group. Lack of a sharp contrast in lithology across the Brushy Gulch/Diamond Creek fault had led to continuation of the Gunsight Formation in the Salmon River Mountains clockwise around the Salmon basin to and south of the Lemhi Pass fault in the Beaverhead Mountains (YI?, fig. 1 insert). We also noted that strata south of the Lemhi Pass fault include chert and anomalously large round quartz grains, more consistent with units above the Swauger than below. This led us to propose that bedrock between the Diamond Creek and Freeman faults might be Apple Creek Formation (fig. 1). Not emphasized were the characteristics of the faults, or the young zircon ages from some of the units. Below we will review the faults and ages, explore what rocks might be on the different thrust plates, suggest how young rocks got “under” the Gunsight Formation, and offer tests for alternative solutions.

A PROBLEM: LOOK-ALIKE UNITS AND LATERAL VARIATION

The Lake Mountain and Trapper Gulch members of the Apple Creek Formation are similar to the Gunsight Formation in being dominated by parallel- or flat-laminated, very feldspathic quartzite. Rocks in both the hanging wall and footwall of the Poison Creek thrust southwest of Salmon (fig. 3) were all

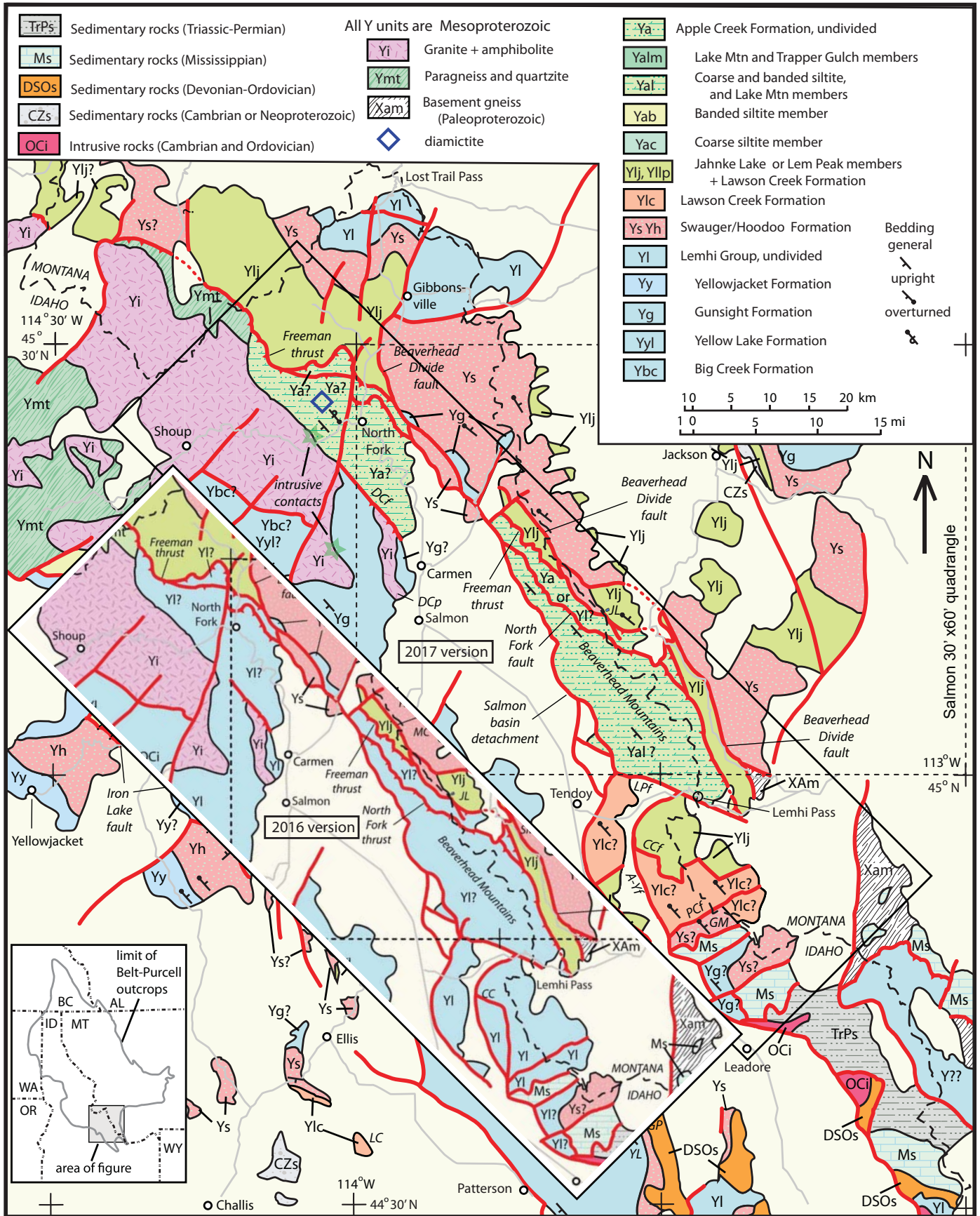


Figure 1. Regional geology around Salmon, Idaho as of 2017, with insert showing previous 2016 version. Some Apple Creek Formation member labels on map explanation omit "a" to save space. Some units in the explanation are hidden by the insert. For type or reference sections, units are in parentheses after location letter codes: A-Yf, Agency-Yearian fault; CCf, Cow Creek fault; DCf, Diamond Creek fault; DCp, Diamond Creek pluton; GM, Goat Mountain; GP, Gunsight Peak (Yg); JL, Jahnke Lake (Yalj); LC, Lawson Creek (Ylc); PCf, Peterson Creek fault; YL, Yellow Lake (Yyl). Stars mark known intrusive contacts of Mesoproterozoic granite with Gunsight and possible Apple Creek Formation strata. Diamonds on all maps approximate diamicrite locations that we have visited.



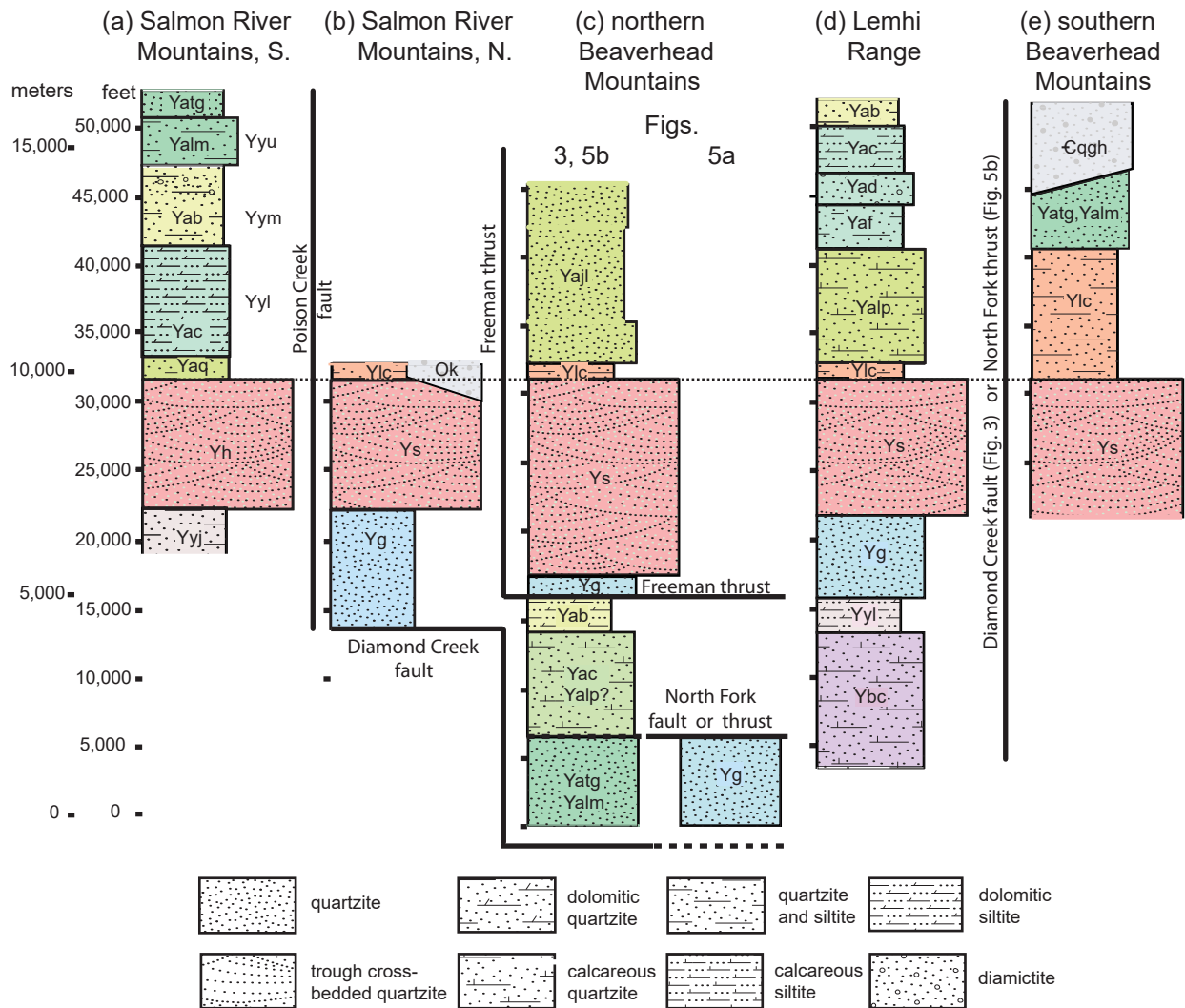


Figure 2. Stratigraphic columns for Salmon River Mountains southwest (a) and northeast (b) of the Poison Creek thrust, Lemhi Range (d), and Beaverhead Mountains north (c) and south (e) of the Lemhi Pass fault. For (a), backsliding on the Iron Lake fault (about Yac/Yh contact) is assumed to make net stratigraphic throw negligible. (a) Includes units from Connor and Evans (1986). Both (a) and (d) are south of the Poison Creek fault (figs. 1, 3, 5a, 5b), so lack of lateral continuity of the Apple Creek Lem Peak, fine siltite, and diamictite members may reflect locally restricted environments of deposition. Alternatives under (c) are for dominant normal motion on the North Fork fault dropping higher Apple Creek members to the southwest (figs. 3, 5b), or thrust motion placing Gunsight over the Freeman plate (fig. 5a). In (e), the quartzite of Grizzly Hill (Cqgh; Lonn and others, 2019) is considered to be Cambrian. Apple Creek Formation (Ya) members are Trapper Gulch (tg), Lake Mountain (lm), banded siltite (b), coarse siltite (c), diamictite (d), fine siltite (f), Lem Peak (lp). Column (a) also shows earlier notations for Yellowjacket Formation upper (u), middle (m) and lower (l) units. Below are Lawson Creek Formation (Ylc), argillaceous quartzite (Yaq), Hoodoo quartzite (Yh), Swauger Formation (Ys), and Lemhi Group Formations Gunsight (Yg), Yellow Lake (Yyl), and Big Creek (Ybc).

mapped as the upper unit of the Yellowjacket Formation by Connor and Evans (1986). The rocks in the hanging wall at Lake Mountain were previously mapped as Gunsight Formation of the Salmon River Mountains by Tysdal (2003) and Evans and Green (2003) but are the Lake Mountain member of the Apple Creek Formation in our current view. Those in the footwall are below the Swauger Formation, therefore Gunsight (fig. 2).

There also is considerable variety in lithologies within any given unit across the region. Figure 2 contrasts the finer grained Apple Creek members of

the Salmon River Mountains and Lemhi Range with the coarser grained members in the Beaverhead Mountains. This lateral variation, reflected in difference in grain size and bedding style, is the basis of our contention that the Trail Gulch–Freeman thrust telescoped strata from distal environments of deposition. It also shows lateral discrepancies in the Apple Creek members between the adjacent Salmon River Mountains and Lemhi Range, which underscores the difficulty in identifying units based on lithology alone.



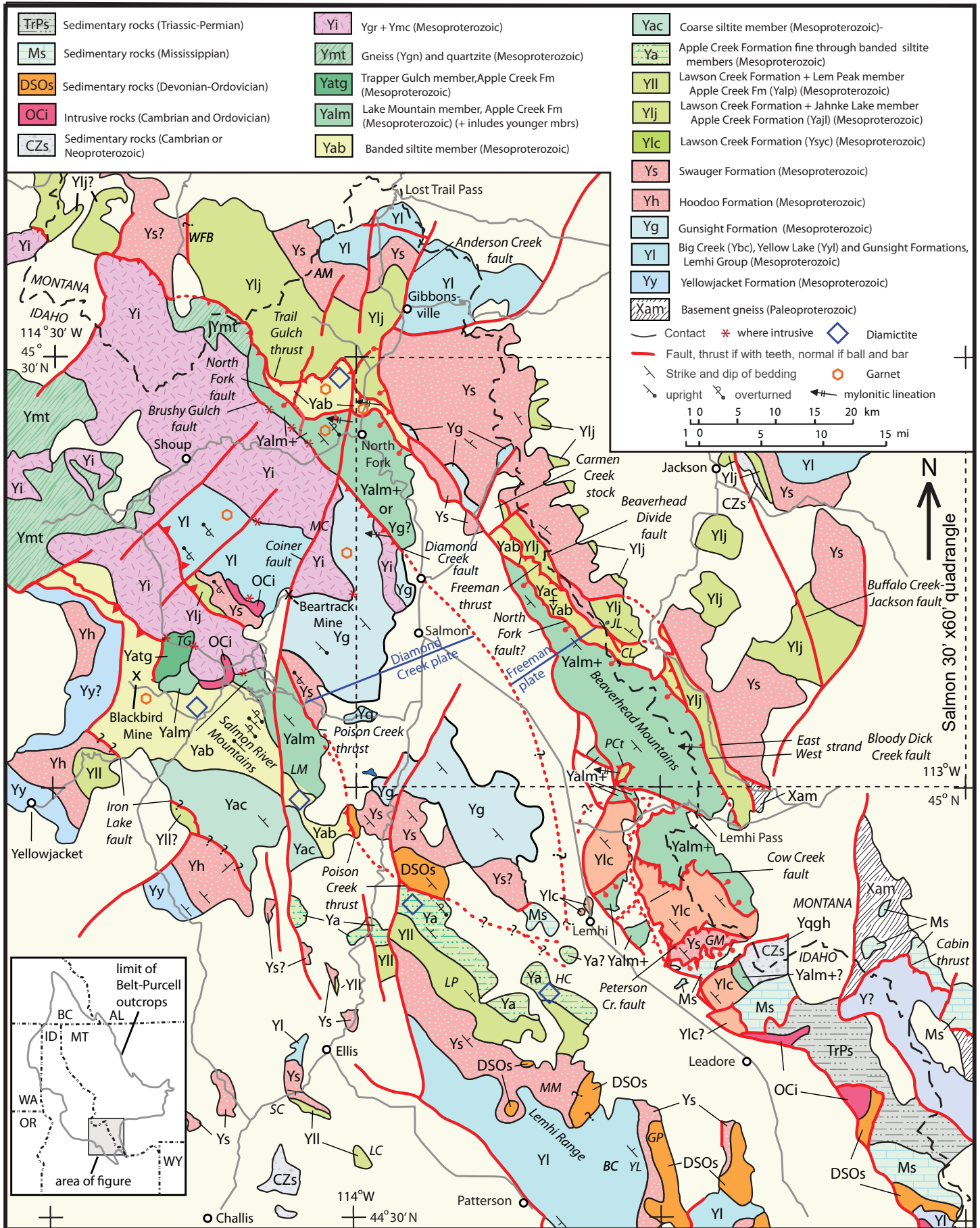


Figure 3—Caption on facing page.



THE FAULTS

Trail Gulch–Freeman Thrust

The Freeman thrust, where named in the Homer Youngs Peak quadrangle northeast of Salmon (Lonn and others, 2008), dips moderately to gently southwest, is mylonitic, and appears to have had reverse movement. It places siltite and argillite over feldspathic quartzite. To the southeast, carbonate-bearing quartzite is in the hanging wall before the fault merges with the west strand of the Beaverhead Divide fault. To the northwest, the fault is intruded by the Carmen Creek stock, beyond which the hanging wall rocks are garnetiferous, phyllitic siltite, and argillite. That portion through the Ulysses Mountain quadrangle northwest of North Fork was renamed the Trail Gulch thrust (Lewis and others, 2019) because of concerns in 2017 that the diamictite-bearing banded siltite member of the Apple Creek Formation in the hanging wall was not the same unit as to the southeast. In contrast to the garnetiferous, faulted and folded hanging wall rocks are greenschist facies quartzite, siltite, and minor argillite of the footwall. That contrast continues to the northwest, at least to the northwest corner of figure 3. The southwest side of an unnamed fault at the state line is quartzofeldspathic gneiss and quartzitic schist that hosts augen gneiss and metagabbro (Berg and Lonn, 1996). Juxtaposition of these intruded and garnetiferous rocks against greenschist facies Apple Creek strata to the northeast must have postdated garnet growth about 1.15 Ga (Lewis and others, 2019).

North Fork Fault

The North Fork fault north of North Fork (Lonn and others, 2013) juxtaposes thin- to thick-bedded siltite and very fine-grained quartzite over the thinly bedded garnet-bearing phyllite of the Trail Gulch–Freeman plate. It dips moderately to gently southwest and exhibits mostly brittle deformation around North Fork. Lineations or definitive shear sense indicators could not be found in outcrop there. Similar footwall

and hanging wall rocks are found on opposite sides of an unnamed thrust southeast of the Carmen Creek stock through the Bohannon Spring quadrangle (Lewis and others, 2009b) and Goldstone Pass quadrangle (Lonn and others, 2009). Mylonite float and east-vergent folding there support thrust motion of west-facing quartzitic hanging wall rocks over east-facing finer grained strata. Evans (1993, unpublished) observed the same, although he placed the fault west of orangish-weathering, carbonate-bearing quartzite. Structural style changes to the southeast. West of Cowbone Lake (CL, fig. 3), more brittle deformation and quartz veining may indicate later normal motion there and to the southeast. The same lithologic boundary is shown on the Kitty Creek map north of Lemhi Pass (Lewis and others, 2009a) as a normal fault that is down on the west. Mostly brittle deformation near North Fork may indicate normal motion there as well. The hanging wall rocks west of North Fork contain garnet; juxtaposition of rocks across the North Fork fault may have been before garnet growth if the age of garnets to the southwest also is about 1.15 Ga.

Diamond Creek–Brushy Gulch Fault System

On the northeast side of the Diamond Creek pluton, the Diamond Creek fault is characterized by mylonitic rock (Lund and others, 2003; Burmester and others, 2012). The pluton on its southwest side and its country rock there (Gunsight Formation) have more widely distributed mylonite zones. Float of mylonite is distributed discontinuously to the northwest, although it is not necessarily exclusively from the Diamond Creek fault. West of North Fork and south of the Salmon River, the igneous–metasediment contact is a narrow zone of transition between undeformed megacrystic granite through augen gneiss to mylonite, similar to the Diamond Creek fault in places, but across the river to the north, contacts of the Mesoproterozoic igneous rocks are intrusive with metamorphic aureoles (Lewis and others, 2019). If the Diamond Creek fault is part of a throughgoing fault system that includes

Figure 3. Pre-Mesozoic bedrock geology around Salmon, Idaho. The coarsest clastic unit (Ys and Yh) separates lower formations of the Lemhi Group from higher Lawson Creek and Apple Creek Formations. Some units are combined where scale or previous mapping makes separating them impractical. Geographic locations are in italics; type or reference sections have units in parentheses: AM, Allan Mountain; BC, Big Creek (Ybc); CL, Cowbone Lake; GM, Goat Mountain; GP, Gunsight Peak (Yg); HC, Hayden Creek (Ya); JL, Jahnke Lake (Yajl); LC, Lawson Creek (Ylc); LM, Lake Mountain (Yalm); LP, Lem Peak (Yalp); MC, Moose Creek; MM, Mogg Mountain (Ys); TG, Trapper Gulch (Yatg); WFB, West Fork Bitterroot River; YL, Yellow Lake (Yyl). Trail Gulch thrust from Lewis and others (2019); Freeman and North Fork thrusts from Lonn and others (2016); Pattee Creek thrust (PCT) from Lewis and others (2011); Coiner fault term usage from American Gold Resources Corporation (Watts, Griffis and McOuat Ltd., 1989); other named faults from Evans and Green (2003). After Burmester and others (2017), figure 1b. Modified to include the Trapper Gulch and possibly higher members of the Apple Creek Formation (Yalm+) between the Diamond Creek and North Fork faults, and to accommodate new mapping north of Leadore (Lonn and others, 2019; Lewis and others, in press, Goat Mountain) and in the Salmon River Mountains.



the Brushy Gulch fault, some faults in that system, possibly as multiple strands or mylonite zones, must be within the plutons or yet to be found outside of the contact aureole.

Poison Creek Fault System

Hansen (2015) detailed the thrust part of this system east and west of the Salmon River and established that the Cretaceous thrusts partly reversed displacement on a large pre-Ordovician, possibly Proterozoic, normal fault that dropped the southwest (in present coordinates) hanging wall block down and tilted the footwall block to the northeast. Incomplete recovery of the normal motion left Apple Creek strata on the southwest against Paleozoic strata (Saturday Mountain Formation and Kinnikinic Quartzite) that unconformably overlie Swauger Formation in the footwall (Hansen, 2015; Hansen and Pearson, 2016). Across the angular unconformity, the Swauger Formation dips less steeply to the southwest by 15 to 30 degrees than overlying Kinnikinic Quartzite. Untilting the Mesoproterozoic section (fig. 4a) so Kinnikinic is horizontal restores the Mesoproterozoic rocks to have a northeast dip of 15 to 30 degrees (Hansen, 2015) during erosion prior to early Paleozoic deposition (fig. 4b). At that time, strata would have younged to the northeast, so strata above the Swauger would be preserved. If the dip were only 15 degrees, crossing 20 km horizontally from the top of the Swauger at that time would expose a 5 km section of Lawson Creek and Apple Creek Formations. Implications of this reconstruction will be revisited below. Hansen (2015) proposed that the present steep attitudes of the Poison Creek fault and adjacent strata are due to thrusting structurally below the Poison Creek thrust, most likely “the Brushy Gulch fault and the North Fork and Freeman thrusts.”

The similarity of attitudes of strata across the Diamond Creek–Brushy Gulch fault would be fortuitous if it were responsible for the back rotation of the hanging wall. If the North Fork fault is a Cretaceous thrust, it could be responsible for the back rotation. The Freeman (Trail Gulch) thrust to the north has the greatest contrast in lithology and metamorphism of the three, and although exposures in the Ulysses Mountain quadrangle show that it is shallowly dipping there, a ramp to the south could have produced back rotation of strata farther south. Back rotation of the Poison Creek footwall block during in-sequence thrust faulting may have led to the present opposite facing of fault blocks

on either side (fig. 3). This contrast in attitude and stratigraphic level continues to the northwest of the Coiner fault where the northeast- and southwest-facing blocks are separated by Mesoproterozoic plutons that have intrusive contacts with both sides (fig. 3). The southwest-directed thrust west of the Beartrack mine also may be a product of the back rotation. Neither Neoproterozoic normal nor northeast-directed Cretaceous thrust faults within the intrusions is obvious, leading to speculation here that normal faulting accompanied and was obscured by the igneous activity.

Mylonite lineations and kinematic indicators show that motion on the Trail Gulch thrust, Diamond Creek fault, west strand Bloody Dick Creek fault, and Pattee Creek thrust window was tops slightly south of east (symbols, fig. 3). This suggests that all were part of the same contractional system. If so, the system likely was active in the Cretaceous based 115–103 m.y. biotite-whole-rock Rb-Sr isochrons of the Diamond Creek pluton near Salmon (DCp, fig. 1; Evans and Zartman, 1990). Most of the obliqueness of the fault traces relative to transport direction was probably inherited from earlier faults, similar to the Poison Creek thrust (Hansen, 2015). East–west portions, such as across the Ulysses Mountain quadrangle northwest of North Fork, are likely lateral ramps.

Cow Creek Fault

Although lack of evidence for east-directed motion on the Cow Creek fault near Lemhi Pass is not evidence against Cretaceous motion, it allows speculation that the Cow Creek fault is older. Nowhere along the Cow Creek fault is there mylonite, breccia, or fault gouge marking its trace or kinematics. It appears to be offset by a pre-Eocene thrust (Burmester and others, 2018). Furthermore, REE-Th mineralization (e.g., Gillerman, 2008) pervades rocks on both sides, consistent with them being in close proximity during the Cambrian and not juxtaposed during Cretaceous contraction. Juxtaposition of Gunsight against Lawson Creek along the Cow Creek fault requires omission of at least Swauger, yet we found no trace of Swauger along it, or fault rocks in proportion to implied slip. This and apparently old deformation in adjacent rocks led us to speculate that motion was very early, with evidence obliterated during later deformation. But if the rocks to the north are Apple Creek, there is no need for large or Cretaceous displacement.



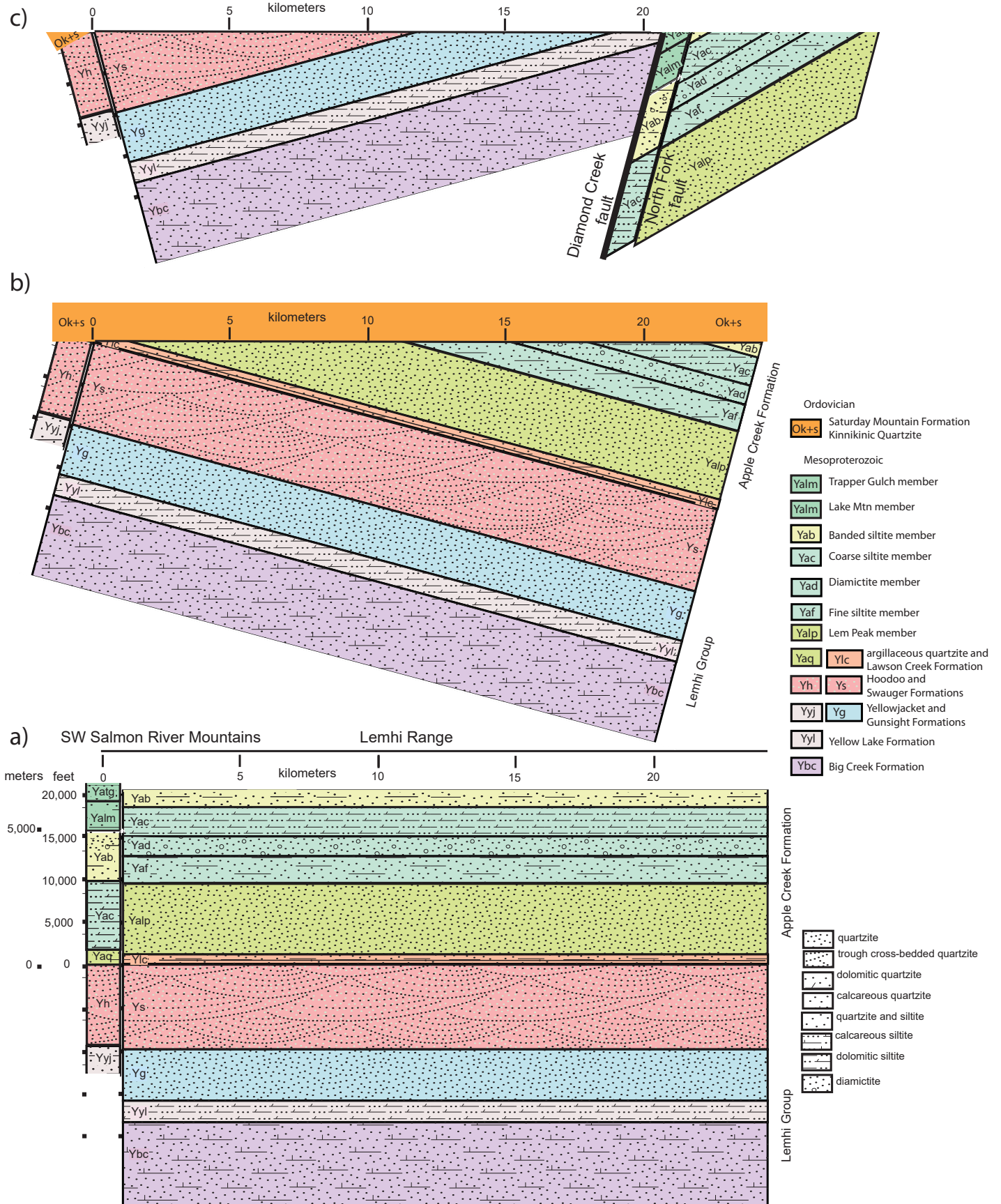


Figure 4. Cartoon of tilt history of Poison Creek footwall: (a) shows southwest Salmon River Mountains and Lemhi Range sections (figs. 2a, 2b), with the latter projected 25 km to imagine what the complete section of the footwall could have been. (b) Sections in (a) tilted 15 degrees, eroded, and unconformably overlain by Paleozoic strata. (c) Section in (b) back tilted and eroded, and relatively uplifted against Apple Creek strata in the footwall of the Diamond Creek fault for map pattern in figure 3. For figure 5, the Diamond Creek fault would replicate part of the Gunsight and displacement of Gunsight over Apple Creek would be on the North Fork thrust, but only west of the gap in 5b.



A CASE FOR OLD FAULTS

Ages of Lemhi subbasin units are close to those of Mesoproterozoic intrusions. Even the lowest unit, the Big Creek Formation (fig. 2), has five concordant detrital zircon grains less than 1400 Ma (11 from 1399 to 1422 Ma; Jesse Mosolf, written commun., 2018), establishing that as its maximum depositional age. The likely Swauger of Goat Mountain (GM; fig. 3) contains a tuff that yielded an age of 1385.4 ± 9.3 Ma (Jesse Mosolf, written commun., 2018). This is insignificantly different from the age of the oldest granite dated (1383 ± 4 ; Aleinikoff and others, 2012). Thus rapid subsidence of the Lemhi subbasin, growth faults in the Apple Creek of the Salmon River Mountains (Hahn and Hughes, 1984), and possibly deformation and metamorphism before some intrusions (Evans and Zartman, 1990; references therein) could be products of tectonic unrest that led to protracted A-type magmatism. The three young detrital zircon ages (1375–1371 Ma; Gillerman, 2008) from both sides of the Lemhi Pass fault are within the age range of the intrusions and similar to age of migmatization along the Salmon River (1370 ± 2.2 Ma; Doughty and Chamberlain, 1996). The youngest intrusion is 1359 ± 7 Ma (Aleinikoff and others, 2012). With such a large range of magmatism there was abundant time for deformation during igneous activity, and it may be difficult to prove how much of the faulting near the intrusions dates from then or later. Some deformation likely accompanied subsidence; burial depth east of Shoup increased from 14 to 20 km during prograde metamorphism (Doughty and Chamberlain, 1996). The originally proposed explanation was burial of the Prichard Formation country rock by the rest of the Belt (Doughty and Chamberlain, 1996). This rationalization does not work if the country rock is not Prichard (Winston and others, 1999) low in the Belt Supergroup, but is near the top and much younger than the 1460 Ma Prichard (Aleinikoff and others, 2015). Instead, subsidence could be due to magma loading (Brown and Burmester, 1991; Brown and McClelland, 2000). If so, perhaps higher-level magmas erupted and blanketed the region with tuff of the same age, e.g., in the Goat Mountain Swauger section, or contributed young zircons to the rock near Lemhi Pass. An implication of this coincidence of ages of magmatism and deposition is that Mesoproterozoic magmatism did not mark the end of Belt deposition, but coincided with late development of at least the Lemhi subbasin. Alternatively,

the overburden might have been emplaced tectonically, despite conventional wisdom that A-type magmas reflect extensional environments. The observation that metamorphic grade and deformation generally increases to the north in and near the Mesoproterozoic intrusions documents that there was greater uplift and erosion there, possibly of that overburden.

WHAT ROCKS ARE IN THE DIFFERENT THRUST PLATES?

Trail Gulch–Freeman Plate

Diamictite in the Trail Gulch thrust plate northwest of North Fork got this ball rolling and led to the 2017 paper and the proposed disconnect with the Freeman plate to the southeast. We hope that a reevaluation of rocks will reunite the two. Around Cowbone Lake (CL, fig. 3) in the Goldstone Pass quadrangle (Lonn and others, 2009), two units were characterized as carbonate bearing, with carbonate as cement in some. One unit contains fine- to rarely medium-grained feldspathic quartzite (40–56% feldspar) with appreciable magnetite in places. The other unit was described as siltite and argillite as distinct, laterally discontinuous laminae and graded couplets with pygmatically folded silt in non-polygonal “crinkle cracks,” and decimeter-scale quartzite that displays hummocky and thin ripple cross lamination, loads, and convolute bedding. Correlations suggested for those units were with the Big Creek and West Fork Formations above the Inyo Creek Formation at the bottom of the Lemhi Group as described at that time (Ruppel, 1975). Non-fault contacts between the two on the 2016 map are consistent with the siltite and argillite unit being above the quartzite in a faulted syncline. If the West Fork and Inyo Creek are fault repetitions of the Yellow Lake (Lonn, 2017), correlation with the Lemhi Group would be Yellow Lake above Big Creek. The 2016 Salmon map also shows Gunsight higher still, east of Cowbone Lake, consistent with Lemhi Group stratigraphy. But is it really Lemhi Group?

Uneven graded siltite and argillite couplets with crinkle cracks and hummocky cross lamination are more abundant in the banded siltite in the Cobalt quadrangle southwest of Salmon than in the Yellow Lake/West Fork rocks that we have seen. Carbonate concentrations were mapped in the banded siltite southeast of Cobalt (Connor and Evans, 1986), and carbonate is known lower in the Apple Creek in the coarse siltite and Lem Peak members in the Lemhi



Range (Tysdal, 2000; Big Creek north of the Lem Peak fault, our reconnaissance), and Lawson Creek Formation (our reconnaissance, Lemhi Range). We did not know until recently that Karl Evans had recognized rocks on the ridge west of Cowbone Lake as similar to the banded siltite of the Salmon River Mountains. The banded siltite south of Lake Mountain grades up through a zone of intense soft sediment deformation into quartzite, which Tysdal (2003) called Gunsight Formation. Evans (1996, unpublished) noted the same characteristics west of Cowbone Lake. The simplest resolution is that rocks between the North Fork fault to the west and the Freeman thrust are these Apple Creek members. However, we know from our work and that of others in the main Belt basin that carbonate varies widely within mapped lithostratigraphic units so should not be taken as essential for a correlation. Magnetite also is not essential for correlation but is common in at least the coarse siltite member of the Apple Creek Formation in the Lemhi Range (Tysdal, 2000) and in the Salmon River Mountains (our reconnaissance).

Also plausible is that the strata between the North Fork fault and Freeman thrust (and its southward continuation as the West Strand Beaverhead Divide fault) continue northwest across a gap of exposure (Carmen Creek stock and detachment of Swauger, fig. 1 insert) past North Fork and through the Ulysses Mountain quadrangle (Lewis and others, 2019). When continuation across that gap, hereafter simply called “the gap,” was questioned in 2017 and upper plate rocks were reassigned to the banded siltite member only northwest of the gap, the northwest extent of the Freeman thrust got a local name, the Trail Gulch thrust. It was deemed to have had considerable translation because it juxtaposes Apple Creek members thought to have originated in widely separated environments. Figures 1, 3, and 5 show the same stratigraphic contrast across the Freeman thrust, which also has mylonite along it. If the two fault segments are the same fault with Apple Creek units of the Lemhi Range and Salmon River Mountains in its hanging wall, the name Freeman should have precedence and the hanging wall constitutes the Freeman plate.

North Fork Plate

Rocks of the North Fork plate are thin- to thick-bedded siltite and feldspathic quartzite with little argillite, and common but dispersed soft sediment deformation. Toward the northwest, we were unable to find

a mappable difference between Gunsight Formation rocks east and northeast of the Beartrack mine under the Swauger in the footwall of the Poison Creek thrust and those near North Fork. To the southeast, the linear trace of the Lemhi Pass fault suggests lateral motion, but the only documented displacement is dip slip (VanDenburg, 1997; VanDenburg and others, 1998; Blankenau, 1999) that is small relative to the apparent thickness of the strata on either side. Similarity of quartzite-dominated rocks with common soft sediment deformation (Stop 6, Lewis and others, 2017) on both sides of the fault support this conclusion. The three young detrital zircon ages (1375–1371 Ma; Gillerman, 2008) from both sides of the fault are consistent with this interpretation and the hypothesis that the rocks are Apple Creek.

Farther south, across the Cow Creek fault, are rocks mapped as the siltite of Yearian Creek that we have correlated with the Lawson Creek Formation (Hobbs, 1980). Below those, south of the Peterson Creek fault and over Goat Mountain, is a quartzite-dominated unit (mapped as quartzite of Goat Mountain but correlated with the Swauger; Lewis and others, in press), from which an interbedded tuff yielded the young age (1385 Ma) mentioned above. Therefore, rocks appear to be younging northward to the Cow Creek fault. The case for rocks north of the Cow Creek fault being younger still and Apple Creek may hinge on the younger age (1373 Ma) from Lemhi Pass.

CONCERNS AND CONSTRAINTS ON ROLES OF THE FAULTS

- (1) Metasedimentary rocks across the Diamond Creek fault are similar and have similar southwest-facing attitudes consistent with the Diamond Creek fault not being responsible for back-tilting of the Poison Creek thrust footwall, and not being a major Swauger-omitting thrust.
- (2) Garnets exist on both sides of the Diamond Creek and North Fork faults, consistent with similar pre-Cretaceous history, unless ages of the garnets differ between fault blocks.
- (3) Similar lithologies and soft sediment deformation between the Diamond Creek and North Fork faults and southeast past the Lemhi Pass fault are consistent with all belonging to the same unit(s).



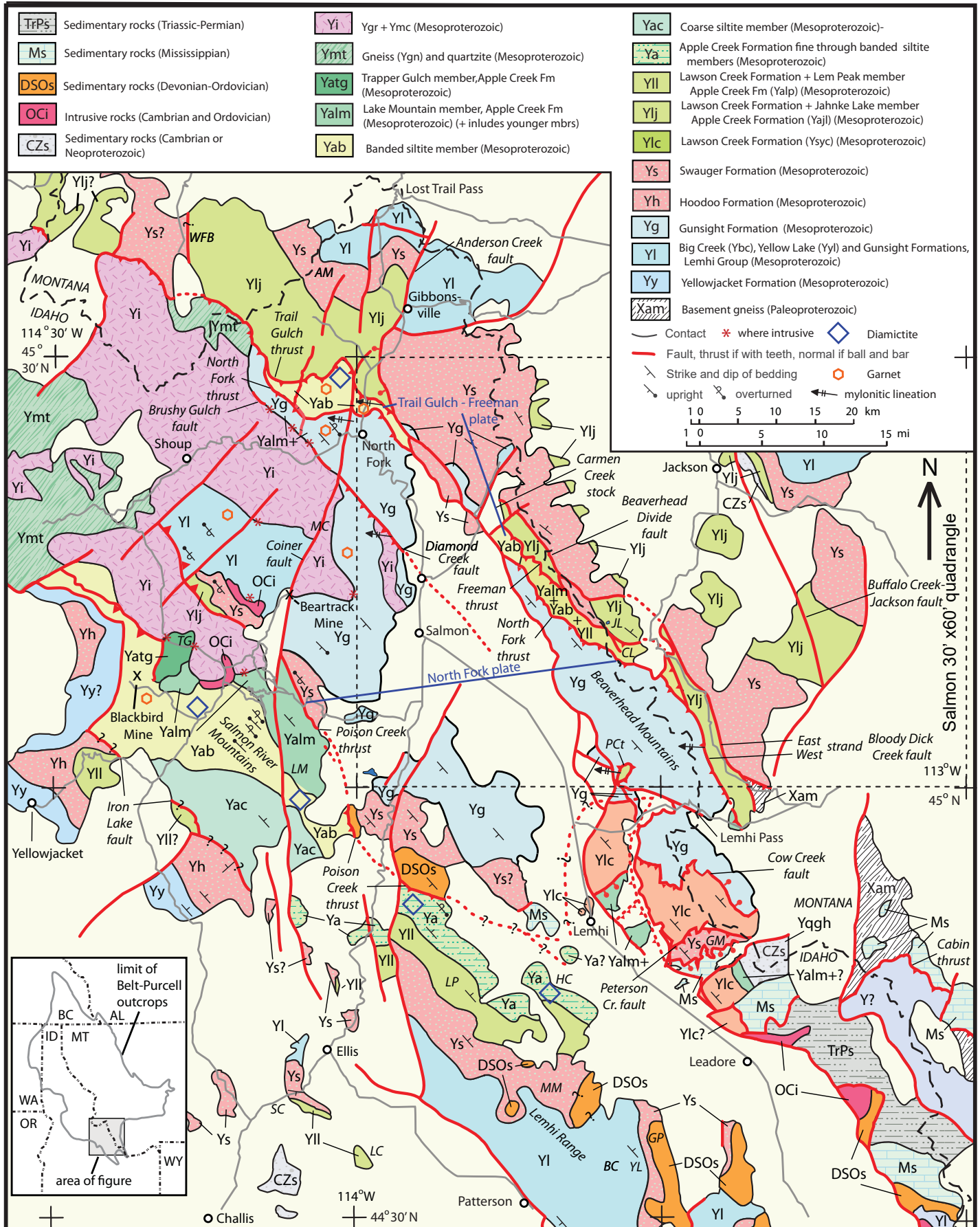


Figure 5a. Same as figure 3 except rock between the Diamond Creek fault and the North Fork thrust are accepted as Gunsight Formation.



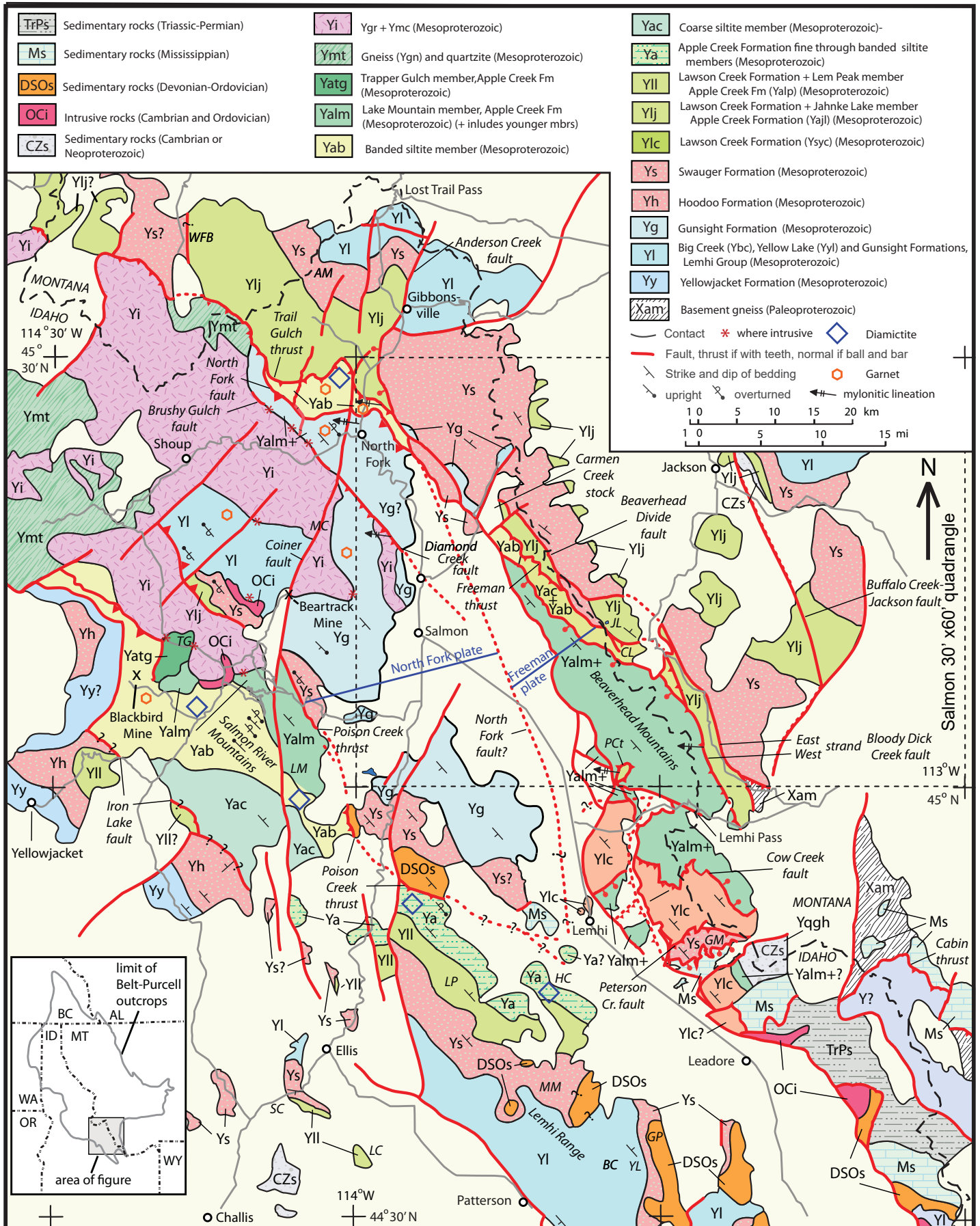


Figure 5b. Same as figure 5a except that the Diamond Creek fault has duplicated some of the Gunsight, which is the hanging wall of the North Fork thrust, which does not continue into the Beaverhead Mountains.



- (4) Young ages near Lemhi Pass are consistent with rocks there being Apple Creek and not Gunsight, but there are only three of them.
- (5) Brittle deformation along parts of the North Fork fault is consistent with at least late normal faulting. Could normal faulting and not thrusting be responsible for juxtaposition of the rocks across it?
- (6) The Freeman and North Fork faults are close to parallel everywhere, suggesting a common origin.
- (7) Contrast between Gunsight on the west and Lawson Creek on the east across the Lemhi Valley north of Lemhi is consistent with a Cretaceous thrust existing beneath the valley fill. That role would fall to the Cow Creek fault in figure 5a.

ALTERNATIVES

While it would be nice if we could say “this is the way it is, guys” and offer a finished map, such is not the case. Figure 3 is a refinement of our 2017 speculation that revives the Diamond Creek fault to major status. Two additional hypotheses, both with reduced offset on the Diamond Creek fault, are shown in figures 5a and 5b. Figure 4 diagrams the history of the Poison Creek fault and how Apple Creek rocks could have gotten northeast of the Diamond Creek fault.

Figure 3 allows the North Fork “plate” to be part of the Freeman plate and entirely Apple Creek strata younger than those between the North Fork fault and the Freeman thrust. One plus is that it maintains continuity of units southwest of the North Fork fault across the northern end of the Salmon basin. It envisions that normal faulting recovered more than original thrust displacement, or that normal faulting after folding during contraction allowed for less. However, this excuse works better for the segment south of the gap where the Freeman thrust footwall rocks are intensely folded than to the west where they are not. The Diamond Creek plate then is everything from the Diamond Creek fault west to the Poison Creek fault. This requires that the Diamond Creek fault is the Lemhi Group–Apple Creek Formation contact as in figure 4c. This option looks good, except for consistency of rock and attitudes across the Diamond Creek fault. Possible tests would be comparison of detrital zircon age spectra and garnet ages across the Diamond Creek fault.

Figure 5a allows the North Fork fault to hog all the glory such that the North Fork plate extends from the Poison Creek fault eastward to the North Fork fault. Its primary positive feature is that it allows the North Fork fault to be a thrust matching east-vergent folding and shearing along its middle part. If the main displacement were the North Fork fault in figure 4c, displacement could be partitioned between it and the Diamond Creek fault such that the latter would duplicate part of Gunsight, and Gunsight would be in the hanging wall of the North Fork thrust. The Diamond Creek fault has mylonite and strain more consistent with Gunsight over Apple Creek than one might imagine would be produced by Gunsight against Gunsight motion, yet similarity of attitudes and lithologies on both sides is consistent with that fault being within Gunsight. This configuration kicks the can down to the Cow Creek fault and requires that ages near Lemhi Pass be erroneous and that the Cow Creek fault have major displacement during the Cretaceous.

Figure 5b is a compromise, sweeping the problem under the Salmon basin rug. It hypothesizes that everything west of the gap is as in figure 5a but beyond that all is as in figure 3. It requires that the fault in the Beaverheads is not the same North Fork fault as around North Fork and leaves unanswered the question of what is covered or intruded out in the gap. The most appeal stems from having the Diamond Creek fault within Gunsight yet also having Apple Creek on the west slope of the Beaverhead Mountains south to the Cow Creek fault. However, that shifts the problem of distinguishing the two units from across the Diamond Creek fault to across the gap. A minor excuse for the change in behavior of the North Fork fault across the gap is the difference in deformation in the footwall of the Freeman thrust mentioned above, but that leaves unexplained why the North Fork and Freeman faults are so parallel everywhere. The activity of the North Fork fault west of North Fork during the Cretaceous might be tested with garnet ages; Cretaceous ages south of the fault would support Cretaceous displacement.

THE TESTS

Being field geologists, we would hope that closer scrutiny of the rocks would reveal diagnostic differences between units above and below the Swauger, and within the Lemhi Group formations and Apple Creek members. Although we have learned a lot dur-



ing our years walking this land about what to look for, the reality is that there are few critical outcrops we haven't seen, exposures are nonexistent in critical areas, and lateral and vertical variation of the units seem to thwart attempts at long-range lithologic correlations. The answers may have to come from geochronology. Maximum age of deposition based on detrital zircon analysis depends on finding elusive young zircons, but given the apparent success with the Big Creek Formation, more widespread collection and analysis of many grains seems warranted. Certainly, resampling the rocks around Lemhi Pass should be on the list to verify or refute the young age there. Samples on either side of the Diamond Creek fault, including metamorphosed ones to the northwest, might reveal similarities or differences that could be used to evaluate whether there is Gunsight Formation on both sides and therefore whether figures 3 or 5 would better reflect reality. Similarly, comparison of rocks across the gap could test the validity of the reconstruction in figure 5b. Grasping for straws would be to examine chert clasts for possible origin as tuffs and to analyze sufficiently large zircons within them in order to better constrain ages of deposition. Also critical would be dating of garnet southwest of the North Fork fault. Grenville ages there similar to those from the banded siltite of the Freeman plate would support pre-Cretaceous displacement on that fault; Cretaceous ages would refute that. Dates from garnets close to the Diamond Creek fault in its hanging wall compared to those in its footwall should reveal differences in the metamorphic histories of those rocks.

SUMMARY

There are several curious aspects of the Burmester and others (2016a) Salmon 30' x 60' map and more recent maps (e.g., Burmester and others, 2018). Some faults, such as the Cow Creek fault, have implied motion far exceeding evidence in the rocks, whereas others, such as the Diamond Creek fault, have evidence of considerable strain but no documented offset. Furthermore, what appears as Gunsight Formation west, north, and east of Salmon is so extensive (and varied) that relabeling it Lemhi Group to mask our inability to map lower Lemhi Group units was suggested at a 2018 field conference with Don Winston, Dave Pearson, Mark McFaddan, and Stuart Parker. Perhaps the reason we could not find Lemhi units below the Gunsight is because not all is Lemhi Group. Instead, if Gunsight continues northeast of the Poison Creek thrust only to

the Diamond Creek fault, and rocks beyond are Apple Creek members, evidence for faulting (strong fabrics) along the Diamond Creek structure better corresponds with implied slip there. However, Gunsight appears uninterrupted below the Swauger Formation west of Salmon, so, unless the Diamond Creek pluton intruded a contact, the rocks northeast from the Mesoproterozoic plutonic rocks to the North Fork fault likely are Gunsight Formation as well. Confinement of Gunsight to near the Mesoproterozoic intrusions, perhaps because of earlier motion on the North Fork fault, allows different strata in the North Fork hanging wall southeast of the gap. Otherwise, the Gunsight Formation would continue all the way to the Cow Creek fault. Paucity of evidence consistent with major thrust faulting on the Cow Creek structure could be because it is older and is part of the North Fork plate. Old faulting may date from deformation before, during, or following intrusion of the Mesoproterozoic plutons, or from block faulting that preceded thrusting along the Poison Creek fault, perhaps during the Neoproterozoic. Angular unconformities under Paleozoic strata south and east of Goat Mountain support at least early Paleozoic deformation there. But old displacement of Gunsight over Lawson Creek requires an unknown fault to juxtapose those rocks across the Lemhi Valley in the Cretaceous. Suggested tests include detrital zircon analyses of the Lemhi Pass rocks, rocks on both sides of the Diamond Creek fault and the gap, and dating of garnets south of the North Fork thrust.

ACKNOWLEDGMENTS

None of this work would be possible without the U.S. Geological Survey Statemap Program and state funding for the Idaho Geological Survey, and the Montana Bureau of Mines and Geology. Clay Martin at the USGS Field Records Library in Denver was most helpful in loaning field maps and notebooks. As always, we greatly appreciate the discussions with Don Winston, Paul Link, Dave Pearson, and others with an interest in these challenging rocks. Mark D. McFaddan and Phyllis Hargrave kindly provided helpful reviews. We also acknowledge the efforts of TRGS to disseminate our current research thoughts in a format that provides a timely release.



REFERENCES CITED

- Aleinikoff, J.N., Slack, J.F., Lund, K., Evans, K.V., Fanning, C.M., Mazdab, F.K., Wooden, J.L., and Pillers, R.M., 2012, Constraints on the timing of Co-Cu ± Au mineralization in the Blackbird District, Idaho, using SHRIMP U-Pb ages of monazite and xenotime plus zircon ages of related Mesoproterozoic orthogneisses and metasedimentary rocks: *Economic Geology*, v. 107, p. 1143–1175.
- Aleinikoff, J.N., Lund, K., and Fanning, C.M., 2015, SHRIMP U-Pb and REE data pertaining to the origins of xenotime in Belt Supergroup rocks: Evidence for ages of deposition, hydrothermal alteration, and metamorphism: *Canadian Journal of Earth Sciences*, v. 52, n. 9, p. 722–745, doi: <https://doi.org/10.1139/cjes-2014-0239>
- Berg, R.B., and Lonon, J.D., 1996, Preliminary geologic map of the Nez Perce Pass 30' x 60' quadrangle, western Montana: Montana Bureau of Mines and Geology Open-File Report 339, scale 1:100,000.
- Blankenau, J.J., 1999, Cenozoic structural and stratigraphic evolution of the southeastern Salmon basin, east-central Idaho: Logan, Utah State University, M.S. thesis, 143 p., 3 plates.
- Brown, E.H., and Burmester, R.F., 1991, Metamorphic evidence for tilt of the Spuzzum pluton: Diminished basis for the Baja British Columbia concept: *Tectonics*, v. 10, no. 5, p. 978–985.
- Brown, E.H., and McClelland, W.C., 2000, Pluton emplacement by sheeting and vertical ballooning in part of the southeast Coast Plutonic Complex, British Columbia: *Geological Society of America Bulletin*, v. 112, no. 5, p. 708–719, doi: [https://doi.org/10.1130/0016-7606\(2000\)112<708:PEBS AV>2.0.CO;2](https://doi.org/10.1130/0016-7606(2000)112<708:PEBS AV>2.0.CO;2)
- Burmester, R.F., Lewis, R.S., Othberg, K.L., Stanford, L.R., McFaddan, M.D., and Lonon, J.D., 2012, Geologic map of the Bird Creek quadrangle, Lemhi County, Idaho: Idaho Geological Survey Digital Web Map 153, scale 1:24,000.
- Burmester, R.F., Lewis, R.S., Othberg, K.L., Stanford, L.R., Lonon, J.D., and McFaddan, M.D., 2016a, Geologic map of the western part of the Salmon 30 x 60-minute quadrangle, Idaho and Montana: Idaho Geological Survey Geologic Map 52, scale 1:75,000.
- Burmester, R.F., Lonon, J.D., Lewis, R.S., and McFaddan, M.D., 2016b, Stratigraphy of the Lemhi subbasin of the Belt Supergroup, in MacLean, J.S., and Sears, J.W., eds., *Belt Basin: Window to Mesoproterozoic Earth*: Geological Society of America Special Paper 522, p. 121–137.
- Burmester, R.F., Lewis, R.S., and Lonon, J.D., 2017, Were we wrong? Second thoughts on geology of the Lemhi subbasin: *Northwest Geology*, v. 46, p. 7–14.
- Burmester, R.F., Othberg, K.L., Stanford, L.R., Lewis, R.S., and Lonon, J.D., 2018, Geologic map of the Agency Creek quadrangle, Lemhi County, Idaho: Idaho Geological Survey Digital Web Map 182, scale 1:24,000.
- Connor, J.J., and Evans, K.V., 1986, Geologic map of the Leesburg quadrangle, Idaho: U.S. Geological Survey Miscellaneous Field Studies Map MF-1880, scale 1:62,500.
- Doughty, P.T., and Chamberlain, K.R., 1996, Salmon River Arch revisited—New evidence for 1370 Ma rifting near the end of deposition in the Middle Proterozoic Belt basin: *Canadian Journal of Earth Sciences*, v. 33, p. 1037–1052.
- Evans, K.V., 1993, Unpublished Bohannon Spring 7.5' quadrangle field map and notebook, U.S. Geological Survey Field Records Library, Denver, Colorado, scale 1:24,000.
- Evans, K.V., 1996, Unpublished Goldstone Pass 7.5' quadrangle field map and notebook, U.S. Geological Survey Field Records Library, Denver, Colorado, scale 1:24,000..
- Evans, K.V., and Zartman, R.E., 1990, U-Th-Pb and Rb-Sr geochronology of Middle Proterozoic granite and augen gneiss, Salmon River Mountains, east-central Idaho: *Geological Society of America Bulletin*, v. 102, p. 63–73.
- Evans, K.V., and Green, G.N., 2003, Geologic map of the Salmon National Forest and vicinity, east-central Idaho: U.S. Geological Survey Geologic Investigations Series Map I-2765, 19 p., scale 1:100,000.
- Gillerman, V.S., 2008, Geochronology of iron oxide-copper-thorium-REE mineralization in Proterozoic rocks at Lemhi Pass, Idaho, and a comparison to copper-cobalt ores, Blackbird mining district, Idaho: Final Technical Report to U.S. Geologi-



- cal Survey, December, 149 p., MRERP Award #06HQGR0170, <https://minerals.usgs.gov/mrerp/reports.html#2006>
- Hahn, G.A., and Hughes, G.J., Jr., 1984, Sedimentation, tectonism, and associated magmatism of the Yellowjacket Formation in the Idaho Cobalt Belt, Lemhi County, Idaho, *in* S.W. Hobbs, ed., The Belt: Abstracts with Summaries, Belt Symposium II, 1983: Montana Bureau of Mines and Geology Special Publication 90, p. 65–67.
- Hansen, C., 2015, An investigation into the Poison Creek thrust: A Sevier thrust with Proterozoic implications: Pocatello, Idaho State University, M.S. thesis, 80 p.
- Hansen, C.M., and Pearson, D.M., 2016, Geologic map of the Poison Creek thrust fault and vicinity near Poison Peak and Twin Peaks, Lemhi County, Idaho: Idaho Geological Survey Technical Report T-16-1, scale: 1:24,000.
- Hobbs, S.W., 1980, The Lawson Creek Formation of Middle Proterozoic age in east-central Idaho: U.S. Geological Survey Bulletin 1483-E, 12 p.
- Lewis, R.S., Burmester, R.F., Stanford, L.R., Lonn, J.D., McFaddan, M.D., and Othberg, K.L., 2009a, Geologic map of the Kitty Creek quadrangle, Lemhi County, Idaho and Beaverhead County, Montana: Idaho Geological Survey Digital Web Map 112 and Montana Bureau of Mines and Geology Open-File Report 582, scale 1:24,000.
- Lewis, R.S., Othberg, K.L., Burmester, R.F., Lonn, J.D., Stanford, L.R., and McFaddan, M.D., 2009b, Geologic map of the Bohannon Spring quadrangle, Lemhi County, Idaho and Beaverhead County, Montana: Idaho Geological Survey Digital Web Map 113 and Montana Bureau of Mines and Geology Open-File Report 583, scale 1:24,000.
- Lewis, R.S., Othberg, K.L., Stanford, L.R., Burmester, R.F., Lonn, J.D., and McFaddan, M.D., 2011, Geologic map of the Goldstone Mountain quadrangle, Lemhi County, Idaho: Idaho Geological Survey Digital Web Map 134, scale 1:24,000.
- Lewis, R.S., Gillerman, V.S., Burmester, R.F., Mosolf, J.G., and Lonn, J.D., 2017, Road log to the geology and mineralization of the Agency Creek and Lemhi Pass areas, Idaho and Montana: Northwest Geology, v. 46, p. 119–132.
- Lewis, R.S., Burmester, R.F., and Lonn, J.D., 2019, Geologic map of the Ulysses Mountain quadrangle, Lemhi County, Idaho: Idaho Geological Survey Digital Web Map 188, scale 1:24,000.
- Lewis, R.S., Stewart, D.E., Burmester, R.F., Stanford, L.R., Othberg, K.L., Stewart, E.D., and Lonn, J.D., in press, Geologic map of the Goat Mountain quadrangle, Lemhi County, Idaho, and Beaverhead County, Montana: Idaho Geological Survey Digital Web Map, scale 1:24,000.
- Lonn, Jeff, 2017, The Lemhi Group type section revisited and revised, east-central Idaho, Northwest Geology, v. 46, p. 15–28.
- Lonn, J.D., Burmester, R.F., Lewis, R.S., and Stanford, L.R., 2008, Geologic map of the Homer Youngs Peak quadrangle, Lemhi County, Idaho, and Beaverhead County, Montana: Idaho Geological Survey Digital Web Map 95 and Montana Bureau of Mines and Geology Open-File Report 575, scale 1:24,000.
- Lonn, J.D., Stanford, L.R., Lewis, R.S., Burmester, R.F., and McFaddan, M.D., 2009, Geologic map of the Goldstone Pass quadrangle, Lemhi County, Idaho, and Beaverhead County, Montana: Idaho Geological Survey Digital Web Map 114 and Montana Bureau of Mines and Geology Open-File Report 584, scale 1:24,000.
- Lonn, J.D., Othberg, K.L., Lewis, R.S., Burmester, R.F., Stanford, L.R., and Stuart, D.E., 2013, Geologic map of the North Fork 7.5' quadrangle, Lemhi County, Idaho: Idaho Geological Survey Digital Web Map 160, scale 1:24,000.
- Lonn, J.D., Burmester, R.F., Lewis, R.S., and McFaddan, M.D., 2016, Giant folds and complex faults in Mesoproterozoic Lemhi Group strata of the Belt Supergroup, northern Beaverhead Mountains, Montana and Idaho, *in* MacLean, J.S., and Sears, J.W., eds., Belt Basin: Window to Mesoproterozoic Earth: Geological Society of America Special Paper 522, p. 139–162.
- Lonn, J.D., Elliott, C.G., Stewart, D.E., Mosolf, J.G., Burmester, R.F., Lewis, R.S., and Pearson, D.M., 2019, Geologic map of the Bannock Pass 7.5' quadrangle, Beaverhead County, Montana, and Lemhi County, Idaho: Montana Bureau of Mines and Geology Geologic Map 76, 1 sheet, scale 1:24,000.



- Lund, K., Evans, K.V., Doughty, P.T., Chamberlain, K.R., Kink, P.K., and Winston, D., 2003, Geology of the Brushy Gulch fault and its hanging wall and footwall rocks, Eastern Idaho: Northwest Geology, v. 32, p. 74–85.
- Ruppel, E.T., 1975, Precambrian Y sedimentary rocks in east-central Idaho: U.S. Geological Survey Professional Paper 889-A, 23 p.
- Tysdal, R.G., 2000, Stratigraphy and depositional environments of Middle Proterozoic rocks in northern part of Lemhi Range, Lemhi County, Idaho: U.S. Geological Survey Professional Paper 1600, 40 p.
- Tysdal, R.G., 2003, Correlation, sedimentology, and structural setting, upper strata of Mesoproterozoic Apple Creek Formation and lower strata of Gunsight Formation, Lemhi Range to Salmon River Mountains, east-central Idaho, *in* Tysdal, R.G., Lindsey, D.A., and Taggart, J.E., Jr., eds., Correlation, sedimentology, structural setting, chemical composition, and provenance of selected formations in Mesoproterozoic Lemhi Group, central Idaho: U.S. Geological Survey Professional Paper 1668-A, p. 1–22.
- VanDenburg, C.J., 1997, Cenozoic tectonic and paleogeographic evolution of the Horse Prairie half graben, southwest Montana: Logan, Utah State University, M.S. thesis, 152 p., 2 plates.
- VanDenburg, C.J., Janecke, S.U., and McIntosh, W.C., 1998, Three-dimensional strain produced by >50 my of episodic extension, Horse Prairie basin area, SW Montana, U.S.A.: *Journal of Structural Geology*, v. 20, no. 12, p. 1747–1767.
- Watts, Griffis, and McOuat Limited, 1989, Review of American Gold Resources Corp. properties Lemhi County, Idaho: Idaho Geological Survey Mineral Property File MPF-EC1184_006, https://idahogeomap.nkn.uidaho.edu/Data/MineDocs/EC1184_006.pdf [Accessed 18 February 2020].
- Winston, D., Link, P.K., and Hathaway, N., 1999, The Yellowjacket is not the Prichard and other heresies—Belt Supergroup correlations, structure, and paleogeography, east-central Idaho, *in* Hughes, S.S., and Thackray, G.D., eds., Guidebook to the geology of Eastern Idaho: Pocatello, Idaho, Idaho Museum of Natural History, p. 3–20.



FIELD GUIDE TO THE GEOLOGY OF THE SLEEPING CHILD METAMORPHIC COMPLEX, SOUTHERN SAPPHIRE MOUNTAINS, WESTERN MONTANA

Jeff Lonn and Jesse Mosolf

Montana Bureau of Mines and Geology, Butte, Montana

INTRODUCTION

The western flank of the Sapphire Mountains along Skalkaho and Sleeping Child Creeks is a poorly understood area underlain by amphibolite-grade metamorphic rocks comprised mostly of quartzite, calc-silicate gneiss, and migmatite. New field work and U-Pb dating have revealed a previously unrecognized regional-scale thrust fault and suggest that: (1) the quartzite has affinities to the strata of the Mesoproterozoic Lemhi subbasin, upper Belt Supergroup; (2) Paleoproterozoic basement rocks are mixed with the Mesoproterozoic Belt rocks; and (3) high-grade metamorphism that generated migmatites occurred in the Cretaceous following or coeval with much of the tectonism/faulting.

The three field trips described here examine some of the interesting features and unresolved problems in this region, named here the Sleeping Child metamorphic complex (SCMC). Field Day 1 is an arduous half-day scramble 1,000 vertical feet up a steep slope to examine a kyanite-bearing shear zone associated with the Stony Lake thrust fault. Field Day 2 is a strenuous all-day hike with 2,000 ft of elevation gain/loss and some off-trail hiking. It examines high-grade Mesoproterozoic Belt rocks and Paleoproterozoic basement rocks, their contacts and possible relationships, and the Stony Lake thrust. Field Day 3 is a short, but steep, half-day, off-trail hike climbing 500 vertical feet to examine a mylonitic fault contact between Paleoproterozoic orthogneiss and Mesoproterozoic quartzite as well as other quartz-feldspar gneiss interlayered within the quartzite.

GEOLOGIC SETTING

The SCMC, on the west side of the southern Sapphire Mountains (figs. 1, 2), is one of the few regions in Montana with Cretaceous-age migmatitic metamorphic rocks. Cretaceous high-grade metamorphic rocks also occur in the West Pioneer Mountains and along the southeast flank of the Anaconda Range, and all three areas may have been continuous before being separated by Tertiary extension. Due to the poly-

deformed high-grade rocks, the complex faulting, and the puzzling Belt stratigraphic section, the SCMC is also one of Montana's least understood regions.

The Sapphire Mountains, in the hanging walls of both the Cretaceous Georgetown–Philipsburg thrust system and the Eocene Bitterroot detachment fault, are underlain by Belt Supergroup strata intruded by Cretaceous and Tertiary plutons. The rocks of the Sapphire Mountains have long been considered a major intact allochthon, the Sapphire tectonic block (Hyndman, 1980), riding atop the east-directed Philipsburg–Georgetown thrust system. However, the Sapphire block is complexly faulted, with numerous thrust faults shown on previous maps (Wallace, 1987; Wallace and others, 1986, 1989, 1992; Lewis, 1998; Lonn and others, 2003a). New mapping (Lonn, unpublished; Lonn, 2017) suggests that many of these thrusts are faulted, disconnected exposures of the same regional-scale thrust (figs. 1, 2). It had previously been named the Stony Lake thrust (Lonn and others, 2003a), although its type locality is now reinterpreted as a normal fault juxtaposing footwall and hanging wall (fig. 2). Sears (2016) recognized the Stony Lake thrust plate as distinct from the Georgetown–Philipsburg plate, and carried the Stony Lake name forward, so we favor retaining this name to avoid confusion.

The flat-dipping, but broadly folded, Stony Lake thrust put Piegan Group rocks of the middle Belt Supergroup, metamorphosed to calc-silicate gneiss, on top of fine- to coarse-grained Belt quartzite (figs. 1, 2). Based on thick, intact sections preserved in the Sapphire and Anaconda Ranges (Lonn, 2014; Lonn and others 2016a,b), those sandy strata are now thought to directly overlie the Piegan Group, and are correlated with the Lemhi subbasin strata that grade into the Missoula Group, upper Belt Supergroup (Lonn, 2014; Lonn and others, 2016a,b; Burmester and others, 2016). Detrital zircon data support this interpretation (Link and others, 2007, 2013, 2016). The minimum age of the Stony Lake thrust is constrained by cross-cutting plutons (Lonn, 2017) with maximum



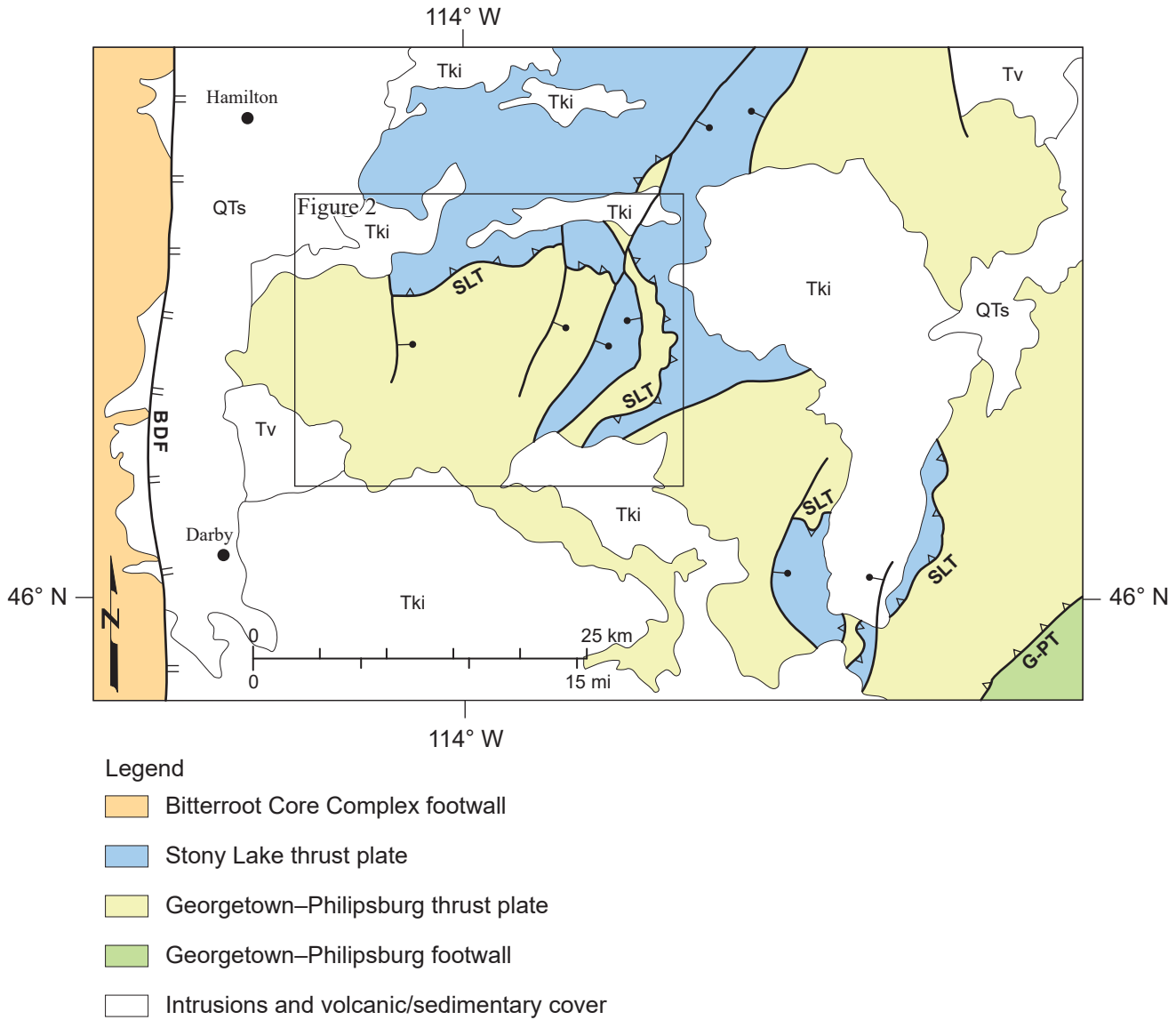


Figure 1. Map showing tectonic features of the southern Sapphire Range, including major thrust allochthons. BF, Bitterroot fault, both Eocene and Quaternary; QTs, sedimentary rocks, undivided; SLT, Stony Lake thrust; G-PT, Georgetown-Philipsburg thrust; TKi, intrusive rocks; Tv, volcanic rocks. Area of figure 2 is outlined. Scale 1:500,000. Modified from Vuke and others, 2007.

crystallization ages of about 78 Ma (Desmarais, 1983). Kinematic indicators along the thrust are scarce and ambiguous, but metamorphic rocks in its footwall consistently show top-to-the-east shear sense (see discussion below).

Detrital zircon data from two samples collected in the Stony Lake thrust footwall quartzite deserve more discussion (fig. 3). A plot from fine-grained quartzite (unit Yql in fig. 2) collected near Field Day 1 (fig. 3C; sample 22PL07 in fig. 2) contains a major peak at 1,700 Ma and much lesser ones at 1,800 Ma and 2,470 Ma. Only one grain is from the North American magmatic gap (1,510–1,625 Ma). Link and others (2007, 2013, 2016) used DZ data to show that the Lemhi strata have the same provenance as the

Missoula Group of the upper Belt Supergroup. These upper Belt Supergroup strata have strong peaks in the 1,700–1,740 range and lack significant 1,510–1,625 Ma grains from the “North American magmatic gap” (NAMG), in contrast to the Prichard Formation and Ravalli Group of the lower Belt, which have strong peaks in the NAMG (Ross and Villeneuve, 2003; Link and others, 2007). New mapping (Lonn, 2014; Lonn and others, 2016a,b), showing that Lemhi strata grade into Missoula Group formations in the northern Sapphire Range, corroborates these proposed correlations. Although this sample was originally thought to be Ravalli Group, lower Belt Supergroup, based on previous maps (Lewis, 1998; Lonn and others, 2003a), new mapping and these detrital zircon data support correlation with the upper Belt Supergroup instead.



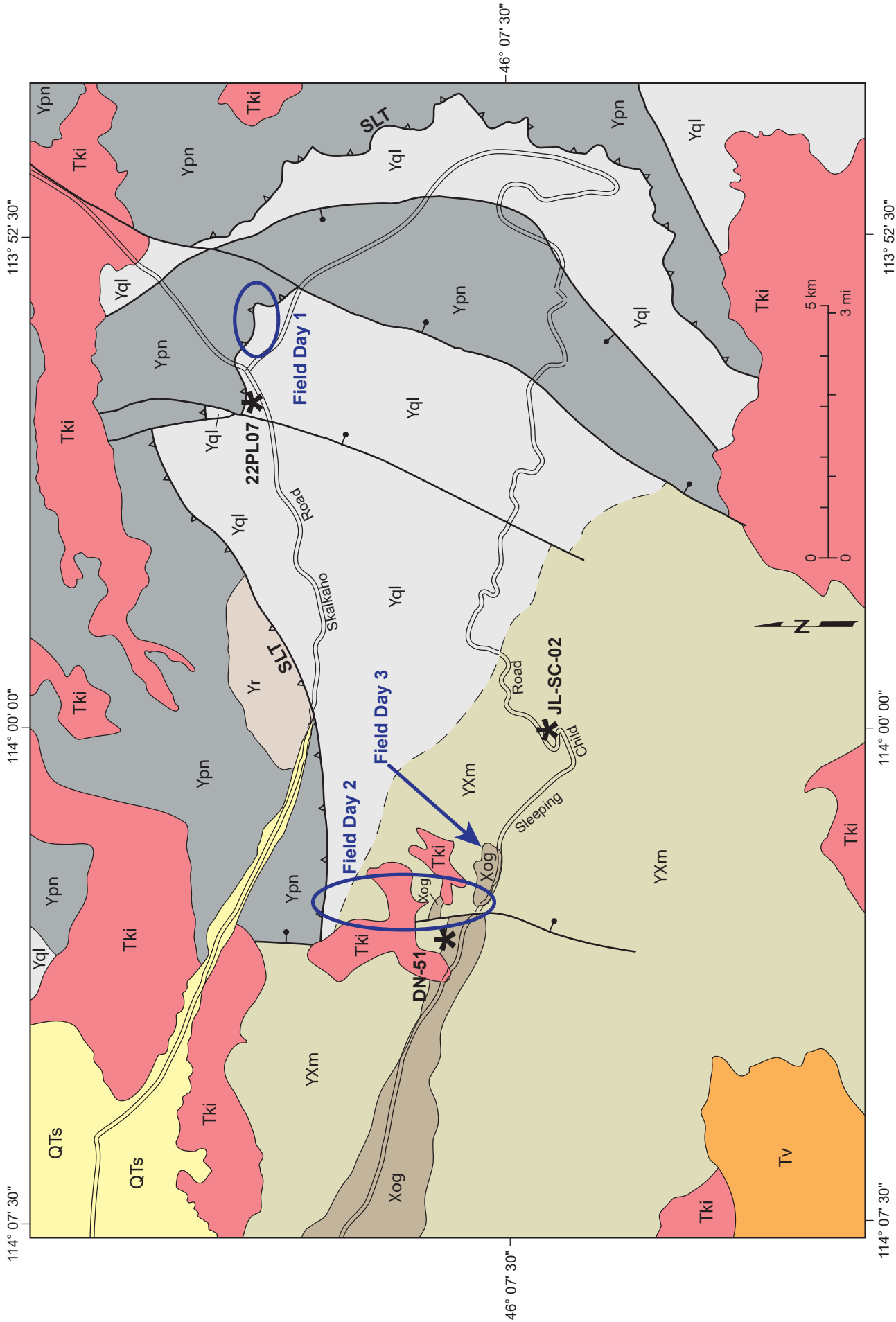


Figure 2. Geologic map of the Sleeping Child metamorphic complex (SCMC) showing field trip locations. Sample locations are shown by stars (see text and fig. 3). QTs, sedimentary rocks, undivided; SLT, Stony Lake thrust; TKi, intrusive rocks; Tv, volcanic rocks; Ypn, Plegan Group, middle Belt Supergroup; Yr, Ravalli Group, lower Belt Supergroup; Yql, Lemhi quartzite, upper Belt Supergroup; YXm, meta-Belt and basement, undivided; Xog, 1,863 Ma orthogneiss. Scale 1:100,000. Modified from Lonn and Berg (1999) and Lonn and others (2003a).



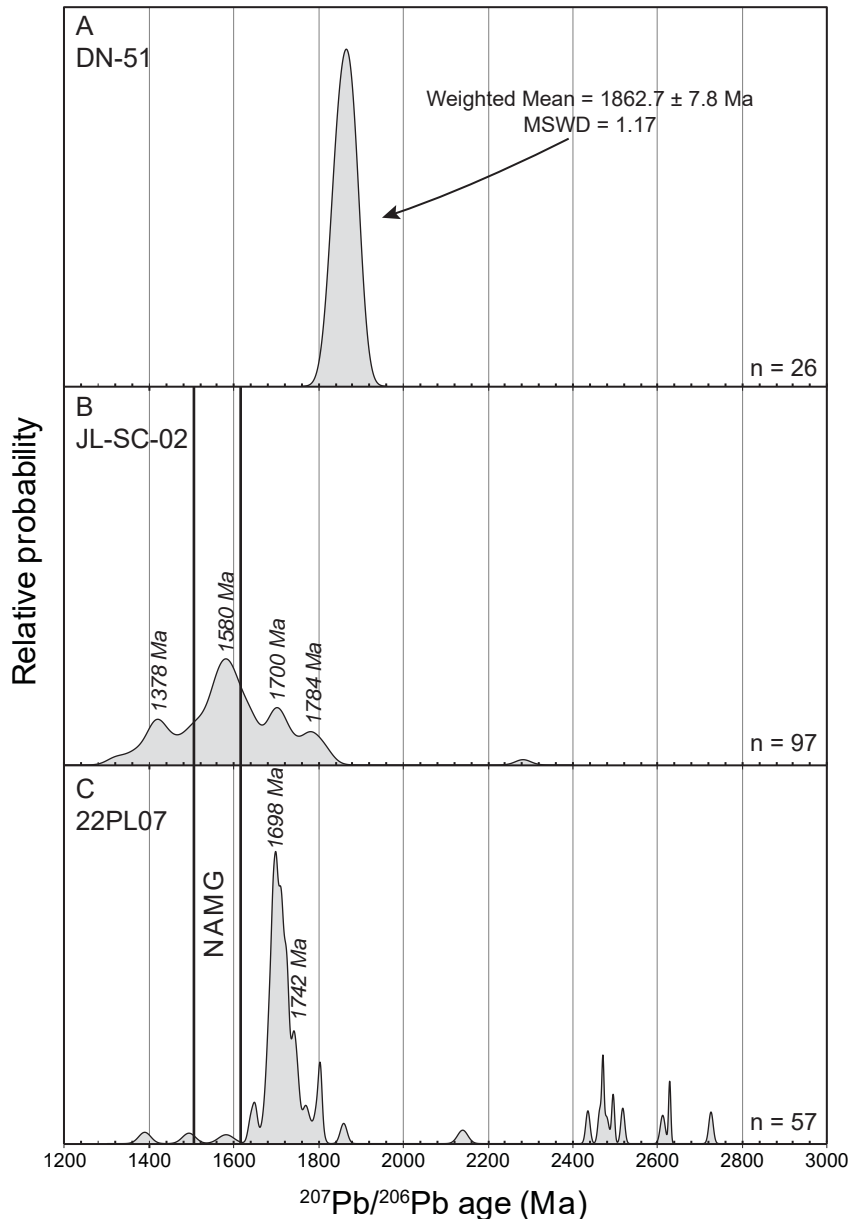


Figure 3. (A) Relative probability plot of concordant $^{207}\text{Pb}/^{206}\text{Pb}$ ages for orthogneiss sample DN-51 (see fig. 2 for location). Approximately 80 zircon grains were analyzed with all but 26 yielding highly discordant data not useful for age determinations. Sample prep and analysis by Jesse Mosolf using laser ablation inductively coupled plasma mass spectrometry at the University of California, Santa Barbara. (B) Relative probability plot of concordant $^{207}\text{Pb}/^{206}\text{Pb}$ ages for fine-grained quartzite sample JL-SC-02 (see fig. 2 for location). Approximately 100 zircon grains were analyzed, with most yielding concordant ages. Sample prep and analysis by Jesse Mosolf using laser ablation inductively coupled plasma mass spectrometry at the University of California, Santa Barbara. (C) Probability plot for fine-grained quartzite sample 22PL07 (see fig. 2 for location). SHRIMP data run at Australian National University by C. Mark Fanning. Sample collected by Paul Link, Idaho State University.

Figure 3B plots data from a fine-grained, amphibolite-grade quartzite (unit YXm in fig. 2) collected near Field Day 2 (sample JL-SC-02 in fig. 2). In contrast to figure 3C discussed above, it shows the strongest peak at 1,580 Ma, in the NAMG, a second peak at 1,700 Ma, and two other significant peaks at 1,378 and 1,784 Ma. While 1,510–1,625 Ma non-North Ameri-

can grains are suggestive of the Ravalli Group and Prichard Formation low in the Belt (Ross and Villeneuve, 2003; Link and others, 2007), the numerous young, 1,378 Ma grains show that this quartzite is near the top of the Belt section, or even Neoproterozoic in age. Its provenance must have included a western, non-North American source, in contrast to upper Belt strata elsewhere.

Therefore, detrital zircon data support the interpretation that both quartzites are upper Belt Supergroup. Correlation with the Lemhi strata is favored because nearly all the Belt rocks exposed in the Stony Lake thrust footwall are very sandy, like the Lemhi strata and unlike typical Missoula Group rocks. In addition, immediately southeast of the SCMC (in the southeastern quarter of fig. 1), an intact 4,000-m-thick section exposes Swauger, Lawson Creek, and Apple Creek Formations of the Lemhi strata (Lonn, 2014; Lonn and others, 2016b), although continuity with the SCMC is disrupted by faults.

In figures 1 and 2, metamorphic grade and deformation intensity increase southward and westward to upper amphibolite-grade, poly-deformed, migmatite gneiss (fig. 4). Protoliths are the Piegan Group, middle Belt Supergroup, in the Stony Lake thrust hanging wall, and Lemhi strata, upper Belt Supergroup, and basement rocks in the footwall. Metamorphic isograds appear to cross the Stony Lake thrust (LaTour, 1974; Lonn and others, 2003a). Peak metamorphism was in the sillimanite–kyanite–migmatite zone with an estimated burial depth of >18 km (Sears, 2016). Clark (1979) similarly estimated peak metamorphic conditions at 600–700°C and 3.5–6.5 kbar, followed by a higher temperature, lower pressure episode that may have been continuous with the earlier event.

Within this high-grade metamorphic terrane is a large body of orthogneiss (fig. 5), first mapped by Clark (1979). A sample of the orthogneiss collected for this study yielded $^{207}\text{Pb}/^{206}\text{Pb}$ ages spanning





Figure 4. (A) Migmatitic biotite quartzite dominates the Stony Lake thrust footwall. (B) Photo of quartzite outcrop shows the complexity of the SCMC. Migmatitic transposed layering has been intruded, folded, and cut by brittle faults.





Figure 5. Photo of the 1,863 Ma orthogneiss intruded at the top and bottom by Tertiary–Cretaceous granite. Elongate quartz–feldspar pods outlined by biotite most commonly define a sub-horizontal east–west lineation.

1,827–1,896 Ma, with a weighted mean age of $1,863 \pm 8$ Ma (fig. 3A; sample DN-51 in fig. 2). Interestingly, the sample appears to exhibit simple U–Pb systematics with no evidence of inheritance (i.e., zircon inherited from Archean crust), and is closely concordant with other meta-igneous Precambrian basement rocks dated in the Pioneer and Little Belt Mountains (Mueller and others, 2002; Foster and others, 2006), and the Priest River and Clearwater complexes (Vervoot and others, 2016). The orthogneiss, however, appears to be ~100 m.y. younger than inherited zircon from the Bitterroot Lobe of the Idaho Batholith (1.75–1.73 Ga; Mueller and others, 1995; Foster and others, 2006). Given the complex deformational history of the Sapphire Mountains, the single radiometric age reported here does not resolve whether this region is solely floored by Paleoproterozoic crystalline basement, or perhaps a complex structural *mélange* of Paleoproterozoic and Archean crust similar to other locales in the northern Rockies such as the nearby Priest River and Clearwater complexes (Vervoot and others, 2016). Because no inherited zircon was detected in the Sapphire Mountains orthogneiss, and inherited zircon in the Bitterroot Lobe of the Idaho Batholith yields Paleoproterozoic

ages, we tentatively interpret the Sapphire Mountains to be underpinned by Paleoproterozoic basement.

Metamorphism and Tertiary–Cretaceous intrusions have obscured the contact relationships between the migmatitic Belt quartzite and the Paleoproterozoic basement, but, because these are uppermost Belt strata, it is unlikely that they were deposited directly on top of the basement. Instead, the basement rocks probably occur as tectonic slices within the Belt rocks. This interpretation, in turn, suggests that at least some metamorphism postdates this tectonism. The oldest plutons in the region, with 78 Ma crystallization ages, have metamorphic fabrics parallel to those in the country rocks (Desmarais, 1983; Lonn and McDonald, 2004), while slightly younger plutons like the Sapphire batholith (Wallace and others, 1989) are undeformed, suggesting that peak metamorphism occurred about 73–78 Ma. It was followed by a high-temperature, lower pressure event (Clark, 1979) that may be related to the voluminous ~73 Ma intrusions like the Sapphire batholith (Wallace and others, 1989), but this interpretation requires considerable exhumation between the two events. Cretaceous intrusive rocks

injected into the migmatite gneiss exhibit progressive deformation ranging from strongly gneissic, boudinaged sills to unfoliated cross-cutting dikes (Sears, 2016), and could be used to further constrain the progression of tectonism and metamorphism. A similar intrusive-tectonic-metamorphic history with nearly identical timing has been proposed for the nearby Anaconda Range (Desmarais, 1983; Grice, 2006; Haney, 2008).

Rare lineations and shear-sense indicators (fig. 6) are scattered throughout the metamorphic terrain, consistently trending due west and showing top-to-the-east shear sense. Although these kinematics are nearly identical to those of the Eocene Bitterroot detachment fault, they are not necessarily related. In this region, older shear zones with similar kinematics have been noted and attributed to thrust faults that pre-date Eocene extension (Foster, 2000; Sears, 2016).

The features discussed above appear to be deformed into a large, ENE-plunging anticline that folds the Stony Lake thrust and exposes the structurally

deepest rocks on its southwest end along lower Sleeping Child Creek (figs. 1, 2). Younger north-northeast-trending, high-angle faults cut across all older features. Although they are shown (fig. 2) as intruded by Cretaceous plutons, the intrusions have not all been dated, and the faults may simply be difficult to follow through the intrusive rocks. The interpretation favored here is that the faults are Tertiary extensional faults related to the Eocene Bitterroot detachment fault.

FIELD DAY 1: STONY LAKE SHEAR ZONE

This field trip is a strenuous half-day scramble 1,000 ft up a steep slope to examine the kyanite-bearing shear zone associated with the Stony Lake thrust fault.

Drive south out of Hamilton on Highway 93 for a few miles and turn left at the flashing yellow light onto the Skalkaho Road (State Route 38). Immediately turn right into the Park and Ride lot. Zero your odometer here.



Figure 6. Northward view of gneissic layer within quartzite, Field Day 3. East is on the right. S-C fabrics and asymmetric feldspar porphyroclasts appear to show top-to-the-east shear sense.



Mile 0.0. Park and Ride lot. Turn right, back onto the Skalkaho Road, and stay on the main highway for 14.5 mi.

Mile 14.5. Turn right on the gravel Skalkaho-Rye road, go 0.1 mi and park in the trashy campground area, avoiding the piles of garbage and staying out of the line of fire. Many 300-yr-old Ponderosa pines and Douglas firs here were logged by the Forest Service as hazard trees because they had been shot so many times. The remaining trees are now taking the bullets, and some have literally been shot down. Shooting and dumping are popular recreational activities in this part of Montana.

Walk up the road a few hundred feet to view large boulders on the right side that rolled down from the cliffs above. Some contain spectacular kyanite crystals more than 3 cm (1 in) long. This was a stop on a 2003 Belt Symposium field trip (Lonn and others, 2003b), but at that time the bedrock source had not been investigated. Since 2003, the boulders have become dust-covered and more weathered, making the crystals harder to find. If you do find some, please leave your hammers holstered and the beautiful specimens in place.

Cross the road and hike up to the lowest outcrops, comprised of gently dipping, fine-grained feldspathic quartzite in beds up to a meter thick. Crossbeds show the beds to be upright. Although the quartzite has equant grains and does not appear highly metamorphosed, at least not to kyanite-grade, as you ascend the slope and section, note that finer grained beds of silt and mud have been metamorphosed to schist.

Continue up the steep slope, staying climber's right of the largest cliffs. Take care not to dislodge loose boulders on any colleagues below. Bedding attitudes remain consistent, dipping moderately into the hill, parallel with the shear zone above. Occasional crossbeds demonstrate that these layers are indeed bedding and still upright. Just a few miles to the southwest, the quartzite is migmatitic and the bedding is completely transposed and severely deformed. No major faults are recognized between the two terranes, but some could exist and have been obscured by later metamorphism.

Reach the ridge at a gentle spot immediately

climber's right of some ridgetop quartzite outcrops (fig. 7, field trip view). There are outcrops of poddy, schistose rock with a NE-dipping, ESE-striking fabric approximately parallel to the bedding attitude of the underlying quartzite (fig. 8A). These outcrops are interpreted to represent the bottom of the Stony Lake shear zone. The pods appear to be strained into asymmetric shapes, but so far, we have not recognized good lineations within the shear zone and shear-sense indicators are ambiguous. Perhaps the large number of sharp eyes viewing these outcrops will discover hidden secrets.

Continue up the ridge, passing upward through the shear zone. Most of the outcrops are obscured by heavy lichen cover, but the float is fresher. The shear zone is quite thick here, >15 m, and a variety of deformed rocks are represented (fig. 8), including knobby mica schist, gneissic rocks with possible igneous protoliths, isolated quartzite clasts or boudins, complexly folded quartz veins, and fine-grained, foliated biotite quartzite. Look carefully for quartzite outcrops that contain blades of kyanite that are concentrated along biotite-rich layers in the quartzite, but randomly oriented across the foliation (fig. 9). The kyanite coexists with the other aluminosilicate polymorphs, andalusite and sillimanite, a relatively rare phenomenon (Whitney and Samuelson, 2019). The order of crystallization appears to be kyanite–andalusite–sillimanite (Colleen Elliott, written commun., 2020). Other metamorphic minerals include staurolite, chlorite, garnet, and others that we need help identifying. Although high-grade metasedimentary rocks dominate the SCMC, kyanite only occurs within this shear zone, and only within this particular segment of the shear zone. The kyanite's limited occurrence has been hard to explain. A literature search revealed a number of other locales where kyanite is restricted to shear zones and attributed to metasomatism involving Al-rich metamorphic fluids moving preferentially along the shear zone (Corey, 1998; McClintock and Cooper, 2003; Buchholz and Ague, 2010; Meighan, 2015). This hypothesis appears to offer the best explanation of the kyanite here. The cross-cutting biotite–kyanite “vein” that occupies a fracture in figure 9B and the numerous quartz veins visible in the shear zone give support to this theory.



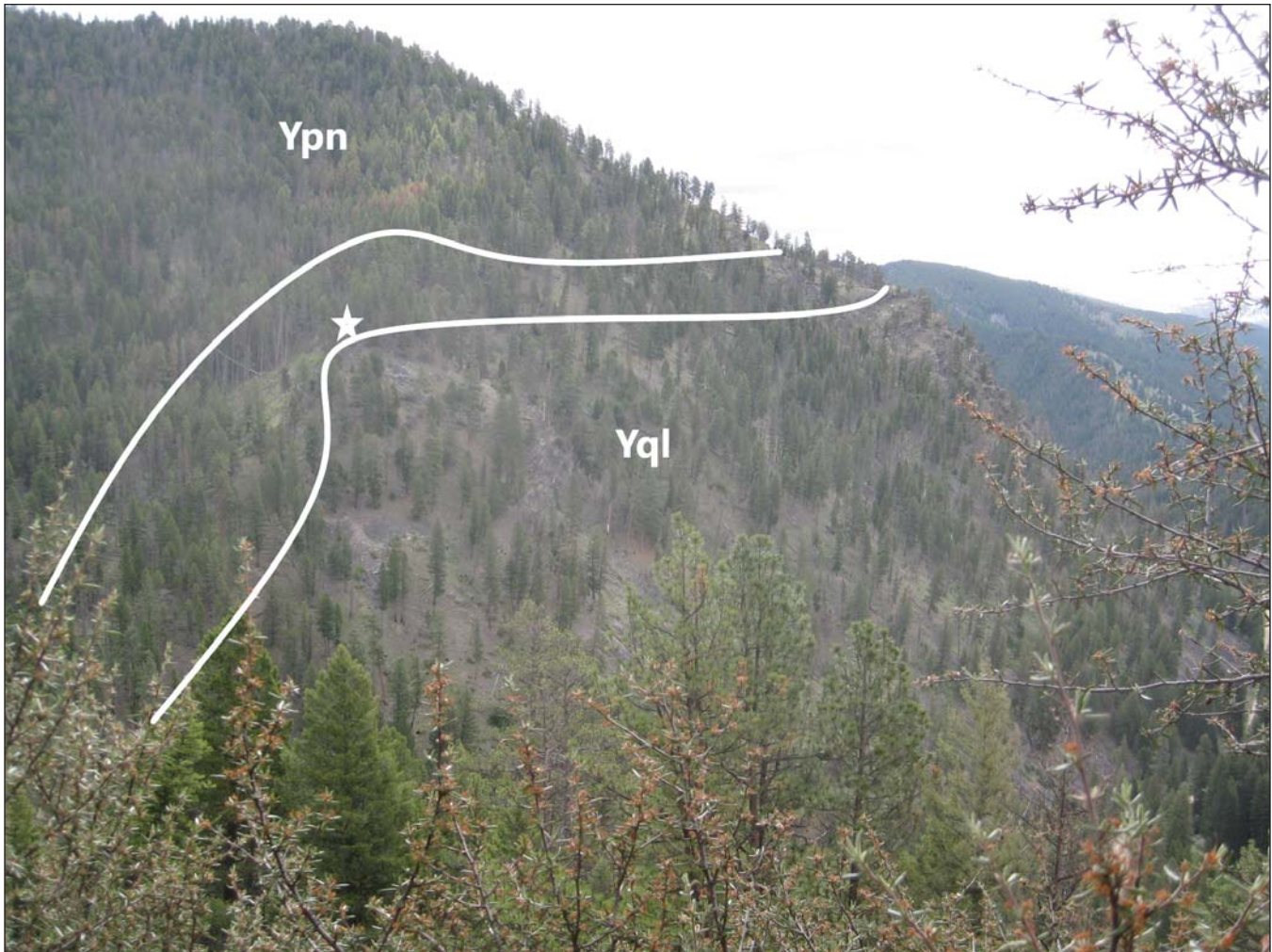


Figure 7. View of Field Day 1 area. Climb up the slope on the right to the star, then proceed up the ridge through the Stony Lake shear zone. White lines enclose the shear zone. Yql, Lemhi quartzite in the footwall; Ypn, Piegan Group of the hanging wall.

The kyanite–andalusite–sillimanite crystallization sequence is relatively rare and possibly indicates two separate metamorphic events (Whitney and Samuelson, 2019). Noted above in the geologic setting section is the possibility of a higher-pressure event followed by exhumation and a high-temperature event (Clark, 1979), similar to that proposed for the Anaconda Range (Desmarais, 1983; Lonn and McDonald, 2004; Grice, 2006; Haney, 2008). However, there is little evidence for Cretaceous exhumation in the Sapphire Range.

Another explanation for the kyanite–andalusite–sillimanite sequence is provided by the aluminosilicate phase diagram (fig. 10). If the kyanite formed close to the triple point, an increase in temperature with a minimal or moderate pressure drop could generate this crystallization sequence in one long, protracted metamorphic event. The higher temperatures could have been caused by the voluminous 73 Ma intrusions like the Sapphire batholith

(Wallace and others, 1989), with slow exhumation provided by erosion.

Finally, an idea in its infancy suggests that differential stress driving deformation in the shear zone could have had a dramatic effect on metamorphic reactions (Schmalholz and Podladchikov, 2014; Wheeler, 2014). This idea challenges the way depths are commonly calculated using metamorphic minerals, and is worth considering here because the coexisting polymorphs are within a shear zone, and kyanite in the SCMC occurs only within this shear zone.

Continue upward to a prospect pit in the shear zone that exposes beautiful knobby schist. Foliation continues to strike east–southeast and dip north. Because this outcrop is fresher, it offers the best chance to find lineations and shear-sense indicators. Try to identify the green mineral.



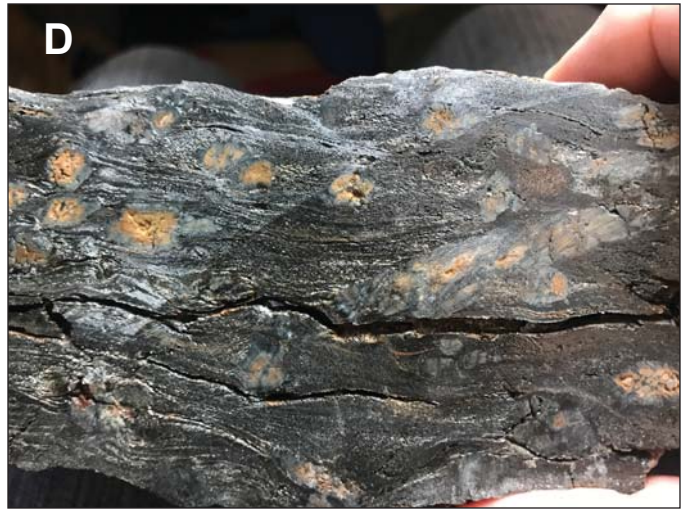


Figure 8. Photos of shear zone rocks. (A) Poddy schist near the bottom of the shear zone. (B) Gneissic rock near bottom of shear zone. Protolith and mineralogy unknown. (C) Knobby muscovite–biotite–chlorite schist. (D) Slabbed knobby schist showing schistosity wrapping around porphyroblasts of unknown mineralogy. Colleen Elliott photo. (E) Quartzite clasts/boudins floating in schist. (F) Slabbed face showing folded layers of recrystallized quartz and biotite. Thickest blob is a folded and dismembered quartz vein. Colleen Elliott photo and mineral ID.





Continuing up, the ridge steepens and becomes bouldery with some large outcrops as you near the top of the shear zone. Find the large outcrop of deformed Piegan Group strata, middle Belt Supergroup, shown in figure 11, in the hanging wall of the Stony Lake thrust. The face of this outcrop is oriented NE–SW, and exhibits offset layers, asymmetric folds, schistose layers, floating quartzite clasts or boudins, and black cataclasite cutting across the layers at low angles. Offset layers show apparent top-to-the-southwest brittle displacement. However, the layers themselves may be sheath folds (fig. 11) recording earlier ductile shear of unknown sense.



Continue upward as long as time and energy permit. The rocks become less and less deformed upward and away from the shear zone, finally passing into recognizable thin-bedded tan siltite grading up into black argillite characteristic of the Wallace Fm, Piegan Group (fig. 12). Return to the cars by walking down the ridge almost to its bottom and then traversing left above the creek to the campground.

Figure 9. Kyanite, andalusite, and sillimanite coexist in the shear zone. (A) Slabbed foliated biotite quartzite showing details and sequence of minerals. Colleen Elliott photo, mineral id, and interpretation. (B) Slabbed foliated biotite quartzite showing kyanite and andalusite concentrated along some layers and also along the cross-cutting fracture/vein on the left side.

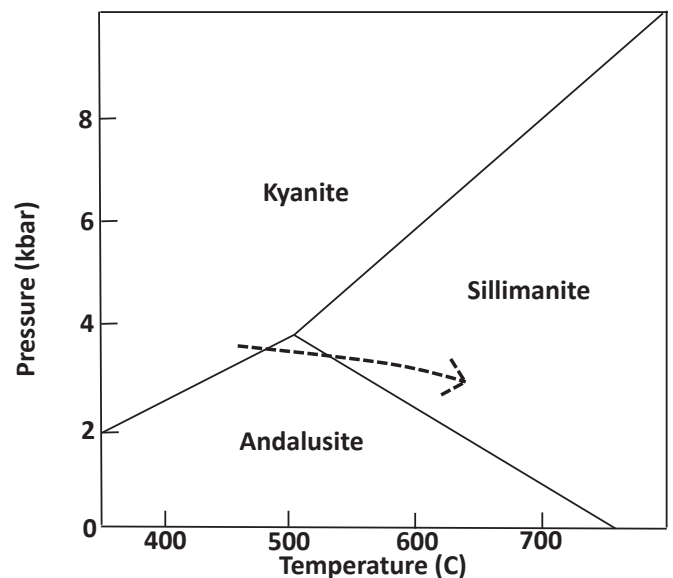


Figure 10. Dashed arrow on aluminosilicate phase diagram shows how the sequence kyanite–andalusite–sillimanite might have formed with an increase in temperature and with minimal or slow pressure decrease that would not require tectonic exhumation.





Figure 11. View of large outcrop in the upper part of the shear zone developed in Piegan Group strata. Outcrop is oriented NE–SW, with SW on the right. Asymmetric folds and a brittle fault drawn in red suggest top-to-the-SW (right) reverse-sense shear. However, note that the quartzite layers are discontinuous and may represent sheath folds developed from earlier ductile shear. Schistosity developed in the darker layers parallels the quartzite layers.



Figure 12. Deformation quickly decreases above the shear zone. Photo shows graded beds of light gray siltite/quartzite grading up to black argillite. Also note the pinch-and-swell character of some siltite–quartzite beds and the gutter in the upper left. These features are characteristic of the Wallace Fm of the Piegan Group.



FIELD DAY 2: ACROSS THE SLEEPING CHILD METAMORPHIC COMPLEX

This field trip is a strenuous all-day hike with 2,000 ft of elevation gain/loss and some off-trail travel. It examines high-grade Mesoproterozoic Belt rocks and Paleoproterozoic basement rocks, their contacts and possible relationships, and crosses the Stony Lake thrust.

Drive south out of Hamilton on Highway 93 for a few miles and turn left at the flashing yellow light onto the Skalkaho Road (State Route 38). Immediately turn right into the Park and Ride lot. Zero your odometer here.

Mile 0.0. Park and Ride lot. Turn right, back onto the Skalkaho Road, and proceed south to a sharp left bend at 0.5 mi.

Mile 0.5. Sleeping Child Road. Turn right at the sharp bend onto Sleeping Child Road. The road parallels the Bitterroot River for a couple miles, then turns east up the valley of Sleeping Child Creek. The surrounding dry hills are comprised of metamorphosed Paleoproterozoic crystalline basement and Mesoproterozoic Belt rocks intruded by Cretaceous to Tertiary granitic plutons. Proceed to mile 7.2, after a sharp right bend.

Mile 7.2. Stop 1. Pull out on the right shoulder across from some outcrops. There is very limited parking. The right side of the roadcut exposes the distinctive coarse-grained 1,863 Ma orthogneiss with near-vertical foliation, and amphibolite-grade schist and gneiss, and at least two types of Tertiary–Cretaceous granite to the left. Across the gulch left of the roadcut is coarse-grained, feldspar-poor quartzite assumed to be Mesoproterozoic upper Belt Supergroup. These outcrops illustrate the difficulties in determining the relationships between the basement orthogneiss and the Belt quartzite. Unfortunately, a Tertiary–Cretaceous granitic intrusion separates the orthogneiss from concordant schist, and the schist is separated from the Belt quartzite by the shallow gulch. Are the schists Paleoproterozoic basement, or are they instead part of the Belt package? Is the thin layer of fine-grained quartz–feldspar gneiss within the schist Paleoproterozoic basement or deformed Cretaceous granite? What is the nature of the contact between the quartzite north of the gulch and the roadcut rocks?

These relationships are equally obscure over most of the SCMC. In one unique locality (Field Day 3), silicified mylonite with due-east lineations and top-to-the-east shear sense separates Belt quartzite from basement orthogneiss, but additional layers of orthogneiss of unknown age also occur within the quartzite.

Return to the vehicles and carefully drive up the Sleeping Child Road with many blind corners. The road passes vertical quartzite layers and then enters a tight canyon. The canyon outcrops are a mix of Cretaceous through Tertiary granite and Paleoproterozoic orthogneiss. Where the canyon opens up, there is a large parking area on the right.

Mile 9.5. Stop 2. Park here to start the hike. Cross the road, go through the wire gate, and ascend the rough logging road converted into 4-wheeler track up Sawdust Gulch. Paleoproterozoic orthogneiss underlies the left (west) side of the gulch, separated from Mesoproterozoic quartzite on the right (east) side by a north–south-trending, down-to-the-east fault (fig. 2). There are also outcrops of Paleoproterozoic orthogneiss on the right side structurally beneath the quartzite, but they are not visible from the trail. Look at the quartzite float along the trail. It is medium-grained and quartz-rich, and interpreted to be from the Lemhi strata, upper Belt Supergroup, based on the detrital zircon data from a nearby sample (fig. 3B). Although the sample was fine-grained and feldspathic instead of medium-grained and clean, we will see the two types of quartzite interlayered later today. Proceed up the trail through lichen- and moss-covered outcrops, noting migmatite float (fig. 4A).

Follow the main road where it switchbacks left and leaves the drainage. Beyond the bend are outcrops of coarse-grained Paleoproterozoic orthogneiss similar to that of the Stop 1 roadcut. Its foliation strikes parallel to the road and dips into the hill. Intrusions of undeformed Tertiary–Cretaceous granite and pegmatite abound. The road then bends right, cuts across the foliation, and passes structurally upward into coarse-grained Belt quartzite similar to that viewed at the beginning of the hike. There is also float of fine-grained, layered and foliated, biotite–quartz–feldspar gneiss with



light-colored elongate pods that cross the layering at small angles. This perplexing rock will be discussed later in the trip when we see it in place. The nature of the Paleoproterozoic orthogneiss–Mesoproterozoic quartzite contact is obscured by metamorphism and Cretaceous–Tertiary intrusions, but it is probably a tectonic one as discussed in the geologic summary above.

Continue up the road, passing through a long area of undeformed Tertiary–Cretaceous granite characterized by massive rounded outcrops.

Leave the road where it switchbacks left and head up the gully towards the large outcrop above. The outcrop consists of thinly layered, fine-grained, feldspathic biotite quartzite most typical of the area, intruded by undeformed gran-

ite. Folds appear to be chaotic and rootless. Although it is tempting to call this quartzite “thin bedded,” original bedding has been completely transposed and deformed during multiple tectonic–metamorphic episodes (fig. 13). It is impossible to put a stratigraphic section together in this area, but other, less deformed and less metamorphosed areas of the Sapphire Range expose stratigraphic sections as thick as 4,000 m composed almost entirely of quartzite. These immensely thick quartzite successions are characteristic of the Lemhi strata in the Salmon, Idaho area.

Continue up the gully and rejoin the road, which then passes through more massive Tertiary–Cretaceous granite.



Figure 13. Isoclines of granite and quartzite in the upper part of this outcrop show that the thin layers of quartzite do not represent original bedding. Bedding has been completely transposed.



At a road intersection, turn left, taking the road less traveled. The road continues to traverse massive granite, but large xenoliths of deformed and migmatitic quartzite also occur. Leave the road to the left in the opening below the ridgetop on a prominent cow trail. Contour west on the trail to soon reach dark-colored amphibolite and light-colored gneiss outcrops. Although the amphibolite appears to be undeformed, quartz veins demonstrate that it, like the surrounding rocks, has experienced severe deformation (fig. 14A). The protolith is

probably a mafic igneous rock that could be of any age from Paleoproterozoic to Cretaceous.

In the light-colored, fine-grained biotite–quartz–feldspar gneiss, elongate pods cross layering and foliation at an acute angle (fig. 14B). The gneiss probably has an igneous protolith, and the pods may be bleached or silicified horizons that have dismembered. They appear to have flattened grains parallel to the elongation direction of the pods, with both defining a lineation that plunges gently



Figure 14. (A) Amphibolite with weakly developed foliation looks relatively undeformed, but the folded quartz veins argue for severe deformation. Amphibolite layers are concordant to the quartzite layering (Clark, 1979), but age is unknown. (B) Light-colored elongate pods are oriented at an angle to the compositional layering of this biotite–feldspar–quartz gneiss and consistently define a gently plunging nearly due-west lineation. Note the tight folds near the bottom of photo.



west–southwest. East–west lineations defined by various features are common in the metamorphic rocks of the area, and it is important to note that they cross-cut and post-date the metamorphic layering. Where kinematic indicators are associated with these lineations, they consistently show top-to-the-east shear sense (fig. 6). Sears (2016) interpreted these fabrics to indicate eastward movement on the Stony Lake thrust, which overlies this quartzite.

From here, walk uphill to beautiful outcrops of folded fine- to medium-grained biotite–feldspar quartzite. The folds appear to be sheath folds, and plunge moderately almost due west (fig. 15). Continue up to the top of the hill. Not far up is an outcrop that displays interlayered fine-grained feldspathic quartzite and clean, medium-grained quartzite. Both must be part of the same upper Belt quartzite succession.

Continue to the top of the hill. At the top, quartzite is almost all medium- to coarse-grained and clean in thick layers. A transposed contact must have been crossed.

Walk down the west ridge, enjoying spectacular views of the Bitterroot Mountains, until you encounter a fence. There, turn right, and walk downhill to the north through a beautiful old growth Ponderosa pine/Douglas fir forest. Stay on the right side of the fence, walking down a ridge. Continue downward on the ridge after the fence leaves the ridge. A dark outcrop of gneiss that appears mylonitic soon appears. This outcrop marks the Stony Lake thrust. Foliation strikes nearly east–west and dips 60° north, with sub-horizontal east–west lineations defined by minerals and elongate porphyroblasts/clasts. It is hard to see through the lichen into the rock, but it appears as though sigma-porphyroclasts show north-side-east shear sense. If the foliation is rotated to horizontal, shear-sense is top-to-the-east, consistent with Sears’ (2016) interpretation of the Stony Lake thrust.

The east–west lineations within the shear zone and the underlying migmatitic quartzite appear to post-date the creation of the metamorphic layers, indicating that transposition predates the thrust. However, the kyanite localized within the shear



Figure 15. These tight folds in quartzite are interpreted as sheath folds. Their axes define a gently west-plunging lineation.

zone (see Field Day 1 discussion) suggests that early movement along the Stony Lake fault occurred while the rocks were still at depth.

Continue down the ridge, first through underformed granite, and then into green calc-silicate gneiss of the metamorphosed Piegan Group, middle Belt Supergroup, in the hanging wall of the Stony Lake thrust (see fig. 2). It appears to be very deformed. Calc-silicate gneiss along the Skalkaho highway below experienced the same high grade of metamorphism and deformation severity as did the rocks in the Stony Lake footwall that you have been examining all day. Temporal relationships between thrusting and metamorphism are obviously complex.

Retrace your steps back to the vehicles, saving some time and effort when you reach the ridge by contouring around the hilltop. Contour back to the road and follow it down to the vehicles and retrace your route back to Hamilton.

FIELD DAY 3: MYLONITIC PALEOPROTEROZOIC GNEISS–MESOPROTEROZOIC QUARTZITE CONTACT

This half-day field trip is a steep, hot, off-trail hike, climbing 500 vertical feet. It examines a mylonitic fault contact between Paleoproterozoic orthogneiss and Mesoproterozoic Belt quartzite, as well as other quartz–feldspar gneiss layers within the quartzite.

Drive south out of Hamilton on Highway 93 for a few miles and turn left at the flashing yellow light onto the Skalkaho Road (State Route 38). Immediately turn right into the Park and Ride lot. Zero your odometer here.

Mile 0.0. Park and Ride lot. Turn right, back onto the Skalkaho Road, and proceed south to a sharp left bend at 0.5 mi.

Mile 0.5. Sleeping Child Road. Turn right at the sharp bend onto Sleeping Child Road. The road parallels the Bitterroot River for a couple miles, then turns east up the valley of Sleeping Child Creek. The surrounding dry hills are comprised of metamorphosed Paleoproterozoic crystalline basement and Mesoproterozoic Belt rocks intruded by

Cretaceous to Tertiary granitic plutons. Proceed to mile 10.6.

Mile 10.6. Park in a small turnout on the left side of the road at the mouth of Twomile Creek. We will start our hike here.

Cross the dry drainage and ascend a hot, weedy slope toward a series of large outcrops. The lower outcrops are coarse-grained orthogneiss (fig. 5) similar to that of Field Day 2. It has a crystallization age of 1,863 Ma (see Geologic Setting section above) and is therefore part of the Paleoproterozoic pre-Belt basement. Note the elongate quartz–feldspar pods outlined by biotite that define a shallow east–west lineation. The biotite defines a weak, gently north-dipping schistosity.

The most rugged outcrops above contain good exposures of the gently dipping contact between the orthogneiss and the overlying quartzite (fig. 16). The contact is mylonitic, but also silicified, making both the contact and the fabrics difficult to see. This is the only location found so far where a fault clearly separates the Paleoproterozoic basement from the Mesoproterozoic Belt quartzite. In other areas, intervening schist or granite obscures the relationships. However, because the quartzite is interpreted as uppermost Belt (see Geologic Setting section above), it is likely that all contacts are tectonic and not stratigraphic.

Mylonitic lineations here bear west–northwest, and sigma-shaped porphyroclasts show top-to-the-east shear. These kinematics are nearly identical to those of the Eocene Bitterroot mylonite located 10 mi to the west. Are they related, or are these the result of older, possibly compressional, tectonism? Lineations defined by various features have similar bearings and shear-sense throughout the SCMC, and probably represent Cretaceous tectonism (see Field Day 2 above, and Foster, 2000; Sears, 2016).

Continue upward, into the overlying quartzite. The quartzite is clean and medium-grained, similar to that near the basement contact on Field Day 2. Although the quartzite is often migmatitic (fig. 4A), there are also thicker layers (0.5 m) of quartz–feldspar gneiss with probable igneous protoliths. One gneissic layer contains isoclinal folds, and others contain asymmetric porphyroclasts suggesting simple shear (fig. 17). Quartzite can be





Figure 16. Top of Brunton and overhang mark the mylonitic and silicified contact between strained Paleoproterozoic orthogneiss and the overlying Mesoproterozoic quartzite. Lineations in the outcrop plunge gently west-northwest and shear-sense indicators show top-to-the-east displacement.



Figure 17. Numerous gneissic layers with probable igneous protoliths occur within the quartzite unit. (A) Axial planes of isoclinal folds are parallel to the layers. (B) Gneiss with strain fabric.

either medium-grained and feldspar-poor, or fine-grained and feldspathic. Both are interpreted to be uppermost Belt Supergroup (see Geologic Setting section above).

At the top of the ridge are slightly displaced exposures of gneiss with porphyroclasts and S-C fabrics showing top-to-the-east shear sense (fig. 5). Are these deformed granitic layers also part of the Paleoproterozoic basement, or are they deformed Cretaceous intrusions as Sears (2016) suggested? It seems as though the latter interpretation is simpler to explain.

Walk the ridge north, to the right, until it intersects a 4-wheeler track. Descend this steep, loose track back to the vehicles and retrace your route back to Hamilton.

Optional stop for those not on the Field Day 2 trip. Drive back down the Sleeping Child road until your odometer reads 13.9 and pull out on the right shoulder next to a distinctive outcrop with a large tree root in its center. This is Stop 1 of Field Day 2, and examines the Paleoproterozoic orthogneiss–schist–quartzite contact.

Refer to Stop 1, Field Day 2, for a complete description of these outcrops. Compare the orthogneiss–quartzite contact to that of Twomile Creek.

REFERENCES

- Buchholz, C.E., and Ague, J.J., 2010, Fluid flow and Al transport during quartz-kyanite vein formation, Unst, Shetland Islands, Scotland: *Journal of Metamorphic Geology*, v. 28, p. 19–39, doi: 10.1111/j.1525-1314.2009.00851.x
- Burmester, R.F., Lonn, J.D., Lewis, R.S., and McFadden, M.D., 2016, Stratigraphy of the Lemhi sub-basin of the Belt Supergroup, *in* MacLean, J.S., and Sears, J.W., eds., *Belt Basin: Window to Mesoproterozoic Earth*: Geological Society of America Special Paper 522, Chapter 5, p. 121–138.
- Corey, M.C., 1988, An occurrence of metasomatic aluminosilicates related to high alumina hydrothermal alteration within the South Mountain batholith, Nova Scotia: *Maritime Sediments and Atlantic Geology*, v. 24, no. 1, p. 83–95.
- Clark, S.L., 1979, Structural and petrological comparison of the southern Sapphire Range, Montana, with the northeast border zone of the Idaho Batholith: Kalamazoo, Western Michigan University, M.S. thesis, 88 p., map scale 1:48,000.
- Desmarais, N.R., 1983, Geology and geochronology of the Chief Joseph plutonic-metamorphic complex, Idaho-Montana: Seattle, University of Washington, Ph.D. dissertation, 150 p., map scale 1:48,000.
- Foster, D.A., 2000, Tectonic evolution of the Eocene Bitterroot metamorphic core complex, Montana and Idaho, *in* Roberts, S., and Winston, D., eds., *Geologic field trips, western Montana and adjacent areas: Rocky Mountain Section of the Geological Society of America*, University of Montana, p. 1–29.
- Foster, D.A., Mueller, P.A., Mogk, D.W., Wooden, J.L., and Vogl, J.J., 2006, Proterozoic evolution of the western margin of the Wyoming craton: Implications for the tectonic and magmatic evolution of the northern Rocky Mountains: *Canadian Journal of Earth Sciences*, v. 43, p. 1601–1619.
- Grice, W.C., Jr., 2006, Exhumation and cooling history of the middle Eocene Anaconda metamorphic core complex, western Montana: Gainesville, University of Florida, M.S. thesis, 260 p., scale 1:100,000.
- Haney, E.M., 2008, Pressure-temperature evolution of metapelites within the Anaconda metamorphic core complex, southwestern Montana: Missoula, University of Montana, M.S. thesis, 110 p.
- Hyndman, D.W., 1980, Bitterroot dome-Sapphire tectonic block, and example of a plutonic-core gneiss-dome complex with its detached supra-structure: *Geological Society of America Memoir* 153, p. 427–443.
- LaTour, T.E., 1974, An examination of metamorphism and scapolite in the Skalkaho region, southern Sapphire Range: Missoula, University of Montana, M.S. thesis, 95 p.
- Lewis, R.S., 1998, Geologic map of the Butte 1° x 2° quadrangle: Montana Bureau of Mines and Geology Open-File Report 363, scale 1:250,000.
- Link, P.K., Fanning, C.M., Lund, K.I., and Aleinikoff, J.N., 2007, Detrital zircons, correlation and provenance of Mesoproterozoic Belt Supergroup and correlative strata of east-central Idaho and southwest Montana, *in* Link, P.K., and Lewis,



- R.S., eds., Proterozoic geology of western North America and Siberia: Society for Sedimentary Geology Special Publication 86, p. 101–128, doi: 10.2110/pec.07.86.0101
- Link, P.K., Steele, T., Stewart, E.S., Sherwin, J., Hess, L.R., and McDonald, C., 2013, Detrital zircons in the Mesoproterozoic upper Belt Supergroup in the Beaverhead and Lemhi Ranges, MT and ID: *Northwest Geology*, v. 42, p. 39–43.
- Link, P.K., Stewart, E.D., Steel, T., Sherwin, J.-A., Hess, L.T., and McDonald, C., 2016, Detrital zircons in the Mesoproterozoic upper Belt Supergroup in the Pioneer, Beaverhead, and Lemhi Ranges, Montana and Idaho: The Big White arc, *in* MacLean, J.S., and Sears, J.W., eds., *Belt Basin: Window to Mesoproterozoic Earth: Geological Society of America Special Paper 522*, p. 163–183, doi: 10.1130/2016.2522(07)
- Lonon, J.D., 2014, The northern extent of the Mesoproterozoic Lemhi Group, Idaho and Montana, and stratigraphic and structural relations with Belt Supergroup strata: *Geological Society of America Abstracts with Programs*, v. 46, no. 5, p. 72.
- Lonon, J.D., 2017, Geologic map of part of the Lick Creek 7.5' quadrangle, southwestern Montana: Montana Bureau of Mines and Geology Open-File Report 690, scale 1:24,000.
- Lonon, J.D., and Berg, R.B., 1999, Preliminary geologic map of the Hamilton 30' x 60' quadrangle, Montana: Montana Bureau of Mines and Geology Open-File Report 340, 6 p., scale 1:100,000.
- Lonon, J.D., and McDonald, C., 2004, Cretaceous(?) syncontractional extension in the Sevier orogen, southwestern Montana: *Geological Society of America Abstracts with Programs*, v. 36, no. 4, p. 36.
- Lonon, J.D., McDonald, C., Lewis, R.S., Kalakay, T.J., O'Neill, J.M., Berg, R.B., and Hargrave, P., 2003a, Preliminary geologic map of the Philipsburg 30' x 60' quadrangle, western Montana: Montana Bureau of Mines and Geology Open-File Report 483, 29 p., scale 1:100,000.
- Lonon, J.D., Lewis, R.S., and Winston, D., 2003b, Belt structure and stratigraphy on the Sapphire block, western Montana: *Northwest Geology*, v. p. 17–28.
- Lonon, J.D., Burmester, R.F., Lewis, R.S., and McFaddan, M.D., 2016a, Giant folds and complex faults in Mesoproterozoic Lemhi strata of the Belt Supergroup, northern Beaverhead Mountains, Montana and Idaho, *in* MacLean, J.S., and Sears, J.W., eds., *Belt Basin: Window to Mesoproterozoic Earth: Geological Society of America Special Paper 522*, Chapter 6, p. 139–162.
- Lonon, J.D., Lewis, R.S., Burmester, R.F., and McFaddan, M.D., 2016b, Mesoproterozoic Lemhi strata represent immense alluvial aprons that prograded northwest into the Belt Sea, Idaho and Montana: Geological Society of America Rocky Mountain Section Meeting, Moscow, Idaho.
- McClintock, M.K., and Cooper, A.F., 2003, Geochemistry, mineralogy, and metamorphic history of kyanite-orthoamphibole-bearing Alpine Fault mylonite, South Westland, New Zealand: *New Zealand Journal of Geology and Geophysics*, v. 46, no. 1, p. 47–62, doi: 10.1080/00288306.2003.9514995
- Meighan, C.J., 2015, PT evolution of the Sentinel Cu deposit, northwestern Zambia: Golden Colorado, Colorado School of Mines, MS thesis, 224 p., <https://mountainscholar.org/handle/11124/20122?show=full> Meighan_mines_0052N_10793.pdf; abstract: https://www.segweb.org/SEG/_Events/Conference_Archive/2014/Conference_Proceedings/data/papers/abstracts/0393-000241.pdf [Accessed June 2020].
- Mueller, P.A., Shuster, R.D., D'Arcy, K.A., Heatherington, A.L., Nutman, A.P., and Williams, I.S., 1995, Source of the northeastern Idaho batholith: Isotopic evidence for a Paleoproterozoic terrane in the northwestern United States: *The Journal of Geology*, v. 103, p. 63–72, doi: 10.1086/629722
- Mueller, P.A., Heatherington, A., Kelley, D., Wooden, J.L., and Mogk, D.W., 2002, Paleoproterozoic crust within the Great Falls tectonic zone: Implications for the assembly of southern Laurentia: *Geology*, v. 30, p. 127–130.
- Ross, G.M., and Villeneuve, M., 2003, Provenance of the Mesoproterozoic (1.45 Ga) Belt Basin (western North America): Another piece in the pre-Rodinia paleogeographic puzzle: *Geological Society of America Bulletin*, v. 115, p. 1191–1217, doi:10.1130/B25209.1
- Schmalholz, S.M., and Podladchikov, Y., 2014, Metamorphism under stress: The problem of relat-



- ing minerals to depth: *Geology*, v. 42, no. 8, p. 733–734.
- Sears, J.W., 2016, Belt-Purcell basin: Template for the Cordilleran magmatic arc and its detached carapace, Idaho and Montana, *in* MacLean, J.S., and Sears, J.W., eds., *Belt Basin: Window to Mesoproterozoic Earth*: Geological Society of America Special Paper 522, p. 365–384, doi: 10.1130/2016.2522(14)
- Vervoort, J.D., Lewis, R.S., Fisher, C., Gaschnig, R.M., Jansen, A.C., and Brewer, R., 2016, Neoproterozoic and Paleoproterozoic crystalline basement rocks of north-central Idaho: Constraints on the formation of western Laurentia: *Geological Society of America Bulletin*, v. 128, p. 94–109.
- Vuke, S.M., Porter, K.W., Lonn, J.D., and Lopez, D.A., 2007, Geologic map of Montana: Montana Bureau of Mines and Geology Geologic Map 62, 2 sheets, scale 1:500,000.
- Wallace, C.A., 1987, Generalized geologic map of the Butte 1° x 2° quadrangle, Montana: U.S. Geological Survey Miscellaneous Field Studies Map MF-1924, scale 1:250,000.
- Wallace, C.A., Schmidt, R.G., Lidke, D.J., Waters, M.R., Elliott, J.E., French, A.B., Whipple, J.W., Zarske, S.E., Blaskowski, M.J., Heise, B.A., Yeoman, R.A., O'Neill, J.M., Lopez, D.A., Robinson, G.D., and Klepper, M.R., 1986, Preliminary geologic map of the Butte 1° x 2° quadrangle, Montana: U.S. Geological Survey Open-File Report 86-292, scale 1:250,000.
- Wallace, C.A., Lidke, D.J., Waters, M.R., and Obradovich, J.D., 1989, Rocks and structure of the southern Sapphire Mountains, Granite and Ravalli Counties, western Montana: U.S. Geological Survey Bulletin 1824, 29 p., scale 1:50,000.
- Wallace, C.A., Lidke, D.J., Elliott, J.E., Desmarais, N.R., Obradovich, J.D., Lopez, D.A., Zarske, S.E., Heise, B.A., Blaskowski, M.J., and Loen, J.F., 1992, Geologic map of the Anaconda-Pintlar Wilderness and contiguous roadless areas, Granite, Deerlodge, Beaverhead, and Ravalli Counties, western Montana: U.S. Geological Survey Miscellaneous Field Studies Map MF-1633C, 36 p., scale 1:50,000.
- Wheeler, J., 2014, Dramatic effects of stress on metamorphic reactions: *Geology*, v. 42, p. 647–650, doi: 10.1130/G35718.1
- Whitney, D.L., and Samuelson, W.J., 2019, Crystallization sequences of coexisting andalusite, kyanite, and sillimanite, and a report on a new locality: Lesjaverk, Norway: *European Journal of Mineralogy*, v. 31, p. 731–737, https://pubs.geoscienceworld.org/ejmin/article-pdf/31/4/731/4881973/ejm_31_4_0731_0737_whitney_2873_online.pdf [Accessed June 2020].





HANGING WALL ROCKS OF THE BITTERROOT DETACHMENT FAULT EXPOSED WEST OF VICTOR, MONTANA

Michael Stickney

Montana Bureau of Mines and Geology, Butte, Montana

This field trip provides an opportunity to see exposures of upper plate rocks of the low-angle Bitterroot detachment in fault contact with the Bitterroot mylonite. At the locale we will visit, this fault contact is a high-angle, post-detachment normal fault. This normal fault offsets the detachment fault, and at nearby locations, offsets glacial deposits, indicating that it remains an active fault. Of particular interest are river gravels with exclusively quartzite cobbles that cap the crest of these foothills. No source area for these gravels exists in today's topography. The slice of upper plate rocks, which these gravels cap, was elevated along a normal fault that lies along the eastern base of the foothills. These features attest to the late Tertiary to post-glacial tectonism along the Bitterroot Range front.

INTRODUCTION

The north-trending, 100-km-long Bitterroot Range lies west of the Bitterroot Valley. Composed primarily of Cretaceous Idaho Batholith granite and less common Precambrian metasedimentary and metamorphic rocks, the Bitterroot Range forms a metamorphic core complex, bounded on the eastern side by a low-angle detachment fault, which—during the Eocene—transported the hanging wall eastward (Hyndman, 1980; Foster and others, 2001). The low-angle detachment fault lies structurally just above the prominent Bitterroot mylonite, which formed in the detachment footwall and is marked by the smooth, gently east-sloping range front. By late Oligocene, steep, east-dipping normal faults developed along the east flank of the Bitterroot Range (Foster and Raza, 2002), offsetting the low-angle detachment fault and down-faulting most of the hanging wall rocks, which Bitterroot Valley alluviation subsequently buried. However, just west of Victor, some of the hanging wall (upper plate) rocks are exposed at the surface where they form some unusual—for the Bitterroot Range front—foothills.

The Bitterroot Range front is marked by a subtle jog between Big and Sweathouse Creeks, just west of Victor (fig. 1). South of Sweathouse Creek, the

range front trends about N.5°W.; from near the mouth of Sweathouse Creek north to near the mouth of Big Creek, the range front trends about N.35°E.; northward from Big Creek, it trends about N.10°E. The 10-km-long section between Sweathouse and Big Creeks is marked by foothills extending east of the prominent range front composed of Bitterroot mylonite. In these foothills, the upper plate rocks of the Bitterroot detachment are exposed because a pair of high-angle normal faults—one tight against the N.35° E.-trending range front, the second lies east of the range front and trends north—intersect at an acute angle near Big Creek. A sliver of upper plate rocks are preserved at the surface between these two normal fault strands. The lead-zinc ores exploited by the Curlew Mine formed at the northern tip of this sliver of upper plate rocks.

ROAD LOG

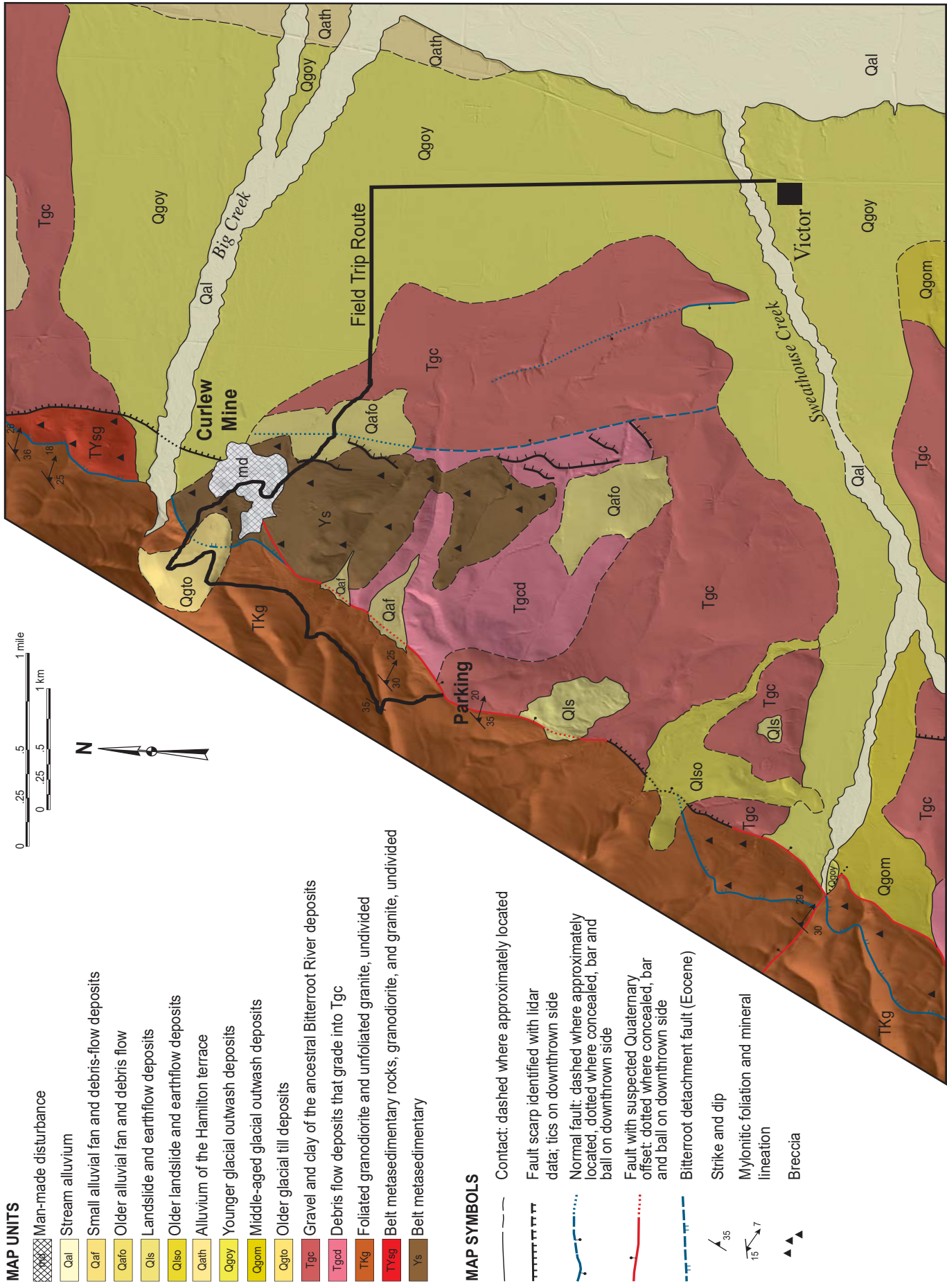
From Hamilton, drive about 11 mi north on U.S. Highway 93 to Victor. At the north edge of Victor turn left on 6th Avenue (46.4195°N., 114.1460°W.). Reset your odometer here. Figure 1 shows the field trip route.

0.0 miles Drive north on Meriden Road.

1.9 miles Turn left (west) on Curlew Orchard Road.

3.0 miles Bear right (northwest) onto Curlew Mine Road.

3.4 miles Crossing the first of two splays of the Quaternary Bitterroot Fault. Down-to-the-east breaks in slope south of the road mark these fault traces. The second (western) trace offsets the glacial outwash terrace both north and south of the modern Big Creek floodplain. The fault scarps are difficult to see from the ground but show up clearly in hillshade images created from LiDAR data (fig. 2).



Adapted from Stickney and Lonn (2018)

Figure 1. Geologic map showing a portion of plate 1 of Stickney and Lonn (2018). The heavy black line indicates the field trip route.

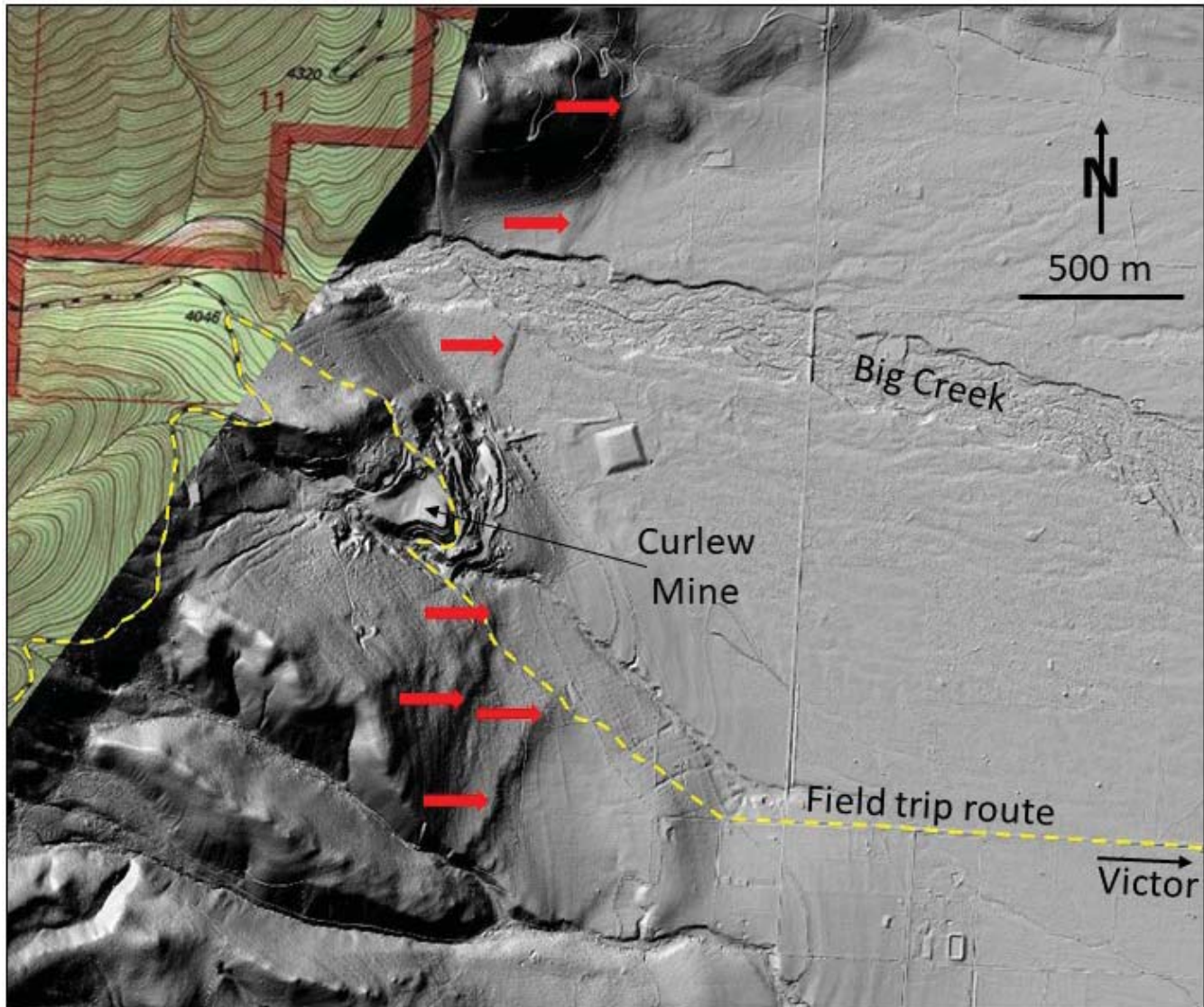


Figure 2. Bare-earth image derived from LiDAR data showing the region around the Curlew Mine. The red arrows mark scarps along a strand of the Bitterroot fault. The smallest scarps, measuring about 2 m, offset the glacial outwash terrace flanking the Big Creek floodplain. The faint horizontal bands visible on slopes and ridges south of the Curlew Mine are Glacial Lake Missoula strand lines.

3.8 miles Approaching the Curlew Mine. Discovered in 1887, the Curlew Mine, by 1892, had a 500-ft shaft and kept a 125-ton mill going steadily (Sahinen, 1957). From 1911 through 1949, the last year of significant underground production, the mine produced nearly 3.4 million lb of zinc, 520,000 lb of lead, 334,000 lb of copper, 194,000 oz of silver, and 4,560 oz of gold. Ore concentrates were shipped to smelters in East Helena, Butte, and Great Falls. In 1968, a small open pit was excavated along with several bulldozer cuts but later production was apparently minimal. The open pit has since been backfilled and the mine and mill sites reclaimed.

The geology surrounding the Curlew Mine is complex and poorly exposed at the surface. Vari-

ous sources in the MBMG Mining Archives mine file describe mineralized faults trending N–S, E–W, N.30°W., and N.30°, and one source maps an asymmetric fold trending northwest with the steeper limb dipping southwest. The Curlew Mine lies within metamorphosed Belt rocks—probably Piegan Group—in the hanging wall of the Eocene Bitterroot detachment fault (fig. 3). Extensive brecciation and silicification characterize these rocks immediately above the detachment fault. A strand of the Quaternary Bitterroot fault trends into the Curlew Mine area from the south, and just north of the mine, this fault offsets the post-Pinedale glacial outwash terrace along Big Creek (fig. 2) about 2 m. There is intriguing information suggesting that Quaternary faulting was encountered in the Curlew Mine workings. USGS geologist



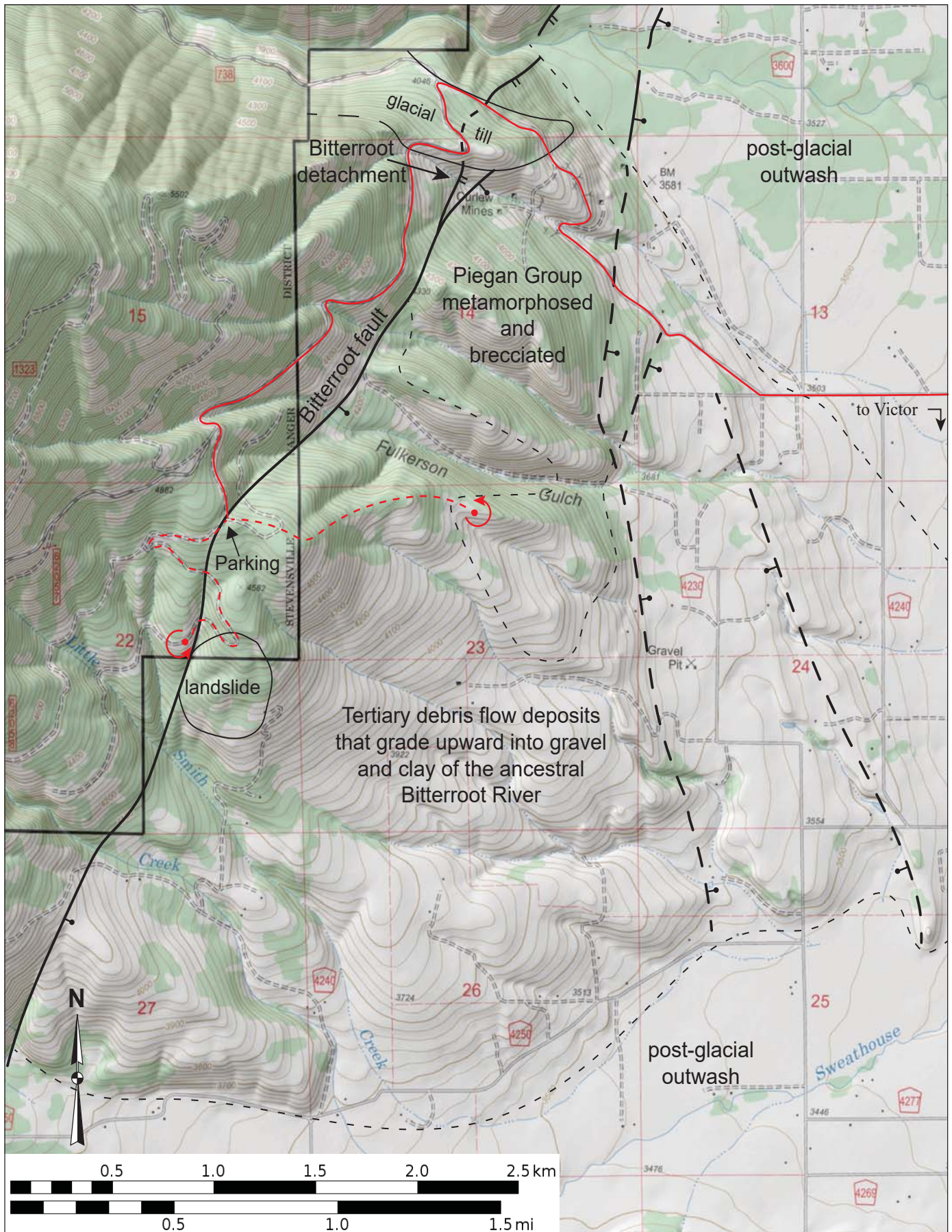


Figure 3. Generalized geologic map, modified from Stickney and Lonn (2018), of the foothills west of Victor showing Neogene strands of the high-angle Bitterroot fault, a small section of the Bitterroot detachment fault, and rocks and deposits that compose the upper plate rocks of the Bitterroot detachment. Solid red line shows the access route; dashed red lines show the walking tours. Note that the land down the slope east of the parking area is privately owned.



Waldemar Lindgren visited the Curlew Mine in about 1903 and published the following account.

“The deposit...strikes north and south and dips 45°E. The ore body was found along a well-defined fissure on an average 10 feet wide and was all along on the east side protected by a thick water-tight cover of clay. Drifts penetrating this clay broke into gravel and sand containing much carbonized wood. From this information, which is doubtless correct, it would appear that the vein occupies a fault fissure between the quartzite and the Pleistocene gravels of the valley. This, besides being most unusual from a mining standpoint, has a structural significance...” (Lindgren, 1904, page 87).

An underground map of the Curlew Mine reproduced by Sahinen (1957) shows several drifts that end against a “line of (granite) wash gravel” striking north and dipping 40°E. No mine workings extend to the east of this plane, suggesting that a normal fault cut off the ore body and placed it in contact with young gravels.

4.5 miles Pass turn off to the Big Creek trail head. Keep left.

4.8 miles Cross the south lateral moraine crest of the Big Creek glacier. The glacier extended eastward just a few hundred meters beyond this point. None of the glaciers of the Bitterroot Range north of Big Creek reached the Bitterroot Valley but most to the south did. Note till containing granite boulders in road cut.

5.0 miles Road turns south onto the east face of the Bitterroot Range front, which is composed of the Bitterroot mylonite. Just before this turn, we crossed the trace of the Eocene Bitterroot detachment fault, which here is buried by the Big Creek moraine.

6.2 miles Bear left onto side road and continue 0.3 mi to a prominent ridge top clearing where the road splits again. Park here (46.4417°N., 114.2035°W.). Note the well-rounded quartzite cobbles—where did they come from and how did they get here?

From here, we can examine the Bitterroot detachment fault hanging wall rocks on foot, along routes shown in figure 3. For a better look at the gravels capping this ridge, walk on the road leading southwest and keep left at the first junction in 0.3

mi. About 0.25 mi beyond this junction, the road cut exposes well-rounded quartzite gravels that cap this ridge. Note the lack of mylonitic and granitic clasts, a potential source area for which lies just west and uphill from here. The next switchback down this road is near the head of a large landslide that extends over 450 ft vertically to the bottom of this south-facing slope. If you continue following the road beyond the switchback, you can find the gully where the gravels are in contact with the Bitterroot mylonite along a high-angle normal fault. Return to parking area.

The gravel cap and underlying deposits are part of the upper plate (hanging wall) of the Eocene Bitterroot detachment fault. At this location, Tertiary debris flow deposits overlie deformed and altered Belt rocks, probably Piegan Group. Recent mapping (Stickney and Lonn, 2018) indicates that remnant bedrock topography existed. Bedrock knobs stick up through the Tertiary debris flow deposits, showing that the bedrock–debris flow contact is irregular. The debris flows seem to have their provenance in local upper plate rocks and include angular blocks of calc-silicate rocks. Although poorly exposed here, exposures at other locations along the Bitterroot Range front suggest that these debris flow deposits may record an unroofing sequence of the Bitterroot dome.

To see these poorly exposed debris flow deposits and the bedrock on which they rest, walk east from the parking area and descend the steep wooded ridge to the northeast. Note that the fence line just below the top of the hill marks the edge of private property, which requires landowner permission to access. The lower contact of the gravel cap is not easy to identify because the gravel cobbles have raveled downhill. Below this, some searching should reveal dark-colored rocks in float with relict bedding and white prismatic crystals up to 2 cm long. I speculate that this is metamorphosed Piegan Group. The white crystals are albite, perhaps pseudomorphs after scapolite. If you descend to a prominent bench on the ridge where a modern ditch crosses (about 0.75 mi and 550 vertical feet below the parking area), there are several large granite boulders. These glacial erratics sit at an elevation of about 4,140 ft, near the high-stand of Glacial Lake Missoula. Just beyond this bench, the ridge narrows and steepens, and brecciated and si-



licified carbonate- and/or calc-silicate-bearing rock is exposed. These rocks have calcite veins and also include some angular clasts of white, fine-grained quartzite. These rocks are probably similar to, and continuous with, those at the Curlew Mine. Slog back up to parking area and retrace route back to Victor.

ACKNOWLEDGMENTS

U.S. Geological Survey National Earthquake Hazards Reduction grant G17AP00051 provided funding for detailed geologic mapping in the Victor area. Thanks to Mr. Robin Hood for granting permission to access the private property. Thanks to Jeff Lonn and Katie McDonald for helpful reviews. Susan Smith's assistance with figures 1 and 3 are gratefully acknowledged.

REFERENCES CITED

- Foster, D.A., Schaferb, C., Fanning, C.M., and Hyndman, D.W., 2001, Relationships between crustal partial melting, plutonism, orogeny, and exhumation: Idaho Bitterroot batholith: *Tectonophysics*, v. 342, p. 313–350.
- Foster, D.A., and Raza, A., 2002, Low-temperature thermochronological record of exhumation of the Bitterroot metamorphic core complex, northern Cordilleran Orogen: *Tectonophysics*, v. 349, p. 23–36.
- Hyndman, D.W., 1980, Bitterroot dome–Sapphire tectonic block, an example of a plutonic core–gneiss–dome complex with its detached supra-structure, *in* Crittenden, M.D., Coney, P.J., and Davis, G.H., eds., *Cordilleran Metamorphic Core Complexes: Geological Society of America Memoir*, v. 153, p. 427–44.
- Lindgren, W., 1904, Geological reconnaissance across the Bitterroot Range and Clearwater Mountains in Montana and Idaho: U.S. Geological Survey Professional Paper 27, 123 p.
- Sahinen, U.M., 1957, Mines and mineral deposits, Missoula and Ravalli counties, Montana: Montana Bureau of Mines and Geology Bulletin 8, 63 p.
- Stickney, M.C., and Lonn, J.D., 2018, Investigation of Late Quaternary fault scarps along the Bitterroot Fault in western Montana: Montana Bureau of Mines and Geology Report of Investigation 24, 16 p., 2 plates, scales 1:12,000 and 1:24,000.



FIELD TRIP GUIDE TO CRYSTAL MOUNTAIN FLUORITE MINE

Chris Gammons and Francis Grondin

Department of Geological Engineering, Montana Tech, Butte, Montana

GEOLOGIC CONTEXT

The Crystal Mountain fluorite mine is located in the southern Sapphire Mountains, 13 mi due east of the town of Darby. Elevations range from 6,730 to 7,260 ft. Bedrock in the area includes late Cretaceous granodiorite (equivalent of the Idaho Batholith) intruded by Paleocene or Eocene, two-mica granite. The two-mica granites are thought to have been emplaced at roughly the same time that the Bitterroot metamorphic core complex was exhumed along a major, east-dipping detachment fault (fig. 1; Foster and Fanning, 1997). The Sapphire Block, in the hanging wall (fig. 1), also contains Belt-aged meta-sediments that have been metamorphosed to amphibolite facies (Hyndman, 1980). Bedrock in the immediate vicinity of the Crystal Mountain mine has been mapped (Lonn and others, 2003) as “Kgdf,” late Cretaceous, foliated granodiorite. However, several different igneous rock types crop out in the mine workings, indicating multiple intrusive events. Grondin (2019) studied the mineralogy of the Crystal Mountain Mine and performed microthermometry on fluid inclusions in fluorite. As of this writing, no detailed geologic map exists of the Crystal Mountain deposit.

MINING HISTORY

Open-pit mining at Crystal Mountain took place between 1954 and 1973 by the Roberts Mining Company of Darby. Despite being the largest historic producer of fluorite in Montana, no data on total production or reserves of fluorite are easily available. This information could possibly be obtained by poring through reports in the Taber Collection stored in the Mining Archives Repository of the MBMG. Ore was hauled from the mine to a mill in Darby that could handle up to 50 T/hr. The mine is currently inactive, although there was interest in the 1980s in reprocessing the mill tailings to recover scandium and other rare metals (Foord and others, 1993; Gambogi, 2014). Current ownership of the mine property is private, with the surrounding land belonging to the Bitterroot National Forest.

According to the USGS Minerals Resource Data System, the primary commodity mined at Crystal Mountain was fluorite at 96% grade. The ore bodies occurred as several east-dipping, tabular masses of nearly pure fluorite, hundreds of feet wide, hundreds of feet long, and dozens of feet thick (fig. 2). Two separate locations were worked, known as the Lumberjack Claims and the Retirement Claims. The main open pit (fig. 3, stop 2) is at the Lumberjack site, and

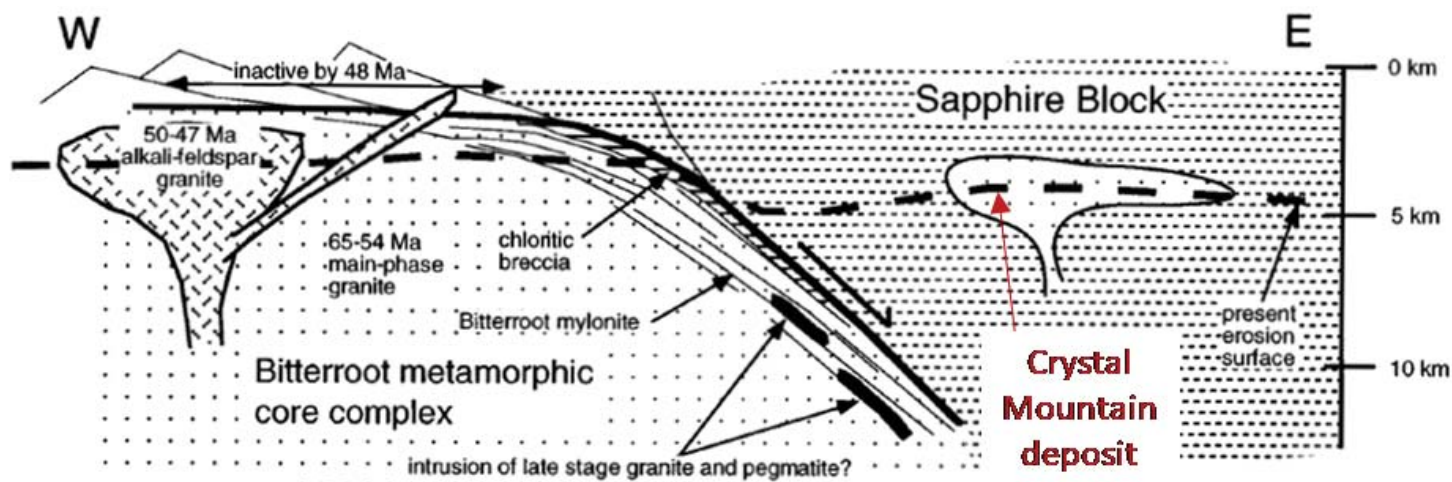


Figure 1. Diagrammatic cross-section showing the relationship between the Bitterroot core complex and the Sapphire Block ca. 51–50 Ma (Grondin, 2019).



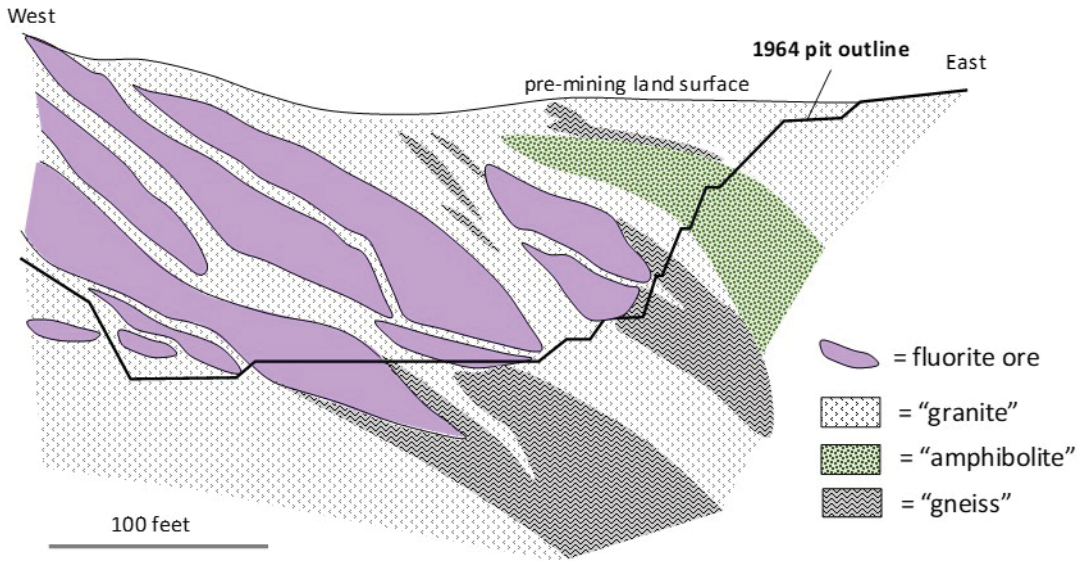


Figure 2. East-west cross-section through the main ore body at the Lumberjack site, showing the outline of the 1964 pit surface and the distribution of massive fluorite ore bodies (Grondin, 2019, redrawn from section E-E' in the Taber Collection, map #53232).

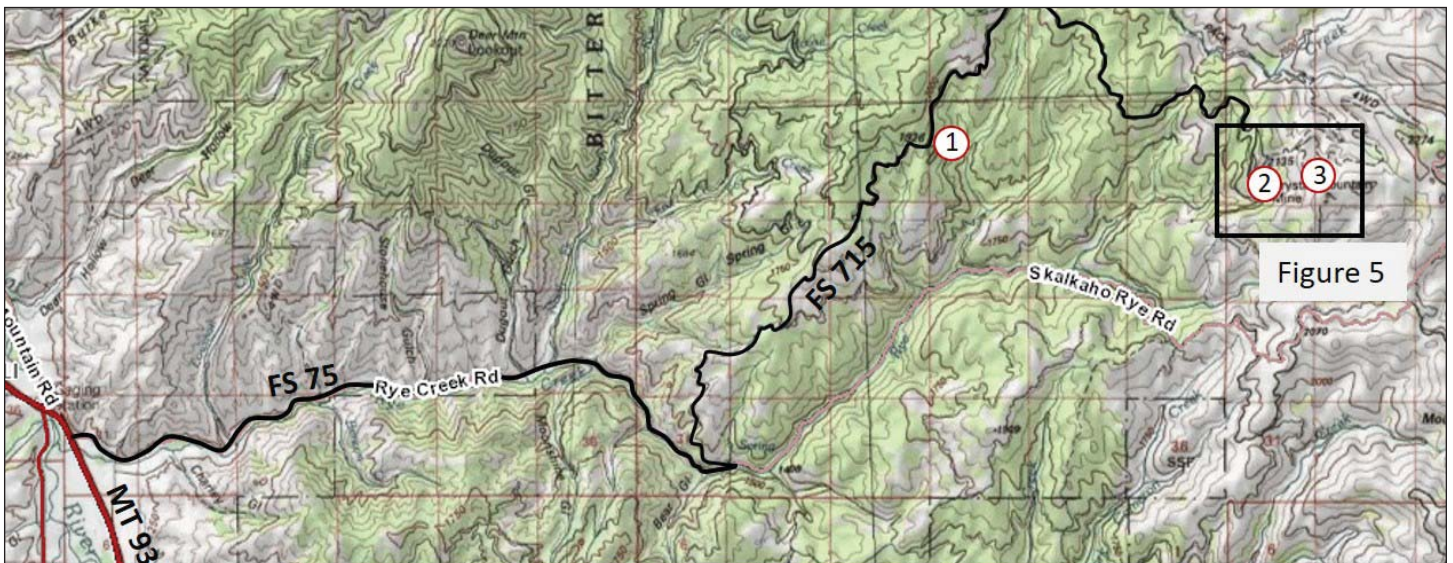


Figure 3. Route to Crystal Mountain showing locations of field trip stops.

most of the fluorite therein has been mined out. The Retirement Claims (fig. 3, Stop 3), which sit at a higher elevation less than a mile east of the main pit, were only mined at a small scale and some large outcrops of fluorite remain in place.

ROAD LOG

0.0 mi Set odometers to zero at the intersection of Rye Creek Road and Montana Hwy 93. Rye Creek Road (Forest Service 75) is about 4.5 mi south of Darby and 0.3 mi after crossing the Bitterroot River. It heads left (east) into the southern Sapphire Range. Turn onto Rye Creek Road and proceed east past the Rye Creek Ranch and many new housing developments (fig. 3).

5.4 mi At an intersection, continue straight on FS-75.

7.7 mi Bear left onto FS-715. The road will switch back and climb steeply. The next 13 mi are very bumpy and washed out in spots, but passable with any vehicle that has higher clearance. The road is not rocky.

9.7 mi Near here it is worthwhile to stop on the road and get out of the car for views to the west and southwest of the southern Bitterroot Mountains. The spectacular peak at the south end of the range is Trapper Peak, with Sugarloaf Peak being the next major mountain to the north. The long, smooth, forested slope that bounds Trapper Peak



to the SE is the trace of the Bitterroot detachment fault (fig. 4). There is about 6,200 ft of vertical relief between the valley floor and the summit of Trapper Peak, more than the Grand Canyon! After stopping, continue on FS-175 about 5 mi to the Stop 1.



Figure 4. View of Trapper Peak (North Peak to the right is slightly lower) and the planar, shallow-dipping trace of the Bitterroot detachment fault. Photo taken from lower Rye Creek Road looking southwest.

14 mi STOP 1—Discovery of the Crystal Mountain Mine

Park on right side of the road at a bend. Here one sees good views to the east towards the crest of the southern Sapphire Mountains, with the dumps of the Crystal Mountain mine visible (unless there is forest fire smoke) 3 mi to the east. Consider how hard it would be to explore for and locate a new mineral deposit in this thickly forested terrain.

The fluorite lodes at Crystal Mountain were discovered by L.I. Thompson and A.E. Cumley in 1937 while building trail for the Forest Service. A glitter on a far hillside was noticed, which proved to be the sun reflecting off of the fluorite masses at the surface. Being toxic to vegetation, no trees or lichens could grow on the fluorite. Thompson and Cumley later claimed the area, but were not good geologists: they thought they had discovered either a beryl or a barite deposit. The area lay dormant until 1951 when a visit by the U.S. Bureau of Mines revealed the site's potential as a high-grade fluorite deposit. Seven outcrops of massive fluorite were mapped, including one mass that measured 180 by 240 ft in area (Taber, 1952).

16.3 mi Keep right (stay on main road).

17.3 mi Keep right (stay on main road).

20.0 mi Continue through open gate.

20.6 mi STOP 2a—Crystal Mountain Mine

The entrance to the Crystal Mountain Mine is at the right hand fork in the road, 20.6 mi from Rte. 93 (fig. 5). There is a gate at the fork, which is normally locked, and room to park. The mine area is on patented (private) land, and the owners frequent the site in the summer for recreation. Visitors need to get written or oral permission before entering the mine site.

From the gate, walk 0.6 mi to the main level of the former mine. As you pass the old mine buildings, the open pit is on your left (northeast), and mine dumps are on your right (west). Follow the main path counterclockwise to the shore of a small pond in the main open pit. From here one can find fluorite veins in place if one knows where to look. Most of the rocks here are ordinary-looking varieties of granite, pegmatite, and amphibolite (fig. 6A). Contacts between fluorite and country rock are sharp, with no obvious signs of hydrothermal alteration (figs. 6B,C). Most of the fluorite is mined out, but the ground is littered with centimeter-sized fluorite crystals, and larger fragments can be found on the dumps. Most of the fluorite here is colorless. Please don't take more than you need as the site is special.

Although the fluorite masses appear mono-mineralic to the eye, in thin section one finds a number of accessory minerals, especially near contacts with country rock. A list of minerals found by Grondin (2019) is given in table 1. Milky white inclusions of plagioclase are fairly common. The plagioclase crystals may have grown in place, or alternatively may have broken off from the surrounding granites when the fluorite masses were emplaced. Small dark spots in the fluorite may be phlogopite or magnetite, or, if surrounded by purple halos, may be radioactive minerals such as xenotime, allanite, thorite, or fergusonite. Thortveitite, a rare scandium-silicate mineral, was reported from Crystal Mountain by Parker and Havens (1963) and later studied in detail by Foord and others (1993). Most of the thortveitite is microscopic, and is more common where fluorite is in contact



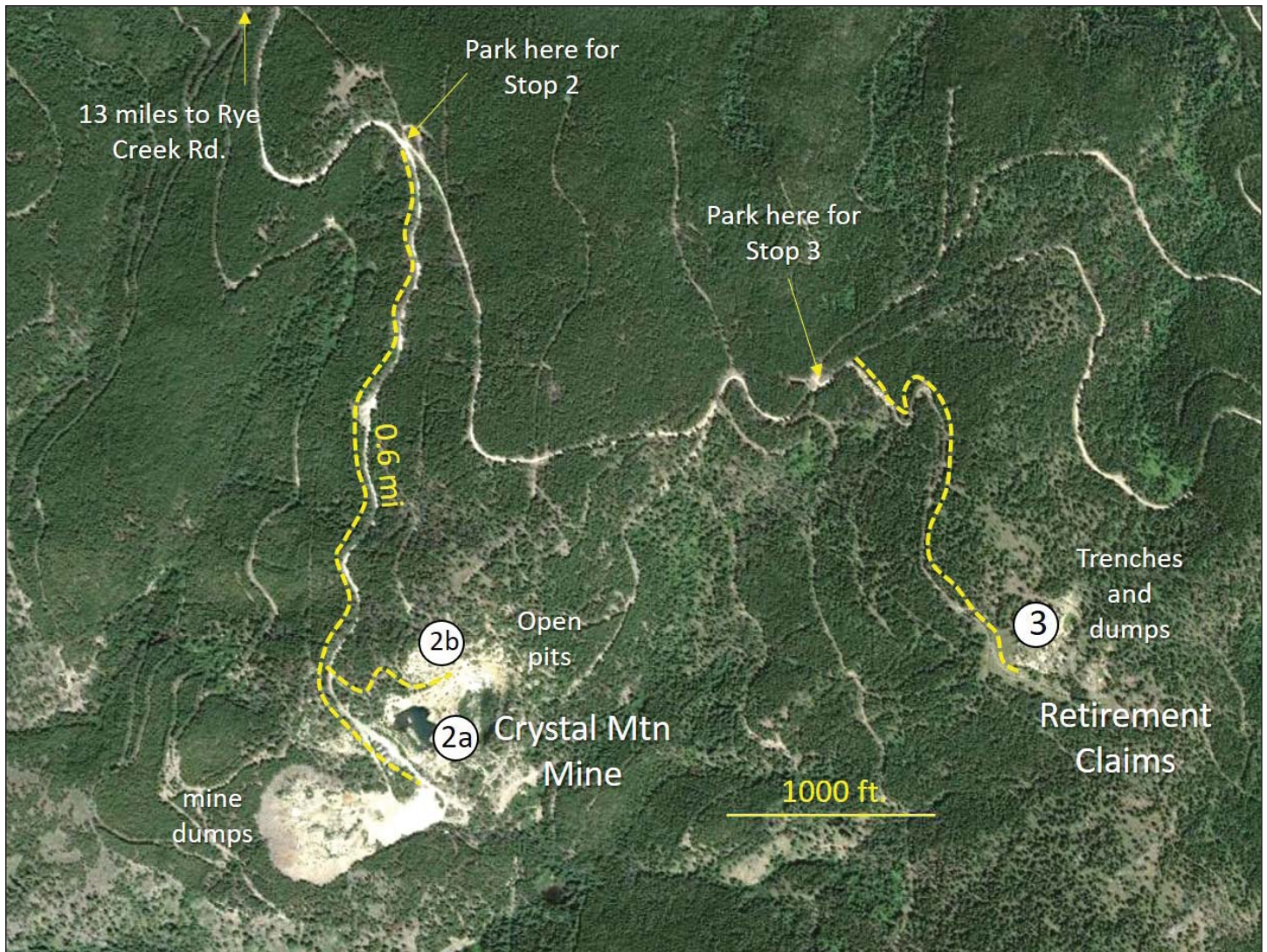


Figure 5. Google Earth image of the Crystal Mountain mine area showing stops 2a, 2b, and 3.

with amphibolite or biotite-rich country rock. Overall, accessory minerals at the Crystal Mountain deposit tend to be enriched in yttrium (Y) and heavier REE, and the fluorite itself is Y-rich (between 0.1 and 1.0 wt% Y, C. Gammons, unpubl. data). This is in contrast to the carbonatites of southern Ravalli County that are enriched in light REE (e.g., Ce, La). Sulfide minerals are rare at Crystal Mountain, although some samples containing chalcopyrite, pyrrhotite, and pyrite were found on the dumps and in drill core by Grondin (2019).

STOP 2b—Upper Level of Crystal Mountain Mine

To get to the upper part of the mine, walk back towards the main gate (about 0.1 mi from the last mine building) and look for a track to the right. This track will lead to the upper mine.

The uppermost bench of the Crystal Mountain mine has some interesting outcrops where one can see the hanging wall contact of a shallow-dipping mass of fluorite (now mostly mined out) overlain by pegmatite and an odd “migmatite” that contains swirls and globules of purple fluorite (fig. 7). Grondin (2019) speculated that the fluorite masses at Crystal Mountain could have formed by separation of an immiscible CaF_2 -rich melt from a granite melt. The intermingling textures seen in the fluorite-bearing migmatite support this idea.

Return to cars at the mine gate. Proceed east on FS-715 by taking the left fork from the parking spot. The road is a bit rough, but passable for most cars with higher clearance.



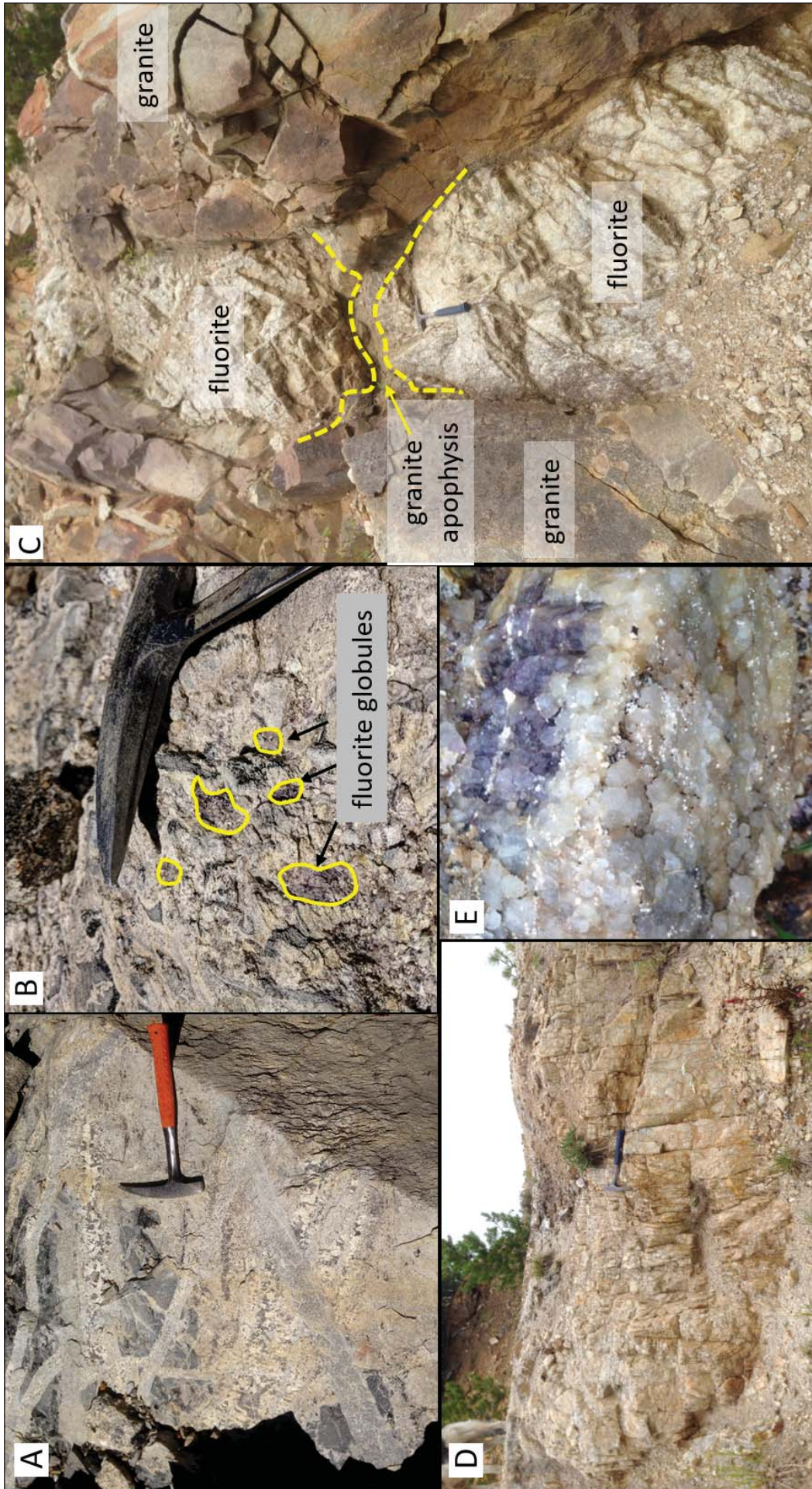


Figure 6. Field photographs from Stops 2a (A, B, C) and 3 (D, E). (A) Intersecting granite-pegmatite-aplite dikes with mafic inclusions. (B) Rounded globules of fluorite in same rock as in A. (C) Large fluorite vein-dike (rock hammer in center) in main pit. (D) Large mass of fluorite at Retirement Claims (rock hammer below bush). (E) Although colorless when exposed to the sun, some of the fluorite has a deep purple color on a fresh surface. Opaque white specks are plagioclase feldspar.



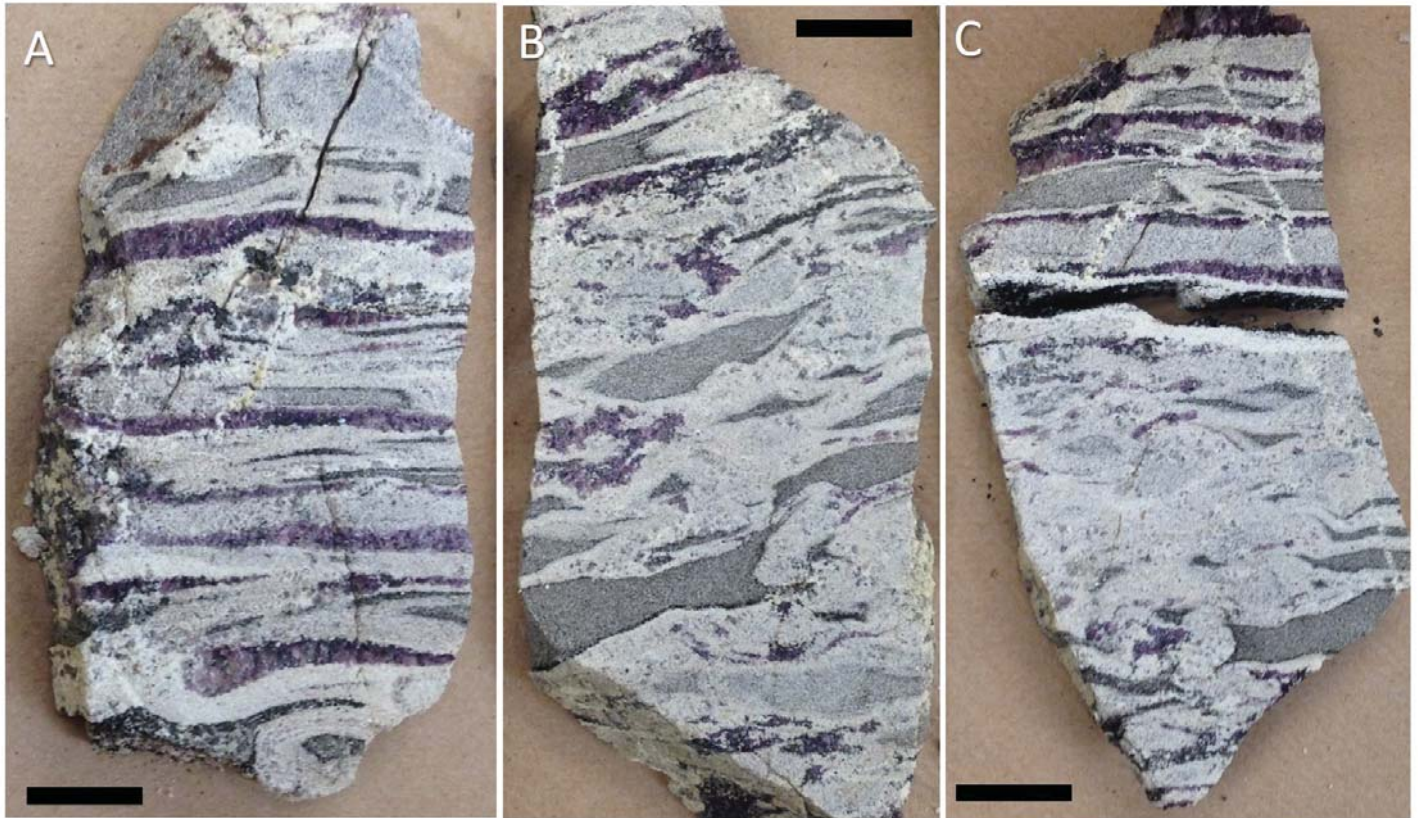


Figure 7. Purple fluorite in “migmatite” from Stop 2b, upper level of main pit at the Lumberjack Claims. Three slabs of the same rock are shown. Black scale bar is 1 in.

21.3 mi STOP 3—Retirement Claims

About 0.7 mi from the parking spot for Stop 2, park in an open area where several roads intersect. Walk less than 100 ft further on FS-715, turn right (south) off the main road onto an old mine road that has been reclaimed, with many downed trees. Follow this road less than half a mile to the Retirement Claims. The main trench (actually a narrow open pit) exposes several outcrops of fluorite in contact with granite and pegmatite (figs. 6D,E). The fluorite is pale where exposed to sunlight, and deep purple on a broken surface. Massive quartz can be found in float and shallow pits to the NW of the main diggings.

Before leaving the mine site it is worth having a discussion about how the fluorite formed. Was it hydrothermal (grew from hot water) or magmatic (crystallized from a melt)? Why are the fluorite masses so large and so pure, and why are there no obvious alteration zones where the fluorite is in contact with country rock? The M.S. thesis of Grondin (2019) has some clues to help solve the puzzle. Grondin found primary fluid inclusions in fluorite that were extremely salty (>50 wt%

NaCl) and homogenized at very high temperatures (up to 500°C and higher). Using fluid inclusion geobarometry, Grondin (2019) concluded that the hot brines were trapped in fluorite at a minimum pressure of 3.0 kbar, which translates to a lithostatic depth of >10 km. These results rule out the idea that fluorite at Crystal Mountain could have formed in an epithermal environment. It is possible that the massive fluorite bodies crystallized directly from an immiscible, fluorite-rich melt (Yang and van Hinsberg, 2019) and exsolved small fluid inclusions as they cooled. More work is needed to discriminate between a high-temperature hydrothermal vs. magmatic origin.

REFERENCES CITED

- Foord, E.E., Birmingham, S.D., Demartin, F., Pilati, T., Gramaccioli, C.M., and Lichte, F.E., 1993, Thortveitite and associated Sc-bearing minerals from Ravalli County, Montana: *Canadian Mineralogist*, v. 31, p. 337–346.
- Foster, D.A., and Fanning, C.M., 1997, Geochronology of the northern Idaho batholith and the Bitterroot metamorphic core complex: Magmatism preceding and contemporaneous with extension:



- Geological Society of America Bulletin v. 109, p. 379–394.
- Gambogi, J., 2014, Scandium: U.S. Geological Survey, Mineral Commodities Summaries, February, 2014, p. 140–141.
- Grondin, F., 2019, Mineralogy and fluid inclusion study of the Crystal Mountain fluorite mine, Ravalli County, Montana: Butte, Montana Tech, M.S. Thesis, 69 p.
- Hyndman, D.W., 1980, Bitterroot dome-Sapphire tectonic block, an example of a plutonic-core gneiss-dome complex with its detached suprastructure: Cordilleran metamorphic core complexes: Geological Society of America Memoir 153, p. 427–443.
- Lonn, J.D., McDonald, C., Lewis, R.S., Kalakay, T.J., O’Neill, J.M., Berg, R.B., and Hargrave, P., 2003, Preliminary geologic map of the Philipsburg 30' × 60' quadrangle, Montana: Montana Bureau of Mines and Geology Open-File Report 483, 1 sheet, scale 1:100,000.
- Parker, R. L., and Havens, R. G., 1963, Thortveitite associated with fluorite, Ravalli County, Montana: U.S. Geological Survey Professional Paper 475-B, p. B10–B11.
- Taber, J.W., 1952, Crystal Mountain fluorite deposits, Ravalli County, Montana: U.S. Bureau of Mines Report of Investigations 4916, 8 p.
- Yang, L., and van Hinsberg, V.J., 2019, Liquid immiscibility in the CaF₂-granite system and trace element partitioning between the immiscible liquids: Chemical Geology, v. 511, p. 28-41.





LATE QUATERNARY FAULT SCARPS NEAR COMO LAKE, MONTANA

Michael Stickney

Montana Bureau of Mines and Geology, Butte, Montana

This field trip to the Como Lake area in the southern Bitterroot area will examine fault scarps developed in a series of glacial moraines of different ages that new LiDAR data have illuminated. We will discuss some of the implications and issues of interpreting faulting history derived from LiDAR data along the way.

INTRODUCTION

The Bitterroot Valley is a half graben developed by normal faulting along the east flank of the Bitterroot Range. Extensional faulting began in the early Tertiary along the low-angle Bitterroot detachment fault and was superseded by more typical high-angle Basin and Range style faulting, now recognized as the Bitterroot fault, which continues to present. The main tectonic basin of the Bitterroot Valley extends for 65 km from just south of Hamilton, north to Lolo, and basin-fill deposits exceed 1,000 m in thickness (Smith, 2006). South of Hamilton at the latitude of Skalkaho Creek, the Bitterroot Valley dramatically narrows, becoming a much less substantial tectonic basin, with the Bitterroot River flowing essentially on bedrock. Despite the dramatic north–south differences in the tectonic character of the Bitterroot Valley, the late Quaternary expression of the Bitterroot fault extends for about 100 km along the Bitterroot Range front.

Barkman (1984) and Lonn and Sears (2001) previously mapped some of the young faults but had not the means to recognize their full extent and youthfulness. The U.S. Geological Survey Quaternary Fault and Fold Database (USGS and MBMG, 2020) includes a generalized trace of the Bitterroot fault but has no other data beyond a Quaternary classification. The fortuitous collection of LiDAR data in the Bitterroot Valley in 2008 and 2010 revealed the presence of fault scarps developed in Quaternary deposits of various ages. This new LiDAR data aided recent geologic mapping in selected areas that reveals greater fault offsets in progressively older Quaternary deposits (Stickney and Lonn, 2018) and provides indisputable evidence for

post-glacial surface faulting events. This evidence implies that large surface-rupturing earthquakes have occurred repeatedly along the Bitterroot fault during the late Quaternary. These new observations seem to be at odds with the very low levels of historical seismicity and classification of the Bitterroot Valley as the area of western Montana having the lowest seismic hazard levels (USGS Earthquake Hazards, 2020).

ROAD LOG

From Hamilton, drive about 13 mi south on U.S. Highway 93. Turn right (west) on Rock Creek Road, marked by a sign for Lake Como Recreation Area. Proceed west on the Rock Creek Road for 2.9 mi to a wide paved pullout (46.0693°N., 114.2232°W.) on the left at the Como Lake Campground Road intersection. Reset your odometer here. Figure 1 shows the route and stops for this field trip.

0.0 miles Drive southwest toward the Como Lake boat launch.

0.2 miles Cross Rock Creek.

0.7 miles Pass turnoff to Como Lake boat launch.

1.2 miles At intersection, keep left on Como Lake Road.

1.9 miles Road crosses the Bitterroot fault scarp near Shannon Creek.

2.4 miles STOP 1 46.0510°N., 114.2268°W.

Road crosses the crest of an older moraine. Park and walk west on a trail that follows the crest of this ridge, which is the south lateral moraine of the Rock Creek glacier of Bull Lake(?) age. An 800-m walk along this gentle ridge will bring you to an irrigation ditch crossing the ridge through a prominent saddle, which is the graben formed where the Bitterroot fault offsets this moraine. The 5- to 6-m

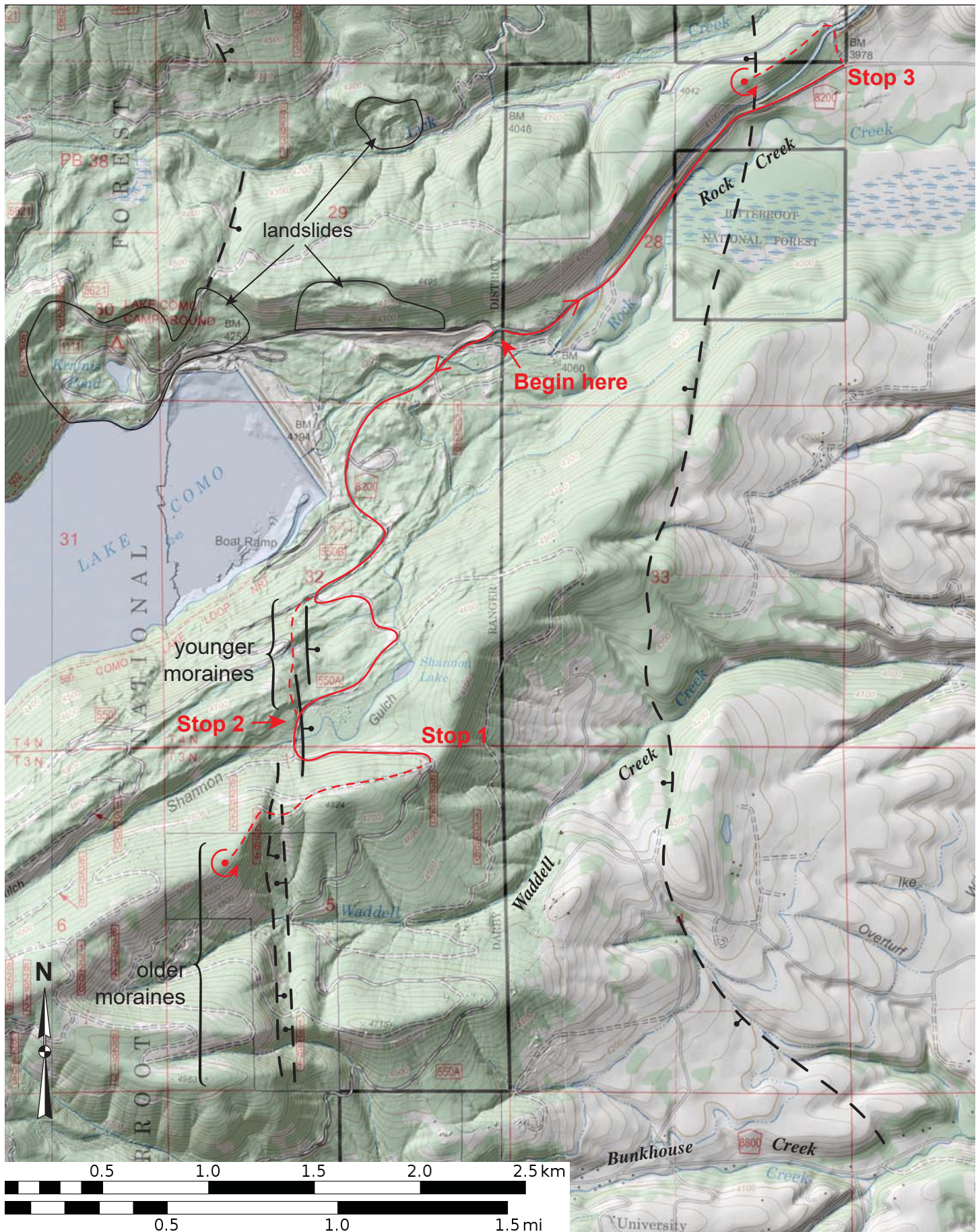


Figure 1. Map showing field trip route, fault traces, and landslides. Dashed red lines show short hikes.



vertical descent into this saddle is the expression of a west-dipping antithetic fault. About 175 m further west along the ridge marks the toe of a steeper east-facing escarpment with a height of about 45 m that marks the main strand of the Bitterroot fault. The toe of this escarpment, with a height of 5 to 8 m, is noticeably steeper than higher parts of the escarpment and probably reflects the most recent offset along this fault. The crest of the escarpment is about 300 m west along the ridge and affords a view to the next ridge south, the divide between Waddell and Bunkhouse Creeks. This ridge appears to be an even older lateral moraine of Rock Creek that has a larger, but otherwise similar, graben where it is offset by the Bitterroot fault (fig. 2).

This graben and the one in the next ridge to the south are obvious geomorphic features that must reflect significant surface offset along the Bitterroot fault since these lateral moraines formed. Topographic profiles along the crests of these two moraines (fig. 3) are difficult to interpret in terms of fault offset. Conservative estimates of the vertical heights of the main (east-facing) scarps measured on the southern and northern profiles are 57 and 41 m, respectively. However, straight lines projected along the moraine crests above and below the grabens don't seem to indicate any net

vertical fault offset. Three possible explanations for this conundrum come to mind.

- (1) Strike-slip instead of normal-slip offset. This explanation seems unlikely because there is no field evidence for horizontal offset along the Bitterroot fault, either here or elsewhere along the length of the Bitterroot fault.
- (2) Pre-existing positive topography along the crest of the moraines that happens to match the location and amount of vertical fault displacement such that the moraine crests now align, interrupted only by the grabens. Certainly moraine crests do have topographic irregularities, but these older moraines seem to have rather smooth profiles except for the grabens. This explanation is simply too coincidental, especially given that two moraines with presumably different ages and with different scarp heights now have similar profiles.
- (3) If the fault producing the grabens had a very shallow dip—matching the eastward slope of the moraine crests—then fault offset could open a graben without causing vertical offsets of the moraine crests beyond the grabens. Although the Bitterroot detachment fault does have a relatively shallow eastward dip (~20 degrees), this dip is significantly



Figure 2. Photograph looking south from the Shannon Gulch–Waddell Creek divide. The dashed white line shows the topography of the moraine crest to the south: the Waddell Creek–Bunkhouse Creek divide. The prominent saddle is the expression of the Bitterroot Fault.



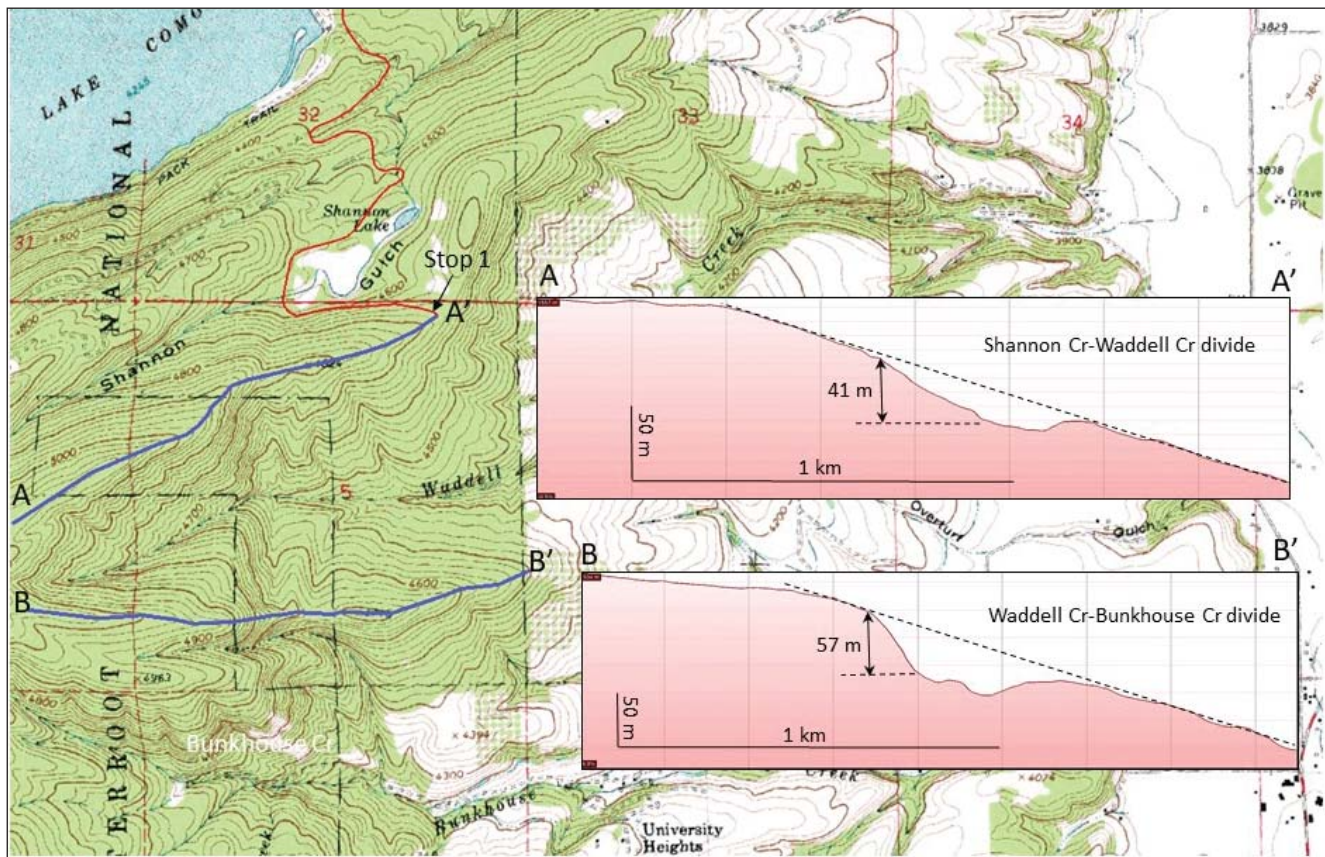


Figure 3. Topographic profiles of the Shannon Gulch–Waddell Creek (profile A–A') and Waddell Creek–Bunkhouse Creek (profile B–B') ridge crests. Both ridges are formed by lateral moraines of the Rock Creek glacier, the southern moraine being older. The prominent saddles in the profiles are the expression of the Bitterroot Fault. Red line shows part of field trip route.

steeper than the slope of the moraine crests. Also, at other locations to the north along the Bitterroot Range front, field relations indicate that the younger and steeper Bitterroot normal fault cuts the older and more gently dipping Bitterroot detachment fault. Furthermore, active range bounding normal faults throughout the Basin and Range province typically dip 45°–60°. Thus, a very low-angle, active normal fault along the Bitterroot Range front seems unlikely. The explanation for the apparent lack of vertical fault offset along the two older moraine crests remains mysterious.

Retrace steps back to Stop 1 and drive back along road for 0.5 mi to Shannon Creek.

2.9 miles STOP 2
46.0526°N., 114.2349°W.

Park along road just north of Shannon Creek. At this stop we will observe the Bitterroot fault scarp where it offsets alluvial/colluvial deposits in Shannon Gulch (fig. 4) and then walk about 0.5 mi north and downhill across a series of small mo-

raine crests with progressively smaller offsets as we descend towards Lake Como.

Shannon Gulch formed when the younger advance (Pinedale) of the Rock Creek Glacier deposited an inset lateral moraine against the higher and older (probable Bull Lake) flank of the lateral moraine to the south. Thus, all fault scarps in the bottom of Shannon Gulch and northward towards Como Lake must be coeval with, or postdate, the Pinedale glacial episode, generally taken to be about 40,000 to 15,000 years before present.

The fault scarp just east of the road is relatively small, with about 3 m of offset. The offset surface in Shannon Gulch appears to be composed of colluvium derived from the adjacent moraines and reworked by Shannon Creek as a weakly developed terrace that may be significantly younger than the Pinedale till from which it was derived.

Follow the scarp north and just beyond the road. The highest, and therefore oldest, Pinedale moraine is offset about 12 m down to the east by the Bitterroot fault. This fault scarp dies out about 150



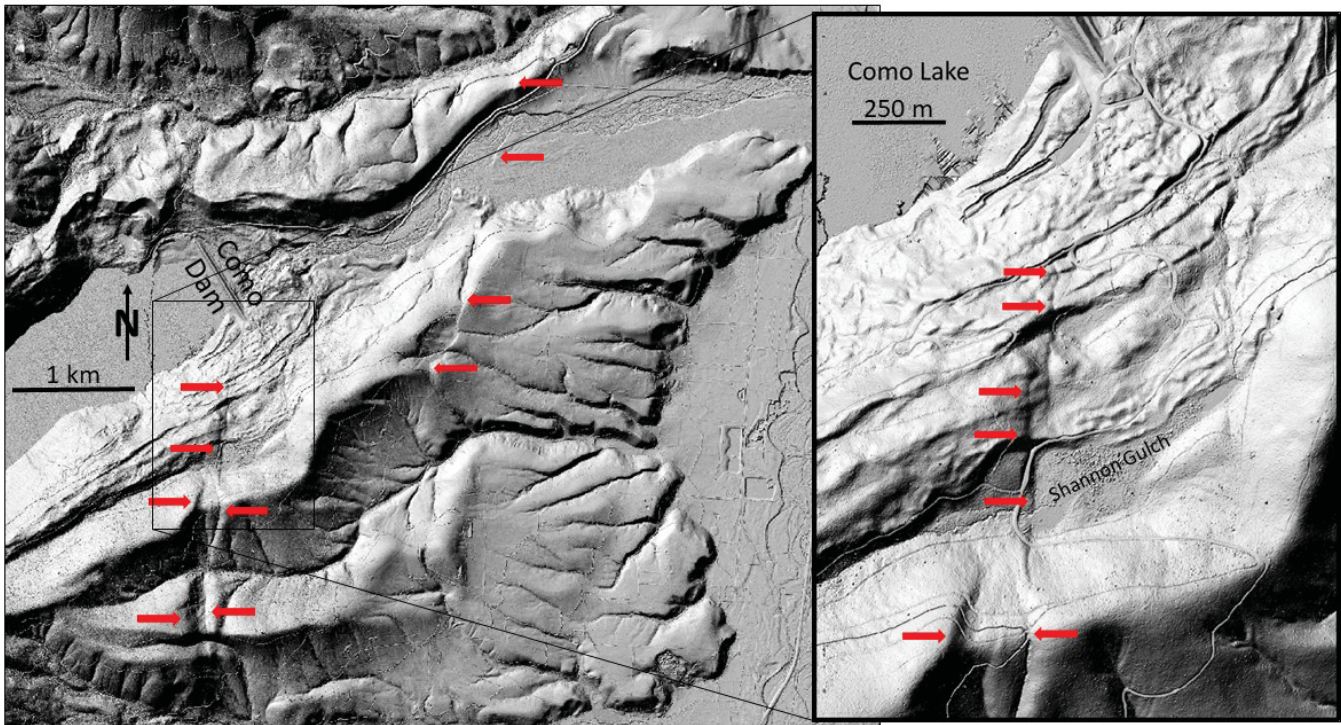


Figure 4. Shaded relief, bare-earth image derived from LiDAR data showing glacial features and faults that offset them. Red arrows mark fault scarps and point towards the down-faulted sides. Inset shows fault scarps just south of Como Dam in greater detail.

m north of here and a right-stepping, *en echelon* scarp about 50 m to the east continues northward (fig. 4). This *en echelon* scarp offsets a prominent moraine ridge by about 6–7 m. Continuing north along the scarp about another 100 m, another small moraine ridge is offset by about 2 m. This is the last visible evidence of surface faulting on the south side of Lake Como. Another small moraine ridge—lower in elevation and therefore younger—just north of the road is clearly not offset by the fault and thus must postdate the last surface rupturing earthquake along this part of the Bitterroot fault. The fact that progressively younger moraines have smaller offsets is clear evidence that multiple earthquakes have occurred during the late Quaternary. If a typical surface-rupturing earthquake produces 2–3 m of offset, then the 12-m offset of the oldest Pinedale moraine implies 4 to 6 major earthquakes during the past ~40,000 years. Given the proximity to Como Dam, further research is needed to determine the timing and recency of major earthquakes on this section of the Bitterroot fault.

Return to vehicles and retrace route back to field trip starting point.

4.8 miles Continue driving down the Como Lake Road past the field trip starting point.

6.2 miles STOP 3 46.0805°N, 114.2016°W

Park along the road where it turns east. Cross the paved road and walk 200 m north up a dirt road and cross the bridge over the Bitterroot irrigation canal. Turn left and follow the ridge southwest for about 400 m to a gentle saddle in the ridge. The slope that descends into the saddle is the expression of a west-facing fault scarp. This ridge is interpreted to be a remnant of an eroded pediment surface that developed on ancestral Bitterroot gravel and clay deposits. The age of this pediment surface is not known, but evidence elsewhere in the western Bitterroot Valley suggests that it is late Quaternary, possibly formed between the Bull Lake and Pinedale glaciations. A short distance southwest of this location, Pinedale till appears to be deposited on top of this surface.

LiDAR data (fig. 5) hints that this fault may offset parts of the Rock Creek floodplain just south of this location. The fault is traceable for at least 5 km to the south. This fault may be antithetic to the fault we saw at Stops 1 and 2.

Return to vehicles. End of field trip.



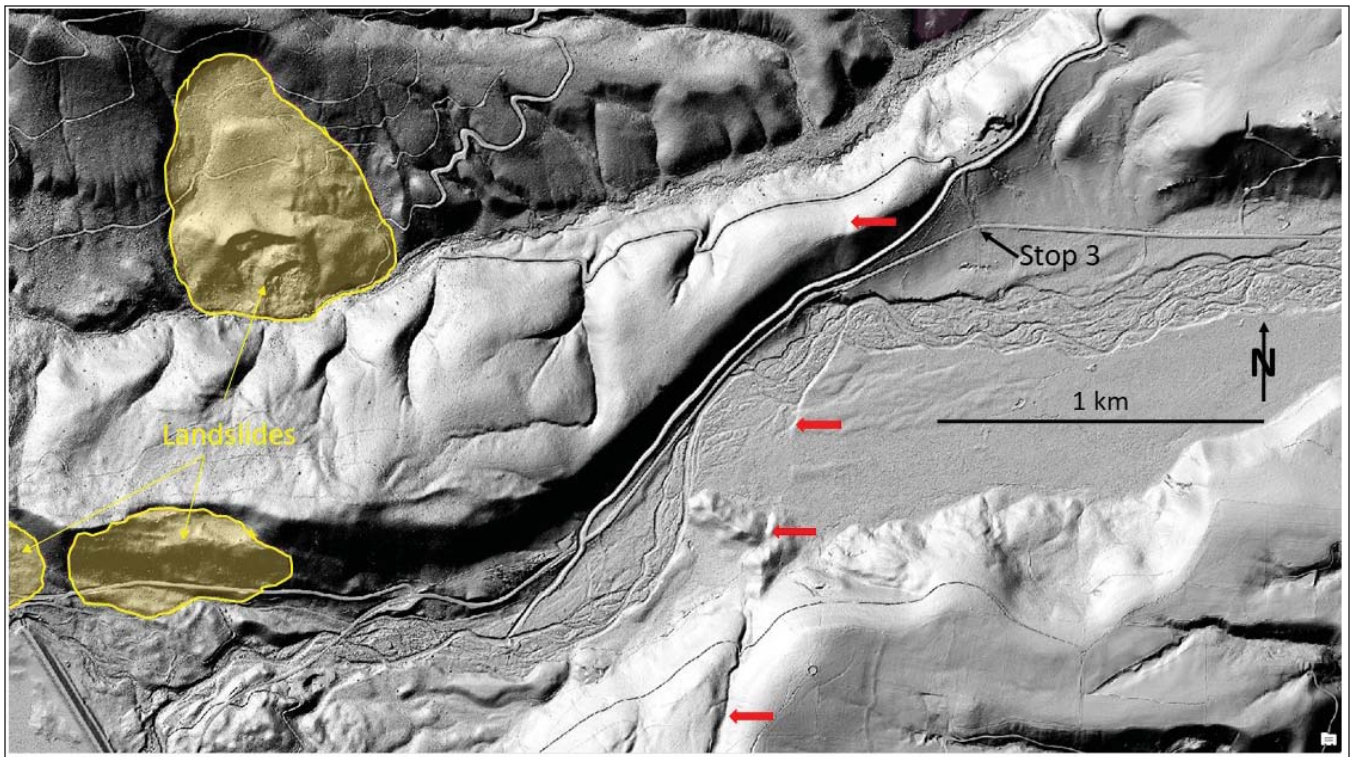


Figure 5. Shaded relief, bare-earth image derived from LiDAR data showing the topography near Stop 3. Red arrows mark the fault trace and point towards the down-faulted side. Landslides are shaded light pink and labeled.

ACKNOWLEDGMENTS

Jeff Lonn provided copies of his field maps for this region, which were most helpful with preparing this field guide. Thanks to Jeff Lonn and Katie McDonald for helpful reviews. Susan Smith's assistance with figure 1 is gratefully acknowledged.

REFERENCES CITED

Barkman, P.E., 1984, A reconnaissance investigation of active tectonism in the Bitterroot Valley, western Montana: Missoula, University of Montana, M.S. thesis, 85 p.

Lonon, J.D., and Sears, J.W., 2001, Surficial geologic map of the Bitterroot Valley, Montana: Montana Bureau of Mines and Geologic Open-File Report 441a, 1 plate.

Smith, L.N., 2006, Thickness of Quaternary unconsolidated deposits in the Lolo-Bitterroot area, Mineral, Missoula, and Ravalli counties, Montana: Montana Bureau of Mines and Geology Ground-Water Assessment Atlas 4B-03, 1 sheet, scale 1:125,000.

Stickney, M.C., and Lonon, J.D., 2018, Investigation of Late Quaternary fault scarps along the Bitterroot Fault in western Montana: Montana Bureau of

Mines and Geology Report of Investigation 24, 16 p., 2 plates.

U.S. Geological Survey and Montana Bureau of Mines and Geology, 2020, Quaternary fault and fold database for the United States, at: <https://www.usgs.gov/natural-hazards/earthquake-hazards/faults> [Accessed May 21, 2020].

U.S. Geological Survey Earthquake Hazards, 2020, at: https://www.usgs.gov/natural-hazards/earthquake-hazards/faults?qt-science_support_page_related_con=4#qt-science_support_page_related_con [Accessed May 21, 2020].



NEW DOCUMENTATION OF A MAJOR MOLYBDENUM–COPPER PORPHYRY SYSTEM IN LOWER WILLOW CREEK, WEST OF THE BLACK PINE MINE, GRANITE COUNTY, SOUTHWESTERN MONTANA

John F. Childs and Darrel A. Dean

Willow Creek Discovery Group, Bozeman, Montana

Figure 1 is a regional geologic and location map showing the locations of the Lower Willow Creek and Smart Creek–Henderson Mountain porphyry systems and other Cretaceous intrusive centers farther west in the Sapphire tectonic block. This allochthonous block was displaced eastward from the present position of the Bitterroot metamorphic core complex at approximately 80 Ma. It was then intruded by a series of granitic centers (fig. 1), including altered rhyolite dikes and molybdenum–copper porphyry mineralization in Lower Willow Creek as shown in figure 2.

In the late 1960s, Bear Creek Exploration drilled two holes west of the Black Pine mine in strongly altered sediments of the Missoula Group of the Middle Proterozoic Belt Supergroup. These holes encountered copper and molybdenum values indicative of a porphyry system. In 1979, Darrel Dean, working for Exxon, drilled a single deep hole (site WC-1 in fig. 2) immediately west of Lower Willow Creek that encountered disseminated molybdenite starting at a depth of approximately 1,200 ft in what was clearly a porphyry system. Mineralization strengthened down-hole with moderate to abundant molybdenite “paint” on veinlet centers from 1,625 ft to the end of the hole at 1,700 ft. However, this hole was never followed up by Exxon for a variety of economic and political reasons.

Further work in 2007 through 2009 by the authors as principals of the Willow Creek Discovery Group (WCDG), and from 2010 through 2011 in a joint venture with Quaterra Resources, confirmed the presence of a large molybdenum–copper porphyry system. This porphyry is one of many porphyry and epithermal mineralized systems that characterize the Great Falls Tectonic Zone of O’Neill and Lopez (1985), sometimes equated to the Idaho–Montana Porphyry Belt (also called the Trans-Idaho Porphyry Belt). This northeast-trending zone of faulting and aligned volcanic and mineralized intrusive centers extends from Boise, Idaho to north-central Montana and into Canada. Porphyry deposits in Montana that form part

of this belt include Cannivan Gulch, Golden Sunlight, Butte, Bald Butte, and Big Ben. In Idaho, deposits include the CuMo porphyry north of Boise and the Thompson Creek porphyry west of Challis, Idaho. Age dates of 67 to 73 Ma have been published for granitic intrusive rocks in the Lower Willow Creek area (Waisman, 1985).

The Willow Creek porphyry is near the eastern end of a string of granitic intrusive centers that trends east–northeast across the Sapphire Tectonic Block (fig. 1). However, the only surface outcrops of the causative intrusive rocks at the Lower Willow Creek prospect are sparse, poorly exposed quartz porphyry dikes in which the quartz phenocrysts are commonly embayed and partially resorbed against the surrounding matrix of the dike. A number of these ENE-striking felsic dikes or sills were mapped in the immediate area by Lonn and others (2003) and by WCDG (fig. 2).

Based on initial geologic reconnaissance, the authors formed WCDG and joint ventured the area with Quaterra Resources Ltd. in 2010. The joint venture embarked on a sampling program including rock and stream sediment samples that led to the drilling of two deep holes west of Lower Willow Creek in 2010, shown as sites WC-1 and WC-2 in figure 2. Hole WC-1, at Stop 5 in fig. 2, was designed to twin the vertical 1979 Exxon hole. The Exxon NC- to BC-size core hole was only surveyed at 500-ft intervals using the acid etch method. We have reinterpreted the results for this hole and we now believe that it deviated to the west where it pierced a molybdenum shell as described above. Hole WC-1 drilled thicker HQ-size core. This hole was surveyed in detail and remained vertical to its total depth of 2,006 ft. The hole intersected weaker porphyry mineralization and we now believe that this hole is separated from the Exxon hole by a major, north-trending, steep to vertical fault zone, the Lower Willow Creek fault (fig. 2). This fault drops the Black Pine block and its contained silver–copper veins on the east down against a deeper portion of the porphyry system on the west.



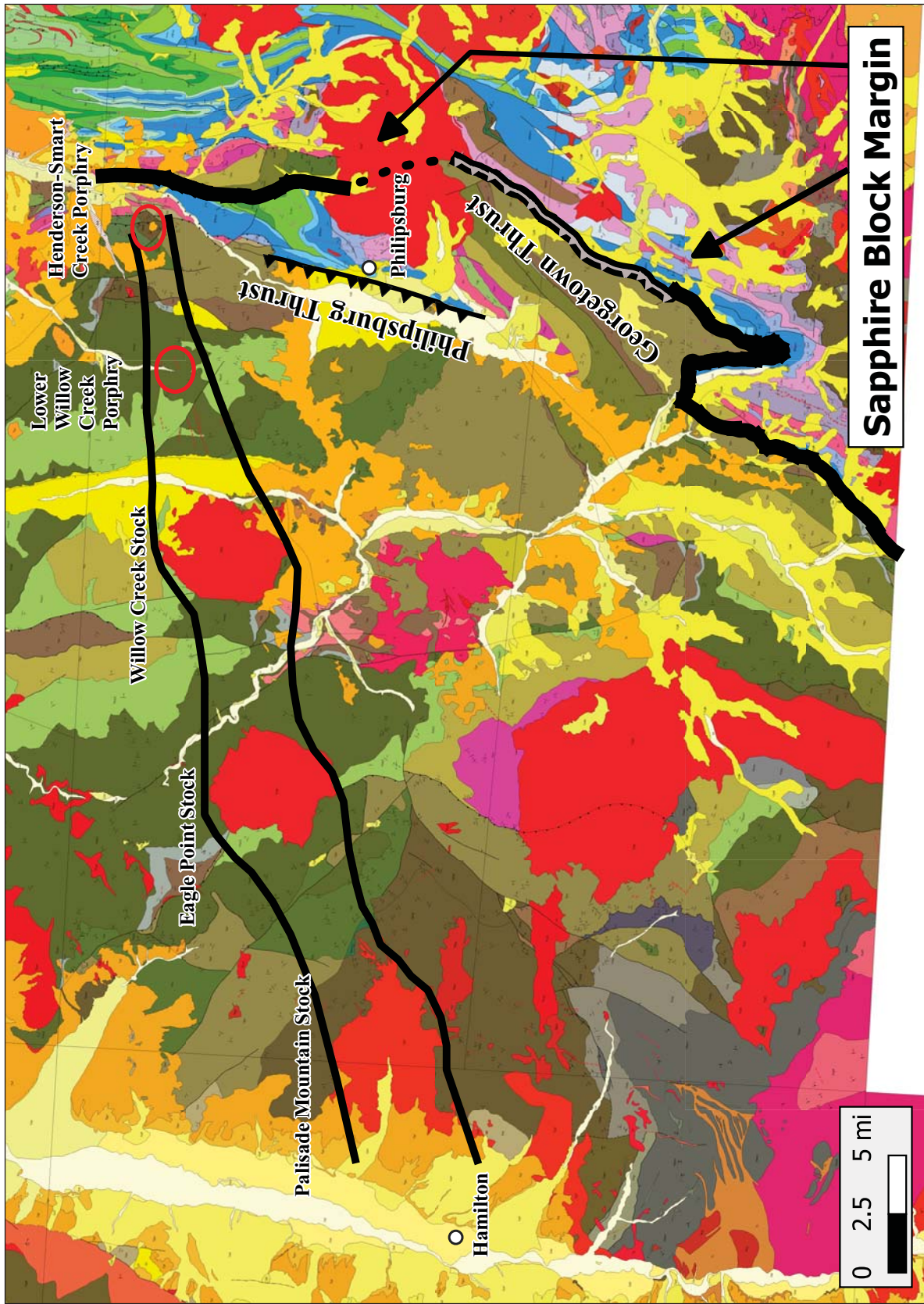


Figure 1. Location map and regional geologic map (after Lonn and others, 2003). The approximate eastern limit of the Sapphire Tectonic Block is shown as a heavy line in the eastern part of the map. The Lower Willow Creek porphyry is the focus of the current field guide and is shown in the northeastern part of the map along with the Henderson Mountain-Smart Creek porphyry system. Dikes and other bodies of granitic rocks in the Lower Willow Creek and Henderson-Smart Creek areas are too small to be shown at the scale of this map, and the Lower Willow Creek area is shown in greater detail in figure 2. Granitic rocks of Cretaceous to Eocene age are shown in shades of red. The five main granitic intrusive centers of the modified Henderson-Willow Creek igneous belt are labeled with informal names.



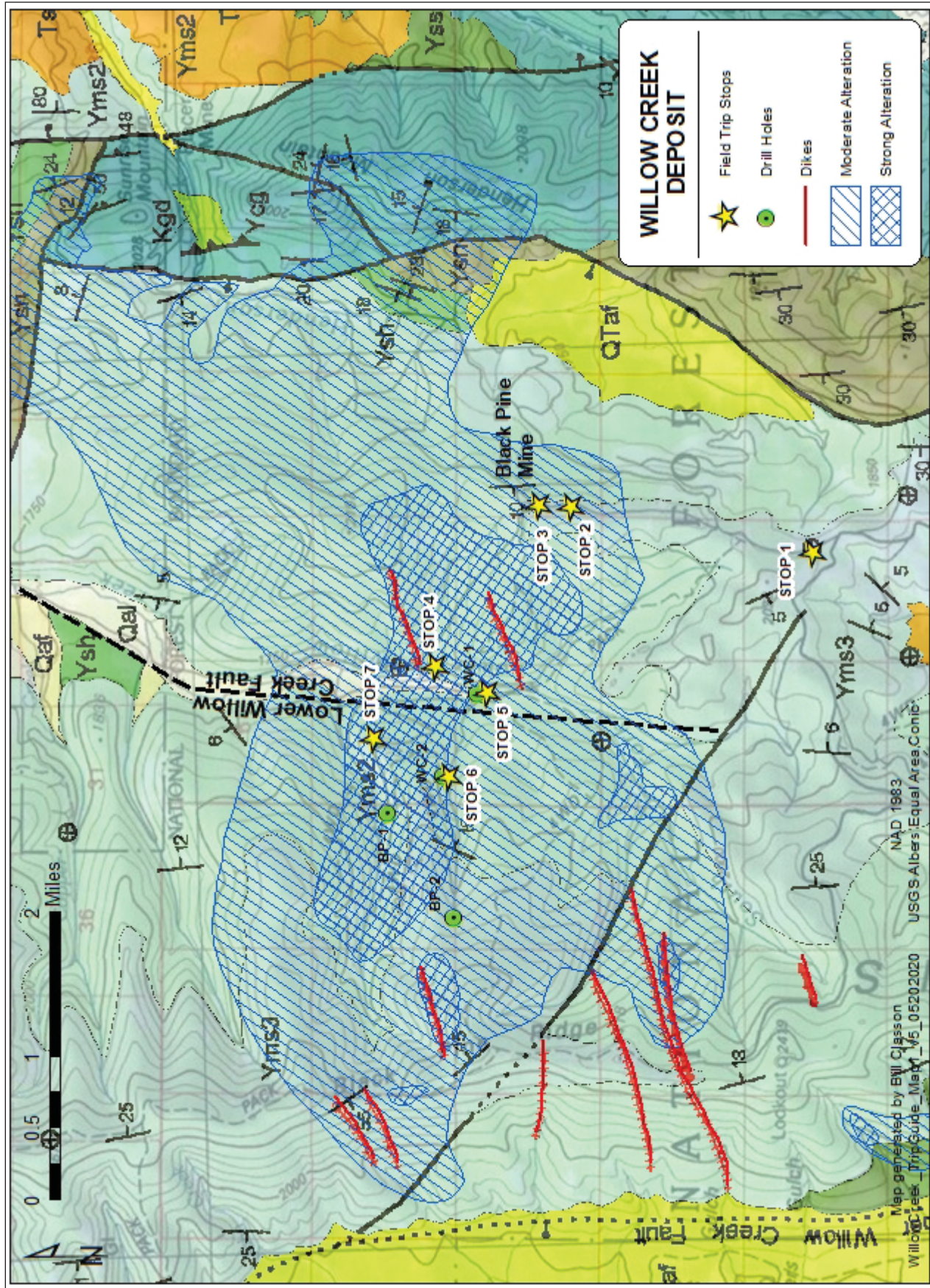


Figure 2. Geologic map of the Black Pine mine area and the Willow Creek prospect in the upper reaches of Lower Willow Creek (Geology from Lonn and others, 2003). Alteration pattern from Bear Creek Mining Company (2007, written commun.). Willow Creek fault based on mapping and drilling by Quaterra Resources/WCDG joint venture.



Drilling in 2010 confirmed the presence of a wide zone of faulting that strikes north–south along the bottom of Lower Willow Creek, here termed the Lower Willow Creek fault zone (WCFZ). There is also evidence for faults along the deeply incised east-flowing tributaries on the west side of Lower Willow Creek. We now believe that high-angle block faulting on the WCFZ and sub-parallel faults uplifted a molybdenite shell that now lies immediately west of the main strand of the WCFZ. When more drilling can better delineate this molybdenite shell, we speculate that it will have a north–south elongation but an unknown east–west thickness and continuation at depth. The upper part of the molybdenite shell was later eroded due to uplift in a horst between the WCFZ and a similar north–south fault that passes east of drillhole WC 10-2 (fig. 2). This fault is unexposed but probably lies approximately midway between holes WC 10-1 and WC 10-2.

The generalized moderate to strong alteration footprint in the Lower Willow Creek area was mapped by Bear Creek Mining Company in the 1960s, and this is shown in figure 2. Later surface sampling and drilling by WCDG has refined the alteration pattern and documented metal zoning typical of a porphyry system. Work to date has defined a core area of strong to intense silica, sericite, and pyrite alteration (QSP) that is locally overprinted by potassic alteration and grades outward to a propylitic zone. Potassic alteration includes secondary biotite and forms an arcuate zone surrounding the strong phyllic zone on the west. Drilling indicates that the pervasive sericitic alteration is locally overprinted by potassic alteration, raising the possibility of more than one mineralizing intrusive pulse. In WCDG/Quaterra core hole WC 10-2, strong phyllic alteration and mineralization were present to a depth of approximately 1,500 ft and are then intercalated with biotitic (potassic) alteration and skarn mineralization deeper in the hole to its total depth of 2,278 ft. Depending on structural interpretation, this hole may have penetrated the carbonate-bearing Shepard or Snowslip Formations or possibly the Middle Belt Carbonate. Overprinting and replacement of phyllic with potassic alteration was noted to the hole's total depth of 2,278 ft.

Detailed vein geochemical sampling in surface exposures and talus within the alteration footprint have defined a systematic progression in metal zoning from a molybdenum center outward through copper

and silver to lead and zinc. Other anomalous metals modeled by Quaterra/WCDG include bismuth, fluorine, and tungsten. The footprint of the moderate to intense QSP alteration covers from 12 to 15 mi², similar in size to the alteration footprint of the porphyry system at Butte, Montana. The importance of the large Lower Willow Creek porphyry system has gone largely unrecognized for two primary reasons. First, the host rocks exposed at surface are argillites, siltites, and quartzites of the Mount Shields Formation of the Missoula Group. These high-silica clastic rocks are largely unreactive and simply appear bleached when they become altered, although they are also typically intensely silicified, recrystallized, and cut by numerous QSP veinlets. Also, the clastic rocks generally lack carbonate units that would have produced more obvious skarn mineral assemblages. Second, expression of the causative plutonic rocks is limited at present levels of erosion to sparse and poorly exposed quartz-eye felsic porphyry dikes or sills. Based upon the 1,200-ft depth to the molybdenum mineralization in Exxon drillhole 1979-1 and the lack of any large intrusive bodies at present levels of erosion, it seems likely that surface exposures represent the upper level of the porphyry system.

Although our understanding of the system is currently limited by the lack of outcrop and general lack of drilling, we interpret the prolific silver–copper mineralization at the Black Pine mine east of Lower Willow Creek as part of the marginal silver–base metal–tungsten zone of the much larger porphyry system to the west. The Black Pine mineralization follows gently west-dipping veins (Waisman, 1985) that Waisman interpreted as thrust faults or ramps in the toe of the Sapphire tectonic block. Waisman dated sericite at the Black Pine mine at 63.9 Ma and proposed that the Black Pine veins were derived from a porphyry system at depth. McClave (2009) described sericitic alteration along the veins, quartz porphyry dikes, small granodiorite bodies, and weak but pervasive sericitic and kaolinitic alteration in and around the Black Pine mine. These features lead McClave, like Waisman, to suggest that porphyry was present at depth below the mine. This is reinforced by the presence of strongly anomalous bismuth and tungsten values at Black Pine.

We agree with this conclusion, but would tentatively place the main porphyry center beneath the strongly QSP and potassic alteration in the uplifted block west of the WCFZ based on alteration zon-



ing and intensity. Hughes (1971) dated stocks in the Henderson–Willow Creek trend at 70.6 to 73.7 Ma and proposed the Henderson–Willow Creek igneous belt to include granitic centers in Upper Willow Creek west of the Lower Willow Creek porphyry described here and the Henderson area farther east. We propose that the Lower Willow Creek porphyry is a third intrusive center in Hughes' igneous belt. We also propose that these three intrusive centers are just the eastern end of a more extensive, structurally controlled string of granitic intrusive centers including that near Eagle Point west of Rock Creek and another farther to the west, centered west of Palisade Mountain and east of Hamilton, MT as shown in figure 1. The east–northeast felsic dikes in the Lower Willow Creek area are interpreted as expressions of the structures that controlled emplacement of intrusive centers within the igneous belt outlined in figure 1.

The west-dipping faults that control the Black Pine veins provided ready conduits for mineralizing fluids emanating from the porphyry system immediately to the west. These structures were likely developed during emplacement of the Sapphire tectonic block at 80–85 Ma (Hyndman, 1980), prior to intrusion of the Henderson–Lower Willow Creek granitic bodies, dikes, and the related porphyry mineralization. We speculate that the Lower Willow Creek porphyry system and its causative intrusive body have a primary, shallow + 20-degree west-dipping orientation that is related to thrust or ramp faults similar to those at the Black Pine mine. These faults provided structural preparation and conduits for intrusive rocks and related porphyry mineralizing fluids. This structural fabric controlled the inferred shallow, west-dipping emplacement of the porphyry system as well as the Black Pine vein system to the east.

The Willow Creek Discovery Group maintains a well-organized core library in Philipsburg that includes all of the core from drillholes WC-1 and WC-2. The group also has available a detailed database including all analytical pulps, rock geochemistry, drill logs, new analytical results for the old Bear Creek drillholes, and other information from the 2007–2011 exploration and drilling program. At present, they control a core group of claims in the central part of the porphyry system.

Mineralized stocks in the Henderson Mountain area, recent drilling of porphyry mineralization in

the Smart Creek area, and our work in Lower Willow Creek suggest to us that this district is underlain by several porphyry centers that may have overlapping alteration haloes. We would further suggest that these intrusive centers are just the eastern expression of a chain of aligned late Cretaceous intrusive centers that extend east–northeast from the Idaho Batholith on the west to just north of the Philipsburg Batholith on the east (fig. 1). This alignment is a proposed extension and revision of the Henderson–Willow Creek igneous belt proposed by Hughes (1971).



ROAD LOG FOR A FIELD TRIP TO THE LOWER WILLOW CREEK PORPHYRY PROSPECT, BLACK PINE DISTRICT, GRANITE COUNTY, MONTANA

Mile 0.0 (UTM 322156 5133834)

Start at the intersection of West Broadway Street and Highway 1 on the west side of Philipsburg, Montana and drive north for 2.1 mi on Highway 1. Turn to the left on Black Pine Road. Head north for 0.2 mi and make a sharp left turn onto Road 178 heading west across Flint Creek.

Stay on Road 178 as it climbs out of the Flint Creek Valley through the foothills of the Sapphire (Long John) Mountains. Proceed west for 1.33 mi and then northwest for 1.1 mi with spectacular views of the Anaconda Range to the south. Cross a cattleguard at 3.1 mi after leaving Highway 1. From here, the road winds to the northwest through horizontal to gently dipping red-weathering interbeds of quartzite, siltite, and lesser argillite mapped as the upper (Yms3; fig. 3) informal member of the Mount Shields Formation of the Missoula Group, Proterozoic Belt Supergroup (Lonn and others, 2003). Continue north for approximately 1.6 mi from the cattleguard to another cattleguard and continue north for 1.7 mi to a third cattleguard. A road splits off to the left just after the cattleguard but stay to the right and go 0.25 mi to Stop 1.

STOP 1

Mile 6.65 (UTM 317593 5143276)

There are two good outcrops of Mount Shields Formation in the 0.9-mi stretch of road north of the cattleguard mentioned above, and we will stop at the first of these locations. These rocks were mapped as informal member 3 of the Mount Shields Formation by Lonn and others (2003). Note the red color of these sediments as this will be in contrast to similar rocks that we will examine in the alteration zone farther north. Here we see interbeds of flat-lying red and pink quartzite and siltite with argillite partings

From Stop 1, drive north for 0.5 mi where more outcrops of Mount Shields Formation are present on the west side of the road, then continue 0.2 mi to a three-way intersection where Forest Road 448 takes off to the right. Continue straight ahead to

the north on Forest Road 8724 following the ridge top for 0.7 mi to a covered shaft on the east side of the road.

STOP 2

Mile 14.7 (UTM 318180 5145983)

Walk up the ramp to the covered shaft. This shaft is part of the Black Pine mine workings. Please stay safe and stay off the shaft cover. We are on the crest of Black Pine Ridge with a view to the west into the allochthonous Sapphire tectonic block and the upper reaches of north-flowing Lower Willow Creek. Look west into the valley of Lower Willow Creek. Drilling and stratigraphy suggest that the down-to-the-east Lower Willow Creek fault runs along the bottom of Lower Willow Creek and likely drops the silver–copper veins of the Black Pine mine hosted by informal member 3 of the Mount Shields Formation down against the phyllic (QSP) to potassic altered rocks of member 2 on the west (fig. 2). The Lower Willow Creek fault is shown in the center of fig. 2.

Note the prominent talus on a ridge west of Willow Creek to the northwest (fig. 4). The talus blocks are intensely altered to QSP and are in the central part of the Lower Willow Creek porphyry (fig. 2). The talus is on the south side of a major east-flowing tributary to Lower Willow Creek that is likely fault controlled. Bear Creek Exploration drilled vertical drillhole BP-1 in 1969–1970 in the western part of this talus. Hole BP-1 intersected significant molybdenum mineralization from 1,600 ft to its end at 2,500 ft, where it assayed 0.035% molybdenum.

There is a second prominent talus barely visible 0.5 mi south of the talus-covered ridge just described (fig. 4, upper left). This second talus is on the north slope of a second, deep tributary valley that drains west into Willow Creek. Bear Creek drilled a second hole (BP-2) to 406 ft in anomalous, but sub-ore grade, molybdenum mineralization approximately 1.0 mi west of the talus in this valley. In 2010 and 2011, Quaterra/WCDG drilled Hole WC-2 in this second talus. Hole WC-10-1




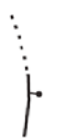



<div style="border: 1px solid black; padding: 2px; width: fit-content;">Qal</div>	<p>ALLUVIUM OF MODERN CHANNELS AND FLOODPLAINS (HOLOCENE) Mostly well-sorted, well-sorted boulders, cobbles, gravel, sand, and silt deposited in modern stream channels and floodplains. Includes both fine-grained overbank deposits and coarse-grained channel deposits. In some areas, older alluvium (Qao) is not divided from Qal.</p>		<p>Fault: unknown series of movement, dotted where concealed</p>
<div style="border: 1px solid black; padding: 2px; width: fit-content;">Qaf</div>	<p>ALLUVIAL FAN DEPOSITS (HOLOCENE AND PLEISTOCENE) Poorly to well-sorted, rounded to sub-angular boulders, cobbles, sand, silt, and clay. Surfaces of these deposits have a distinct fan shape. Deposited by both stream flow and debris flow processes in alluvial fan environments. In some areas, older alluvial fan deposits (Qafo) are not divided from Qaf.</p>		<p>Normal fault: dotted where concealed; bar and ball on downthrown side</p>
<div style="border: 1px solid black; padding: 2px; width: fit-content;">QTraf</div>	<p>ALLUVIAL FAN DEPOSITS (EARLY PLEISTOCENE AND LATE TERTIARY) Poorly to well-sorted, rounded to sub-angular boulders, cobbles, sand, silt, and clay. Surfaces of these deposits have a distinct fan shape and now stand more than 15 m (50 ft) above modern deposits.</p>		<p>Reverse or thrust fault: teeth on upthrown block</p>
<div style="border: 1px solid black; padding: 2px; width: fit-content;">Ts</div>	<p>SEDIMENTARY ROCKS, UNDIVIDED (TERTIARY) Include both coarse- and fine-grained rocks.</p>		<p>Strike and dip of bedding</p>
<div style="border: 1px solid black; padding: 2px; width: fit-content;">Kgd</div>	<p>GRANODIORITIC ROCKS (LATE CRETACEOUS) Biotite-hornblende granodiorite, biotite granodiorite, and tonalite.</p>		<p>Horizontal bedding</p>
<div style="border: 1px solid black; padding: 2px; width: fit-content;">Yme2</div>	<p>MOUNT SHIELDS FORMATION, MEMBER 2, INFORMAL (MESOPROTEROZOIC) Pink to gray, flat-laminated, fine- to medium grained quartzite, with tan-weathering dolomitic blebs. Contains some crossbeds. In the Anaconda Range of the southernmost part of the map area, and in the Skalkaho region, the Mount Shields contains abundant pebbles and crossbeds, making it difficult to distinguish from the Bonner Formation. However, in contrast to the Bonner, Lewis (1998b) found subequal amounts of plagioclase and potassium feldspar and a total feldspar content of 25–35% in the Mount Shields.</p>		
<div style="border: 1px solid black; padding: 2px; width: fit-content;">Yme3</div>	<p>MOUNT SHIELDS FORMATION, MEMBER 3, INFORMAL (MESOPROTEROZOIC) Mostly red siltite to argillite couples and couplets with abundant mudcracks, mud chips, and salt casts.</p>		
<div style="border: 1px solid black; padding: 2px; width: fit-content;">Yes</div>	<p>SHEPARD AND SNOWSLIP FORMATIONS, UNDIVIDED (MESOPROTEROZOIC) Total thickness as much as 1,067 m (3,500 ft).</p>		
<div style="border: 1px solid black; padding: 2px; width: fit-content;">Ysh</div>	<p>SHEPARD FORMATION (MESOPROTEROZOIC) Dark green siltite and light green argillite in microlaminae and couplets that are dolomitic and have a characteristic orange-brown weathering rind. Upper part is red, thinly bedded dolomitic quartzite and siltite. Poorly exposed but weathers into thin plates. Estimated to be 152 m (500 ft) thick.</p>		
<div style="border: 1px solid black; padding: 2px; width: fit-content;">Ysn</div>	<p>SNOWSLIP FORMATION (MESOPROTEROZOIC) Mostly red sand to clay couplets with abundant ripples and mud cracks. Green and red, dolomitic siltite-argillite laminae are common near the base. Increasing amounts of siltite and quartzite up section. Some fine- to medium-grained, feldspar-poor quartzite is present in beds less than one foot thick. The upper portion is mostly flat-laminated, medium- to coarse-grained quartzite that is difficult to distinguish from the Mount Shields Formation. Mudcracks and mud chips are abundant throughout. In the Anaconda Range are some thin lenticular beds of coarse-grained quartzite that contain granule-sized lithic fragments. Thickness as much as 914 m (3,000 ft).</p>		
<div style="border: 1px solid black; padding: 2px; width: fit-content;">Ysg</div>	<p>CALC-SILICATE GNEISS OF THE METAMORPHOSED PIEGAN GROUP (MESOPROTEROZOIC) Greenish, diopside-rich, calc-silicate gneiss, fine-grained quartzite, marble, and minor schist. Metamorphic equivalent of the Piegan Group.</p>		

Figure 3. Abbreviated explanation for the geologic map in figure 1. For full explanation please refer to Lonn and others (2003).





Figure 4. View looking northwest from Stop 2. Workings of the inactive Black Pine mine are in the foreground. The fault-controlled valley of the north-flowing Lower Willow Creek runs from left to right behind the knoll in the middle distance. Field trip Stops 6 and 7 are in the large snow-covered talus piles on the west side of Lower Willow Creek. Holes WC-10-2 and BP-1 are 0.5 mi apart and were drilled in a central zone of strong QSP alteration and molybdenum–copper veinlets.

and the 1979 Exxon hole that WC-1 was intended to twin were collared where the east–west tributary containing Holes BP-2 and WC-10-2 joins Willow Creek. This deep tributary, like the one 0.5 mi to the north, is probably underlain by a fault. Surface samples collected by WCDG in the area of these drillholes carried up to 0.07% Mo. Ore minerals include chalcocite, molybdenite, pyrite, ferrimolybdenite, sphalerite, and galena. Gangue minerals include quartz, sericite, clays, chlorite, calcite, and fluorite.

The material around the shaft at Stop 2 includes ore mined from the Black Pine veins. Quartz vein fragments here include chalcopyrite, chalcocite, blue copper oxides, galena, sphalerite, and manganese oxides. Note also the light green to tan color of the quartzites due to alteration to sericite and clays.

Field trip Stops 2, 3, and 4 are underlain by the workings of the Black Pine mine, which was developed in gently west-dipping veins dated at 63.9 Ma. The veins are interpreted to have developed along preexisting reverse faults associated with eastward translation of the Sapphire tectonic block

between 75 and 80 Ma (Hyndman, 1980; Kerrich and Hyndman, 1986).

Continue north on Forest Road 8724 for 0.24 mi to Stop 3.

STOP 3 **Mile 14.94 (UTM 318256 5146441)**

As at Stop 1, we will examine relatively unaltered interbeds of argillite, siltite, and quartzite of the Mount Shields Formation. This outcrop is close to the contact between the informal upper member (Yms3) and the underlying informal member (Yms2) of the Mount Shields Formation (Lonn and others, 2003). Note the abundant well-preserved desiccation cracks, ripple marks, mud chip breccias, and salt casts diagnostic of Mt Shields member 3 in these red sediments.

Just north of Stop 3, turn west on Forest Road 678 and proceed for 0.5 mi though a major reclamation site where mine dumps have been recontoured and capped with topsoil as part of reclamation supported by funds that were set aside by ASARCO. The headframe and other structures of the Black Pine



underground mine are visible on the ridge south of the road. Continue west down the eastern slope of the Lower Willow Creek Valley for 1.1 mi. We are dropping down through poorly exposed sections of the Yms2 member of the Mount Shields Formation to Stop 4. The Yms2 member of the Mount Shields is described by Lonn and others (2003) as pink to gray, flat-laminated, fine- to medium-grained quartzite with tan-weathering dolomitic blebs.

STOP 4

Mile 16.54 (UTM 316429 5147575)

Here we will examine a dump from the lower part of the Black Pine mine complex. Note the bleaching and strong alteration here. Brown, elongate huebnerite (MnWO_4) crystals are fairly common in this dump and elsewhere in the porphyry system.

The flats on the east side of Lower Willow Creek are underlain by un-reclaimed mill tailings from the Black Pine mill. These extend for approximately 1.5 mi downstream, where they have been eroded by flooding events and washed even farther down Lower Willow Creek.

Continue downhill for 0.18 mi and the road bends to the right before crossing Lower Willow Creek. After crossing the bridge, turn left at the intersection and go south for 0.26 mi to Stop 5 at a drillsite on the west side of the road.

STOP 5

Mile 16.98 (UTM 316071 5147071)

This is the site of the 1979 hole drilled by Exxon that intercepted strong molybdenum mineralization with phyllic alteration at a depth of approximately 1,200 ft. The hole reportedly drilled 100 ft of 0.17% Mo from 1,650 ft to the end of the hole at 1,750 ft that was hosted in strongly QSP altered quartzite, siltite, and argillite with some carbonate. The last 20 ft of the hole contained 0.22% Mo. These footages and values are based on Darrel Dean's recollection, as Exxon's original data are no longer available. Darrel was the project geologist running the drilling program for Exxon. This hole was twinned by vertical hole WC-1 (fig. 1) in 2010 to 2,006 ft. The new hole intersected scattered molybdenite intervals from 280 ft to the end of the hole. This hole drilled through a near-sur-

face, high-angle fault zone (WCFZ), then through strong QSP alteration for its entire length, but did not intercept ore grade mineralization. Our interpretation is that because core size of the Exxon hole was relatively small (NQ and reduced to BQ at depth), it likely deviated to the west into stronger mineralization as it passed through the WCFZ. In contrast, the 2010 hole stayed more vertical and was drilled east of the WCFZ and within the Black Pine mine block, which was dropped down on the east against an uplifted block on the west in which the Exxon hole encountered strong molybdenum mineralization. This interpretation is reinforced by the occurrence of four intervals that are strongly anomalous in lead in hole WC-1 between depths of approximately 500 and 1,000 ft. We infer that these four anomalous zones are the down-dip extensions of the veins that were mined at the Black Pine mine up slope to the east.

STOPS 6 OR 7

At this point we have two options depending on the time remaining and road conditions. We can walk north 300 ft from Stop 5 along the road we drove in on and then hike 0.45 mi uphill in direction North 60° West to Stop 6. Alternatively, if road conditions permit, we can reach Stop 6 by vehicle after visiting Stop 7, as described below.

STOP 6

(UTM 315369 5147466)

Here we can examine alteration features along a drill road in a large talus. This site is where drill-hole WC-2 was collared. This hole was drilled vertically for 1,820 ft in 2010 and deepened to 2,278 ft in 2011. Here, as with hole WC-1, the hole was entirely in strong alteration, but with only sub-ore grades of molybdenum, copper, silver, zinc, and lead. The hole drilled through strong phyllic alteration that transitioned into potassic alteration, with some skarn, and ended in potassic alteration and skarn within a quartz porphyry dike swarm.

If road conditions permit, we can reach Stops 6 and 7 following the route described below.

Backtrack to the north from Stop 5; do not turn right to re-cross the bridge we came in on. Stay to the left on the road that leads north along the west



side of Lower Willow Creek for 0.7 mi. The road splits here, with the right branch heading to the north down Lower Willow Creek. Stay left through a switchback and follow the road uphill to the southwest for 0.7 mi where the road switchbacks again and continues for 0.4 mi to the north–northwest onto a large talus overlooking a deep, east-flowing branch of Lower Willow Creek at Stop 7. This last 0.4 mi is very hard on tires, so you may want to walk or leave some vehicles at the switchback.

STOP 7

Mile 18.78 (UTM 315550 5148177)

This is the more northern of two talus piles that were visible from overview Stop 2. These rocks were mapped as part of informal member 2 of the Mount Shields Formation by Lonon and others (2003). Excellent vuggy QSP alteration textures and strong stockwork veining are visible in the boulders of this large talus. The blocks of Mount Shields Formation in the talus are intensely bleached, recrystallized, and altered to QSP. Thin, vuggy quartz-sulfide veinlets are pervasive and some contain fluorite. Bear Creek drilled Hole BP-1 approximately 0.5 mi west of Stop 7 in the central part of this large talus pile in 1969-70.

STOP 6

Mile 19.08 (UTM 315369 5147466)

If we have not chosen previously to walk uphill from Stop 5 to Stop 6, we can reach Stop 6 by walking or driving south–southwest from Stop 7 for 0.3 mi to a wide area at a switchback in the road. Park the vehicles here and walk another 0.2 mi on contour following the drill road to the south to Stop 6. The description for Stop 6 is provided above.

ACKNOWLEDGMENTS

We would like to thank Bill Classon at Childs Geoscience, Inc. and Nick Fox at Fox Geoscience, Inc. in Bozeman, MT for their help creating the figures for this report. Jeff Lonon and Phyllis Hargrave edited and greatly improved the report.

REFERENCES

- Hughes, G.J., 1971, Petrology and tectonic setting of the igneous rocks in the Henderson-Willow Creek igneous belt, Granite County, Montana: Houghton, Michigan Technical University, Ph.D. dissertation, 236 p.
- Hyndman, D.W., 1980, Bitterroot dome-Sapphire tectonic block, an example of a plutonic-core gneiss-dome complex with its detached superstructure, in Crittenden, M.D., Jr., Coney, P. J., and Davis, G. H., eds., Cordilleran metamorphic core complexes: Geological Society of America Memoir 153, p. 427–443.
- Kerrich, R., and Hyndman, D., 1986, Thermal and fluid regimes in the Bitterroot lobe-Sapphire block detachment zone, Montana: Evidence from $^{18}\text{O}/^{16}\text{O}$ and geologic relations: Geological Society of America Bulletin, v. 97, p. 147–155.
- Lonon, J.D., McDonald, C., Lewis, R.S., Kalakay, T.J., O'Neill, J.M., Berg, R.B., and Hargrave, P., 2003, Preliminary geologic map of the Philipsburg 30' x 60' quadrangle, western Montana: Montana Bureau of Mines and Geology Open-File Report 483, scale 1:100,000.
- McClave, M.A., 2009, A geologic review of the Black Pine mine, Granite County, Montana: Northwest Geology, v. 38, p. 27–34.
- O'Neill, J.M., and Lopez, D.A., 1985, Character and regional significance of the Great Falls Tectonic Zone, East-Central Idaho and West-Central Montana: American Association of Petroleum Geologists, v. 69, no. 3, p. 437–447.
- Waisman, D., 1985, Geology and mineralization of the Black Pine Mine, Granite County, Montana: M.S. thesis, University of Montana, Missoula, 66 p.



GEOLOGY ALONG THE LATE QUATERNARY BITTERROOT FAULT SCARPS, AND IMPLICATIONS FOR SEISMICITY IN THE BITTERROOT VALLEY, WESTERN MONTANA

Jeff Lonn

Montana Bureau of Mines and Geology, Butte, Montana

INTRODUCTION

This all day, 8-mi hike follows the Coyote Coulee trail in the forested Bitterroot Mountain foothills south of Hamilton. Although the topography is gentle, the ups and downs add up to about 1,100 ft of elevation change. Drinking water is not available on the route and, with elevations of less than 5,000 ft, it is likely to be hot in July. The trail offers a surprisingly good look at the major geologic features that shaped the Bitterroot region, including exposures of the two major fault systems that uplifted the mountains, one old (Eocene), and one young and still active. We will also view the Cretaceous–Tertiary granite that underlies the mountains, the Eocene Bitterroot mylonitic gneiss, the unconsolidated Tertiary deposits that fill the valley, and Quaternary deposits and landforms, which include glacial features, pediments, and fault scarps.

REGIONAL GEOLOGIC SUMMARY

The oldest rocks in the area are 1,863 Ma crystalline basement rocks exposed along Sleeping Child Creek in the Sapphire Mountains immediately east of this field trip (see Field Guide to the Sleeping Child Metamorphic Complex, this volume). Siliciclastic rocks of the 1,380–1,470 Ma Belt Supergroup were presumably deposited atop this basement, and accumulated to thicknesses of up to 15 km (50,000 ft). These rocks remained largely undisturbed until the Sevier–Laramide orogeny 1.2 billion years later. The Late Cretaceous tectonism buried and metamorphosed these rocks to upper amphibolite-grade, and they were intruded by voluminous 120–50 Ma granitic plutons. The 53–30 Ma (Foster and Raza, 2002), top-to-the-ESE Bitterroot detachment fault exhumed these mid-crustal rocks from depths of >20 km (12 mi; Foster and others, 2001). Through time, the detachment fault transitioned from amphibolite-grade mylonitization to greenschist-grade shearing to brittle faulting as structural levels became increasingly shallow. The Bitterroot Mountains, in the detachment's footwall, comprise the metamorphic infrastructure of the well-

studied Eocene Bitterroot metamorphic core complex (e.g. Hyndman, 1980; Foster and others, 2001), although high-grade metamorphic rocks also occur in parts of the hanging wall. The plutonic–metamorphic core forms a broad, elongate, north–south dome that defines the high Bitterroots and is bounded by the top-to-the-east detachment fault on all sides.

From the Oligocene through at least late Miocene (Konizeski, 1958; McMurtrey and others, 1972; Dale Hanson, Museum of the Rockies, written commun., 2018), debris flow, fluvial, and floodplain deposits (Lonon and Sears, 2001; Stickney and Lonon, 2018) as thick as 700 m (2,300 ft; Norbeck, 1980) were deposited in the ancestral Bitterroot Valley. Facies relationships suggest that both the Sapphire and Bitterroot Mountains flanked the north–south valley at this time (Jeff Lonon, unpublished mapping).

Pediment surfaces are extensively developed in the Bitterroot Valley and plane off Proterozoic through late Pleistocene rocks, suggesting that at least some pediments formed during interglacial periods in the late Quaternary.

At least three glacial advances left late Quaternary deposits (Weber, 1972; Stickney and Lonon, 2018); the youngest and least extensive was the Pinedale advance ending at 11–14 ka (Stickney and Lonon, 2018). Glacial Lake Missoula filled the valley at times to elevations as high as 4,200 ft, with its last stand estimated at 13.7–13.4 ka (Smith and others, 2018).

The steeper Miocene (?) to Late Quaternary Bitterroot fault (fig. 1) developed in response to Basin and Range extension. Associated fault scarps vertically offset late Pinedale glacial till and outwash surfaces by as much as 2.4 m (8 ft). Deposits and geomorphic surfaces interpreted as early Pinedale and older have vertical fault offsets from 8 to 11 m (26 to 36 ft). Pediment surfaces of older, but unknown, age have vertical fault offsets ranging up to 43 m (141 ft). Without age control for the faulted deposits and surfaces, fault slip rates cannot yet be accurately estimated. However,



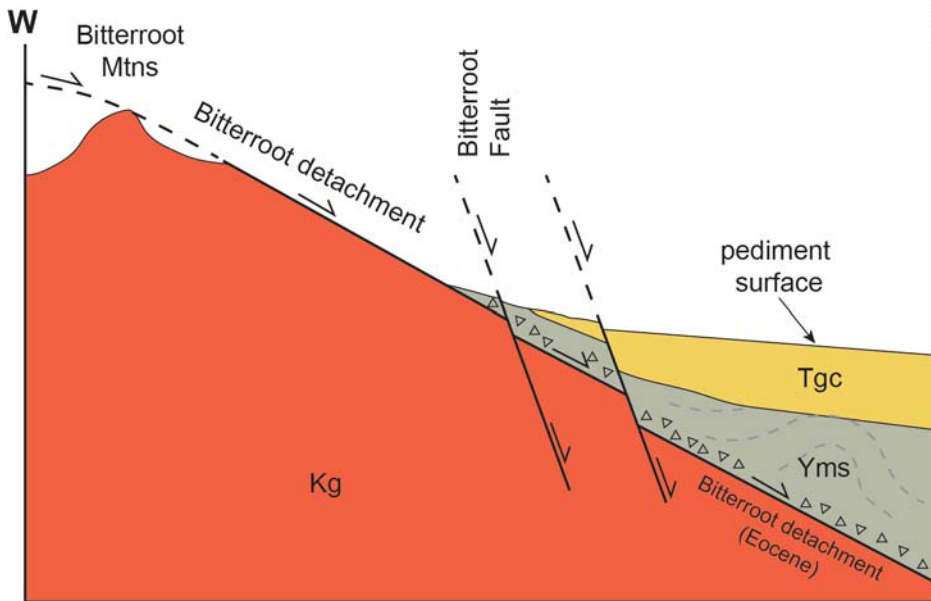


Figure 1. Simplified cross-section showing relationships between the Eocene Bitterroot detachment fault and cross-cutting Quaternary Bitterroot normal fault. Kg, granitic rocks; Tgc, gravel and clay; Yms, metasedimentary rocks. From Stickney and Lonn (2018).

progressively larger fault offsets of older deposits and surfaces demonstrate repeated surface-rupturing earthquakes have occurred along the Bitterroot fault during the latest Pleistocene (Stickney and Lonn, 2018). Earthquake magnitudes of >6.5 are required to generate surface ruptures (dePolo, 1994), and these repeated ruptures suggest that other significant earthquakes along the Bitterroot fault are likely to occur in the future.

TRAILHEAD ACCESS

From Hamilton, proceed south along U.S. Highway 93 for 10 mi. The spectacular Bitterroot Mountains are to the west, with the more subdued Sapphire Range to the east.

Where Highway 93 widens to four lanes, stay in the right lane and turn right on Lost Horse Road at the top of the hill. The highway roadcuts expose Proterozoic–Cretaceous high-grade metamorphic rocks of the Cretaceous Sleeping Child metamorphic complex and unconsolidated Tertiary fluvial and floodplain deposits. Lost Horse Road ascends a flat-topped hill that represents a pediment surface carved across the Tertiary and

E Proterozoic rocks. Prominent peaks to the southwest, from left to right, are the Shard, the Como Sisters, the Lonesome Bachelor, and El Capitan, ranging from 9,100 to 10,000 ft.

Proceed on Lost Horse Road for 2.5 mi to the second fork in the road, where the pavement ends. Take the right fork 0.25 mi to the large parking area on the right at the Coyote Coulee trailhead.

THE HIKE

Coyote Coulee Trailhead 46° 7.2915', -114° 13.7366'

Figure 2 shows the hiking route superimposed on a geologic map.

Begin by following the trail a few hundred feet north to a fork and take the right fork. Proceed across a gently undulating surface containing scattered, enormous, angular gneissic and granitic boulders that are badly weathered, and abundant, fresher, rounded cobbles and boulders. Based solely on its fan-shaped topographic surface, without fieldwork, Lonn and Sears (2001) incorrectly mapped this landform as an alluvial fan deposited where Hayes Creek emerges from the mountains. However, in 2019, Lonn, attempting to increase his domestic water supply, drilled a water well on this feature. The well was dry, and penetrated glacial till overlying granite bedrock, prompting a revised (and expensive) reinterpretation of this landform. The drillhole data and new fieldwork suggest that this feature is a pediment surface that was carved on older till (Bull Lake age?) and then subsequently dissected during a later deglaciation. The giant weathered boulders represent exposed older till, and the rounded fresher boulders were deposited as younger (Pinedale?) glacial outwash emanating from the Hayes Creek cirque far above. We will cross the original,

Figure 2. Geologic map of the field trip area superimposed on a LiDAR image base. The hiking route is shown by green dots. Walk the northern loop in a counterclockwise direction as shown by the arrows. Map units are: Qal, modern alluvium; Qaf, alluvial fan deposits; Qath, river terrace deposits; Qgdo, older debris flow deposits; Qgdy, younger debris flow deposits; Qgoo, older glacial outwash; Qgom, middle-ages glacial outwash; Qgoy, younger glacial outwash; Qgto, older glacial till; Qgty, younger glacial till; Qpa, Paludal deposits; Tgc, gravel and clay; TKg, granitic rocks. Black lines represent fault scarps with tics on downthrown side. Blue lines represent the Bitterroot detachment fault with tics on hanging wall. Black triangles represent brecciated rocks in the hanging wall of the Bitterroot detachment. Foliation/lineation are orientation data for mylonitic gneiss in the footwall of the Bitterroot detachment. Scale: 1:24,000. Modified from Stickney and Lonn (2018).



undissected pediment surface shortly, and will have more discussion there. About 10–15 min of walking will bring you to Hayes Creek.

Hayes Creek Bridge

46° 7.7122', -114° 13.6230'

Cross Hayes Creek and ascend to a striking pediment surface that was not eroded by the younger Hayes Creek deglaciation. Huge, angular boulders are visible within the next few hundred yards that suggest this pediment surface was formed on Pleistocene glacial till during an interglacial period. This particular pediment remnant is extensive, and is also underlain by Tertiary sediments and Tertiary–Cretaceous granite in addition to Pleistocene till. The underlying glacial till challenges the commonly accepted theory that pediments require millions of years and tectonically quiescent conditions to form. This pediment appears to have formed relatively quickly in a tectonically active area. Supporting this concept is a paper by Larson and others (2016) showing that pediment surfaces in an area of rapidly changing base level were able to form within just one glacial–interglacial cycle, in as short as 50,000 years. Stickney and Vuke (2017) also interpreted pediments in the Helena Valley to be of Pleistocene age. The Lost Horse fault scarp cuts this pediment immediately to the east, and vertically offsets it 10.8 m (35 ft; Stickney and Lonn, 2018). An absolute age for this surface would be invaluable in determining slip rates.

This area was farmed as an apple orchard a century ago, and apple trees can still be found under the Ponderosa pines that have far surpassed them. Bitterroot National Forest acquired this private land in the late 1970s to preserve elk winter range, but commercial logging here a decade ago caused excessive soil disturbance that allowed extensive knapweed fields to develop. Knapweed must be important elk forage! The trail soon intersects a 4-wheeler track; turn right and proceed down the track past the Coyote Coulee trail split, until the road descends a shallow gully.

Granite Outcrop beneath the Pediment

46° 8.1406', -114° 13.3333'

Roadcuts here expose brecciated and iron-stained two-mica granite interpreted to lie just above the

Eocene Bitterroot detachment fault, in its hanging wall. The granite is not gneissic; it is instead brittlely deformed. Farther down this track, unconsolidated Tertiary deposits unconformably overlie the granite, and the pediment surface cuts across both. Ascend the road cut and walk the pediment surface northwest. Note that not a single rounded boulder, cobble, or pebble lies on this surface, suggesting that the pediment did not form through lateral corrasion by migrating streams, a commonly accepted explanation for pediment formation. In a literature review, Twidale (2014) concluded that pediments like this one, that are not covered by exotic material, form through a poorly understood weathering process called etching. Etching is driven by “subsurface moisture attack” and results in an “etch plain” covered with weathered, in-place, autochthonous material (Twidale, 2014). Also noteworthy is that pediment development is not restricted to arid climates, nor do sheet floods drive their formation; the planar pediment surface must already exist for a sheet flood to occur (Dohrenwend and Parsons, 2009). Pediments are extensively developed in the Bitterroot Valley, and most appear to have formed through etching. Are most also Quaternary in age? The region is ripe for a pediment study that may have far-reaching implications.

Continue northwest to intersect a new logging road and follow it until it crosses the Coyote Coulee trail. The low roadcuts expose *grus*, silt, clay, and sub-rounded pebbles and small cobbles, suggesting the pediment here is developed on Tertiary sedimentary deposits (unit Tgc in fig. 2). Turn right onto the continuation of the trail. After 1 min, reach a saddle at the head of a drainage running southeast. Note that this is a headless drainage cutting across the pediment. It appears to have developed from meltwater originating from the Camas glacier that filled the larger valley to the north during one of the early glacial advances.

Descend the trail into this dry valley, aptly named Coyote Coulee. The bottom of Coyote Coulee is covered with fresh rounded boulders and cobbles that clearly have a fluvial origin. Continue to a trail intersection and note the huge boulders up the slope to the northwest unearthed by the logging road construction. The huge boulders are part of the Pinedale terminal moraine of the Camas gla-



rier. Coyote Coulee developed along the southern margin of this moraine, and was an ice-marginal channel transporting outwash into the main Bitterroot Valley. The LiDAR coverage shows that this outwash (unit Qgoy in fig. 2), with an estimated age of 11–14 ka, is cut by a fault scarp (figs. 2,3) on its lower, eastern end with a vertical offset of 2.4 m (8 ft; Stickney and Lonn, 2018).

Hayes Creek Loop–Homestead Lane Trail Junction

Continue straight at the trail junction, down Homestead Lane, a connector that joins the Hayes Creek and the Brown Jug loops. On your left is the terminal moraine of the Pinedale Camas Glacier, characterized by enormous, unweathered boulders. This is the youngest moraine of the Camas glacier, and was deposited about the same time as the Coyote Coulee outwash material. The mapping shows that at least two older moraines surround this Pinedale moraine.

The open hillside that appears after a few minutes of walking is underlain by gneissic granite bedrock

that has been brecciated along the 53–30 Ma Bitterroot detachment fault. We will take a closer look at this fault later this afternoon.

Modern Camas Creek soon appears, incised into the outwash. Fault scarps do not cut any modern stream deposits in this region, but, because the stream processes are active, scarps might not last long. Cross Camas Creek and ascend to the intersection with the Brown Jug Loop.

Brown Jug Loop Intersection 46° 8.8245', -114° 13.1104'

Look to your right and view the small break in the mostly flat surface. The LiDAR image shows that this break is a small, straight fault scarp parallel to the main scarp farther east. The angular boulders indicate this is glacial till in an older moraine deposited by the Camas glacier. This scarp is interpreted to be the southern continuation of the Ward Fan scarp we will soon see.

Take the trail's right fork, going across a shallow drainage containing rounded boulders that must



Figure 3. Southwestward view of the fault scarp that cuts the Pinedale outwash near the east end of Coyote Coulee (fig. 2). Scarp has 2.4 m of vertical offset (Stickney and Lonn, 2018).



represent another glacial meltwater channel. The prominent hill to the left is bedrock composed of broken, brecciated gneissic granite that we will view later. The trail curves east down the valley, then contours along the hillside and follows an old irrigation ditch. Note that the angular boulders disappear and are replaced by an abundance of well-rounded cobbles and pebbles. Continue to a large cut in the hillside.

Tertiary Gravel

46° 8.9218', -114° 12.8641'

Stop and examine some of the well-rounded cobbles and pebbles that clearly have a fluvial origin. Most are quartzite and porphyritic volcanic rocks that today are not found in the Bitterroot Mountains, only in the Sapphire Mountains. Because these gravel deposits (unit Tgc in fig. 2) contain cobbles representative of the entire Bitterroot River drainage, and are interbedded with clay and volcanic ash interpreted as floodplain deposits, Lonn and Sears (2001) called them the Ancestral Bitterroot River (ABR) deposits. Fossils collected from fine-grained interbeds within these Tertiary ABR deposits range in age from 7 to 25 Ma (Konizeski, 1958; McMurtrey and others, 1972; Dale Hanson, Museum of the Rockies, written commun., 2018).

Note the complete absence of round Bitterroot mylonite clasts and the scarcity of any round granitic clasts, suggesting that the Bitterroot core complex's core had not yet been exposed when these rocks were deposited. The mylonite and granite clasts here are angular and were probably deposited unconformably on top of the Tgc by Pleistocene glaciers. Farther north along the flanks of the Bitterroot Mountains, Stickney and Lonn (2018) found quartzite-dominated debris flow deposits that grade into and interfinger with the fluvial deposits towards the valley center, suggesting that quartzite of the hanging wall was preserved in the Bitterroot Mountains until late Miocene time. It is possible that the gneissic footwall of the Bitterroot detachment was not exposed until the steep Basin and Range Quaternary Bitterroot fault became active. Near Victor, the ABR deposits can also be found as much as 450 m (1,500 ft) above the current level of the river, and are interpreted to have been uplifted by the Bitterroot fault.

Continue around the east edge of the hill. The flat, open plain below you is another pediment surface. This one is cut on Tertiary deposits (unit Tgc in fig. 2). Well above, to the left, is the continuation of this pediment surface, 40 m (130 ft) above the lower surface, representing offset along the Bitterroot fault scarp. The scarp here is not obvious on LiDAR imagery because the Tertiary gravel deposits erode easily and do not preserve scarp morphologies.

Rather than following the trail, go left on the new logging road. In 2016, the Bitterroot National Forest constructed 3 mi of new logging roads in this previously roadless area. Roads, like weeds, also apparently improve elk winter range. The roadcuts expose rounded quartzite and granitic cobbles, angular granitic material, grus, and ashy material. These different lithologies represent different interbedded facies of the Tgc unit. Near the crossing of a small creek, the hummocky topography upstream represents landslides developed in the clay-rich facies of Tgc. In this area, virtually all landslides are developed in the Tgc unit.

After passing through a clearcut, the road again intersects the trail. Turn left on the trail and take it upwards across a planar sloping surface that contains large, sub-rounded, granitic gneiss boulders. While this surface appears similar to the pediment developed on glacial till that we crossed earlier, a slightly different interpretation is proposed here. This surface undulates more, and lobes and levees can be seen on the LiDAR image and in the field (fig. 4). The boulders are more rounded than those of the moraines we have seen, and they can be followed upward to their origin at the outermost glacial moraine of Ward Creek. Incised drainages expose these bouldery deposits as a thin mantle above a buried pediment surface carved on Tertiary deposits (Tgc) and gneissic bedrock (TKg). These observations suggest that we are on debris flow deposits (Qgdo on fig. 2) that issued from the Ward Creek cirque and spread out atop the pediment surface. Age is unknown, but the boulders' association with the outermost Ward Creek glacier moraine indicates that this surface is older than Pinedale.

Continue up the rocky, but flat, fan surface until you converge on a swampy drainage to the left. A





Figure 4. Levees visible on the Ward Creek fan confirm that it formed from debris flows descending from the Ward Creek glacier. (A) Boulder train marks a levee in older debris flow deposits. (B) A prominent levee of subrounded boulders in a Pinedale-age debris flow deposit. Note the large size (3 m) of some boulders.



hill immediately ahead breaks the flat fan surface; this is the fault scarp so prominent on the LiDAR image (fig. 2).

Fault Scarp View

46° 9.3766', -114° 13.0499'

The hill ahead is a fault scarp cutting the debris flow (fig. 5), and has a vertical offset of 3.3 m (11 ft; Stickney and Lonon, 2018). One half mile north of here is a younger, Pinedale-age debris flow (Qgdy in fig. 2), inset into this one, with a vertical offset only 2 m (6 ft). Still farther north is an even older debris flow that exhibits 14 m (46 ft) of vertical offset (Stickney and Lonon, 2018). These numbers show that the older the surface, the greater the offset, but without absolute ages an accurate slip rate cannot be estimated.

Earlier geologic maps postulated the scarp's existence here (Barkman, 1984; Lonon and Sears, 2001), but the recent LiDAR coverage confirmed

its presence and extended its length far to the south. However, we should not be surprised by its existence: almost all big mountain ranges are bounded by active faults, and the Bitterroot Mountains are certainly big mountains.

Continuing, the trail crosses the scarp where it intersects the drainage and soon leaves the bouldery material and enters bedrock. Where the trail follows an old roadcut across a south-facing slope, bedrock is exposed in the road cut. It is weathering into thin plates of gneissic granite developed through ductile shear along the Eocene Bitterroot detachment fault. Lineations plunge moderately ESE, consistent with the regional top-to-the-east transport direction. Continue along the trail until some large bedrock slabs appear above the trail. Note the severe burn above the trail from the 2016 wildfire. The area along the trail experienced only a ground fire.



Figure 5. Southward view of the fault scarp cutting the Ward Creek fan near the trail. Vertical offset here is measured at 3.3 m (Stickney and Lonon, 2018). Note the slight back tilting of the hanging wall into the base of the fault scarp.



Bedrock Slabs

46° 9.2654', -114° 13.4367'

Walk up to these slabs. They are layered granitic gneiss, and the surfaces are parallel to the Bitterroot detachment fault plane. The first outcrop contains some chloritic breccia that developed during the late stages of faulting when these rocks were close to the surface. The outcrop 100 ft farther displays ESE-plunging mineral lineations along the slab. Shear sense indicators on both the eastern and western (Lonon, unpublished mapping) sides of the Bitterroot Mountains consistently show top-to-the-ESE transport, indicating that the domal uplift of the Bitterroot Mountains occurred after movement along the detachment fault. Continue up a steep hill until the trail levels out.

Glacial Till

46° 9.1571', -114° 13.5049'

Hummocky terrain here is underlain by glacial till (Qgto in fig. 2) as indicated by the large boulders. The glacier that deposited them occupied a small cirque 500 m (1,640 ft) higher. However, a subtle fault scarp visible on the LiDAR image, cutting through bedrock to the north and extending into this till, may be responsible for some of the topography. A spring along the fault just above the trail creates a swampy area here. The Quaternary Bitterroot fault appears to be expressed by several parallel and *en echelon* strands. LiDAR coverage does not extend west into the mountains, and more fault scarps may exist on the Bitterroot face. Continue on the trail through a beautiful mature Ponderosa pine forest. This area escaped the logging only because it is in an Inventoried Roadless Area, and it is still shady and weed-free. Reach an open area on a hilltop.

Como Peaks View

The Como Peaks are visible to the south. Like the hill you are standing on, the peaks are underlain by granitic gneiss formed along the Bitterroot detachment fault. The ductile shear zone and layered gneiss are more than 300 m (980 ft) thick (Hyndman, 1980) and extremely resistant to weathering. The resistant gneiss underlies all of the highest peaks of the Bitterroot Mountains. However, it was the Quaternary glaciers that were responsible

for carving the peaks into their rugged forms. The Como Peaks are good examples of glacial horns, pyramidal peaks with steep sides formed by intersecting glacial cirques.

Eastward, the more subdued Sapphire Range is visible. Why do these two mountain ranges differ so? One reason might be that the Bitterroot Mountains are still undergoing active uplift along the Quaternary Bitterroot fault. Another is that the Bitterroot Mountains have a much snowier climate, which resulted in more extensive glaciation during the ice ages.

Leave the trail and walk east on another pediment surface, crossing reddish, iron-stained rocks that mark the trace of the Eocene Bitterroot detachment fault. Drop onto the open, south-facing hillside.

Breccia Outcrops

46° 8.8204', -114° 13.3626'

Outcrops are composed of angular clasts of brecciated gneiss cemented together. As the rocks along the detachment fault were brought to shallower levels, the deformation progressed from forming amphibolite-grade gneiss to greenschist-grade mylonite to angular breccia. The breccia indicates that we are at the top of the Bitterroot detachment fault, and its trace is mapped at the breccia–gneiss contact. The breccia is often hundreds of feet thick, and grades upward into unbroken rocks of the hanging wall.

Climb back up the hill and follow its edge north-eastward, crossing a steep drainage and then turning east along a game trail that traverses brecciated bedrock. As you pass onto flatter terrain, reddish iron-stained soil marks a fault, the southern continuation of the prominent scarp we viewed earlier. The fault scarp here, although not obvious on the LiDAR coverage, cuts the pediment and can be seen in profile if you look north. After crossing it, rounded quartzite cobbles of the Tertiary ABR gravel (Tgc) appear. The fault here separates Tgc from brecciated TKg, although there are also angular boulders of mylonitic gneiss on the surface deposited by Pleistocene glaciers. Walk down the south-facing hillside.



Bedrock–Tertiary Gravel Contact
46° 8.9486', -114° 13.1973'

Not far below the top of the hill is the unconformable Tgc–TKg contact, suggesting that the normal fault dropped the east side down enough to preserve Tgc above the TKg. The bedrock here is brecciated, and the Tertiary gravel contains rounded quartzite cobbles. Field mapping shows considerable topography existed on the bedrock surface prior to deposition of the Tertiary sedimentary rocks. Knobs of bedrock protrude through the Tgc throughout the region.

Continue to the base of the hill and head southeast to intersect the trail. Turn right on the trail and retrace your steps back to the trailhead, about 2.5 mi (4 km).

REFERENCES CITED

- Barkman, P.E., 1984, A reconnaissance investigation of active tectonism in the Bitterroot Valley, western Montana: Missoula, University of Montana, M.S. thesis, 85 p.
- dePolo, C.M., 1994, The maximum background earthquake for the Basin and Range Province, western North America: *Bulletin of the Seismological Society of America*, v. 84, pp. 466–472.
- Dohrenwend, J.C., and Parsons, A.J., 2009, Pediments in arid environments, *in* Parsons A.J., and Abrahams A.D. (eds), *Geomorphology of Desert Environments*: Springer, New York, p. 377–411, doi: http://dx.doi.org/10.1007/978-1-4020-5719-9_13
- Foster, D.A., and Raza, A., 2002, Low-temperature thermochronological record of exhumation of the Bitterroot metamorphic core complex, northern Cordilleran orogen: *Tectonophysics*, v. 349, p. 23–36.
- Foster, D.A., Schaferb, C., Fanning, C.M., and Hyndman, D.W., 2001, Relationships between crustal partial melting, plutonism, orogeny, and exhumation: Idaho–Bitterroot batholith: *Tectonophysics*, v. 342, p. 313–350.
- Hyndman, D.W., 1980, Bitterroot dome–Sapphire tectonic block, an example of a plutonic core–gneiss dome complex with its detached suprastructure, *in* Crittenden, M.D., Coney, P.J., and Davis, G.H. (eds.), *Cordilleran Metamorphic Core Complexes*: Geological Society of America Memoir, v. 153, p. 427–443.
- Konizeski, R.L., 1958, Pliocene vertebrate fauna from the Bitterroot Valley, Montana, and its stratigraphic significance: *Geological Society of America Bulletin*, v. 69, p. 325–345.
- Larson, P.H., Kelley, S.B., Dorn, R.I., and Seong, Y.B., 2016, Pace of landscape change and pediment development in the northeastern Sonoran Desert, United States: *Annals of the American Association of Geographers*, v. 106, no. 6, p. 1195–1216.
- Lonon, J.D., and Sears, J.W., 2001, Geology of the Bitterroot Valley, shaded relief: Montana Bureau of Mines and Geology Open-File Report 441-C, 1 sheet, scale 1:48,000.
- McMurtrey, R.G., Konizeski R.L., Johnson, M.V., and Bartells, J.H., 1972, Geology and water resources of the Bitterroot Valley, southwestern Montana: U.S. Geological Survey Water Supply Paper 1889, 80 p., scale 1:125,000.
- Norbeck, P.M., 1980, Preliminary evaluation of deep aquifers in the Bitterroot and Missoula valleys in western Montana: Montana Bureau of Mines and Geology Open-File Report 46, 15 p.
- Smith, L.N., Sohbati, R., Buylaert, J.P., Lian, O.B., Murray, A., and Jain, M., 2018, Time of lake-level changes for a deep last-glacial Lake Missoula: Optical dating of the Garden Gulch area, Montana, USA: *Quaternary Science Reviews*, p. 23–35, doi: 10.1016/j.quascirev.2018.01.009
- Stickney, M.C., and Lonon, J.D., 2018, Investigation of Late Quaternary fault scarps along the Bitterroot Fault in western Montana: Montana Bureau of Mines and Geology Report of Investigation 24, 16 p., 2 sheets, scales 1:12,000 and 1:24,000.
- Stickney, M.C., and Vuke, S.M., 2017, Geologic map of the Helena Valley area, west-central Montana: Montana Bureau of Mines and Geology Open-File Report 689, 1 sheet, 11 p., scale 1:50,000.
- Twidale, C.R., 2014, Pediments and platforms: problems and solutions: *Geomorphologie*, v. 20, p. 3–56, <https://journals.openedition.org/geomorphologie/10480?lang=en#text> [Accessed June 2020].
- Weber, W.M., 1972, Correlation of Pleistocene glaciation in the Bitterroot Range, Montana, with fluctuations of glacial Lake Missoula: Montana Bureau of Mines and Geology Memoir 42, 42 p.



ROADSIDE GEOLOGIC TRAVERSE ALONG THE BITTERROOT FRONT FROM HAMILTON TO LAKE COMO

George Furniss

Geologist, Darby, Montana

INTRODUCTION

This field trip introduces us to eroded bedrock of the Bitterroot Front, ancient river gravels, alluvial fans, pediments, glacial moraines, and beaches of Glacial Lake Missoula and Lake Como, originally impounded by an ice age moraine. Following uplift of the Rocky Mountains, the crust was being stretched, and a fault made the Bitterroot Valley. Erosion took hold and streams washed in gravels, the wind carried volcanic ash, lakes deposited sand, and peat accumulated in bogs. A river found its way out toward the north and began clearing out a drainage basin. Unconsolidated valley-fill once deposited at higher levels became incised, leaving terrace benches. Flowing water redeposited material all along the river bottom, reworking it, and carrying it out of the valley. The picturesque Bitterroot River remains wild today, a headwaters stream deepening its valley each year by transporting sediment out to the greater Columbia River basin and to the Pacific.

FIELD GUIDE

0.0 Begin at the Hamilton Fairgrounds; set odometer to zero.

Turn right (west) out of the parking lot and cross US Highway 93 at the stoplight, and continue west on Adirondack.

While traveling across town, note that we are driving on old valley floor river sediment with soil cover. This surface is called the Hamilton Terrace (Weber, 1972) and is composed of **outwash** that is a gravelly remnant of ice-age valley-fill. **Blodgett Canyon** in the Bitterroot Mountains to our west is one of many **glacially widened and deepened canyons**. Alpine glaciers once flowed slowly down many of the Bitterroot canyons into the valley from an ice cap perched over the highest part of the Bitterroot Range.

0.4 Turn left (south) on 7th Street.

1.0 Turn right (west) on Main Street.

1.6 Cross the Bitterroot River travelling west. Continue west on paved road.

2.5 Note **glacial moraines and erratic boulders**.

3.3 Merge west (left) with Blodgett Camp Road and continue west.

4.1 Follow signs to Canyon Creek Trailhead 3; dirt road now.

4.7 Turn left (west); follow road signs to Blodgett Overlook Trail 3, Canyon Creek Trail 3.

This sidehill after the turn that we are driving on is **lateral moraine** from Blodgett Canyon.

6.0 Switchback and glacial erratic.

6.6 Outcrops of mylonite texture.

7.2 Good turn-around place. All outcrops here are mylonite texture (Vuke and others, 2009).

Turn around and travel back downward a short distance to stop and view this long exposure of **mylonite texture**.

7.4 STOP 1—Mylonite of the Bitterroot Front

Outcrops here have slabby texture of sheared, dynamically metamorphosed and recrystallized granite called mylonite with a thin-blanket foliation that dips toward the valley. Mylonite textures develop in ductile shear zones under pressures and temperatures conforming to depths of at least 4 km where high rates of strain are focused. They are deep crustal counterparts of brittle faults that create fault breccia. Feldspar crystals form most of the eye-shaped resilient mineral grains called augens that appear to be slightly rotated by asymmetric shearing, while mica crystals and quartz within the layering create the easily split foliation and slickensides. Many of the augens show similar direction of drag folding tapering on either side,



providing shear direction information. When we look at the flat-iron slopes of the Bitterroot Mountains tilting into the valley, we are often looking at mylonite surfaces (Vuke and others, 2009). This sheared rock was a zone of deep crustal horizontal movement between the Bitterroot Dome and the Sapphire tectonic block (Hyndman, 1980). This slabby surface, now exposed by erosion, represents the sliding contact between the rising igneous **Idaho Batholith** plutons and the ridged **Sapphire Block** of metamorphosed Belt sediments. This sliding contact is called a detachment fault, and it was a thick zone of slow continuous transferal of mass spanning millions of years between Late Cretaceous to Early Eocene that fractured brittle cover rocks and allowed weathering and erosion to penetrate deep into the crust, initiating the Bitterroot Valley as a long narrow south–north structural basin. The west–east Bitterroot Canyons draining to the valley today probably owe their spacing to minor alternating ridges and grooves within the once active and deep planar detachment fault zone. In map view today the western basin margin along the Bitterroot Mountains, edged with mylonite, meets the valley in a relatively straight north–south line that corresponds with the alignment of the Late Quaternary Bitterroot fault.

7.7 Returning downward, note another long exposure of **mylonite** with room to pull over.

9.5 Turn right back on to Blodgett Camp Road.

10.1 Reach pavement.

10.9 Turn right on to Canyon Creek Road again.

11.9 At stop sign turn right (south) on Westside Road.

12.1 Cross Canyon Creek.

14.6 Cross Roaring Lion Creek.

14.8 Cross another channel of Roaring Lion Creek.

At stop sign turn right onto Roaring Lion Road and pull off the side of the road.

16.4 STOP 2

46° 11'36" N., 114° 10'33" W.

We are parked on the **outwash surface** of the

Hamilton Terrace (Weber, 1972). Look to the southwest toward the Como Peaks where we can see, in the middle distance, a **higher terrace or bench** with the same top slope as the one we are standing on, a slope of about 2½–3 degrees. That surface is older by millions of years, an alluvial fan surface like the one we are standing on, but draped over an even older bedrock surface exposed along Gold Creek Loop that protected it from lateral erosion of the Bitterroot River. That higher terrace or bench that we see in the middle distance is now a pediment surface incised by stream erosion on either side. The Hamilton Terrace fan of glacial outwash on which we are standing grades to the glacial moraines up ahead mapped by Weber (1972). That higher bench in the middle distance is now only a remnant of a pediment that grades to the bedrock slopes of mylonite along the Bitterroot Front (Lonn and Sears, 2001). When that higher bench surface was the broad valley floor, rhinoceroses and camels and, by association with stratigraphic correlations to nearby basins, smallish horses such as *dinohippus*, roamed the valley (Wilkins, 2017; Konizeski, 1958). Only the Bitterroot Valley benches preserve that older valley floor. A rhinoceros skull retrieved from approximately that age surface (estimated 7–9 million years before present, Miocene), but from a bench on the other side of the valley above Corvallis, resides at the Museum of the Rockies at Bozeman (Hanson, 2018).

Look to the east; the Bitterroot River has incised downward into the Hamilton Terrace, indicating that streams have changed the shape of the valley floor since the last glacial age, and since Glacial Lake Missoula.

Continue west on Roaring Lion Road.

As we pass **Little Lion Lane** on the right, note the scattered **extra-large boulders**. These are the outermost remnants of terminal moraine from glaciers emerging from Roaring Lion Canyon, dating to the Early Wisconsin Glaciation (Weber, 1972). Local names for the moraine are Charlos or Bull Lake Glaciation, occurring perhaps 70,000 years ago.



17.4 STOP 3

46° 11' 36" N., 114° 11', 59" W.

Notice the **mounds of large and small boulders**. This is a **glacial moraine**, a record of the Late Wisconsin Glaciation. Local names for this moraine are Lost Horse, or Pinedale Glaciation, perhaps 30,000–13,000 years ago.

Continue driving west on Roaring Lion Road.

17.8 STOP 4

46° 11'36" N., 114° 12'26" W.

Another example of **glacial moraine**, but here we can also see a well-sorted **beach sand**, deposited by **Glacial Lake Missoula**, which lapped onto the side of the moraine, mapped by Weber (1972). This large lake, dammed periodically by glacial ice between Thompson Falls, MT and Sandpoint, ID, flooded the Bitterroot Valley up to about elevation 4,200 ft occasionally, and drained and refilled a number of times.

Continue driving west on Roaring Lion Road. Pass Judd Creek Hollow Road on the left.

Continue past Judd Creek Hollow Road about 0.3 mi on Roaring Lion Road to where the road turns sharply right (north).

18.3 STOP 5

46° 11'29" N., 114° 12' 59" W.

Here, at 4,200 feet elevation, we see another **beach sand** and an example of younger moraines that are remarkably steeper (perhaps as young as 13,000 years ago), younger than the moraines at Stops 3 and 4.

Continue on Roaring Lion Road through the burned area (2016) to the Ward Mountain Trail-head, and the road junction wide enough to turn around.

18.7 STOP 6

46° 11'28" N., 114° 13' 19" W.

We make a U-turn here, but stop for a moment.

Observe the **freshness of the granite boulders** and cobbles in the moraine. The boulders are granite from the **Idaho Batholith**, carried out of the

canyon by glacial ice, and have been mechanically and chemically weathering at the surface since the last ice age. Weathering has not softened them; our hammers will bounce when striking them.

Return to Judd Creek Hollow Road and turn right (south) to follow the Judd Creek Road. This will take us sideways, parallel to the mountain front, through the lateral Roaring Lion glacial moraines (Weber, 1972). Follow the Judd Road almost all the way to Judd Creek, where water can be seen surging through a large culvert. Stop at some smooth moraines.

20.1 STOP 7

46° 11' 11" N., 114° 12' 49" W.

At this stop we can dig around in search of **extremely weathered granite boulders** in the smooth looking and ancient Judd moraine. This glacial moraine is from a previous glacial period, perhaps the Illinoian Glaciation, of about 200,000 or more years ago, or perhaps even Pre-Illinoian Glaciations. The feldspar crystals in the granite have reacted with carbonic acids from rain and organic decomposition in soil to become clay, and the mica crystals have converted to rusty clay and iron oxide. The boulders in this moraine simply fell apart due to physical and chemical weathering over large amounts of time.

Travel back to US Highway 93.

23.1 At US Highway 93, turn right (south).

24.4 Turn right (west) on North Gold Creek Road. We climb up onto the higher (estimated to be Miocene) bench surface now that we could see from Stop 2, from Roaring Lion Road. This incised alluvial fan surface draped over and buttressed by bedrock, and thus protected from river erosion, is perhaps 7–9 million years old. The upper surface could actually be a pediment carved onto older fan sediments representing a higher ancient valley floor, mantled now with a thin veneer of younger gravels and occasional erratic boulders.

24.9 STOP 8

46° 10' 43" N., 114° 11' 31" W.

Glacial erratic. How did that large rock get onto this flat surface? Possibly stowed within an ice-



berg floating on Glacial Lake Missoula? Look to the low hills to the east across the river. Do you see any Glacial Lake Missoula **shorelines**?

Elevation here: 3,850 ft.

Continue west on North Gold Creek Road for 0.3 mi. We pass through Judd Moraine of the Pre-Bull Lake, Pre-Charlos Glaciation (? Illinoian Glaciation).

Turn left (south) to stay on North Gold Creek Road.

26.0 STOP 9
46° 10' 2" N., 114° 12' 1" W.

Notice **ancient extremely weathered cobbles of granite and quartzite river gravels** (Lonn and Sears, 2001).

Continue to stop sign. Turn right (south) onto Gold Creek Road.

26.8 STOP 10
46° 10' 2" N., 114° 12' 1" W.

- **Peat Lands** ~300 acres, the post-mining base of the peat at a depth of 4 ft yielded a mass spectrometer radiocarbon date of **7,940 ± 30 years before present**; Mazama ash can be detected in numerous areas of the peat deposit above this base at greater depth on the west side than the east side of the deposit, indicating the **peat deposit tilts toward the west**.
- Notice the Bitterroot Fault on the map (Stickney and Lonn, 2018) provided by your guide.

Continue south on Gold Creek Loop.

Reaching Camas Creek Loop, turn left (toward US Highway 93).

29.3 Turn right (south) onto US Highway 93. We are driving on the Hamilton Terrace.

30.6 Turn right (west) at the top of the hill onto Lost Horse Road. Continue along the road to the highest point, only a short distance, where there is room to park.

30.8 STOP 11
46° 7' 14" N., 114° 10' 55" W.

From this **high point** on Lost Horse Hill observe the distant **moraines along the Bitterroot Front (timbered areas extending out into the valley from the canyons)**.

Elevation: 3,890 ft

We are parked on another incised (**Miocene**) **alluvial fan bench, which is draped over bedrock pediment, or is itself a pediment surface**. This surface extends out from the sides of Lost Horse Canyon and grades into the mylonite flat-irons of Bitterroot Front. The metamorphic Belt bedrock core protecting this surface from river erosion is exposed in the roadcut on the east side of US Highway 93 just behind us. Similar to the North Gold Creek, this surface is much older than the "Big Flat" valley floor to our north and the valley floor on which Hamilton stands.

Continue west on Lost Horse Road and stay left on the paved road at the next junction and continue west into Lost Horse drainage.

33.0 At junction keep to the left (south). Continue on Lost Horse Road. We are driving through **large erratic boulders and moraine** of Late Wisconsin Glaciation, locally referred to as Pinedale, or Lost Horse Glaciation. Weber mapped these moraines (1972), and we can review his maps from the vantage point of Stop 13 up ahead.

33.6 STOP 12
46° 7' 51" N., 114° 14' 7" W.

This is a sorted **beach sand**, deposited by Glacier Lake Missoula, on glacial moraine, and partly mined by local entrepreneurs. Elevation here is 4,100 ft.

35.2 **Restroom stop** at USFS toilets.

35.4 Turn left, toward Lake Como. **Cross bridge over Lost Horse Creek** (look for road sign #5621). Note, since the beach sand we've been traveling in moraine. Weber (1972) mapped these moraines in his thesis, *Correlation of the Pleistocene glaciation in the Bitterroot Valley*.



36.9 STOP 13

46° 5' 33" N., 114° 14' 40" W., elevation 4,580

“**Missing incised Miocene**” alluvial fan. Stop to view the canyon below us that was eroded by glaciers emerging from Lost Horse drainage. If we had lived in the Miocene, 7–9 million years ago, we would have been able to walk north from here across this gaping emptiness to the other side of the canyon on an alluvial fan surface, without elevation change. The glaciers emerging from Lost Horse Canyon gouged out that alluvium and melted, leaving airspace and erratic boulder moraines far below out into the valley. This is a huge amount of missing material, much of which probably became outwash on the valley floor past Hamilton all the way to Missoula and out to the Pacific Ocean!

Continue toward Lake Como; note that we are driving on lateral moraines from Lost Horse Canyon smoothed by the weathering of feldspar to clay.

41.0 Crossing over Lick Creek.

Downstream, a quarter mile east, there is a meadow that captured **Mazama ash**, high in sodium and easy to lick. This ash is proposed because whitish clots of clay in the bioturbated soil where ungulates lick tested similar to Mazama ash in sodium values. Thousands of generations of deer and elk have licked and ingested great craters into the meadow’s surface, comprised of this weathered salty volcanic ash altered to clay. The ash came from eruptions about 7,000 years ago at Crater Lake in Oregon. The eruptions sent ash clouds to Montana that washed into and accumulated in small basins and mixed with soil.

A source most often hypothesized for these licks are the Tertiary-age volcanic clays lining Lick Creek both upstream and downstream of the meadow. These are much older, however, leached of sodium, and don’t seem to attract animals quite as much as the clots and thin layers of clay-altered Mazama ash in our region.

41.8 Crest the lateral moraine of Rock Creek (Lake Como drainage), elevation 4,500 ft, and descend toward Lake Como.

42.1 To your right below is an unusual **kettle**

pond, where Three Frogs Campground is located, but this common interpretation may not be the origin. Jeff Lonn (MBMG, written commun., 2020), using LiDAR data, suggests a landslide origin for this pond because glacial till here was deposited on top of clay-rich Tertiary sediment, which failed, bringing the till down and damming the pond.

42.5 At stop sign, turn sharply right to visit the beach at Lake Como.

42.6 STOP 14—Lake Como

Marker: **Glacier Lake Missoula Rock at Lake Como**, placed by the Missoula Chapter of the Ice Age Floods Institute.

Across the lake to the south, observe the timber-covered ridge of **lateral moraine**. A corresponding terminal moraine can be located 1.5 mi east of the dam. The base of the dam is recessional **terminal moraine**. The last glacier to exist here would have been at least 1,500 ft high at this location. Across the lake we can see the Little Rock Creek drainage, just below the **Como Peaks**, a good example of a **hanging valley**. The **Como Peaks are horns**, rock faces bounded by the intersecting walls of **cirques** cut back into the mountain by the headward erosion of **glaciers**.

The current elevation of the water in Lake Como at full pool is about 4,200 ft. This corresponds to the maximum water level of Glacial Lake Missoula. If Glacial Lake Missoula existed today at that level, it would extend over the entire Bitterroot Valley.

A projection of the **Bitterroot Range-Front fault** can be interpreted through the Lake Como dam (Stickney and Lonn, 2018). A prominent **scarp of the Bitterroot fault is easy to find in the ridge of lateral moraine** on the south side of Lake Como, conveniently utilized by a water supply ditch and easy to locate.

Lake Como, named by the Italian priest Anthony Ravalli in 1845, is a reservoir providing vital drinking water and irrigation in Ravalli County. A man-made dam was completed over the glacial moraine in 1910. The dam has been modified, the last time in 1994 to 85 ft high with a crest length of 2,550 ft and a spillway elevation of 4,246 ft. At full pool the reservoir capacity today is



38,500 acre-ft. The lake feeds a canal fondly called the Big Ditch, operated by the Bitter Root Irrigation District that facilitates a net annual transfer of 70,000 to 75,000 acre-ft of water along a 72-mi route, almost to Florence. The Big Ditch crosses from the west side of the valley to the east side onto Miocene alluvial fans underlain by bedrock pediment or vice versa, a pediment carved onto alluvial fans called benches, irrigating 17,000 acres on the east side of the Bitterroot Valley. The canal is unlined and leaks water to the valley aquifers at the rate of 1.05 ft³ per second per mile, where measured east of Hamilton over a 5.8-mi reach (Todd Myse, MBMG, 2016 written commun.), and thus supplies drinking water to numerous homeowner wells in alluvial aquifers along most of the east side of the Bitterroot Valley. Lake Como is stocked with Rainbow and West Slope Cutthroat Trout by Montana Fish, Wildlife & Parks.

Wilkins, Megan, 2017, A closer look at John Day Fossil Beds National Monument: Discover Your Northwest, 58 p.

REFERENCES

- Hyndman, D.W., 1980, Bitterroot Dome-Sapphire tectonic block, an example of a plutonic-core gneiss-dome complex with its detached superstructure: Geological Society of America Memoir 153, p. 427–443.
- Konizeski, R.L., 1958, Pliocene vertebrate fauna from the Bitterroot Valley, Montana, and its stratigraphic significance: Geological Society of America Bulletin 69, p. 325–345.
- Lonn, J.D., and Sears, J.W., 2001, Surficial geologic map of the Bitterroot Valley, Montana: Montana Bureau of Mines and Geology Open-File Report 441a, scale 1:100,000.
- Stickney, M.C., and Lonn, J.D., 2018, Investigation of Late Quaternary fault scarps along the Bitterroot Fault in western Montana, Montana Bureau of Mines and Geology Report of Investigation 24, 28 p., scales 1:24,000 and 1:12,000.
- Vuke, S.M., Porter, K.W., Lonn, J.D., and Lopez, D.A., 2009, Geologic map of Montana field notebook: Montana Bureau of Mines and Geology Geologic Map 62E, scale 1:500,000.
- Weber, W.M., 1972, Correlation of Pleistocene glaciation in the Bitterroot Range, Montana, with fluctuations of glacial Lake Missoula: Montana Bureau of Mines and Geology Memoir 42, 42 p.



FAULTS AND FLOODS OF THE MISSOULA VALLEY

J.W. Sears

University of Montana, Missoula, Montana

INTRODUCTION

Missoula Valley occupies the depressed southeast corner of a triangular, Cenozoic graben. It is one of an *en echelon* series of grabens that cross the central-western Montana Rockies along the Lewis and Clark shear zone. The northwest-trending Clark Fork–Ninemile fault bounds the graben on the north, and the northeast-trending Mount Sentinel fault zone bounds it on the east (fig. 1). Both fault zones experienced movement in Eocene and Miocene times, as shown by the structure and stratigraphy of the Missoula Valley.

The Missoula Valley is the namesake of Glacial Lake Missoula because of its excellent lake shore strand lines and lake-bottom sediments (Pardee, 1910).

This field guide visits several key localities to consider the evolution of the Missoula graben and Lake Missoula.

MISSOULA GRABEN STRATIGRAPHY

The Missoula graben exposes thick Paleogene sediments that are overlain with angular unconformity by Neogene sediments. They are equivalent to the Renova and Sixmile Creek Formations, respectively, of southwest Montana (Fields and others, 1985).

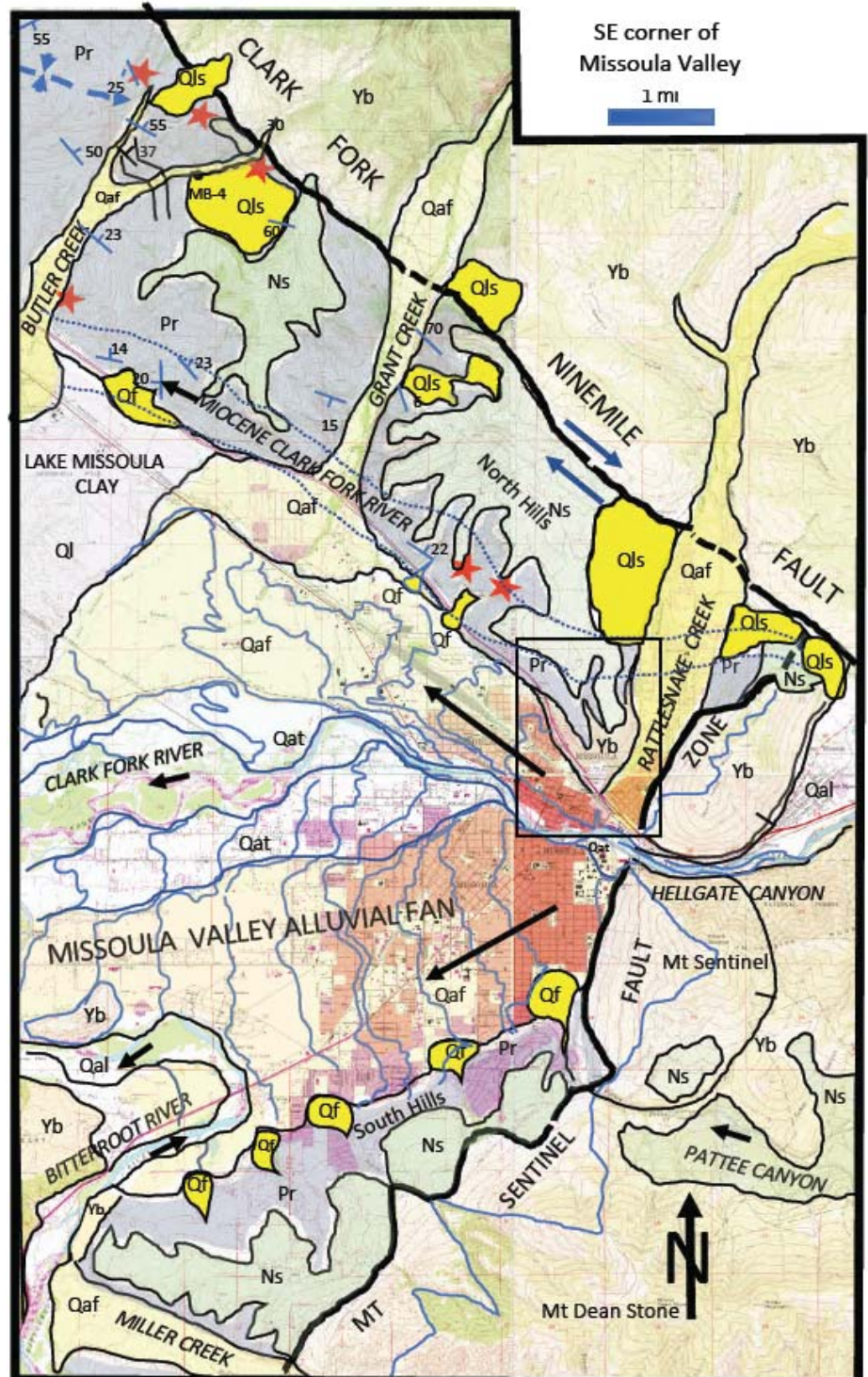


Figure 1. Geologic map of SE Missoula Valley. Yb, Belt Supergroup; Pr, Renova Formation; Ns, Sixmile Creek Formation; Ql, Lake Missoula lake-floor sediment; Qaf, Alluvial fan; Qat, alluvial terrace; Qal, alluvium; Qls, landslide; Qf, fan. MB-4, Test well. Blue lines in Missoula Valley floor, 10-ft contours from U.S. Geological Survey topographic base. Zig-zag blue lines show triangular facets of Mt Sentinel fault zone. Red stars, ash beds in Renova Formation. Dotted lines, edges of Miocene river channel. Rectangle, area of figure 6. Some data from Lonn and others (2007, 2010).

Paleogene Renova Formation Equivalent

In the Missoula graben, the Renova equivalent beds exceed 4,000 ft in thickness. They are not properly named, but are equivalent to the Renova Formation of southwest Montana, and I use that name in this field guide. Like the Renova, the unit overlies rhyolite flows dated at 48 Ma, and is overlain with angular unconformity by Miocene–Pliocene alluvial fans, here assigned to the Sixmile Creek Formation. No fossils have been found in the Missoula area, but a tephra bed yielded an apatite fission-track age of 39 Ma. The beds are dominantly of fluvial facies. Lithologies include pebbly gravels with exotic clast types derived from the Bitterroot Valley and sources in central Idaho, tephra beds, lignite beds, granitic sands, and swelling clays derived from volcanic ash. The beds are generally poorly lithified, but some gravel is tightly cemented by hematite, opal, or carbonate. The muds are susceptible to landslides.

Although correlative, the Missoula unit differs lithologically from the Renova of southwest Montana, which is dominated by thick volcanic ash that has been diagenetically degraded into swelling clay. The Renova of southwest Montana is richly fossiliferous, and interbedded with dated lava flows and welded tuffs, so its age range is well established at latest Eocene to early Miocene.

Neogene Sixmile Creek Formation

In the Missoula graben, the Sixmile Creek Formation is dominantly a coarse-grained unit that stands in contrast to the dominantly fine-grained Renova equivalent. It is made up of alluvial fan facies that grade downslope into fluvial deposits along the axes of grabens. It is correlative and lithologically similar to the type Sixmile Creek Formation of southwest Montana, so I use that formation name in this field guide. The unit is as thick as a few hundred feet in the Missoula area. Facies include well-rounded fluvial gravel and angular alluvial fan gravel. The formation overlies the Renova and older rocks on an angular unconformity marked by a red laterite soil zone of Middle Miocene age. The formation was dissected by significant erosion beginning in the Pleistocene.

In southwest Montana, vertebrate fossils and volcanics date the Sixmile Creek Formation to Middle Miocene to late Pliocene age, from 16 Ma at the base to 2 Ma at the top. In southwest Montana, the Sixmile

Creek Formation has been heavily faulted in the border zone of the Yellowstone hotspot, but in the Missoula Valley it appears to have been relatively undisturbed by tectonics.

Pleistocene Units

Pleistocene units in the Missoula graben include glacial lake beds, widespread alluvial fans, fluvial terraces and alluvium, and landslides. Landforms include ravines, gulches, braid plains, floodplains, strandlines, and narrow bedrock canyons that incise older fans and valleys.

Lakeshore strand lines preserved on Mount Jumbo and Mount Sentinel, along with lake-bottom sediments preserved in the valley to the west, led Pardee (1910) to recognize that the giant ice-age Lake Missoula had filled the valley.

FIELD TRIP STOPS

This guide visits critical field stops around Missoula that constrain the geometry and timing of faulting, sedimentary filling, and erosional incision of the Missoula Valley graben. Field stops are numbered in figures 2 and 3. The guide begins on the University of Montana campus, to discuss ideas about Glacial Lake Missoula (Stop 1). It then visits Rattlesnake Creek Valley at Lincoln Hills to observe red soils at the Neogene unconformity (Stop 2). Next, it goes to Cherry Gulch (Stop 3) for a hike up to Randolph Hill (Stop 4). The round-trip hike covers 2.5 mi and climbs 500 ft. The hike crosses from the Belt Supergroup to unconformably overlying Eocene sediments, and summits in Miocene river gravel. Randolph Hill has a fabulous 360-degree view of the Missoula graben and its surroundings. Finally, the guide loops back to the Cherry Gulch trailhead by way of the radio tower (Stop 5) to visit the Belt Supergroup/Renova contact.

STOP 1—University of Montana Campus Oval. Lake Missoula and Mount Sentinel Fault.

Lake Missoula

The surface of the UM Campus Oval, at an elevation of 3,200 ft, is the depositional top of a wide, late Pleistocene gravel fan that spread westward across the floor of the Missoula Valley from the mouth of Hellgate Canyon (fig. 1). The fan is correlative with a broad, boulder-strewn gravel



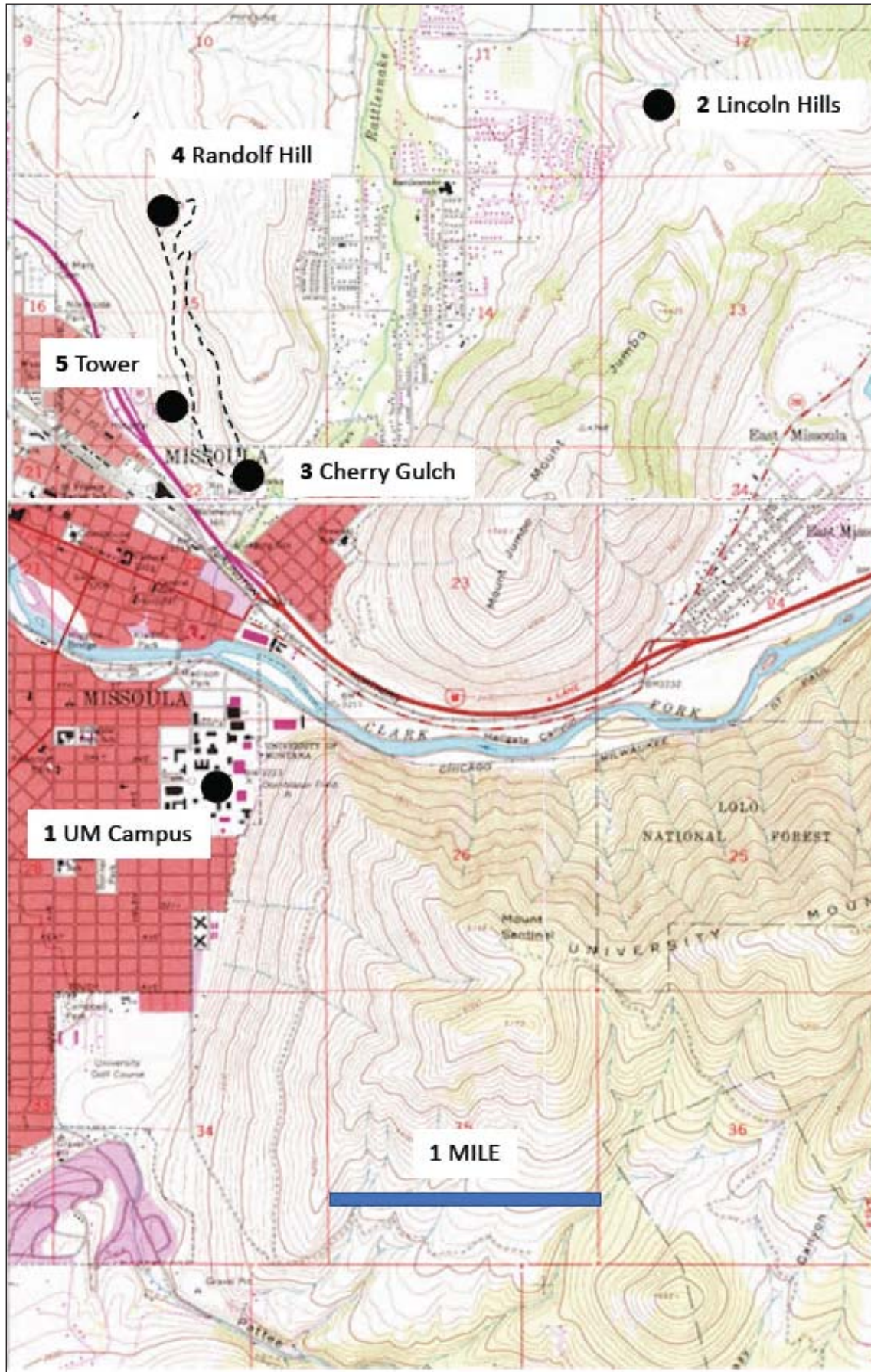


Figure 2. Topographic map of Missoula Valley. Field stops discussed in guide.





Figure 3. Google Earth image of Missoula Valley, view north. Field stops discussed in guide.

bed that floors Rattlesnake Valley directly across the Clark Fork River from campus. Alden (1953) concluded that the gravel of Rattlesnake Valley is outwash from late Pleistocene glaciers on the north flank of Stuart Peak, 10 mi northeast of Missoula, and is therefore about 10,000 years old. The Missoula Valley fan eroded Lake Missoula beds near the Missoula Airport, and was not covered by younger lake beds. It therefore post-dates the last filling of the lake.

Numerous building excavations around campus and on the north side of the Clark Fork River exposed the upper 20–30 ft of the Missoula Valley fan deposit. The top few feet are dominated by fluvial channels filled with well-rounded Belt Supergroup cobbles and pebbles. Beneath that, a chaotic layer contains large angular blocks, the largest of which exceed 10 ft in length. The top of one such block projects to the surface in the northwest quadrant of the Oval. It has the date “1898” carved into it. Most of the blocks are dense white quartzites that resemble massive quartzite cliffs in Hellgate



Canyon about a half-mile east of campus. The large blocks are scattered in a matrix of smaller angular blocks within the layer. Ten-foot-long blocks have been excavated from construction stops as far west as Higgins Avenue. A water main along Third Street encountered angular blocks in the layer that systematically decrease in size to a few feet long, 1 mi west of campus. The layer of blocks appears to be the deposit of a massive debris flow that spread out westward from the mouth of Hellgate Canyon in the Missoula Valley fan (Alt, 2001).

The Missoula Valley fan was cut by numerous fluvial terraces that step down to the present floodplain of the Clark Fork River (fig. 1). Enough of the original depositional top of the fan is preserved to allow a reconstruction of its essential form. Figure 1 traces preserved topographic contours of the surface. The top of the fan descends smoothly westward from 3,200 ft at the UM campus to 3,100 ft 8 mi to the west, near the confluence of the Bitterroot River. As the fan slopes down to the west by 100 ft, the river drops by only 75 ft. The contours arc from a scarp along the base of the North Hills to a scarp along the base of the South Hills. The fan carved a 45-ft scarp in the lake-floor sediments of Lake Missoula near the Missoula Airport. (The airport was constructed on the lake-bottom sediments.)

The Missoula Valley alluvial fan includes the highly productive gravel of the Missoula aquifer. Well logs across the valley show that the fan is about 200 ft thick and has three stratigraphic units—an upper bouldery gravel (including the large blocks), a middle clay-rich layer, and a lower gravel (Morgan, 1986). The fan gravels unconformably overlie Renova Formation sediments, indicating that Lake Missoula beds were scoured out before deposition of the fan.

I postulate that the Missoula Valley alluvial fan is the deposit of the final catastrophic draining of Glacial Lake Missoula. As the waters drained through Hellgate Canyon, they scalloped the quartzite cliffs on the south side of the river, eroding the quartzite blocks found in the fan deposit on campus. In the valley, the current scooped a 200-ft-deep scour pit in the soft lake-floor sediment and underlying Renova Formation. The scour reached from the North Hills to the South Hills. The subsiding current then aggraded the Missoula alluvial fan sediments in the scour pit. Over time, the Clark Fork River eroded a series of river terraces through the fan deposit, down to the level of the present floodplain.

Mount Sentinel Fault Zone

The west face of Mount Sentinel (fig. 3, 4) is un-

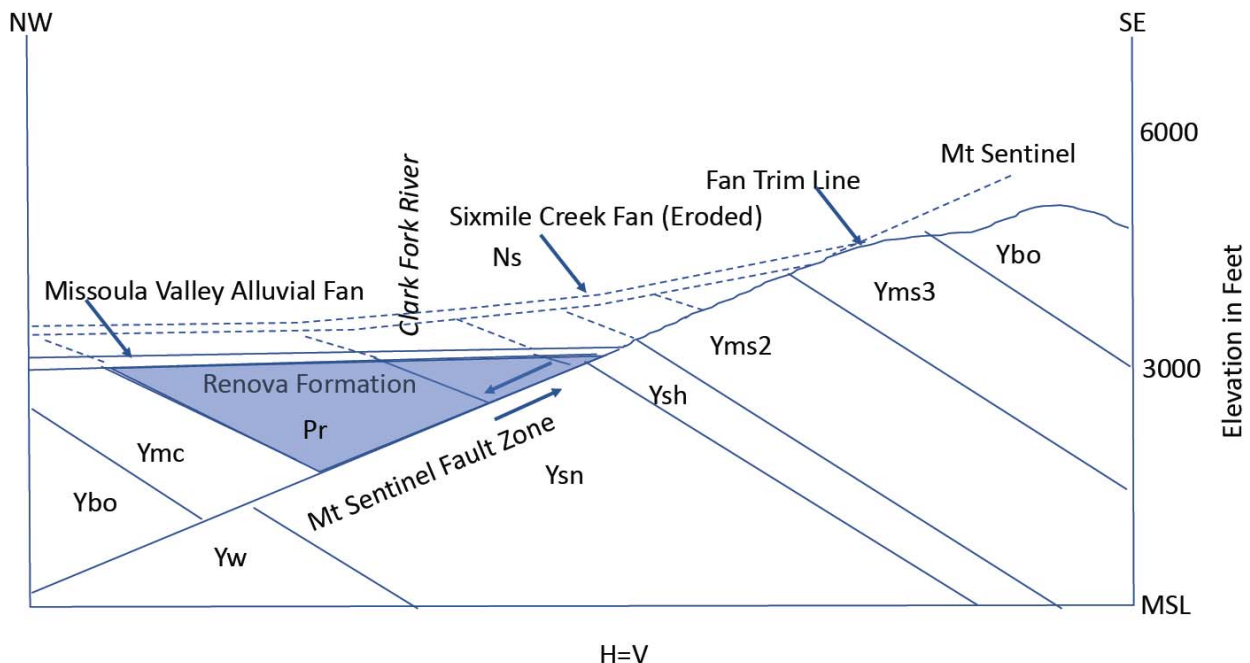


Figure 4. Geologic cross section of Mount Sentinel Fault zone. Dashed lines indicate material eroded from hanging wall of fault. Yw, Wallace Formation; Ysn, Snowslip Formation; Ysh, Shepard Formation; Yms2, Mt Shields Formation, member 2; Yms3, Mt Shields Formation member 3; Ybo, Bonner Formation; Pr, Renova Formation (equivalent); Nsc, Sixmile Creek Formation (equivalent).



usually smooth and planar from its base at 3,200 ft to about 4,000 ft elevation (about the level of the fire road above the “M”). Above that elevation, at about 4,200 ft, there are three broad valleys covered with thick forests. What did these hanging valleys lead to? South of Pattee Canyon, Mount Dean Stone has similar broad valleys above 4,200 ft (fig. 1). These lead down to alluvial fan surfaces that slope toward the bottom of the Missoula Valley. The alluvial fans are assigned to the Six Mile Creek Formation of Late Miocene and Pliocene age, and were deposited under an arid climate (Thompson and others, 1982). The fans onlap the Belt Supergroup on the footwall of the Mount Sentinel fault zone, and spread across tilted Renova-equivalent sediments on the hanging wall. The fans are about 200 ft thick and comprise angular and poorly sorted gravel derived from the neighboring footwall.

Pattee Canyon is a hanging valley that crosses the footwall of the fault zone, and preserves a thick section of Sixmile Creek Formation between the elevations of 3,600 and 4,400 ft (Lonn and others, 2010). It is generally concordant with the alluvial fans and likely flowed into the graben, across the Mount Sentinel fault zone, as a major point-source of sediment. The Mio–Pliocene floor of Pattee Canyon was incised by Pleistocene erosion down to the level of the floor of the Missoula Valley. It built a small Quaternary fan out onto the surface of the larger Missoula Valley alluvial fan.

Similar hanging valleys appear to be present in the south wall of Hellgate Canyon and on the east side of Mount Jumbo, down to the same elevations as the ones along the west face of Mount Sentinel. That would indicate that Hellgate Canyon was present in Middle Miocene, and was deepened by Pleistocene incision, similar to the incision of Pattee Canyon.

Several springs occur at the base of the alluvial fan deposits at the permeability barrier between the gravelly Six Mile Creek Formation above and the clay-rich Renova Formation below (Harris, 1997). One large spring occurs in a deep gulch near High Park in the South Hills, accessible from Parkview Way on a public trail. That spring seeps out of the Sixmile/Renova contact zone, fills a pond, and has a significant flow down a tree-lined gulch. Other

springs occur in the North Hills above the 1890s Moon-Randolf Homestead. These provided water for domestic use and livestock. Several seeps occur near the contact at Stop 2 in Lincoln Hills. Landslides are common in Renova mudstones where they are saturated by springs or seeps from the base of the Sixmile Creek Formation (Harris, 1997).

There is commonly a break in slope at the Six-mile–Renova contact, with the gravelly Sixmile Creek Formation forming a rim above the slope-forming Renova Formation. Combined with the red soil outcrops, springs, and common Renova landslides, the topographic profile helps in mapping the contact.

At campus, the fans and underlying Renova Formation were completely removed by Pleistocene erosion, revealing the northwest-dipping surface of the Mount Sentinel fault plane (fig. 4). A trim line at the 4,200-ft contour marks the erosional level of the valley during deposition of the Sixmile Creek Formation from 16 to 2 million years ago. Below the erosional scarp, the fault plane was buried by the Renova Formation, which was tilted toward the fault. An unknown amount of Renova Formation was eroded prior to deposition of the Sixmile Creek Formation. As the Sixmile alluvial fans aggraded, the footwall eroded back, broadening the hanging valleys. Where the fans onlapped the Mount Sentinel fault, they etched a ~200-ft-high erosional scarp on the fault plane, which corresponds to the thickness of the fans. Pleistocene erosion incised the alluvial fans, cutting down into the underlying Renova. On campus, erosion stripped away all of the alluvial fans as well as the underlying Renova Formation, down to 3,200 ft elevation.

That erosion took place before the incision of the Lake Missoula shorelines across the west face of Mount Sentinel, but after deposition of the Sixmile Creek fans, probably during many previous episodes of filling and draining of Lake Missoula.

Mount Jumbo and Mount Sentinel may be horst blocks that collapsed into the Missoula graben in Middle Miocene time before being crossed by drainages through the Mount Jumbo saddle, Hellgate Canyon, and Pattee Canyon.



STOP 2—Lincoln Hills. Red Soil Zone at Base of Sixmile Creek Formation.

Directions: Take Van Buren Street north from I-90 for 2 mi, to the turnoff to Lincoln Hills. Turn right on Lincoln Hills Drive and proceed for about 1.5 mi, to the Mount Jumbo Trailhead parking area (fig. 5).

The parking area is in the basal Sixmile Creek Formation, which is here characterized by well-rounded river cobbles and boulders. The cobbles are dominated by Belt Supergroup quartzites, but careful examination also reveals fine-grained, cross-bedded, white quartzite cobbles ornamented with small pits. They may be quartzites from the Devonian Maywood Formation channels found in the Potomac and Cramer Creek areas, 20 mi to the east. This may indicate that the river gravel deposit flowed from the east. The base of the Sixmile Creek river gravel exposed here is nearly 500 ft above the modern Clark Fork River channel, due to falling base level between Middle Miocene and Pleistocene times.

Mount Jumbo is a Missoula City Park with many hiking trails. These are closed during much of the year because an elk herd shelters here in the fall and winter and calves in the spring. The area is mostly covered by soil and vegetation, but the trails commonly show traces of well-rounded river pebbles, cobbles, and pea-gravel. The saddle in Mount Jumbo appears to be the channel of a west-flowing river that aggraded some 200 ft of river gravel. The north boundary of the saddle is the Clark Fork–Ninemile fault zone. A road cut in the Clark Fork Valley 1 mi to the east exposes a 1,000-ft-wide zone of pulverized rock along the fault zone.

At this stop, the Sixmile Creek river gravel overlies an angular unconformity that cuts across tilted and faulted Renova Formation and Belt Supergroup. It onlaps the Clark Fork–Ninemile fault in the saddle. Seeps and springs along the hillside come out of the basal Sixmile Creek Formation. These zones are marked by dense, bushy vegetation.

The unconformity is marked by a bright red laterite soil zone that crops out in a cut along Lincoln Hills Drive, 0.2 mi northwest of the parking area.

It also occurs on the east side of the Mount Jumbo saddle beneath the Sixmile Creek gravel, in East Missoula. The red soil records the brief period of warm and wet climate of the Middle Miocene climatic optimum, around 16 million years ago. The unconformity has been mapped across the graben valleys of southwest Montana and adjacent Idaho (Thompson and others, 1982). It coincided with tectonic tilting, graben formation, and drainage rearrangement in the Basin-Range Province, and outbreak of the Yellowstone hot spot (Sears and others, 2010).

In the Missoula area, the bright red soils help to define the geometry of the sub-Sixmile Creek unconformity in the poorly exposed hillsides. The soils are mainly seen in road cuts and construction stops. The soils were the sources of clay for some bricks in Missoula's early buildings. The soil zone is as much as 200 ft thick within the Renova Formation beneath the unconformity. The weathering that produced the soil also affected the Belt Supergroup, along fault footwalls. This indicates that both the faulting and tilting of the Renova occurred before the soils zone formed in Middle Miocene time, as also documented in southwest Montana.

Across Rattlesnake Creek to the west, in the middle distance, is Randolph Hill (Stop 4). It is capped by river gravel of the Sixmile Creek Formation, which overlies Renova Formation and Belt Supergroup on an angular unconformity.

STOP 3—Cherry Gulch Trailhead at Waterworks Hill. Belt Supergroup Overlain by Renova and Sixmile Creek Formations.

Directions: From Stop 2, return to Van Buren Street on Lincoln Hills Drive. Turn left on Van Buren Street and drive 0.8 mi south to Lolo Street. Turn right on Lolo Street and drive 0.5 mi to Duncan Drive. Turn left on Duncan Drive, and drive 0.85 mi to where Duncan Drive starts down a hill. Make a hairpin right turn and go uphill into the parking area for the Waterworks Trailhead. Take the Cherry Gulch Trail for 1.3 mi to the summit of Randolph Hill (a climb of about 500 ft). Figure 6 shows a detail of the geology of the route. See figure 1 for location of figure 6.



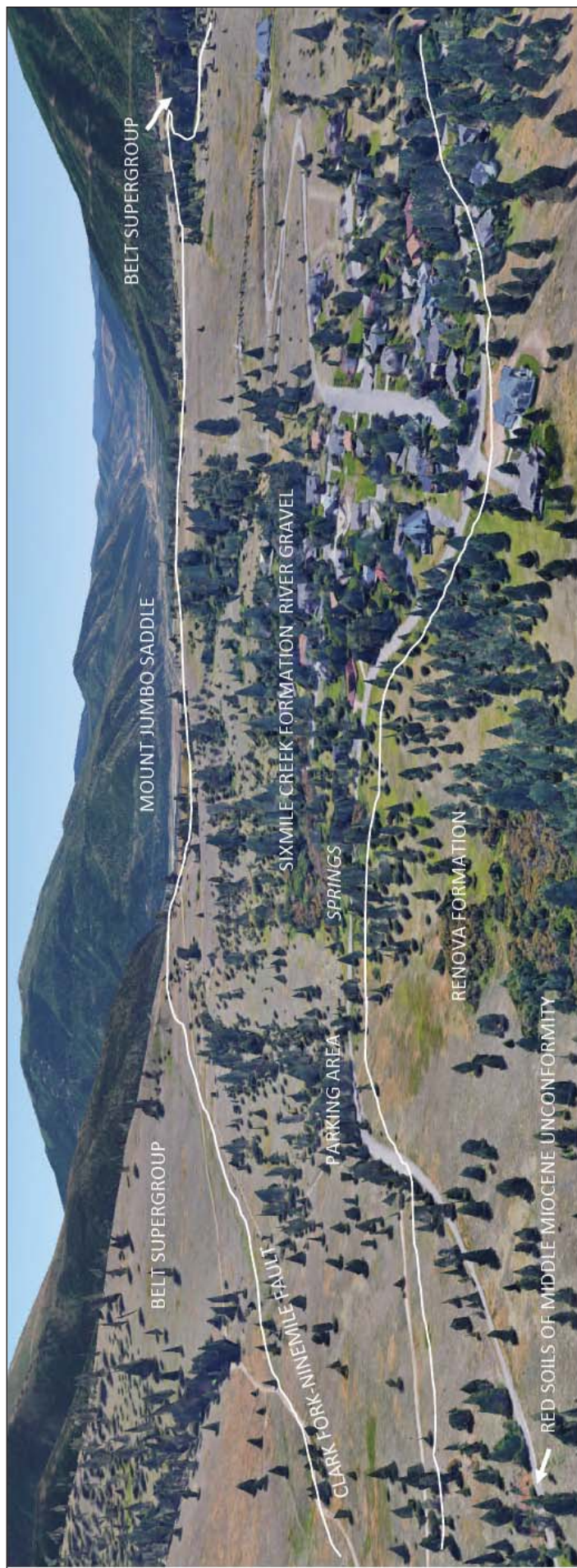


Figure 5. Google Earth image of Mount Jumbo saddle, Lincoln Hills, view east. Field Stop 2.



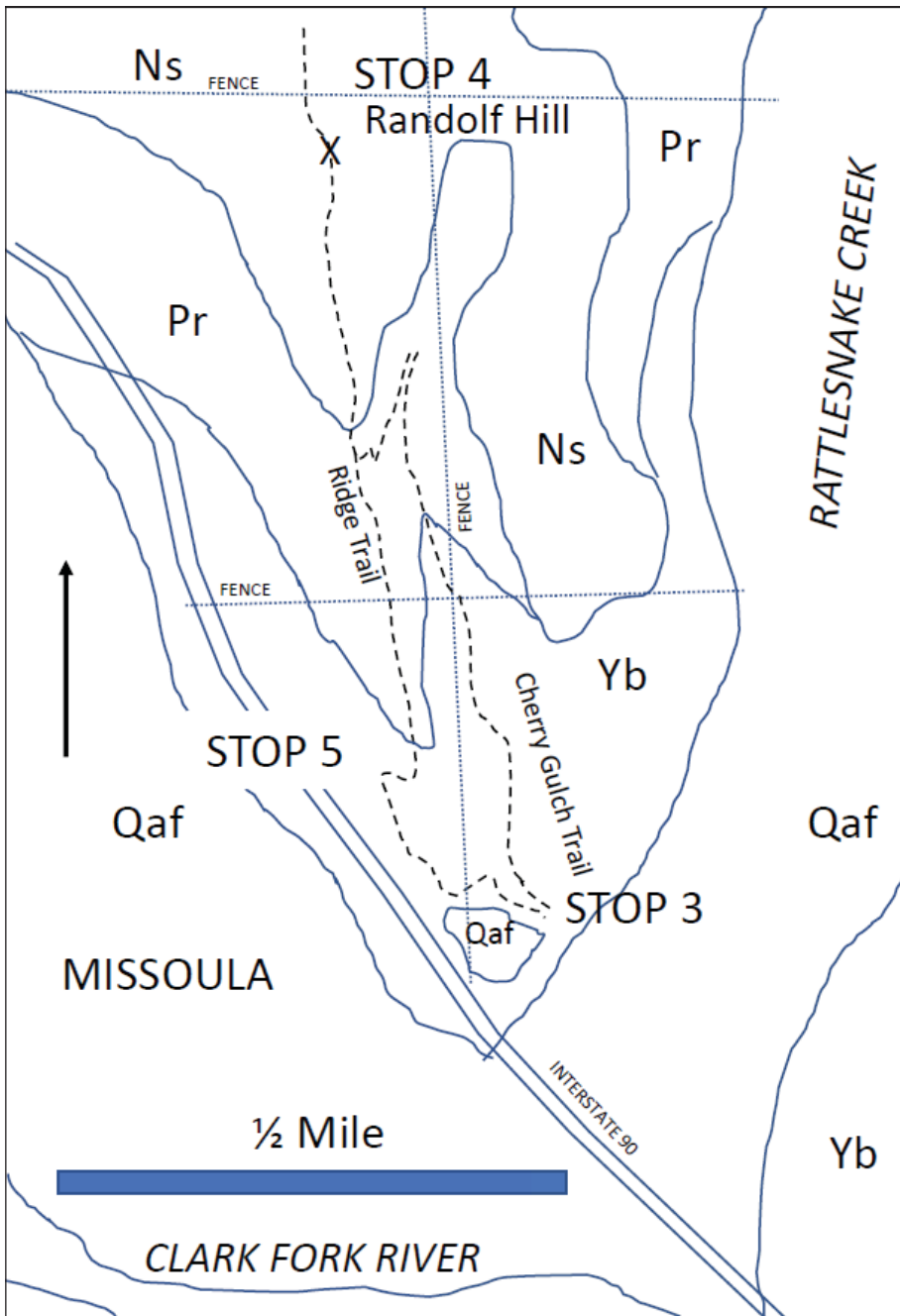


Figure 6. Simplified geologic map of Cherry Gulch–Randolf Hill area, North Hills of Missoula. Figure 1 shows location. Yb, Belt Supergroup; Pr, Renova Formation equivalent; Ns, Sixmile creek Formation; Qaf, alluvial fan.

The trail begins in Pleistocene terrace gravel of Waterworks Hill, about 200 ft above the surface of the Rattlesnake Valley fan. That gravel was likely deposited in a pre-Pinedale fan at the mouth of Rattlesnake Creek. The trail follows the bottom of the gulch past small outcrops of the Belt Supergroup, and through a thick, covered section of Renova Formation. It then climbs out of the gully and up to Randolph Hill, crossing into the Sixmile Creek Formation. The route returns to the Waterworks Trailhead parking area on the Ridge Trail past the radio tower.

Belt Supergroup

The first outcrops along the trail are thin, gently southeast-dipping beds of argillite and quartzite assigned to the Snowslip Formation, the basal unit of the Missoula Group. The Missoula Group is the uppermost unit of the Belt Supergroup, and is about 15,000 ft thick. The Belt Supergroup totals >45,000 ft thick in the Missoula area. It was deposited from 1.5 Ga to 1.4 Ga in an intracontinental rift basin.

Renova Formation

In Cherry Gulch, the Renova Formation overlies the Snowslip Formation of the Belt Supergroup on an angular unconformity. The Renova is not well exposed along the trail. It can be mapped, however, by carefully searching slope-wash soils on the hillsides for distinctive pebbles of lineated mylonitic granite likely derived from the Bitterroot mylonite zone, which crops out 35 mi south of Missoula along the east flank of the Bitterroot Mountains. Rare pebbles of chert-clast litharenite of the Mississippian Copper Basin Group of central Idaho also occur. In the Missoula area, the Sixmile Creek Formation lacks these clasts. Ghostly traces of bedding on the west slope of Cherry Gulch indicate a gentle northerly dip of the Renova, above its contact with the Snowslip Formation.

The Renova Formation is a minimum of 2,300 ft thick where it was logged in exploration well MB-4 in Butler Creek, 6.6 mi northwest of here (Harris, 1997). The well started in the Renova and the base was not encountered in the well. A 500-ft-thick section of gravel that was logged in the well strikes toward this area. The gravel contained mylonite cobbles, and dipped northeast, toward the Clark Fork–Ninemile fault, at 37 degrees.

Landmark: The Cherry Gulch Trail passes a North Hills City Park map exhibit at the intersection of two quarter-section fences. The Belt–



Renova contact appears to cross Cherry Gulch Trail about 300 ft north of the point where the two quarter-section fences cross.

At about 1,000 ft beyond the quarter-section fence, the trail starts up Randolph Hill in a ravine. The constructed trail switchback away from the ravine to the south and then back to the north. The switchbacks are in the Renova Formation.

Sixmile Creek Formation

Where the constructed trail returns to the ravine, take a small footpath to the right for about 100 ft. This leads to a bouldery gravel bed at the base of the Sixmile Creek Formation. The gravel bed is at approximately the same elevation as the boulder bed at the base of the Sixmile Creek Formation at Stop 2. The boulders are smooth, very well rounded, and are similar in compositions to those at Stop 2. This is likely part of the same river channel as at Stop 2, which is visible at the Mount Jumbo saddle, 2 mi to the east of this location. It may represent the Middle Miocene paleochannel of the Clark Fork River. The boulder bed ends abruptly in the ravine just to the west of here at what appears to be the channel margin, cut into the Renova Formation. The same boulder bed emerges about 500 ft farther to the west on the other side of Randolph Ridge. The boulder bed is also found about a half-mile to the northeast, in line with the boulder bed at Stop 2. A similar boulder bed occurs about a mile north of this location, and 100 ft higher in elevation. It may indicate that the channel shifted across the valley through time as the river gravel aggraded.

Note that the Miocene channel is nearly horizontal, overlies Renova gravels that are tilted at about 30 degrees, and has different clast sizes and provenances, indicating westward transport of the Miocene paleo Clark Fork River, rather than northerly transport of the Eocene–Oligocene paleo Bitterroot River. The paleo-Clark Fork River evidently cross-cut the paleo-Bitterroot River channel when the Missoula graben collapsed along the Clark Fork–Ninemile Fault.

From the boulder bed, return to the switchback trail, and continue up the hill. The trail approximately follows bedding in the Renova Formation up to the ridge crest. A stratigraphic section of

approximately 1,000 ft of Renova Formation may be present in Cherry Gulch from the basal contact with the Snowslip Formation to the base of the Sixmile Creek Formation.

Landmark: Four concrete posts at the Ridge Trail junction on ridge crest. The posts were the footings of the locally infamous aluminum communication panel that was graced with a hand-painted “peace sign.” It was the image of Missoula from 1980 to 2000, when it was dismantled.

At the concrete footings, the trail joins the main Ridge Trail to Randolph Hill. There are small fragments of Bitterroot mylonite pebbles in the soil. Continue up the trail to Randolph Hill. The contact with the Sixmile Creek Formation occurs about 500 ft up the trail to the north. Several thin beds of Sixmile Creek cobble gravel along the climb suggest aggregation of a braided river bed. The crest of Randolph Hill is a boulder facies of Sixmile Creek gravel. It is at the same elevation as a similar boulder gravel about 1 mi north of here. It may represent a broad, braided, bouldery river system.

STOP 4—Randolf Hill: View of Missoula Valley.

The views from Randolph Hill highlight the story of the faults and floods of the Missoula Valley.

View Southeast (fig. 7)

To the southeast, the “M” decorates the grassy slopes of the west face of Mount Sentinel. The west face of the mountain is essentially a large, somewhat eroded, faceted spur of the Mount Sentinel fault plane. The plane dips gently to the west, at about 25 to 30 degrees. It is bounded on the north by Hellgate Canyon and to the south by Pattee Canyon. Three broad, forested “hanging valleys” (HV in fig. 7) scallop the faceted spur, down to the elevation of about 4,200 ft, where they end abruptly. Below that, the hanging valleys pass into straight and narrow ravines. To the southwest of Pattee Canyon, Miocene–Pliocene Sixmile Creek Formation alluvial fans are preserved up to 4,200 ft, and onlap forested valleys that are equivalent to the hanging valleys of Mount Sentinel. This shows that the hanging valleys were the headwaters of alluvial fans that formerly spread into the Missoula Valley.





Figure 7. Google Earth image of Mount Sentinel Fault, view SE. HV, hanging valley.

In the South Hills, the Sixmile Creek fans cover Renova Formation, which is exposed along a Pleistocene erosional scarp. The lower, forested part of the South Hills subdivision was built in the Renova, which was more easily landscaped than the overlying, rocky Sixmile Creek. The Renova was downfaulted and tilted against the Belt Supergroup on the Mount Sentinel fault plane, was deeply eroded, and then was overlapped by the Sixmile Creek alluvial fans. At Mount Sentinel, the Sixmile Creek fans and Renova Formation were stripped away by Pleistocene erosion to reveal the Mount Sentinel fault surface. The Mount Sentinel fault surface was cut by Pleistocene Hellgate Canyon. The Mio–Pliocene floor of Pattee Canyon was concordant with the 4,200 ft trim line of the Sixmile Creek fans against the Mount Sentinel fault zone, and also with the saddle in Mount Jumbo. It accumulated alluvial deposits that are locally preserved. It was a feeder channel for alluviation of the valley. Pleistocene erosion entrenched the Mio–Pliocene valley floor of Pattee Canyon.

Glacial Lake Missoula shorelines are well displayed across the west face of Mount Sentinel. These shore lines are not deep—they were merely cut into soil zones on the fault surface. They are thought to record the last fillings and drainings of Lake Missoula. They are not expressed on the south wall of Hellgate Canyon, possibly because of talus disruption. They are expressed on the north wall.

The floor of the Missoula Valley is a large Pleistocene alluvial fan that incised the South Hills. Hellgate Canyon is at the head of the fan, and the largest clasts in the fan gravels are near the canyon mouth. The fan slopes west and descends by 100 ft across 8 mi. The modern Clark Fork River incises the fan by 45 ft near the mouth of Hellgate Canyon. The fan contains the Missoula aquifer, which is recharged by the Clark Fork River.

View East (fig. 8)

To the east, the Mount Sentinel Fault plane makes up the steep face of Mount Jumbo. Like on Mount Sentinel, the fault plane is smooth below an elevation of about 4,200 ft, and above





Figure 8. Google Earth image of Mount Jumbo and Rattlesnake Valley, view east. CF-NM, Clark Fork–Ninemile fault.

that several hanging valleys mark the heads of Miocene–Pliocene fans that filled the Missoula Valley before Pleistocene erosion. Mount Jumbo saddle (Stop 2) was the Miocene–Pliocene paleo-valley of the Clark Fork River before it shifted to Hellgate Canyon in the Pleistocene. The Clark Fork–Ninemile Fault zone (CF-NM in fig. 8) forms the north side of the saddle. The saddle contains well-rounded river gravel from about 3,600 ft to 4,200 ft elevation. It was concordant with the Sixmile Creek fans in the South Hills. Thus, the paleo-river evidently flowed through the saddle and into the aggrading valley in harmony with the deposition of the fans. The gravel rests on the bright red, Middle Miocene soil zone that was weathered in the underlying Renova Formation. The base of the Sixmile Creek Formation in the saddle is concordant with its base on Randolph Hill. A Pleistocene erosional scarp along Rattlesnake Creek exposed the Sixmile Creek and underlying Renova Formations.

View North (fig. 9)

The view north shows the high footwall block of the Clark Fork–Ninemile fault, rising to 8,500 ft elevation in the Jocko Mountains, nearly 5,000 ft above the Clark Fork River (fig. 9). The footwall block exposed in this view is mostly made up of Piegan and Missoula Groups, the highest two divisions of the Belt Supergroup. The hanging wall is mostly Renova and Sixmile Creek Formations. The Renova Formation is likely >4,000 ft thick, so that the vertical offset of the Clark Fork–Ninemile fault is likely >9,000 ft. The fault line follows a break in slope near the lower tree line. Trees prefer the bedrock of the footwall to the sediments of the hanging wall. As in the other views (figs. 7, 8), alluvial fans of the Miocene–Pliocene Sixmile Creek Formation onlap the fault zone. The fans grade southward into the fluvial gravels of Randolph Hill. The Sixmile Creek Formation overlies the angular unconformity on the tilted and faulted Renova Formation. Likely half of the displacement on the fault took place in the Eocene–Oligocene to accommodate deposition of the Renova, and the other half took place in the Middle Miocene, before deposition of the Sixmile Creek Formation.

A large area on the west side of Rattlesnake Valley is marked by landslides, where the Renova





Figure 9. Google Earth image of Jocko Mountains and Clark Fork–Ninemile fault zone, view north. CF-NM, Clark Fork–Ninemile fault.

mudstones gave way beneath the Sixmile Creek Formation and slid toward Rattlesnake Creek. The scarps of the landslides cut the Sixmile gravels but the sliding surfaces were within the Renova. There are several such landslides in similar settings along the trend of the Clark Fork–Ninemile fault (fig. 1). Note that the landslides have no shorelines preserved, compared with other nearby surfaces. This tells that the landslides post-dated the last filling of Glacial Lake Missoula. It is possible that draining of the lake precipitated the collapse of the landslides.

Rattlesnake Valley emerges from a bedrock canyon as it crosses the Clark Fork–Ninemile fault. In the foreground, the valley is underlain by a bouldery Pleistocene alluvial fan. This surface is concordant with the UM campus oval surface at the top of the Missoula Valley alluvial fan. They both may reflect the final draining of Glacial Lake Missoula.

View West (figs. 10A–10C)

This view is along the Clark Fork–Ninemile fault toward Ninemile Valley and Siegel Pass (on the horizon). The ridge to the southwest of Siegel Pass is a tilted fault block that clearly slopes toward the fault zone, which trends through the pass. The surface of the ridge is the Eocene erosional surface. Middle Eocene volcanics overlie the surface near the mouth of Ninemile Valley. The hanging wall exposes the top of the Missoula Group and overlying Cambrian strata near the mouth of Ninemile Creek. The adjacent footwall exposes the base of the Missoula Group, so that the fault there has a minimum of 15,000 ft of vertical stratigraphic displacement.

In the foreground we see a large landfill excavated in the Renova Formation. The tight clay-rich layers isolate the landfill from the Missoula aquifer. The landfill pit exposes gently northeast-dipping beds of the Renova that include a red-weathered clay-rich unit and a white ash bed (fig. 10B). The ash bed gave a fission-track age of 39 million years (Eocene). The pit exposed thick, northeast-dipping gravel beds (Harris, 1997), but these are now buried to the south of the open pit. The stratigraphic section continues upward to the northeast, and includes a coalbed, a lignite bed with fossil *Metasequoia*, and a second ash bed. The tilted section is





Figure 10. (A) Google Earth image of Missoula Valley and tilted Renovia Formation bedding, view west. (B) Detail of Moon-Randolf Homestead and Renovia exposed in pits.



overlain with angular unconformity by the Sixmile Creek Formation.

The Sixmile Creek Formation is made up of alluvial fans to the north, and fluvial gravel to the south. The fluvial gravel makes flat terraces and shows the trend of the Clark Fork paleovalley.

The Missoula Valley floor south of I-90 is the surface of the large Pleistocene alluvial fan that spread westward from the mouth of Hellgate Canyon, possibly during the final draining of Glacial Lake Missoula.

If you hike over the peak of Randolph Hill for about 500 ft, you may see two small gravel pits on the side of the hill (fig. 10C). These expose gravel of the Renova Formation, which contains pebbles of Bitterroot mylonite. The Renova gravel is overlain by the Sixmile Creek river gravel on the ridge top.

View South (fig. 11)

This view highlights the Pleistocene Missoula Valley alluvial fan in the foreground, cut into the Renova Formation of the South Hills in the middle ground. Note that the older parts of the South Hills subdivision are entirely on the more gently sloping surface of the Renova Formation, as it is more conducive for excavating roads, yards, and home stops than the rocky Sixmile Creek Formation. It is, however, also susceptible to mass wasting.

On the horizon is the Bitterroot metamorphic core complex. Lolo Peak is metamorphosed Prichard Formation (the oldest unit of the Belt Supergroup) in the upper sillimanite–migmatite zone. The Bitterroot mylonite zone forms the sloping surface on the east side of the Bitterroot Mountains. It was exhumed by crustal extension in Middle to Late Eocene time, coevally with the collapse of the Missoula graben along the Mount Sentinel and Clark Fork–Ninemile fault zones. The collapse of the graben made accommodation space for deposition of the thick Renova Formation.

STOP 5—Below Radio Tower. Renova/Snowslip Contact.

On the hike back down to the Cherry Gulch (Waterworks) trailhead, take the Ridge Trail past the tall radio tower. From the “Peace Sign” footings

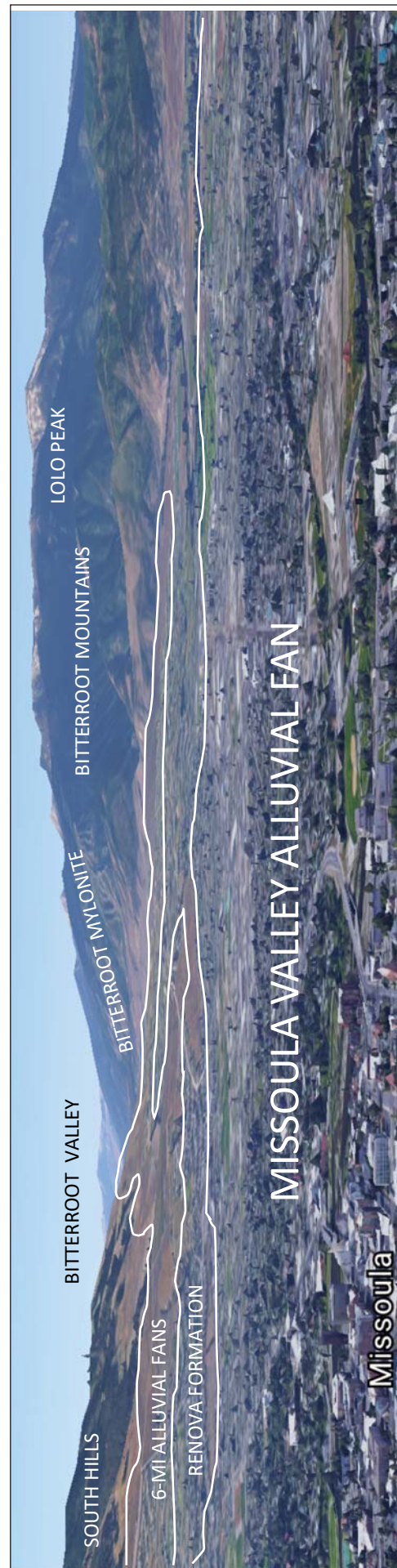


Figure 11. Google Earth image of Missoula Valley and Bitterroot Mountains, view south.



down to the radio tower, the path is in Renova river pea-gravel. Take the branch trail toward Froehlich Trail Head to the right, just past the small communication tower, for about 300 yards, to a small outcrop of Snowslip Formation. The beds dip about 25 degrees toward the east. This is near the basal contact of the Renova, where it rests directly on the Snowslip Formation. Map interpretation from here to Butler Creek (fig. 1) suggests that the Renova may be as thick as 4,000 ft along the north edge of the Missoula graben.

I-90 road cuts visible to the northwest expose red laterites of the Middle Miocene soil zone that weathered the Renova Formation. The soils appear to be 200 ft thick here, beneath the Sixmile Creek contact.

Return to the Ridge Trail and proceed downhill, past the water works, to the Waterworks Trailhead parking area.

End of Field Guide

REFERENCES CITED

- Alden, W.C., 1953, Glacial geology of western Montana and adjacent areas: U.S. Geological Survey Professional Paper 231, 210 p.
- Alt, D., 2001, Glacial Lake Missoula and its humongous floods: Mountains Press, 208 p.
- Fields, R.W., Rasmussen, D.L., Nichols, R., and Tabrum, A.R., 1985, Cenozoic rocks of the intermontane basins of western Montana and eastern Idaho, *in* Flores, R.M., and Kaplan, S.S., eds., Cenozoic paleogeography of the west-central United States: Denver, Colorado, Rocky Mountain Section of the Society of Economic Paleontologists and Mineralogists, p. 9–36.
- Harris, W.J., 1997, Defining benefit and hazard: Distribution of upper and lower Tertiary units on the northeast flank of the Missoula Valley, Montana: Missoula, University of Montana, MS thesis, 127 p.
- Lonn, J.D., Smith, L.N., and McCulloch, R.B., 2007, Geologic map of the Plains 30' x 60' quadrangle, western Montana: Montana Bureau of Mines and Geology Open-File Report 554, scale 1:100,000.
- Lonn, J.D., McDonald, C., Sears, J.W., and Smith, L.N., 2010, Geologic map of the Missoula East 30' x 60' quadrangle, western Montana, scale 1:100,000.
- Pardee, J.T., 1910, The Glacial Lake Missoula: Journal of Geology, v. 18, p. 376–386.
- Sears, J.W., McDonald, C., and Lonn, J.D., 2010, Lewis and Clark Line, Montana: Tectonic evolution of a crustal-scale flower structure in the Rocky Mountains, *in* Morgan, L.A., and Quane, S.L., eds., Through the generations: Geologic and anthropogenic field excursions in the Rocky Mountains from modern to ancient: Geological Society of America Field Guide 18, p. 1–20.
- Thompson, G.R., Fields, R.W., and Alt, D., 1982, Land-based evidence for Tertiary climatic variations: Northern Rockies: Geology, v. 10, p. 413–417.



ROADSIDE GEOLOGIC TRAVERSE THROUGH THE SAPPHIRE MOUNTAINS, MONTANA: STATE HIGHWAY 38, WEST TO EAST

Bruce Cox¹ and George Furniss²

Geologists: ¹Missoula, Montana and ²Darby, Montana

INTRODUCTION

Outcrop and roadcut exposures along Montana Highway 38 (fig. 1 and plate 1) reveal a wide range of Precambrian sedimentary and metamorphic lithologies and provide an introduction to tectonic processes that formed the Sapphire Range. Short traverses away from the highway will visit Proterozoic quartzites and the Tertiary volcanic terrain that hosts the Rock Creek sapphire deposits.

Don Hyndman described the tectonic setting of the Sapphire Range (Hyndman, 1980) as follows: “The Bitterroot dome–Sapphire tectonic block appears to be a well-developed example of a plutonic-core gneiss–dome complex or infrastructure separated from the adjacent suprastructure by a gently dipping zone of mylonitic shearing.” Don considered the Sapphire Range to be the suprastructural block now lying 60

km east from its original position atop the Bitterroot dome infrastructure. Gneiss–dome processes continue to be the favored model for Sapphire Range tectonics, but new mapping is revealing subtleties or constraints to the model and many areas that need more detailed structural work. Ongoing mapping is redefining stratigraphic correlations in the Belt quartzites (Lonn and Mosolf, this volume).

Mineral deposits in the immediate vicinity of Highway 38 include gold placers, vermiculite and fluorite deposits and the currently operating sapphire mines. Most of the mineralogic and mining engineering data for these deposits is proprietary but is slowly coming into the public domain. An exception is data for the Rock Creek sapphire deposits, which we will visit at STOP 11.

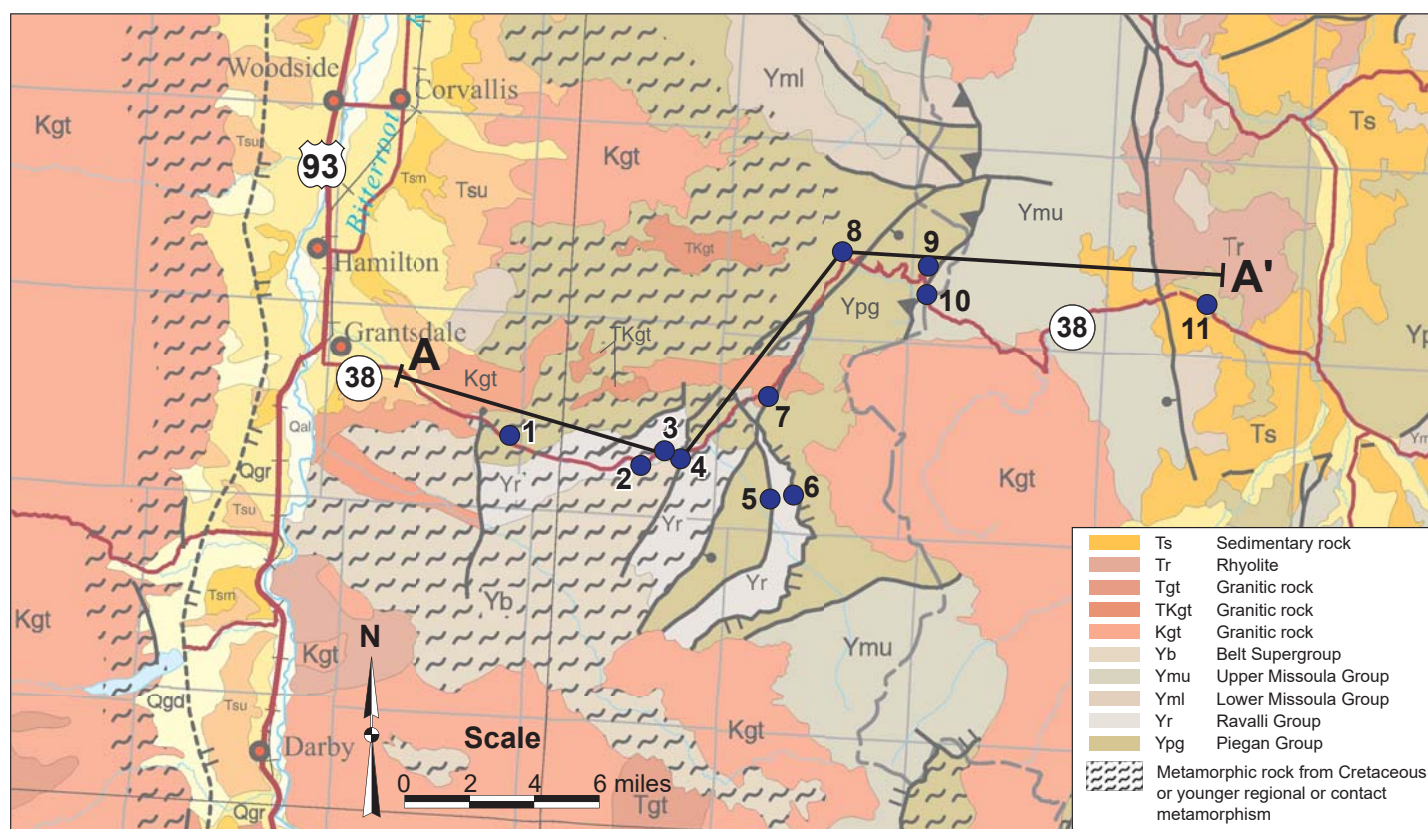


Figure 1. Geologic map of the southern Sapphire Range, Montana. Modified from Vuke and others (2009). Numbered dots, Field Trip Stops. A–A', cross-section, plate 1.

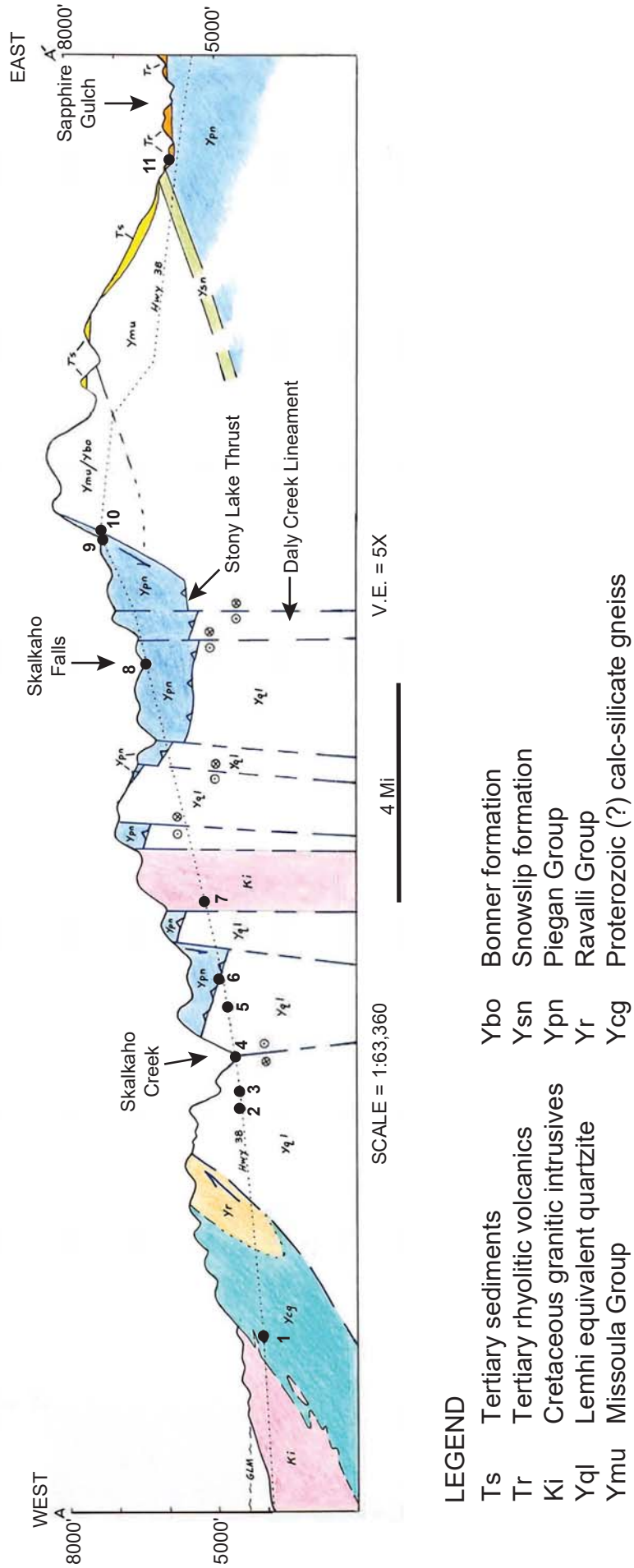


Plate 1. Lithologic and structural contacts are transposed from Yuke and others, 2009, and modified from recent mapping by Lonm, 2020. Refer to figure 1 for the line of section.

FIELD GUIDE

(fig. 1 and plate 1)

Miles Travelled

(total miles/reset above mouth of Daly Creek)

0.00 Junction Highway 93 and Highway 38 (2 mi south of Hamilton)

Turn eastward onto Highway 38 (toward Skalkaho Falls and Philipsburg)

5.7 Entering Skalkaho intrusive igneous complex. Note spheroidal weathering of granitic bedrock.

6.0 STOP 1—Paragneiss of the Proterozoic Y Piegan Group

(figs. 2 and 3)

Park on right shoulder of highway. Roadcuts expose quartzofeldspathic gneiss and calc-silicate gneiss intruded by quartz veins and pegmatitic dikes and sills. Examine the metamorphic textures, mineral assemblages and cross-cutting relationships.

7.0 Milepost 7. Elevation 4,200 feet—approx. Highest shoreline of Glacial Lake Missoula.

11.8 STOP 2—Centennial Grove Interpretive Site and Trail

(fig. 4)

Examine the lithology and roundness of boulders as you walk the interpretive trail. One interpretive sign suggests the hummocky topography here was formed by a landslide which broke away from the steep quartzite cliffs on the north side of the canyon. Another interpretation might be downstream deposition of debris flow sediment at a constriction in Skalkaho Canyon. Closer examination of boulder lithologies might indicate the boulders' origins.

12.4 STOP 3—Yql quartzites

(fig. 5)

Turn left into mouth of road aggregate quarry. These quartzites were formerly considered part of the Ravalli Group and are now believed to be younger Lemhi quartzites equivalent to Missoula



Figure 2. STOP 1. Highway 38 road cut exposures Ycg gneiss and Ki intrusive rock. (a) West section shows calc-silicate and quartz-feldspar gneiss intruded by granitic rocks. (b) Mid-section with normal fault, down-to-left. (c) East section; Ki dikes, sills and pegmatitic veins.

Group (Lonn, personal communication). Note overall character of these rocks for comparison with quartzites at Stop 6.





Figure 3. STOP 1. Metamorphic textures in Ypn. (a) Remnant fining upward graded beds; (b) Garnet-rich boudins.



Figure 4. STOP 2. Centennial Grove debris flow mound. Note the size and lithology of rounded boulders.

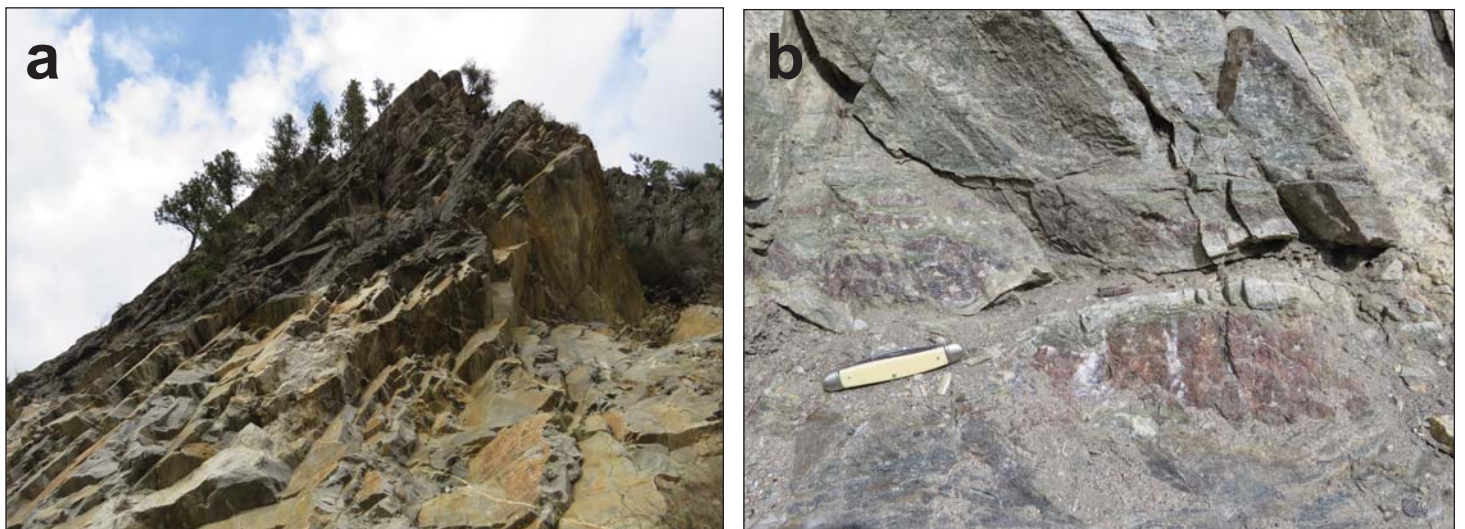


Figure 5. STOP 3. (a) Thick-bedded, fine-grained Yql quartzite dipping west (left). (b) Pegmatite dikes intruding fine-grained Yql quartzite.



13.1 STOP 4—Black Bear Campground

Pit stop. The campground is located along the trace of a north-striking, right-lateral fault (see plate 1).

13.7 Turn right on Road 75 toward Railroad Creek.

15.2 Turn left on Railroad Creek Road #711.

15.8 STOP 5

(fig. 6)

(optional)—Mazama ash exposed in roadcut on left.



Figure 7. STOP 6. (a) Sole marks or long-wavelength oscillation ripple marks. (b) Fine-grained quartzite showing climbing ripple cross laminations. (c) Differential weathering along crenulation cleavage(?).



Figure 6. STOP 5. Mazama ash layer between paleosol and modern soil/talus.

16.4 STOP 6

Blocky talus of Yql quartzites. Park along shoulder on opposite side from talus. Use caution examining talus boulders, as some are unstable. Quartzites display a variety of sedimentary textures and structures (fig. 7). How do these features compare with those at STOP 3 and what do they tell us about the depositional environment?

16.5 Road junction. Turn around and return to Highway 38.

17.8 Junction with Road #75, turn right.

19.4 Junction with Skalkaho Road (Highway 38). Turn right, reset odometer to 0.0 (optional).

19.4/00.0 Junction Road #75 and Highway 38.

19.6/0.2 Traverse passes from Yql quartzites into Ypn Piegan Group rocks in the Stony Lake thrust



hanging wall. Daly Creek Lineament: for the next 8 mi, Highway 38 is centered along a set of NE-trending linear features herein called the “Daly Creek Lineament.” This trend might be considered a segment of the Trans Challis–Great Falls Tectonic Zone. It is evidenced by a distinct topographic grain, local fault segments, and the location of prominent springs.

21.9/2.5 STOP 7 (optional)

Landslide “breccia.” Note the overall character of this deposit (fig. 8) for comparison with the Ypg breccia at the next stop, Skalkaho Falls.



Figure 8. STOP 7. Landslide debris, mixed provenance.

25.4/6.0 OPTIONAL STOP

Note gnarly deformation texture of lithologies exposed in roadcuts. Potential sedimentary and structural processes that might generate these textures are discussed at STOP 8.

27.5/8.1 STOP 8

Ypn breccia at Skalkaho Falls (figs. 9, 10). The middle belt carbonate “breccia” has been the subject of numerous academic investigations and lay person headscratchings. Overocker (2006) provided the following observations: “A series of enigmatic breccias in the Wallace Formation [Piegan, Ypn], Mesoproterozoic Belt Supergroup, have been variously interpreted as originating from: (1) syndepositional downslope slumping; (2) syndepositional evaporite dissolution and collapse; or (3) post-depositional tectonic faulting. Each hypothesis carries its own implications regarding



Figure 9. STOP 8. (a) Skalkaho Falls. (b) View SW along Daly Creek lineament. (c) View NE along Daly Creek lineament.

the depositional and diagenetic history of the Belt basin.” Other processes that have been suggested for specific breccia textures and structures are:

- soft-sediment deformation triggered by gas overpressuring along growth faults,
- turbidite breccias deposited in subaqueous debris flows,



Examine roadcut exposures and discuss breccia origin. Ypn exposures and float continue for the next 4.6 mi.

31.7/12.3 STOP 9

Qtg, Glacial till (fig. 11). Unsorted and unconsolidated surficial deposits here are glacial till previously unmapped.



Figure 11. STOP 9. Glacial till (?) deposited along the hangingwall trace of the Stony Lake thrust.

32.1/12.7 STOP 10

West-verging Stony Lake thrust. Fault places Ypn over Ymu (upper Missoula Group) and forms this subdued topography. Lonn (oral commun.) now interprets this fault as a down-west normal fault that juxtaposes hanging wall and footwall of the Stony lake thrust. Quartzite around the top of the pass contains chert rip-ups suggesting correlation with McNamara Formation. Note the transition from gray-green-tan siltite float into hematitic siltstone and quartzite float as you traverse west-to-east.

32.1/12.8 Skalkaho Pass.

43.2/23.8 STOP 11

Rock Creek Sapphire District (fig. 12). Turn left on Road 129. The following discussion is an excerpt from the website of Potentate Mining and describes a new interpretation for occurrence of sapphires in the historically productive Dann Placer:

“Dann Placer is known for phenomenal mining grades, often over 1,000 carats per cubic meter, but mining exposures showed no evidence of sorting and concentrating of the gravels and sapphires by rivers or streams.



Figure 10. STOP 8. Middle Belt (Ypn) carbonate breccia. (a) Weakly brecciated Ypn with molar tooth texture. (b) Wavy bedded Ypn with incipient breccia. (c) Fine-clast, matrix-supported Ypn breccia.

- thickly graded bedded mudstone facies deposited in a wave-dominated environment, or
- molar tooth structures generated by carbonate filling of microbial gas channels.



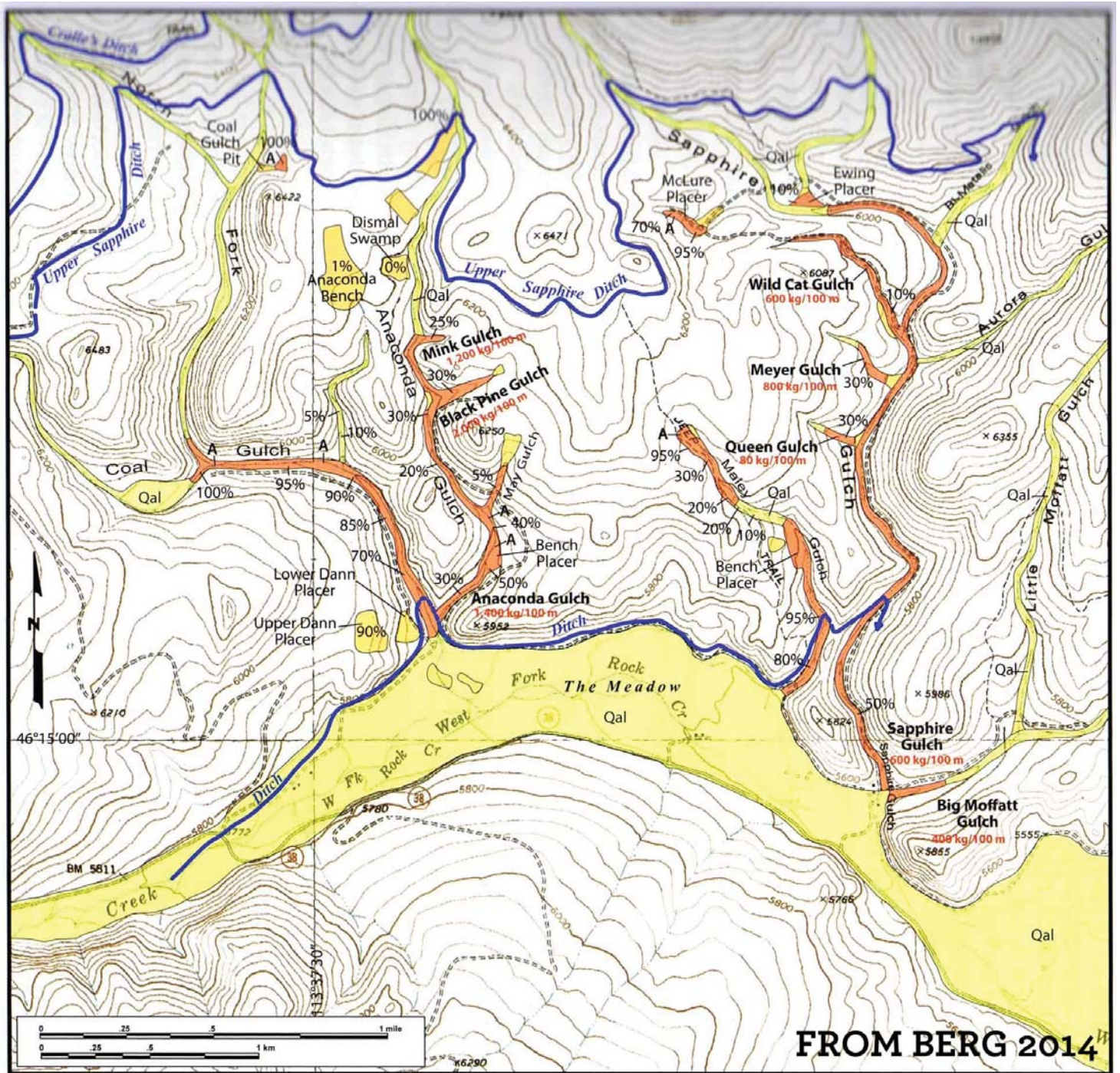


Figure 12. STOP 11. Map of the Rock Creek sapphire deposits. The debris-flow hosted Dann placer is at the mouth of Coal Gulch, center left. Modified with permission from Berg (2014).

The host material was a random mixture of rounded and angular rock fragments in a muddy and clay-rich matrix with the sapphires distributed throughout this matrix. There was only rudimentary bedding, unlike the typically well-bedded and sorted alluvial gravel deposits. [It was]...determined that the sapphire rich deposits are actually colluvium, or debris flow deposits, produced by a geological process known as mass wasting.”

The Potentate property has recently yielded some very fine ruby-grade sapphire stones.

End of the Field trip. You can follow Highway 38 west, returning to Hamilton, or east toward Philipsburg and Anaconda.

ACKNOWLEDGMENTS

We express our thanks to Jeff Lonn and Katie McDonald for their review of the manuscript and help with the figures and to Keith Barron for permission to visit the Potentate Sapphire operations. Larry Johnson and Jay Johnson (not related, that we know) assisted with development of the road log and energetic discussion of processes which formed the middle-Belt carbonate breccias.

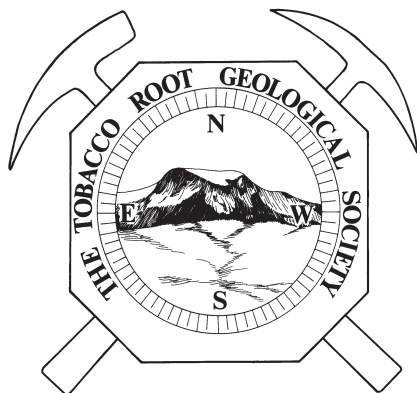


REFERENCES

- Berg, R.B., 2014, Sapphires in the southwestern part of the Rock Creek sapphire district, Granite County, Montana: Montana Bureau of Mines and Geology Bulletin 135, 86 p.
- Furniss, G., Rittel, J., and Winston, D., 1998, Gas bubble and expansion crack origin of “molar-tooth” calcite structures in the middle Proterozoic Belt Supergroup, western Montana: *Journal of Sedimentary Research*, v. 68(1): p. 104-114.
- Godlewski, D.W., 1981, Origin and classification of the Middle Wallace breccias: Missoula, University of Montana, M.S. thesis, 74 p.
- Hyndman, D.W., 1980, Bitterroot dome-Sapphire tectonic block, an example of a plutonic-core gneiss-dome complex with its detached suprastructure: *Geological Society of America Memoir* 153, p. 427-443.
- Johnson, D. Jay, 1999, Sedimentary structures and facies in the Helena and Wallace formations, Middle Proterozoic Belt Supergroup, Montana: Missoula, University of Montana, PhD thesis, 169 pages.
- Lonn, J.D. and Mosolf, J., 2020, Field guide to the geology of the Sleeping Child metamorphic complex, southern Sapphire Mountains, western Montana: *Northwest Geology*, this volume.
- Lonn, J.D., et al, 2003, Preliminary Geologic Map of the Philipsburg 30' X 60' Quadrangle, Lonn, J.D., McDonald, C., Lewis, R.S., Kalakay, T.J., O'Neill, J.M., Berg, R.B., Hargrave, P., 2003, revised 2009, Geologic map of the Philipsburg 30' x 60' quadrangle, western Montana: Montana Bureau of Mines and Geology Open-File Report 483, scale 1:100,000.
- Overocker, Q.M., 2006, Origin and classification of Middle Wallace breccias, Mesoproterozoic Belt Supergroup, Montana and Idaho: Knoxville, University of Tennessee, M.S. thesis, 64 p.
- Vuke, S. M., Porter, K.W., Lonn, J.D., and Lopez, D.A., 2009, Geologic Map of Montana Field Notebook: Montana Bureau of Mines and Geology Geologic Map 62-E, 59 p., scale 1:500,000.







NORTHWEST GEOLOGY

The Journal of The Tobacco Root Geological Society

Requirements for Contributions

TEXT FORMAT: Word Doc (not docm), or plain text (TXT or RTF)

IMAGE FORMAT: JPG—do not embed in Word Docs

DO NOT SUBMIT TABLES OR IMAGES AS EXCEL SPREADSHEETS

FINAL DEADLINE FOR RECEIPT BY EDITORS: JUNE 1 (may be earlier; check website)

Generally, follow USGS style for writing. See COMPLETE REQUIREMENTS at trgs.org. YOU MUST READ AND FOLLOW.

Text should be submitted to the Editor(s) in MS Word-compatible (DOC) format (plain TXT or RTF is fine). **Please DO NOT provide formatting.** Do not assign page numbers, do not double space, do not use columns or backgrounds, **do not indent** anything. Especially, **PLEASE do not include images within Word documents** – they have to be removed, re-formatted, re-sized, and introduced into the publisher program. Word formats images in a way that makes files huge. Do not include large tables in text – make a separate file or image for tables. IMAGES PROVIDED AS WORD DOCUMENTS WILL BE RETURNED.

Photographs and other images should be submitted as JPG or PDF files, **separate** from text. Dimensions should be so that the full size of the image is approximately as it will be displayed – that is, if it will be 3 inches wide when printed, 3 inches wide when displayed on the computer monitor will be adequate. We can interpret most image formats; **this does not include Word or Excel, which are not image formats. ANYTHING SENT AS AN EXCEL SPREADSHEET WILL BE RETURNED.**

Scanned images and line drawings should be at NO MORE than 300 dots per inch resolution. The native size, as displayed on a computer screen should generally be no larger than the screen. If necessary, we can scan hard-copy drawings or photos for you – this is preferable to submitting images in unusual file formats. Figure captions should be submitted as a separate text file, or part of the text file.

Road Logs **must** be accompanied by (at a minimum) a location map of stops; ideally, a geologic map with stops would be included. Such maps should be provided separately from the text.

Please use the following bibliographic format. Note especially capitalization and use and position of commas and colons. For journals, do not abbreviate except J. for “journal” and U.S. in “U.S. Geological Survey.”

Sears, J.W., and Hendrix, M., 2004, Lewis and Clark Line and the rotational origin of the Alberta and Helena Salients, North American Cordillera: *in* Sussman, A., and Weill, A., eds., *Orogenic Curvature: Geological Society of America Special Paper 383*, p.173-186.

Tikoff, B., and Teyssier, C., 1992, Crustal-scale, en-echelon P-shear tensional bridges: a possible solution to the batholithic room problem: *Geology*, v.20, p. 927-930.

Color images are accepted at our discretion, and will only be included if the color is critical to the understanding of the image (e.g., a complex geologic map). Images including photographs can be submitted in color, but expect that we will likely convert them to grayscale. Each color page adds about \$200 to the cost of a normal press run of the guidebook.

Topics: In general, papers published in Northwest Geology do NOT need to be directly related to a particular TRGS Field Conference.

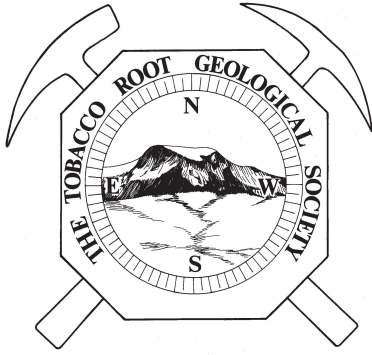
Abstracts: In general, we prefer to NOT publish stand-alone abstracts. Exceptions may be made, but we encourage you to create a short paper (which can be thought of as an expanded abstract) including at least one informative map, cross section, or image.

The Tobacco Root Geological Society, Inc.

P.O. Box 118

Butte, Montana 59703

<http://trgs.org>



NORTHWEST GEOLOGY

The Journal of The Tobacco Root Geological Society

Volume 49, July 2020

Geology of the Bitterroot Region and Other Papers

TABLE OF CONTENTS

FIELD GUIDES

Skye W. Cooley	Sheeted clastic dikes in the megaflood region, WA-OR-ID-MT 1
Burmester, Lonon, and Lewis	Further speculation on Belt stratigraphy and structure around Salmon, Idaho: Alternative interpretations and tests..... 19
Lonon and Mosolf	Field guide to the geology of the Sleeping Child metamorphic complex, southern Sapphire Mountains, western Montana..... 35
Michael Stickney	Hanging wall rocks of the Bitterroot detachment fault exposed west of Victor, Montana..... 57
Gammons and Grondin	Field trip guide to Crystal Mountain fluorite mine..... 63
Michael Stickney	Late Quaternary fault scarps near Como Lake, Montana 71
Childs and Dean	New documentation of a major molybdenum–copper porphyry system in Lower Willow Creek, west of the Black Pine mine, Granite County, southwestern Montana..... 77
Jeff Lonon	Geology along the Late Quaternary Bitterroot fault scarps, and implications for seismicity in the Bitterroot Valley, western Montana..... 87
George Furniss	Roadside geologic traverse along the Bitterroot Front from Hamilton to Lake Como 97
J.W. Sears	Faults and floods of the Missoula Valley 103
Cox and Furniss	Roadside geologic traverse through the Sapphire Mountains, Montana: State Highway 38, west to east..... 119